Use of Sol Chemistry and Fine Grained Precursors in the Production of Controlled Microstructural Polycrystalline Continuous Oxide Fibres

Craig John Freeman BSc. (Hons.)

A thesis submitted in partial fulfilment of the requirements of the University of Wolverhampton for the degree of Doctor of Philosophy

May 2005

This work or any part thereof has not previously been presented in any form to the University, or to any other body, whether for the purposes of assessment, publication or for any other purpose. Save for any express acknowledgements, references and/or bibliographies cited in the work. I confirm that the intellectual content of the work is the result of my own efforts and no other person.

Signature: Craig Freeman

Date: 17.11.05

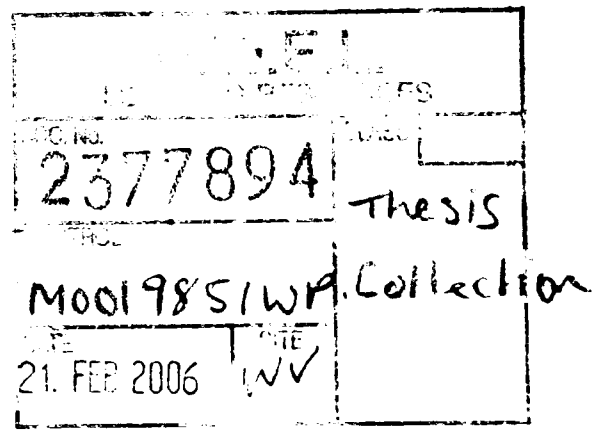

Acknowledgements

I sincerely thank Prof. Craig Williams for directing my studies and my second supervisor and colleague Dr. Roger Bayliss for their continuous support, encouragement and advice throughout my studies and most especially through the long days of writing up.

I wish to thank my ex-colleagues of Morgan Group Technology for their encouragement and assistance in preparing samples for analysis. Also TEM imaging of fibres at Warwick University.

Thank You to my dear wife, Michelle who has put up with me and looked after our young son Euan allowing me to complete my work without interruption. Also to my family who have encouraged me, both recently and through my earlier studies – Thank You.

And yes this is the end of my studies Michelle!

Contents

	Page
Contents	i
List of Figures	viii
List of Tables	xii
List of Equations	xiv
Abstract	xvi
Hypothesis and Aims	xviii
Chapter Introductions	xx
Chapter 1 Introduction to Ceramic Fibres	
1. Introduction	pg 1
1.1. Fibre Characteristics	pg 5
1.2. Use of Fibres For Composite Reinforcement	pg 6
1.3. Polycrystalline Fibre Characteristics	pg 9
1.4. Non Oxide Fibres	pg 11
1.4.1. Fibres Produced by Chemical Vapour Deposition	pg 11
1.4.2. SiC Ceramic Fibres Produced From Polymer Precursors	pg 13
1.4.3. Si-C-N Ceramic Fibres Produced From Polymer Precursors	pg 10
1.5. Oxide Fibres	pg 18
1.5.1. Continuous Single Crystal Monofilaments	pg 18
1.5.2. Melt Derived Amorphous Ceramic Oxide Fibres	pg 23
1.5.3. Commercial Polycrystalline Oxide Fibres	pg 25
1.6. References	pg 33

Chapter 2 Selection of Precursors for Preparation of Non Oxide and Oxide Fibres

2.1. Historical Review of Silane and Carbosilane Polymers pg 39

2.2. Development of Spinnable Carbosilane Polymers pg 40

2.2.1. Mark 1 Fibre pg 41

2.2.2. Mark 2 & 3 Fibre pg 43

2.3. Precursors used in Oxide Ceramic Fibres pg 44

2.3.1 Historical Review of Sol-Gel pg 44

2.4. The Sol-Gel Process pg 46

2.5. The Alkoxide Route pg 48

2.6. The Aqueous Route pg 51

2.7. Specific Precursor Selection For Commercial and Experimental Polycrystalline Sol-Gel Derived Fibres pg 52

2.7.1. Alumina Precursor Materials pg 52

2.7.2. Silica Precursor Materials pg 61

2.7.3. Zirconia Precursor Materials pg 62

2.7.4. YAG Precursor Materials pg 63

2.7.5. Spinel and Other Aluminate Precursor Materials pg 64

2.7.6. Mullite Precursor Materials pg 64

2.7.7. Summary pg 66

2.7.8. Aims pg 67

2.8. References pg 68

Chapter 3 Methods of Analysis

3. Introduction pg 78

3.1. Controlled-Stress Rheometry (Cone and Plate) pg 78

3.2. Thermal Analysis (TGA, DT/TGA, DSC) pg 79

3.3. Fourier Transform Infrared Spectroscopy (FT-IR) pg 80

3.4. Inductively Coupled Plasma Emission Spectroscopy (ICP) pg 81

3.5. X-ray Fluorescence (XRF) pg 81

3.6. X-ray Diffraction (XRD) pg 83

3.7. Nuclear Magnetic Resonance Spectroscopy (NMR) pg 86

3.8. Scanning Electron Microscopy (SEM) pg 87

3.9. Transmission Electron Microscopy (TEM) pg 90

3.10 Room Temperature Mechanical Tensile Tests pg 92

3.11. References pg 94

Chapter 4 Formation of Fibres and Firing (Preliminary Work)

4. Fabrication and Firing of Continuous Polycrystalline Oxide Fibres from Sol-Gel Precursors pg 95

4.1. General Processing Considerations pg 95

4.2. Wet and Dry Fibre Spinning pg 96

4.2.1. The Slurry Process pg 97

4.2.2. Solution or Sol-Gel Spinning pg 98

4.2.3. Filtration pg 99

4.2.4. Rheology For Spinning pg 100

4.2.5. Drying pg 102

4.3. Mullite As a Material For Use in Polycrystalline Continuous Fibres pg 103

4.3.1. Precursor Selection For Sol-Gel Fibre Production pg 103

4.4 References pg 109

Chapter 5 Experimental Polycrystalline Fibre Production Using Chloride Free Mullite Sol-Gels

5.1. Alkoxide Mullite Sol pg 111

5.1.2. Mixing Procedure pg 112

5.1.3. Rotary Evaporation pg 113

5.1.4. Fibre Formation, Stability and Rheology pg 115

5.1.5. Sol Extrusion to Produce Green Fibres pg 115

5.1.6. Thermal Analysis pg 117

5.1.7. XRD (X-ray Diffraction) Analysis pg 117

5.1.8. SEM Analysis pg 118

5.2. Inorganic Salt/Colloidal Sol - AAT Mullite Sol System pg 119

5.2.1. Properties of Aluminium Carboxylates pg 119

5.2.3. Commercial Grade Aluminium Acetotartrate (AAT) pg 119

5.2.4. Commercial AAT/Ludox AM-30 Mullite Sol pg 120

5.2.5. Thermal Analysis pg 122

5.2.6. XRD (X-Ray Diffraction) Analysis pg 123

5.2.7. SEM Analysis pg 123

5.3. Summary of Chloride Free Mullite Sols pg 124

5.4. References pg 127

Chapter 6 Optimisation and Characterisation of Fired Fibres

6.1. Commercial AAT Mixed Mullite (50:50) Fibres pg 128

6.1.1. Thermal Analysis pg 128

6.1.2. SEM Analysis of Fired Fibre pg 132

6.1.3. SEM – Elemental Mapping pg 133

6.1.4. XRD Analysis pg 134

6.2. Alternative Colloidal Silica pg 135

6.3. Precursor Ratio Optimisation of Commercial AAT Mixed Mullite Fibres pg 138

6.3.1. SEM Analysis of Fired Fibres pg 139

6.3.2. Commercial AAT 55:45 Mixed Mullite Fibres pg 140

6.4. Commercial AAT (55:45) Zirconia Additions pg 140

6.4.1. SEM of Zirconia Doped Fired Fibres pg 142

6.5. Alternative Lab AAT With Low Impurity Levels pg 143

6.6. Lab AAT (55:45) 5% Zirconia Additions pg 144

6.6.1. Thermal Analysis pg 146

6.6.2. XRD Analysis pg 147

6.6.3. TEM Analysis pg 148

6.7. Lab AAT (55:45) With Incremental Zirconia Additions pg 149

6.7.1. XRF Analysis pg 149

6.7.2. TEM Analysis pg 150

6.7.3. XRD Analysis pg 151

6.8. Stabilising Additives for Zirconia pg 152

6.9. Porosity in 5% ZrO_2 Fibre pg 152

6.10. Sulphur Free Lab AAT pg 154

6.11. Sol Rheology pg 155

6.12. Pyrolysis and Low Temperature Phase Formation pg 160

6.13. Porosity pg 162

6.14. Low Angle XRD Non Intrusive Porosity Measurements pg 163

6.15. Fibre Characterisation Using Solid State NMR pg 165

6.16. Preliminary Room Temperature Mechanical Tensile Tests pg 167

6.17. Effect of Firing Rate on the Microstructure pg 169

6.18. Low Angle XRD Non Intrusive Porosity Measurements Slow Fire pg 172

6.19. Comparison of Microstructural & Mechanical Properties of Commercial Nextel 720 & 650 and Experimental Mullite and Zirconia Polycrystalline Fibres pg 173

6.19.1. Seeding with Fe^{3+} Compounds pg 173

6.19.2. Microstructural Stability of Nextel 720 and 650 With Temperature pg 175

6.19.3. Tensile Test Evaluations pg 117

6.19.4. High Temperature Creep Properties – Bending Stress Relaxation Creep Test pg 180

6.20. References pg 183

Chapter 7 Conclusions and Further Work

7.1. Introduction pg 186

7.2. Simple Chloride Free Mullite Sols pg 188

7.3. Blending Sols pg 190

7.4. Substitution of Commercial AAT Precursor With a Lab Produced Precursor pg 192

7.5. Microstructural Refinement Using Nano Dispersed Tetragonal Zirconia pg 193

7.6. Sol Rheology and Ageing With Time pg 194

7.7. Effects of Firing on Microstructure and Mechanical Properties pg 195

7.8. Microstructural Comparison of Commercial and Experimental Fibres pg 196

7.9. Mechanical Testing pg 196

7.10. Further Work pg 197

7.11. References pg 200

Figures

Chapter 1

Figure 1.1: Boron Fibre with a Tungsten Core pg12

Figure 1.2: YAG - Alumina Eutectic Monofilament pg 21

Figure 1.3: Alumina - Silica Phase Diagram pg 23

Chapter 2

Figure 2.1: Schematic of Aqueous Route to Polycrystalline Silica pg 51

Figure 2.2: α-Alumina Formation From Hydrated Alumina's and Associated Intermediate Oxides pg 57

Chapter 3

Figure 3.1: Controlled Stress Rheometer Equipment Schematic pg 78

Figure 3.2: Thermo Gravimetric Analysis Equipment Schematic (SEM) pg 79

Figure 3.3: Schematic of a Fourier Transform Infrared Spectrometer pg 80

Figure 3.4: Simultaneous ICP Apparatus pg 81

Figure 3.5: Schematic of a Typical Scanning Electron Microscope (SEM) pg 88

Figure 3.6: Schematic of a Transmission Electron Microscope (TEM) pg 91

Figure 3.7: Card Fibre Testing Template (For 25mm Gauge Length) pg 92

Figure 3.8: Watson Image Shearing Eyepiece (WISE) Used to Measure Fibre Diameters pg 93

Chapter 4

Figure 4.1: SEM Micrograph of an ACH/SiO_2 fibre fracture surface fired at 180°C/hr to 1400°C/4 hrs pg 104

Figure 4.2: Al_2O_3 - SiO_2 - B_2O_3 Ternary Phase Diagram pg 108

Chapter 5

Figure 5.1: Buchi R152 10 litre Rotavapor pg 114

Figure 5.2: Sol-Gel Fibre Extrusion Rig pg 116

Figure 5.3: Spinnerette used for Fibre Extrusion - 100μm pg 116

Figure 5.4: dt/TGA Trace For a 2AIP:1AN/TEOS Mullite Fibre at 180°C/hr to 1400°C pg 117

Figure 5.5: SEM Micrograph of 2:1 AIP:AN/TEOS fired at 180°C/hr to 1400°C/4hrs pg 118

Figure 5.6: Surface Substitution by Al^{3+} of Ludox AM-30 Colloidal Silica pg 122

Figure 5.7: dt/TGA Trace For a Commercial AAT/Ludox AM-30 Mullite Precursor sol at 180°C/hr to 1400°C pg 122

Figure 5.8: Extruded Green AAT/Ludox AM-30 Fibre pg 123

Figure 5.9: High Magnification image of AAT/C.SiO_2 Fibre Showing Grain Growth and Porosity after 1400°C Heat Treatment pg 124

Chapter 6

Figure 6.1: Pyrolysis Profile of Mixed Mullite Sol Fibres 50:50 pg 128

Figure 6.2: SEM Micrograph of Mixed Mullite 50:50 Green Extruded Fibres pg 132

Figure 6.3: Mixed Mullite 50:50 Extruded Fired Fibre 1200°C/24hrs pg 132

Figure 6.4: EDS Elemental Mapping of a Fibre Cross Section pg 133

Figure 6.5: XRD Patterns for Mixed Mullite 50:50 Fired Fibres pg 134

Figure 6.6: Mullite Crystallite Size of Experimental and Commercial Fibres pg 137

Figure 6.7: SEM 50:50 Mullite Fibre 1400°C/4hrs pg 139

Figure 6.8: SEM 60:40 Mullite Fibre 1400°C/4hrs pg 139

Figure 6.9: SEM 30:70 Mullite Fibre 1400°C/4hrs pg 139

Figure 6.10: SEM 20:80 Mullite Fibre 1400°C/4hrs pg 139

Figure 6.11: 55:45 Mixed Mullite Fibre Heat Treated 180°C/hr to 1400°C/4 hours pg 140

Figure 6.12: 55:45 Mixed Mullite + 5% MEL ZrO_2 Fibre Fired to 1400°C/4hrs pg 141

Figure 6.13: MEL Sol - Zirconium Hydroxynitrate Linear Polymeric Species pg 142

Figure 6.14: Lab AAT Mixed Mullite Fibre Fired to 1400°C/4 hrs (55:45 + 5 wt% Nyacol ZrO_2) pg 146

Figure 6.15: XRD Trace with Varying Pyrolysis Temperatures pg 147

Figure 6.16: Mixed Mullite (55:45) 1400°C/4 hrs pg 148

Figure 6.17: Mixed Mullite Fibre + 5% ZrO_2 1400°C/4 hrs pg 148

Figure 6.18: TEM Image 1% ZrO_2 1400°C/4hrs pg 150

Figure 6.19: TEM Image 2% ZrO_2 1400°C/4hrs pg 150

Figure 6.20: TEM Image 3% ZrO_2 1400°C/4hrs pg 151

Figure 6.21: TEM Image 4% ZrO_2 1400°C/4hrs pg 151

Figure 6.22: Mullite Crystallite Size Comparison of Doped and Non Doped Fibres pg 151

Figure 6.23: SEM 1500°C/4hrs Porosity in Mullite + 5% ZrO_2 Fibre pg 153

Figure 6.24: SEM 1500°C/4 hrs (Polished) pg 153

Figure 6.25: Polished SEM Micrograph of Mullite + 5% ZrO_2 Fibre Heat Treated to 1300°C/4 hrs and EDS Map pg 154

Figure 6.26: Viscosity Vs Time at a Shear Rate of $1s^{-1}$ pg 157

Figure 6.27: Low Solids Sol Shear Stress and Viscosity Vs Shear Rate pg 158

Figure 6.28: High Solids Sol Shear Stress and Viscosity Vs Shear Rate pg 159

Figure 6.29 TGA/DSC Trace of Extruded Fibres (Heating Rate 20°C/min) pg160

Figure 6.30: Mullite + 5% ZrO_2 Fibres Fired to 900°C/24hrs pg 160

Figure 6.31: Mullite + 5% ZrO_2 Fibres Fired to 1100°C/24hrs pg 160

Figure 6.32: Mullite + 5% ZrO_2 Fibres Fired to 1400°C/24hrs pg 161

Figure 6. 33: Low Angle XRD of Fast Fired (180°C/hr)

Mullite + 5% ZrO_2 fibres pg 165

Figure 6.34: Typical ^{27}Al spectra of a mullite and 5% zirconia sol-gel prior to

extrusion pg 167

Figure 6.35: Bubble (Left) and Crack (Right) Defects of Fired Fibres pg 168

Figure 6.36: Rate of Weight Loss/Second @ 180°C/hr pg 170

Figure 6.37: Rate of Weight Loss/Second @ 18°C/hr pg 170

Figure 6.38: Representation of Mullite+ 5% ZrO_2

1400°C/24hrs (180°C/hr) pg 171

Figure 6.39: Representation of Mullite + 5% ZrO_2

1400°C/24hrs (Slow Firing) pg 171

Figure 6.40: Mullite Crystallite Size Analysis (Fast and Slow Firings) pg 172

Figure 6.41: Low Angle XRD of Slow Fired Mullite + 5% ZrO_2 fibres pg 172

Figure 6.42a: SEM Nextel 650 1300°C/4 hrs pg 176

Figure 6.42b: SEM Nextel 650 1400°C/4 hrs pg 176

Figure 6.43: TEM Nextel 650 As Made Fibre pg 176

Figure 6.44: Tensile Strength of Nextel 720 and 650 vs Heat

Treatment Temperature and Time pg 177

Figure 6.45: Dicarlo BSR Test Schematic pg 181

Figure 6.46: Dicarlo BSR M Ratio Values Vs Temperature pg 181

Tables

Chapter 1

Table 1.1 Properties of Ceramic Fibres Produced by Chemical Vapour Deposition

pg 13

Table 1.2 Properties of SiC Ceramic Fibres Produced From Polymer Precursors

Pg 15

Table 1.3 Properties of SiN/SiCN Ceramic Fibres Produced From Polymer Precursors

pg 18

Table 1.4: Continuous Oxide Ceramic Fibres pg 29

Chapter 2

Table 2.1: Examples of Some Alumina/Silica Precursors Used For Fibre Production

Pg 65

Chapter 4

Table 4.1: Potential Alumina Precursor Materials for Sol-Gel Fibre Preparation

pg 107

Chapter 5

Table 5.1: Advantages and Disadvantages of the Alkoxide Mullite Sol pg 125

Table 5.2: Advantages and Disadvantages of the Inorganic Salt/Colloidal Sol

Pg 125

Chapter 6

Table 6.1: XRD Mullite Crystallite Size Data (nm) For Alternative Silica Sols

pg 136

Table 6.2: Sol Ratio Optimisation Results After Extrusion pg 138

Table 6.3: Oxide Impurities In Commercial AAT Determined By XRF Analysis

pg 142

Table 6.4: XRF Analysis of Fired Fibres pg 149

Table 6.5: Shear Rates for Standard Spinnerette and Hole Geometries pg 156

Table 6.6: Main Chemical Shift Peaks For ^{29}Si Nuclei pg 166

Table 6.7: Main Chemical Shift Peaks For ^{27}Al Nuclei pg 167

Table 6.8: Room Temperature Tensile Testing

Characterisation of Heat Treated Fibres pg 168

Table 6.9: Multi Step Slow Firing pg 169

Table 6.10a: Nextel 650 Heat Treatments vs Duration at Temperature pg 175

Table 6.10b: Nextel 720 Heat Treatments vs Duration at Temperature pg 175

Table 6.11: Tensile Test Results of Best Commercial Fibres

after 1250°C/4hrs Heat Treatment pg 178

Table 6.12a : Tensile Test Results of Batch A Experimental

Fibres after 1250°C/4hrs pg 178

Table 6.12b: Tensile Test Results of Batch B and C Experimental

Fibres after 1250°C/4hrs Heat Treatment pg 179

Equations

Chapter 1

Equation 1.1: Si–C–O Ceramic Thermal Decomposition pg 17

Chapter 2

Equation 2.1: Hydrolysis Reactions of Metal Alkoxides pg 50

Equation 2.2: Condensation Reactions of Metal Alkoxides pg 50

Chapter 3

Equation 3.1: The Bragg Equation pg 85

Equation 3.2: Transposed Bragg Equation pg 85

Equation 3.3: Pore Size Calculation in nm pg 85

Equation 3.4: Relationship Between Magnification
and Electron Beam Width pg 88

Equation 3.5: Calculation of Tensile Strength of a Single Fibre pg 93

Chapter 4

Equation 4.1: Stable Newtonian Jet Length of a Sol During Extrusion pg 100

Equation 4.2: Period of Stable Newtonian Jet Length
of a Sol During Extrusion pg 101

Equation 4.3: Cohesive Energy Density Change with Spin/Draw Ratio pg 101

Equation 4.4: Shear Rate of a Sol During Extrusion pg 102

Chapter 5

Equation 5.1: Hydrolysis of Mullite Alkoxide Sol Precursors pg 111

Chapter 6

Equation 6.1: Debye-Sherrer Equation for Mullite
Crystallite Size Estimation pg 136

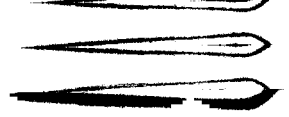

Equation 6.2: Shear Rate of a Sol During Extrusion pg 156

Equation 6.3: The Bragg Equation pg 164

Equation 6.4: Transposed Bragg Equation pg 164

Equation 6.5: Pore Size Calculation in nm pg 164

Abstract

Novel mullite fibres have been produced on a laboratory scale by pyrolysis of sol-gel spun precursors, having nanosized grains or discrete atomic dispersion, stabilised by in-situ precipitation of a minor phase addition of zirconia. A complex blend of chloride free precursors in aqueous media enabled good extrusion and drying characteristics, exhibiting Newtonian flow behaviour and draw down to fired fibre diameters, typically in the range of 10 - 20μm, the finest being almost defect free. The inorganic salt/alkoxide precursor ratio was optimised to 55:45 weight % addition after firstly using commercial grade precursors and then further optimised using lab produced aluminium acetotartrate (AAT) in order to remove unwanted alkali and alkaline earth oxide impurities. Various colloidal silca sols were also evaluated, the finest particle size (7nm) preferred for extrusion and sintering properties. Flow characteristics (rheology) and ageing with time were determined by cone and plate rheometry on three different sol concentrations, the highest concentration was found to age (thicken) faster but was easily extruded to make fibre over a 5 week period due to its shear thinning Newtonian flow behaviour.

Various spectroscopic and microscopic techniques including ICP, XRF, XRD, solid state NMR, SEM and TEM were employed to determine the purity, oxide phase evolution and microstructural stability with temperature and time. During conversion of the sol-gel fibres to the polycrystalline fibre SEM imaging and elemental analysis showed that careful heat treatment was necessary to remove volatile components such as sulphate in order to avoid large residual porosity and week fibres. Densification of fibres between 900 - 950°C was critical, as up to 26% linear shrinkage would result.

The formation of nano porous γ-alumina was apparent from low angle XRD scans and concurred from Al^{27} solid state NMR analysis which manifested itself as deformations in the fibre longitudinally resulting in "kinks" further exacerbated during sintering and mullite formation above 1200°C.

Si^{29} NMR confirmed that tetrahedral peaks at 110ppm between 990 – 1100°C were due to heterogeneous colloidal silica, which subsequently reacted to form a fine stable orthorhombic mullite ($3Al_2O_3.2SiO_2$) above 1200°C in and around which the zirconia existed in the tetragonal form, as defined by XRD analysis. TEM imaging demonstrated that the mullite microstructure had been stabilised and porosity removed due to in-situ precipitation of zirconia and subsequent sintering. The microstructure was compared to 3M Nextel 720 mullite/alumina fibre and found to be of similar dimensions. Optimisation of the zirconia addition was found to be 5% by weight, which also allowed the fine microstructure to be maintained without severe grain growth up to 1400°C. A relatively slow firing rate was shown to almost half the size of the mullite crystals due to controlled sintering and densification, although commercially firing rates of several hundred degrees per hour are more desirable. Such fibres exhibited an average tensile strength of 3.4GPa after heat treatment to 1250°C and superior Dicarlo ratio creep rate properties at and above this temperature compared to the 3M Nextel 720, the best commercial fibres that were currently available on the market.

Discussions with QinetiQ (Farnborough) are being held with the aim of exploiting the sol chemistry within a development project with the ambition of scale up from lab to production scale in order to supply fibres for fabrication of ceramic matrix composites.

Hypothesis and Aims

The main aim of this project is to address the need to produce a stable, single phase, fine grained polycrystalline ceramic fibre via extrusion of sol-gel precursors. The ideal fibre for such applications would be both chemically and microstructurally stable up to 1400°C, have a diameter of less than 20 μm to ensure flexibility, a strength of above 2GPa at room temperature, and retain a strength of at least 1.5GPa at 1200°C. The fibre should also be economical to use to broaden its potential use. Stoichiometric mullite ($3Al_2O_3.2SiO_2$) was considered as a potential material for the fabrication of fibres due to its high melting point, intrinsically low diffusivity compared to simple oxides and hence reduced diffusional creep. Mullite is also highly resistant to shear plasticity at high temperatures and the absence of a large free alumina content also reduces its susceptibility to fracture stress at intermediate temperatures. The fibres will be formed using traditional dry spinning (extrusion) of suitable viscosity sol-gels containing alumina and silica precursors that exhibit gel forming tendencies with reasonable oxide yield (>20%). A shelf life enabling extrusion over several days, without the use of organic fugitive fiberising aids is also a target.

Tensile strength after heat treatment at >1200°C with improved creep properties at temperature, are the intended resulting mechanical properties. The approach will be based on manufacturing small batches of stoichiometric single phase pure mullite fibres using high purity precursors excluding persistent anions such as chloride or sulphate due to their adverse effects on residual porosity, sintering and defect formation. The materials will be characterised in the sol form using cone and plate Controlled-Stress Rheometry, Thermal Analysis, Fourier Transform Infrared Spectroscopy (FT-IR) and as fired fibres by Inductively Coupled Plasma Emission

Spectroscopy (ICP), X-ray Fluorescence (XRF), X-ray Diffraction (XRD), Nuclear Magnetic Resonance Spectroscopy (NMR) and Scanning and Transmission Electron Microscopy (SEM/TEM). Mechanical properties will be established using room temperature tensile testing and at temperature Dicarlo creep ratio determinations.

Chapter Introductions

Chapter 1 provides an overview of the many kinds of high temperature fibres that are available for reinforcement purposes. This covers fibres such as non-oxide silicon carbide, melt derived single crystal and vitreous oxide fibres, concluding with polycrystalline oxide fibres made from the sol-gel process. Chapter 2 discusses the precursors used for polycrystalline silicon carbide and various oxide fibres, that are currently commercially available or topics of research. The inadequacies of these fibres are highlighted and reasons given for the need to develop new oxide materials within this research project. Chapter 3 outlines the various analytical tools used to characterise the oxide precursors, unfired and fired oxide fibres, chemically, physically and structurally. Chapter 4 overviews the general processing considerations for making polycrystalline sol-gel fibres using hand drawing and dry spinning of fibres through spinnerette holes. Selection of precursors is discussed with emphasis on inherent fibre forming ability, purity and oxide yield. Chapter 5 details the experimentation used in the preliminary stages of the work to assess potential candidate systems with stoichiometric mullite composition ($3Al_2O_3.2SiO_2$) that fit the criteria assigned in chapter 4. In chapter 6 these concepts are then developed further and optimised using precursors synthesised to give high purity, stable sol-gels, which formed precursor fibres via dry spinning and were subsequently converted to dense polycrystalline phase pure fibres. Characterisation was carried out through all of these stages to assist in developing fibres with excellent mechanical properties, both after and during exposure to high temperatures.

Chapter 7 concludes the findings of the experimental work in relation to the current state-of-the-art and proposes further work, which may produce a more consistent mechanical performance of as made fibres based on improved processing. Another approach would be to further develop the work on YAG based fibres, which suffer from excessive porosity. A similar mixed sol approach may give the trade off that has been seen for mullite.

CHAPTER 1 INTRODUCTION TO CERAMIC FIBRES

1. INTRODUCTION

Polycrystalline ceramic fibres hold great potential as high temperature reinforcement materials at high temperatures, as they are chemically inert and resistant to oxidation in air. Silicon carbide and other non-oxide fibres are extruded into filaments from organo-silicon precursor polymers, cured and heat treated with oxygen excluded to form the desired phase and preclude the formation of oxide phases. They posess excellent mechanical properties at room temperature, but suffer from oxidation during prolonged use at 1200°C. Fibres have been developed with low oxygen contents (<0.5%) resulting in better oxidation resistance, but their applications are limited. Current commercial continuous polycrystalline oxide ceramic fibres are manufactured from sol-gel precursors, which are extruded through small diameter holes (<100μm), drawn down in diameter, dried and fired to convert them into the oxide form. The resulting fibres are normally high in alumina providing chemical inertness and oxidation resistance, but suffer from loss of strength, grain growth and creep limiting them to a maximum use temperature of 1200°C. 3M are the market leaders in the manufacture of such polycrystalline oxide continuous fibres and initially developed aluminosilicate fibres with considerable levels (>10%) of boric oxide (i.e. 62% Al_2O_3, 24% SiO_2, 14% B_2O_3). The boron levels have been reduced over the years and the alumina:silica ratio adjusted nearer to stoichiometric $3Al_2O_3.2SiO_2$ mullite and more recently alumina rich mullite. Mullite has long been used as a high temperature refractory material in industry, but is not widely abundant as a natural mineral, the exception being on the Isle of Mull in Scotland. Mullite exhibits a high melting point (1920°C), good modulus, thermochemical stability and superior creep strength retention at high temperatures.

A historical problem with these types of fibres is that they are not processed sufficiently and are thermally instable. This results in either a mixture of intermediate alumina, alumino silicate or amorphous phases, which will either result in further reactions at temperature or uncontrolled grain growth and loss of strength. The exception is the more recent Nextel 720 multiphasic α-alumina/2:1 mullite ($2Al_2O_3.SiO_2$) alumina rich fibre. The alumina-rich 2:1 mullite phase becomes unstable and converts to stoichiometric ($3Al_2O_3.2SiO_2$) mullite at temperatures above 1200°C. Minor phase formation is also initiated by impurities, such as sodium leading to residual glass formation at grain boundaries. More recently, during the life of this project, the focus has been on development of a non-silicate system based on a fine α-alumina matrix with yttria stabilised nano-dispersed zirconia. The fibres retain their tensile strength very well up to 1200°C, but become very brittle above this temperature due to crystallisation and grain growth. As such they are regarded as being inferior to the Nextel 720 fibre and the maximum use temperature is limited to 1080°C, whilst Nextel 720 is 1150°C. The challenge remains to produce a stable polycrystalline oxide fibre with superior mechanical properties to those currently available at room temperature, during and after exposure to temperatures of 1200°C or more. This would enable the true realisation of ceramic matrix composites where currently only superalloys perform.

Mullite as a Candidate for Polycrystalline Continuous Fibres

Stoichiometric mullite ($3Al_2O_3.2SiO_2$) was considered as a potential material from which to fabricate fibres due to its high melting point, intrinsically low diffusivity compared to simple oxides, such as alumina, and hence reduced diffusional creep.

Mullite is also highly resistant to shear plasticity at high temperatures and the absence of a large free alumina content also reduces its susceptibility to fracture stress at intermediate temperatures. The fibres will be formed using traditional dry spinning (extrusion) of suitable viscosity sols containing alumina and silica precursors that exhibit gel forming tendencies with reasonable oxide yield (>20%).

Precursors and Selection

An additional factor in selection of mullite is the low cost and large number of readily available precursors for sol-gel production. Traditionally many alumina and mullite fibres have been based on the use of simple aqueous sol-gel systems which utilise aluminium chlorhydrate (ACH - typically $Al(OH)_5Cl$) as the main alumina precursor and colloidal silica. Both aluminium and silicon precursors are widely and economically available in a variety of grades. 3M prefer the use of aluminium carboxylates, which have similar gel and fiberisation properties to ACH, but do not contain persistent anions such as sulphate and chloride, only organic groups that are easily converted to CO_2 and H_2O during pyrolysis. Other manufacturers like Sumitomo have favoured the use of alkoxides, allowing conversion to inorganic polymers via hydrolysis in an alcoholic system, however they are more expensive and difficult to handle. An aqueous based system is preferable, as this reduces the health and safety issues associated with volatile organic solvents and reduces the cost of manufacture, making the fibre more economical, broadening its potential use. The approach will be to manufacture small batches of stoichiometric mullite fibres using high purity precursors excluding persistent anions such as chloride or sulphate due to their adverse effects on residual porosity, sintering and defect formation.

The spinning dope or sol should have a good shelf life enabling extrusion over several days, without the use of organic fugitive fiberising aids which contribute to the volatile components that reduce the final ceramic yield and economics of the material.

Improved Mechanical Properties

A specific target is an improvement over the microstructural stability of Nextel 720 above 1200°C. The ideal fibre for such applications would be both chemically and microstructurally stable up to a maximum of 1400°C, have a diameter of less than 20 μm to ensure flexibility, and a strength above 2GPa at room temperature, and retain a strength of at least 1.5GPa at 1200°C. An improvement in creep properties at temperature is also desirable, especially with inherently low creep of pure mullite. Careful processing and firing of the as made dried green fibre and conversion to the oxide will be required. The fired fibre will contain only phase pure stoichiometric mullite as the major phase with minimal amorphous content and impurities, with a dense, stable fine-grained microstructure. Additives to control sintering and crystal growth may also be required to control the microstructure to provide the mechanical properties.

Characterisation

The materials will be characterised in the sol form using cone and plate Controlled-Stress Rheometry to enable evaluation of sol rheology, shear characteristics during extrusion and sol stability with time (ageing).

Thermal Analysis will evaluate the pyrolysis profile and rate of oxidation of constituent components during conversion from the green to the polycrystalline fibre state. Fourier Transform Infrared Spectroscopy (FT-IR) will be used to assess the preparation of precursors from their "finger print structures".

Both precursors and fired fibres will be evaluated for purity and oxide composition using Inductively Coupled Plasma Emission Spectroscopy (ICP) and X-ray Fluorescence (XRF). X-ray Diffraction (XRD), Nuclear Magnetic Resonance Spectroscopy (NMR), Scanning and Transmission Electron Microscopy (SEM/TEM) will determine crystalline phase formation, atomic homogeneity and environment, and micro/nanostructural evolution and dispersion respectively. Mechanical properties will be established using room temperature tensile testing of heat treated fibres and at temperature Dicarlo creep ratio determinations.

1.1. Fibre Characteristics

A fibre is a long fine filament of material that is flexible and strong in contrast to ceramics, which are hard and brittle materials that break easily under any type of shock. The flexibility of a fibre is a function of its diameter (to the inverse power of four), so that materials that in bulk form appear very inflexible can be made into fine filaments that can then behave like textile fibres. A good example are glass fibres, the flexibility of which comes from their small diameter (typically 5 and 20 μm) allowing them to be woven into cloth in the same way as nylon fibres. The Young's moduli of most synthetic textile fibres are usually low, ~5 GPa. Fine filaments of steel may reach 210 GPa, carbon 800 GPa and diamond 1200 GPa, which is the stiffest material known. However, ceramics are brittle and show much scatter in their mechanical properties, which is also exhibited in ceramic fibres. Even if a stiff material can be made flexible in filament form, its intrinsic properties will control its ultimate behaviour. A glass fibre can be bent easily but only down to a minimum radius of curvature because the tensile stresses developed in the convex surface will eventually reach the tensile failure stress of the glass and the fibre will break.

Glass is not a material that deforms plastically at room temperature, so that even in the form of a flexible fibre it will break by the same processes as bulk glass. The presence of defects on the fibre surface or within its volume will also affect fibre strength. Bulk ceramic materials exhibit variation in strength because of such defects that are distributed throughout its volume, which can also be related to the large sizes of the grains that make up its microstructure. Hence the fine dimensions of a filament require the control of a very fine microstructure to a higher degree to that typically found with bulk ceramics. With a reduction in fibre diameter the ratio of surface area to volume increases, which reduces the importance of flaws in the volume. Thus polycrystalline ceramic fibres are stronger than their counterparts in bulk form and like glass and carbon fibres, they remain elastic at room temperature and fail when their failure stress is reached.

1.2. Use of Fibres For Composite Reinforcement

The primary use of these polycrystalline ceramic fibres is for reinforcement of composite materials with metal or ceramic matrices, for use at high temperatures. In the last 30 years, great progress has been made in the development of high performance materials. One of the important reasons for this progress has been the production of inorganic or ceramic fibres with high tensile strength and modulus values as well as resistance to high temperatures [1]. These fibres when used with polymers and metals have produced composites with superior properties, which have created new engineering possibilities. As a result, composites containing these inorganic fibres are used in space vehicles because of their lightweight, high strength, and resistance to high temperatures. Composites are used in military and civilian aircraft because they increase range, payload, and fuel consumption.

The role of the fine ceramic fibres used to toughen ceramic matrices is very different from that of fibres used in a metal matrix, the difference arises from the nature of the matrix materials used. Resin and most metal composites exploit the lower rigidity and the ability of the matrix material to deform plastically. This together with the greater rigidity of the reinforcements allows stresses to be transferred to the fibres through the matrix and their extraordinary mechanical properties to be conferred to the composite structure as a whole. In contrast, ceramic matrix composites (CMC's) are usually composed of a very stiff matrix and more flexible fibres. The role of the fibres is to mitigate against the brittleness of the matrix, allowing the fibres to inhibit crack propagation in the ceramic matrix. Two mechanisms exist for this, i.e. the de-bonding of the fibre matrix interface, and the bridging of cracks by fibres and their subsequent pullout. In both of these processes the interfacial bond is of primary importance.

Historically the first important inorganic fibres were asbestos and glass. Fibres containing a mixture of alumina and silica have a high melting point and are mainly used for insulation applications involving high temperatures and for composites production. Only if the SiO_2 content is high (~50%) can these fibres be produced by melt spinning, similar to that used in making glass fibres. Carbon fibres have small diameters and are made with a wide range of Young's moduli, however above 400°C they begin to suffer greatly from oxidation. Carbon fibre reinforced carbon composites are used for re-entry heat shields for space vehicles as well as in brakes for trucks and planes, but these are short duration applications and even if the carbon fibre reinforced carbon matrix can resist temperatures up to 3000°C oxidation limits its use [2]. The ultimate challenge is to develop fibres that are stable up to very high temperatures in an oxidizing atmosphere.

The environment in which the fibres are to be exposed to at high temperatures is important because in the absence of oxygen the choice for most applications would be immediately carbon fibres, as oxidation would not be a problem. The applications that define the temperature range required for fine ceramic fibres are those that presently rely on nickel superalloys used in aircraft engines. The maximum use temperature of these alloys is ~1100°C but they can be used with ceramic insulating coatings and sophisticated air cooling engineering in environments that are much hotter than this temperature. However the metal must not experience temperatures higher than 1100°C.

A number of routes have been adopted to produce ceramic fibres, the earliest method was chemical vapour deposition of the ceramic onto a supporting filament of boron, silicon carbide (SiC) or silicon nitride (Si_3N_4), resulting in large diameter fibres (100 to 140 μm) which are not flexible and cannot be woven or used to make complex shapes. They are used in the boron aluminium tubular frame of the U.S. space shuttle and more recently, such silicon carbide fibres embedded in a titanium matrix have been considered as a prospective structural material for jet engines. These fibres are light in weight and have high strengths and moduli, but are usually very costly to produce. Later fibres based on alumina and often combined with silica are produced from slurries or sol-gels and then sintered. These oxide fibres were originally produced for refractory insulation and then used to reinforce light metal alloys. Related fibres are being examined for use as reinforcement for ceramics. Single crystal oxide filaments have much larger diameters (>100μm) produced from melt drawing, which is very slow resulting in a product which is inflexible and expensive, although does exhibit superior creep and tensile properties to their polycrystalline analogues.

A third group of fibres, based on silicon carbide, has been developed through the pyrolysis of organosilicon precursor filaments in an analogous fashion to the technique used to make the most successful carbon fibres, which are produced by carbonising precursors of polyacrylonitrile filaments. These silicon carbide based fibres first allowed ceramic matrix composites to be developed and are at present the most widely used reinforcement for this type of composite. Engineered designs of composites are limited in their performance and if more efficient engines are to be produced, then materials capable of operating uncooled in air in the range of 1400 - 2000°C are required and retention of their properties for periods of up to 60,000 hours. The fibres currently available reveal the interest in reinforcing a ceramic matrix but also demonstrate certain limitations. The ideal fibre for such applications would be both chemically and microstructurally stable up to 1400°C, have a diameter of less than 20 μm to ensure flexibility, possess a Young's modulus around 200 GPa or higher and a strength of above 2 GPa at room temperature, and retain a modulus of 150 GPa and a strength of at least 1.5 GPa above 1200°C. The fibre should also be economical to use to broaden its potential use.

1.3. Polycrystalline Fibre Characteristics

Synthetic ceramic fibres have been available for the reinforcement of light alloys from the beginning of the 1960's. The earliest fibres were produced by chemical vapour deposition (CVD) onto a tungsten substrate, first to give boron and then silicon carbide fibres. Carbon fibres were also developed around this time and attempts were soon made to use them as reinforcements for aluminium. Composite structures consisting of aluminium or magnesium reinforced with these fibres have been developed and have found a limited number of applications.

The reactivity of carbon with the metal matrix has still not been completely resolved and research continues in this area. However the oxidation of carbon above 400°C limits the use of carbon fibres at high temperature in the presence of oxygen. Silicon carbide fibres produced by CVD onto tungsten or carbon cores today represent the only viable reinforcement for titanium metal matrix composites. Such fibres are produced with a sophisticated protection barrier that makes possible titanium matrix composites for use up to 600°C. Short fine alumina silica fibres were produced in the early 1970's and these fibres, under the trade name Saffil (ICI), today represent the most widely used filamentary reinforcement for light alloys. Amorphous continuous fibres, based on mullite with boron added, were also produced around this time by 3M under the trade name of Nextel 312. Small diameter continuous α-alumina fibres (FP) were produced, first by Du Pont, in the 1970's and began to be incorporated into metal matrix composites toward the end of that decade. The composites that were produced showed great improvements in stiffness and creep resistance when compared to un-reinforced aluminium; however, high cost and the brittleness of the fibres then available limited their use. Since 1980 other fibres have been developed based on alumina, often with a small amount of silica or zirconia. Mullite fibres with varying alumina:silica stochiometry have been produced and are easier to handle. Often the presence of silica results in the reduction of Young's modulus and creep resistance.

The development in Japan, in the early 1980's, of small diameter fibres, based on silicon carbide and produced by the conversion of an organosilicon precursor has generated much interest in the possibility of producing ceramic composites capable of being used for long periods in air above 1000°C.

These fibres retain their properties up to 1000°C when heated in air, although above this temperature their strength falls due to pitting of the surface due to oxidation. Also, because of their nonstoichiometric microstructure their mechanical properties are not those of bulk silicon carbide. The most recent generation of small diameter ceramic fibres of this type have been produced with a modified microstructure destined to improve their high temperature stability. Long-term stability in air at 1300 - 1400°C is the aim for this type of fibre. For temperatures above this range hope resides with oxide fibres, either with carefully controlled microstructures, so as to avoid grain boundary sliding but also to limit dislocation mobility inside the grains, or with the development of orientated single continuous crystal filaments. Advances in this field are occurring rapidly and the goal is to enable composites to be produced that will considerably extend the temperature range of advanced structural materials.

1.4. Non-oxide Fibres

1.4.1. Fibres Produced by Chemical Vapour Deposition

Boron and silicon carbide fibres with diameters of 140 μm were first produced by CVD onto a core in the 1960's and their manufacture, properties, and microstructure are well described [3]. Boron fibres were produced by a reaction of H_2 and BCl_3 gases and deposition onto typically a tungsten core (**Figure 1.1**) although other substrates have also been used. Boron fibres have been produced with both B_4C and SiC coatings to limit fibre degradation during metal matrix processing. These fibres are limited in their possible temperature range as reactions occur at the interface at around 1000°C. Fibres of large diameter (140 μm), consisting of silicon carbide deposited onto carbon or tungsten cores, are made using various chlorosilanes such as CH_3-Si-Cl_3 which yield SiC and 3HCl.

The fibre that is produced has a mantle of silicon carbide, which in the case of a tungsten core is a pure SiC whereas carbon can be included in the mantle if a carbon core is used. Carbon can migrate to the fibre surface, which in any case is further modified to prevent loss of fibre properties during composite manufacture.

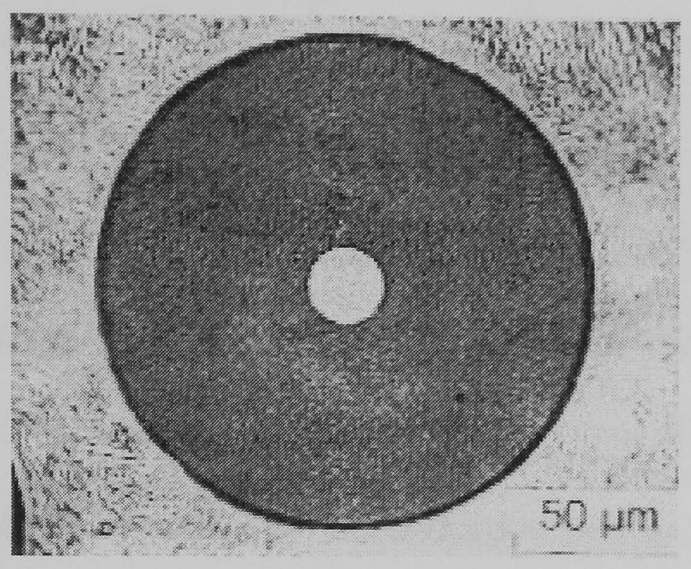

Figure 1.1: Boron fibre with a tungsten core

The Textron fibres were originally developed for metal or polymer matrix composites [4] and are known as SCS-n, where n is the thickness in microns of surface coating added onto the diameter. The variations of the silicon/carbon content of this layer is closely controlled to permit optimum fibre protection for different matrices so that the SCS-6 fibre is seen as being particularly attractive for titanium matrix composites. Similarly SiC fibres using a tungsten core are made by QinetiQ (formerly DERA) in the U.K. These Sigma fibres have a diameter of 100 µm. Because of their large diameter (>100µm), they are usually not acceptable for ceramic matrix composites. However they are included in this section because of their superior high temperature properties relative to the small diameter ceramic fibres [5]. CVD fibres tend to be stable to slightly higher temperatures due to the finer ~1nm grains, but are more costly and difficult to fabricate into the woven fabric required for composite manufacture. The properties of some CVD fibres are shown in **Table 1.1:**

Fibre *CVD*	Manufacturer	Composition %	Grain Size (μm)	Diameter (μm)	Strength (GPa)	Max Use Temp °C
SCS-6	Avco/Textron	β-SiC Carbon Core	0.04 - 0.01	143	3.9	1300
	Avco/Textron	Boron On Tungsten Core	N/A	100 - 140	3 - 6	1300
Sigma	Dera (QinetiQ)	β-SiC Carbon Core	N/A	100	3.4 – 4.1	1300

Table 1.1: Properties of Ceramic Fibres Produced by Chemical Vapour Deposition

1.4.2. SiC Ceramic Fibres Produced From Polymer Precursors

The Japanese have led the way in the development of SiC fibres [6] was the first to publish work in this area in the mid 1970's and gave rise to the first and so far the most successful fine ceramic fibres [7]. Nippon Carbon produced this fibre under the name of Nicalon. The most widely used fibre in this family at present is the Nicalon 202. The manufacture of Nicalon fibres involves the production of polycarbosilane (PCS) precursor fibres that consist of cycles of six atoms arranged in a similar manner to the diamond structure of β -SiC. The elastic modulus of SiC is lower than diamond (>450GPa) but greater than alumina making it an ideal strong reinforcement material. The molecular weight of this polycarbosilane is low (around 1500g mol^{-1}) which makes drawing of the fibre extremely difficult, because the viscoelastic nature and strength is lower than that for higher molecular weight polymers. In addition, methyl groups (CH_3) in the polymer are not included in the Si-C-Si chain, so that during pyrolysis hydrogen is driven off, leaving a residue of free carbon. The production of the Nicalon-202 fibre involves subjecting the precursor fibres to heating in air at about 200°C to produce crosslinking of the structure. This oxidation makes the fibre infusible but has the drawback of introducing oxygen into the structure, which remains after pyrolysis.

A further slow increase in temperature in an inert atmosphere up to 1200°C follows to produce a majority of β - SiC, around 2 nm, but also significant amounts of free carbon of less than 1 nm, and excess silicon combined with oxygen and carbon as an intergranular phase. Excess carbon arises from the precursor nominally C:S 5 2 for PCS: –(SiHMe–CH_2)n–. The strengths and Young's moduli of Nicalon fibres tested in air or in an inert atmosphere show little change up to 1000°C. Above this temperature both of these properties fall with the greatest change being in the strength of the fibre [7,8]. When a load is applied to the fibres, it is found that a creep threshold stress exists above which creep occurs. The free carbon and the oxygen in the structure have been shown to play a determining role in the degradation of the microstructure of the Nicalon-202 fibres above 1200°C and the fibre is seen to creep above 1000°C due to the presence of the oxygen rich intergranular phase. The properties and composition of these fibres are shown in **Table 1.2**.

The Tyranno LOX-M fibre produced by Ube Industries is made with a similar precursor to that used for the Nicalon-202 fibres, but with the addition of titanium. This was presumable, added to avoid infringement of patents initially, as no technical improvement was initially proposed from the titanium addition. The structure of this polytitanocarbosilane (PTC) precursor is complex due to condensation of Si-H bonds and crosslinking of titanium compounds occurring simultaneously [9]. The precursor fibre is crosslinked by heating in air at about 180°C and then converted to a ceramic fibre by treatment in nitrogen above 1000°C. The resulting fibre contains a small amount of titanium, around 2% by weight, which is said to inhibit crystallization and offer better resistance to oxidation of the carbon by the formation of Ti-C bonds.

The Tyranno LOX-M fibre contains 13 wt% of oxygen, which limits its use over 1000°C because of the same processes seen in the Nicalon-202 fibre. The Tyranno fibre properties are also listed in **Table 1.2.**

Fibre ***SiC (Ti/Zr)***	**Manufacturer**	**Composition %**	**Grain Size (μm)**	**Diameter (μm)**	**Strength (GPa)**	**Max Use Temp °C**
Nicalon NLM-202	Nippon Carbon	56% Si, 32%C, 12% O	1.7nm SiC	14	2	1200
High Nicalon	Nippon Carbon	62.4% Si, 37% C, 0.6% O	1.7nm SiC	14	3.0	1200
High Nicalon S	Nippon Carbon	62.4% Si, 37.1% C, 0.5% O	1.7nm SiC	13	2.4	1200
Tyranno Lox-M	Ube Industries	54% Si, 31.6% C, 12.4% O, 2% Ti	Amorphous (~1nm)	8.5	2.5	1300
Tyranno Lox-E	Ube Industries	54.8% Si, 37.5% C, 5.8% O, 1.9% Ti	Amorphous (~1nm)	11	2.9	1300
Tyranno ZMI	Ube Industries	56.6% Si, 34.8% C, 7.6% O, 1% Zr	Amorphous (~1nm)	11	3.4	1300
Tyranno ZE	Ube Industries	58.6% Si, 38.4% C, 1.7% O, 1% Zr	Amorphous (~1nm)	11	3.5	1300

* = Oval Cross Section

Table 1.2: Properties of SiC Ceramic Fibres Produced From Polymer Precursors

This family of fibres, in common with all of the silicon carbide based fibres, will suffer from oxidation from 1200°C, resulting in the formation of a silica layer that would modify the properties of the SiC matrix interface in the composites used in oxidizing conditions. For this reason silicon carbide fibres are likely to be limited to a maximum longterm use temperature of 1200°C.

The silica is initially present in the amorphous amorphous form which is stronger than the ultimate crystalline phase cristobalite, resulting in a reduction in tensile strength with an increase in layer thickness. Fibres with a thick cristobalite layer exhibit crack formation at the fibre surface [10]. The cracks act as flaws resulting in weak fibre. The reason for crack formation seems to be due to a mismatch in thermal expansion for amorphous SiO_2, cristobalite and SiC being 0.5×10^{-6}, $\sim 10 \times 10^{-6}$, and 3×10^{-6} respectively [11].

During cooling, the high temperature β-cristobalite shrinks more than the SiC based fibre, due to its higher coefficient of thermal expansion. Additionally a phase transition of the cristobalite from β to α during cooling, accompanied by a volume decrease (-8.8%), is reported to occur at 200°–270°C [12] which further promotes crack formation. Oxidative degradation affects a fine diameter SiC fibre (high surface area) more seriously than the usual monolithic SiC body, because the diameter of the fibre is much smaller than the dimensions of a monolithic body, even given the same oxide thickness. The strength of a SiC fibre is sensitive to surface flaws arising from the resulting oxide structure. The latest generation of Nicalon and Tyranno fibres has been produced by cross-linking the same precursors by electron irradiation, so avoiding the introduction of oxygen at this stage, [13-14]. The oxygen present in the fibre permits oxidation of SiC to amorphous SiO_2 at high temperatures, which is more prone to creep due to softening and plastic deformation. These fibres are known as Hi-Nicalon, which contain 0.5 wt% oxygen, and Tyranno LOX-E, which contains approximately 5 wt% oxygen (the higher value of oxygen in the LOX-E fibre is due to the introduction of titanium alkoxides for the fabrication of the PTC).

Significant improvements in the creep resistance are found for the Hi-Nicalon fibre compared to the Nicalon-202 fibre Takeda [15, 16], whereas the creep properties of the LOX-E fibre appear similar to that of the LOX-M fibre due to the insufficient reduction of oxygen content in the electron cured fibre [17]. A more recent polymer polyzirconocarbosilane (PZT), has allowed the titanium to be replaced by zirconium and the oxygen content to be reduced, as the percentage of oxygen in this oxide is 14% less. The resulting fibres, known as Tyranno ZE, show increased high temperature creep and chemical stability. Si–C–O ceramics and Nicalon 202 fibres are thermodynamically unstable and decompose along with CO gas evolution at high temperatures. Decomposition of the fibre results in CO gas formation, according to the equation:

$$\mathbf{SiC_xO_y \rightarrow SiC + {}_yCO + {\sim}(x - y - 1)\ C}$$

Equation 1.1: Si–C–O Ceramic Thermal Decomposition

The gas can be trapped resulting as bubbles, which behave as new strength controlling flaws in the fibre structure. Stoichiometric silicon carbide fibres like Hi-Nicalon type S possess better creep resistance than all of the present SiC based fibres [18]. Hi-Nicalon type S fibres can retain their strength, even after 1600°C exposure and demonstrate high strength (1.8 GPa) after 10 hr exposure in argon at 1600°C [19-21]. This result shows that SiC-based fibres with reduced internal oxygen content exhibit superior thermal stability. A faster rate of strength degradation is seen in air, as oxygen is available for oxidation of SiC [22].

1.4.3. Si-C-N Ceramic Fibres Produced From Polymer Precursors

These ceramic fibres are produced from polycarbosilazane precursors, based on the silicon carbide-silicon nitride system have been studied but have not given rise to commercial fibres. Various routes for the manufacture of these fibres are possible [23] examples of some of these fibres are given in **Table 1.3**.

Fibre Name *SiN/ SiNC*	Manufacturer	Composition %	Grain Size (μm)	Diameter (μm)	Strength (GPa)	Max Use Temp °C
HPZ	Dow Corning Celanese	59% Si, 25% N, 10% C, 3% O	Amorphous	10 - 12	1.7 – 2.1	N/A
MPDZ	Dow Corning Celanese	49% Si, 30% N, 15% C, 8% O	Amorphous	10 - 15*	1.75 - 2.45	N/A
Tonen	Tonen	58.6% Si, 38.2% N, 2.7% O, 0.5% C	Amorphous	10	2.5	N/A

Table 1.3: Properties of SiN/SiCN Ceramic Fibres Produced From Polymer Precursors

This type of fibre was initially studied for the dielectric properties that can be obtained with this class of material as the electrical resistivity of silicon carbide-silicon nitride is superior by a factor of 1000 times to that of graphite.

1.5. Oxide Fibres

Fibres for use in reinforced ceramic composites may be expected to provide reinforcement for parts while being exposed to very hostile environments, high temperature, corrosive and oxidising. Therefore, properties such as resistance to reactive atmospheres and matrices as well as creep and fatigue at very high temperature must be considered along with strength and stiffness. A broad range of ceramic fibres for different applications and environmental conditions are required to meet requirements for future developments in ceramic composites [24].

Oxide ceramic fibres, though generally having lower reinforcement property values than some non-oxide fibres are more oxidation resistant.

1.5.1. Continuous Single Crystal Monofilaments

The production of continuous single crystal monofilaments was first reported by LaBelle [25] who recognised that certain refractory materials, such as BeO, MgO and $A1_2O_3$ exhibited a marked improvement in mechanical properties (tensile strength and creep resistance) when produced in single crystal monofilament form. He devised a series of experiments for producing single crystal alumina monofilaments for reinforcing high performance metal and plastic matrices. The apparatus was based around a modified Czochralski crystal puller and consisted of a molybdenum crucible containing pure alumina powder, which was melted using radio frequency heating. In the first experiments a molybdenum washer with a small diameter hole at its centre was placed on the surface of the melt. A seed crystal is then inserted through this orifice and grows down into the melt by dendritic growth. The seed is withdrawn at a constant rate producing a continuous alumina dendrite and this produced single crystal monofilaments with diameters in the range 50-250μm at rates up to 30mm/min [26]. The tensile strength of these first filaments was around 0.5GPa. This was attributed to a lack of accurate control of temperature at the solidification interface caused by the molybdenum washer sinking into the crucible as the source material was depleted.

LaBelle solved this problem by developing the "Self-Filling Tube Technique" [27]. The washer was replaced by a molybdenum capillary tube, which ensured that the solidification interface was always at a fixed height in relation to the crucible, which resulted in a marked improvement in crystal quality and strength (1 GPa - 2.8 GPa).

This method was a big improvement over the earlier "floating orifice technique". but there were still problems associated with accurate diameter control. The diameter of the grown monofilaments was found to be a function of the growth rate (determined mainly by capillary tip speed) and the shape of the capillary tip. The first capillary tubes had a knife-edge opening so that the angle between the surface of the opening and the vertical was typically less than 30°. It was later discovered that if the capillary opening were made horizontal then the molten liquid would flow to the outer edge of this surface so that the dimensions of the growing crystal would be determined by the size and shape of the capillary surface.

This method of crystal growth became known as "Edge-Defined Film-Fed Growth" or EFG [28]. The diameters of monofilaments produced by the EFG process were found to be far less dependent on the growth rate and both the melt temperature and pulling speed could be varied over a wide range without a substantial change in diameter. This led to far more accurate diameter control than the self-filling tube technique. Modification of the apparatus enabled sapphire filaments to be produced continuously by incorporating a continuous pulling mechanism and a method for replenishing the melt without having to interrupt the growth process. The EFG process is capable of producing crystals of virtually any cross-sectional shape or size. For example it is possible to grow hollow tubes, multi-bore tubing and ribbon, as the shape of the crystal is determined by edges formed by both the outside diameter and edges of blind holes in the capillary surface [29-31]. It is also possible to grow many crystals simultaneously from the same crucible through the use of multiple dies. The EFG technique proved so successful that the American company "Saphikon" was set up to exploit EFG crystal growth.

Saphikon have developed large diameter (typically >100μm) continuous single crystal filaments grown from molten alumina, which is a slow process and at high cost. The stoichiometric composition of these fibres (with the absence of grain boundaries) ensures that they should be more stable at high temperatures above 1600°C. Careful orientation of the seed crystal enables the crystalline orientation to be controlled so that creep resistance can be optimised [32]. Published data on the strength of Saphikon fibres as a function of temperature reveal that strength variation is not a function of temperature alone. Bubble defects are characteristic of these fibres most probably due to convection during fibre growth at the meniscus point between the solid and the melt [33]. The limitations of the sapphire filaments has led to the investigation of multiphase oxides with low intrinsic creep properties, such as mullite ($Al_6Si_2O_{13}$), magnesium aluminate or spinel ($MgAl_2O_4$) [34] and yttrium aluminium garnet (YAG - $Y_3Al_5O_{12}$) eutectic alumina fibre which can also be made using the same process. The later consisting of interpenetrating phases of α-alumina and YAG [35].

The structure depends on the conditions of manufacture, specifically the drawing speed, but can be lamellar and oriented parallel to the fibre axis. **Figure 1.2** shows a longitudinal cross section of the fibre, as revealed by scanning electron microscopy, showing the elongated YAG (dark) and alumina (light) phases.

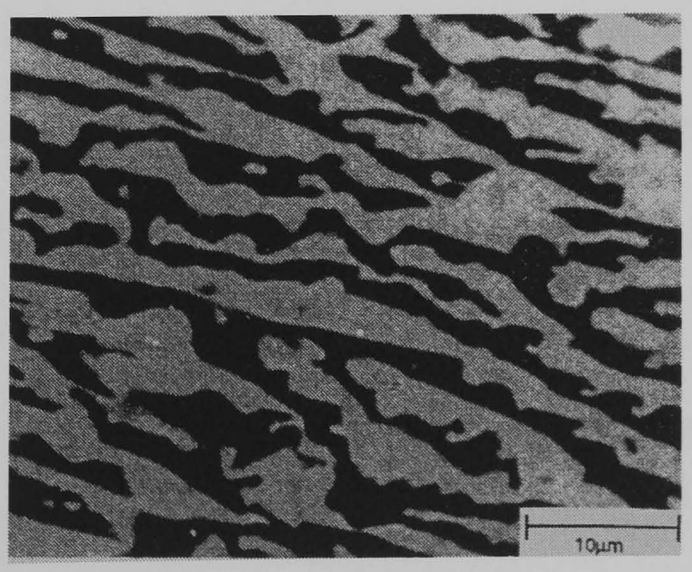

Figure 1.2: YAG - Alumina Eutectic Monofilament

Such fibres are seen to relax above 1100°C but are not as strongly dependent on temperature as the polycrystalline oxide fibres [36, 37]. Converting such large diameter fibres into woven fabrics for use in ceramic matrix composites (CMC's) is difficult, as the filaments do not flex easily without breaking. In order to obtain oxide fibres of high refractoriness with single or multiphasic structures at a viable cost, alternative processing was required.

An alternative method for growing single crystal monofilaments is to use the Laser Heated Floating Zone (LHFZ) method also referred to as Laser Heated Pedestal Growth (LHPG). This technique was developed for producing single crystal monofilaments for high performance composites. [38]. However after its introduction it was more commonly applied to the production of monofilaments for optical devices such as fibres for neodymium doped:YAG lasers [39]. The design of equipment for the LHFZ process has evolved over the years, but the basic principle remains the same. One or more laser beams are focused onto the end of a rod of feed material (compacted polycrystalline powder or a larger single crystal rod/bar). The power of the laser is increased until a molten pool is formed on the end of the feed material, at which point a seed crystal is dipped into the pool and then withdrawn at a constant rate to form a single crystal monofilament. The rate at which the feed material is fed into the laser beam and seed crystal is withdrawn determines the overall change in cross-sectional area from the feed material to the seed crystal. The laser growth technique is particularly suited to producing small single crystals of virtually, any congruently melting compound for evaluation purposes. Its major advantage over EFG growth is that the purity of the grown crystals is determined solely by the purity of the source material, as there is no crucible involved which can lead to contamination problems in the EFG process.

1.5.2. Melt Derived Amorphous Ceramic Oxide Fibres

Fibre formation of molten oxide compositions, as in the manufacture of glass fibres, is limited by the viscoelastic properties of the final oxide composition. Usually the composition requires the presence of significant percentages of glass forming oxides such as SiO_2, P_2O_5, or B_2O_3, thus limiting the potential refractoriness or elastic modulus.

Aluminosillcate Melt Fibres

Traditional melt spun kaolin based fibres are short, discontinuous and sometimes refered to as "staple fibres". They contain ~54% by weight silica and can only be used in insulation up to about 1400°C because of the low melting silica-rich eutectic (1595°C) [40]. High alumina fibres (>60%) cannot be made by conventional melt spinning processes, as the surface tension/viscosity characteristics for fiberisation are too narrow [41].

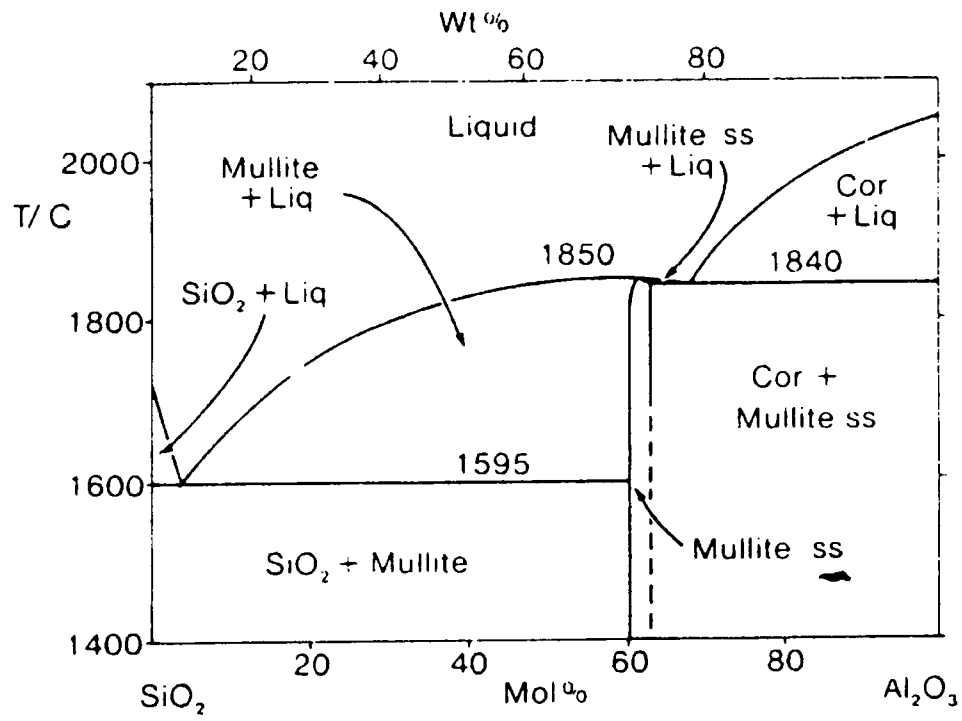

Figure 1.3: Alumina - Silica Phase Diagram

For use at higher temperatures, Al_2O_3:SiO_2 fibres containing less SiO_2 (28%) than mullite (which includes all available continuous fibres) are most desirable since the relevant eutectic temperature is then 1840°C.

The high temperature equilibrium phases in this region of the phase diagram (**Figure 1.3**) are mullite ($3Al_2O_3$-$2SiO_2$) and corundum (α-Al_2O_3). As made fibres may not have reached this equilibrium phase composition but may contain low temperature phases dependant on the heat treatment during sintering. The first melt blown aluminosilicate fibres were produced by the Babcock and Wilcox Company, just after World War II [42]. Silicate melts solidify to a glassy product and are relatively easy to spin. Progressive replacement of silica by alumina improves refractory performance but reduces the spinnability and the 47% alumina in fibres derived from kaolin being typical. The range of composition of melt spinnable aluminosilicates is about 45 - 60 wt% $A1_2O_3$ with SiO_2 as the other major component and with minor amounts of Fe_2O_3, TiO_2, CaO and other oxides [43]. The fibres are usually manufactured from kaolin or a related clay mineral, or from blends of alumina and silica (allowing closer control of composition than with clay minerals). The raw material is melted and made into fibres in one of two ways; The melt may be poured into a stream of compressed gas (air or steam) which breaks the melt into staple fibres, or the melt may be fed to a rapidly rotating spinning disk from which fibres are thrown by centrifugal force [44]. The latter method produces longer and silkier fibres, but in both processes a wide range of fibre diameters (<1 to > 10 μm) are formed together with a significant fraction (about 50% of the product mass) of non fibrous material termed shot [45].

For vitreous aluminosilicate fibres the usual temperature limit is governed by the devitrification of the glass (nucleation and growth of mullite ($3A1_2O_3.2SiO_2$)), which reduces mechanical strength drastically and results in dimensional shrinkage.

Temperature resistance increases with increasing alumina concentration, fibres containing up to about 46% Al_2O_3 being suitable for use at temperatures up to 1250°C, and those containing higher levels (up to about 54%) being capable of use at up to 1400°C [43]. Small additions of chromia (~5% as Cr_2O_3) and higher levels of zirconia (15% ZrO_2) also improve temperature resistance by controlling grain growth at up to 1400°C. Aluminosilicate fibres are processed into a number of forms such as bulk wool, blanket, felt, paper and board. The major application of aluminosilicate fibres is in the insulation of furnaces in the metallurgical, ceramic and chemical industries, with a resulting considerable saving in weight and fuel usage. There may be up to a tenfold difference between the mass of a fibre-lined furnace and the mass of one constructed conventionally from refractory brick. This brings very considerable advantages in construction and the low thermal mass allows rapid heating and cooling in cyclic operations and a reduction in fuel usage of as much as 40% is not uncommon. Not surprisingly, the use of refractory fibres in high temperature technology has grown rapidly and around 300,000 metric Tonnes are currently produced worldwide.

1.5.3. Commercial Polycrystalline Oxide Fibres

The incentive to produce inorganic fibres higher in alumina content is largely for use in thermal insulation at temperatures >1400°C and exploitation of the high modulus of alumina (α-alumina, 530 GPa), its relatively low density (α- alumina, 4.0 g/cm^3) and its non reactivity for use in composite manufacture especially metal reinforcement [46]. The low viscosity of molten alumina and its high melting point (2070°C) preclude melt spinning, so processes had to be developed to avoid the melting step. Most alumina based fibres are made by sol-gel processes, in which a low temperature precursor is spun to a gel fibre and then calcined to the ceramic.

The earliest developments were again by Babcock and Wilcox [47] in a drive to make fibres with less silica and improved refractory properties. A further advantage of the sol-gel process is that the precursor is spun in a low temperature process that can be refined to give a good quality fibre product.

Saffil alumina fibre is a staple fibre with a geometric mean diameter of ~3μm, first manufactured by Imperial Chemical Industries (ICI) [48] and now by Dyson Ltd, consisting of 96-7% of δ-alumina and 3-4% of silica. Saffil was a "science led" product originally conceived as an asbestos replacement but was quickly developed as a high temperature insulating material. Its widest use is high temperature thermal insulation, for automotive catalyst wraps or, when blended with aluminosilicate fibres, it extends the range of temperature application from 1200°C to 1600°C. Fibre insulating blankets are lighter than refractory insulating bricks giving lower thermal mass, also the inherent flexibility of the fibre increases the resistance of an individual ceramic material to thermal shock. A number of manufacturers, i.e., Denka Kagaku Kogyo [49], Carborundum, Mitsubishi Chemical Co Ltd and Nichias, followed ICI with staple sol-gel products of mainly mullite composition. Toyota used Saffil for the reinforcement of aluminium piston crowns and since then it has been the prominent fibre for light metal reinforcement [50].

Continuous polycrystalline fibres started to emerge commercially in 1974 with 3M launching their continuous Nextel 312 fibre based on a mullite composition but with an essentially amorphous structure [51]. The main use of this product was not composite reinforcement initially, but as a fire curtain as it could be woven into a fabric because of the long flexible fibres. Small diameter continuous, almost pure α-alumina fibres became available in 1979 from Du Pont and were called Fibre FP [52].

This fibre was made by blending alumina powder with a soluble aluminium rich precursor to form a mixture that could then be spun. The filaments were extruded through spinnerettes, drawn, and fired in air to 1300°C to produce the α-alumina fibre. A silica surface layer increased fibre strength by healing surface flaws as the fibre exhibits a granular structure and also helps wettability with light alloys. Some properties of the FP fibre, which had a grain size of 0.5μm and a diameter of 20μm, are shown in **Table 1.4**. The fibre had a low strain to failure that made it difficult to handle; this limited its use and eventually caused its withdrawal from production. However the FP fibre retained its strength to approximately 1000°C after which intergranular plasticity accompanied by grain growth occurred when the fibre was under load, generally weakening it. This fibre was not suitable for reinforcement of light alloys so a new fibre was developed called PRD 166.

This fibre was microcrystalline based on α-alumina but containing approximately 20% of zirconia partially stabilized with yttrium oxide [53]. The largest α-alumina grains were of the order 0.3μm also present was zirconia 0.1μm (located at triple points of alumina grains) its role was to improve strength and toughness. This resulted in a slight improvement in strain to failure (better handling) compared to the FP fibre [54]. At high temperatures the PRD 166 fibre showed greater resistance to creep, which began at 1100°C. The PRD 166 fibre was produced on a pilot plant and none of the alumina-based fibres from Du Pont were never developed into commercial products. Almax fibres based on α-alumina have been commercialised by Mitsui Mining, which has a diameter of 10μm, allowing it to be woven. **Table 1.4** shows the differences between the properties of the almax and FP fibres. These differences are due to the more porous microstructure of the almax fibre which which exhibits considerable internal stresses.

This leads to a lower density, failure stress, and Young's modulus of the almax fibre and at high temperature easier grain boundary sliding and grain growth. Several fibres contain additions of silica to form other intermediate phases of alumina and inhibit the formation and grain growth of α-alumina. The highest percentage of silica provides the greatest strength but lowers the Young's modulus and resistance to creep [55] due to amorphous phase formation. Altex fibre from Sumitomo Chemicals contains 15wt% of silica with a predominance of γ-alumina, leading to a much lower Young's modulus than that of the α-alumina fibres but a greater strain to failure and therefore easier handleability. The alumina crystallises in the γ phase with a very fine grain size, a low density, and an active surface. The role of the silica, which is amorphous and makes up 15% of the structure, is to stabilize the alumina in the γ phase [56-9]. The fibres retain their strength and stiffness with little noticeable loss in tensile strength at 1000°C and above this temperature it falls rapidly. The fibre suffers considerably from creep above 1000°C, above 1100°C softening of the silica accounts for the rapid acceleration of the creep processes, above 1127°C it reacts with alumina to form crystalline mullite.

The Nextel 312, 440, 480 and 550 series of fibres produced by 3M are mainly based on a mullite composition, 312 and 440 with varying percentages of boric oxide (B_2O_3) to restrict grain growth [60-1]. Boric oxide creates both crystalline and amorphous phases. The fibres are 11μm in diameter, oval in cross section, due to solvent evaporation and shrinkage induced by filament drying during the sol-gel fabrication process. The Nextel 312 fibre is predominantly amorphous and is composed of 62% Al_2O_3, 24% SiO_2 and 14% B_2O_3.

Fibre	Manufacturer	Composition %	Grain Size (μm)	Diameter (μm)	Strength (GPa)	Max Use Temp °C
Alumina						
Saphikon	Saphikon	>99% Al_2O_3	S.C.	125 - 600	2	2000
Fibre FP	Du Pont ICI	>99% α-Al_2O_3	0.5	20	1.4	1320
Saffil HA		96% α-Al_2O_3, 4% SiO_2	<1.0	3	2	1600
Almax	M. Mining	>99% α-Al_2O_3		10	2	1250
Altex	Sumitomo Chemical Co.	85% α-Al_2O_3 15%SiO_2		17	1.5	1250
PRD 166	DuPont	80% α-Al_2O_3 ~20% tet-ZrO_2	0.5 0.1 - 0.3	20	2.1	1400
Mullite						
Nextel 312	3M	62% Al_2O_3, 24% SiO2 14% B_2O_3 (Am. + mullite)	<0.5	11*	1.7	1200
Nextel 440	3M	70% Al_2O_3, 28% SiO_2, 2% B_2O_3	<0.5	11*	2	1420
Nextel 480	3M	70% Al_2O_3, 28% SiO_2, 2% B_2O_3 (mullite)	<0.5	11*	1.9	1000
Nextel 550	3M	72% Al_2O_3, 28% SiO_2 (γ - Alumina + Am. Silica	-	10	-	1000
Nextel 610	3M	>99% Al_2O_3, 0.35% SiO_2, 0.65% Fe_2O_3	0.1	10	3.3	1000
Nextel 720	3M	86% Al_2O_3, 14% SiO_2 (mullite + α-Alumina)	<0.5	12	2	1150
Nextel 650	3M	89% Al_2O_3, 10% ZrO_2, 1% Y_2O_3 (α-Alumina + cubic-ZrO_2)	0.1	11	2.5	1080

Table 1.4: Continuous Oxide Ceramic Fibres

It has the lowest production cost of this group of fibres and is widely used. The amorphous phase helps the fibre retain strength after exposure to high temperature because it slows the growth of the crystalline phases that weaken the fibre but the creep properties are poor due to the viscous flow of the amorphous phase.

Another limit to high temperature use is poor thermal stability due to aluminium borate compounds becoming volatile from 1000°C, which induces severe shrinkage above 1200°C. The Nextel 440 fibre contains more alumina and less B_2O_3 (70% $A1_2O_3$/28% SiO_2/2% B_2O_3) present as 20 nm γ-alumina crystals with amorphous silica. The more crystalline Nextel 480, which is no longer available, contained only mullite as a crystalline phase [62]. The grain size was only 50nm and the microstructure was stable up to 1200°C except for the completion of the mullite crystallisation. The fibres were reported to retain at least 75% of their properties up to 1000°C and that they creep over 1000°C.

The Nextel 550 is 10μm in diameter and does not contain B_2O_3 and therefore does not have an excessive glassy phase, it is predominantly γ-alumina and mullite and amorphous silica. At exposure temperatures higher than 1200°C the strength of Nextel 550 is lower than Nextel 440 due to the formation of larger grained mullite, however because Nextel 550 has little amorphous phase it retains its strength better at temperature. The composite grade fibres Nextel 610, 650, and 720, have more refined crystal structures based on α-Al_2O_3 and do not contain any amorphous phases, allowing the fibres to retain their creep strength at higher temperatures. The Nextel 610 fibre has a diameter of 10μm and is composed of α-alumina with 1.15% total impurities including 0.65% Fe_2O_3 as a nucleating agent and 0.35% SiO_2 as grain growth inhibitor. It has the highest strength at room temperature (3.3GPa) of all the Nextel fibres. The grain size is a fifth of the size of the alumina grains in the FP fibre at only 0.1μm. The properties of the fibre can be seen in **Table 1.4**. Because it is essentially single-phase, the strength rapidly decreases at higher temperatures due to grain growth, correspondingly improving creep resistance, but not to the extent of the FP fibre [63].

Both Nextel 650, which is 89% Al_2O_3 (α- Al_2O_3), 10% ZrO_2 (cubic) and 1% Y_2O_3 and Nextel 720 which is composed of 85 wt% Al_2O_3 15 wt% SiO_2 forming α- Al_2O_3 / mullite, have good room temperature strength (2.5 and 2.1 GPa respectively) and better strength retention at temperature than the preceeding fibres due to reduced grain boundary sliding. These additions also help to "pin" the grains and reduce grain growth when exposed to thermal ageing. Further confirmation of the effect of additional phases and removal of the amorphous phase is shown in the improved creep properties. The Nextel 720 fibre does not have the composition of mullite found in other Nextel fibres, as it is richer in alumina. These fibres are composed of 85% Al_2O_3 15% SiO_2 resulting in around 55% mullite and 45% α-alumina. As a result its microstructure is distinctive from that of the other Nextel fibres as it contains α-alumina in the form of randomly oriented needles and large mosaic grains. This microstructure results in much improved creep properties with a creep rate at 1200°C, which is reported to be three orders of magnitude less than that of the FP fibre. Stress induced slow crack growth seems to limit use under steady loads at this temperature so the maximum use temperature is restricted to 1150°C [63-4]. The ceramic fibres based on alumina seem to be possible candidates for reinforcing light alloys. Such reinforcements permit metal structures to be made with enhanced properties, notably creep resistance at high temperatures.

All of the alumina based fibres begin to lose strength between 900°C and 1000°C and retain almost no strength above 1150°C, which would seem to exclude these fibres from most ceramic matrix composite materials. Creep is clearly inhibited in the Nextel 720, two-phase fibre, but its loss in strength above 1000°C seems due to stress induced slow crack growth. Nextel 650 has been developed for high temperature composite reinforcement applications.

Nextel 650 fibres which have the composition Al_2O_3+ 10 wt % ZrO_2 + 1 wt % Y_2O_3 are reported to have 10-100 times lower creep rate than Nextel 610 fibres. This represents an improvement in high temperature creep capability of 80°C relative to Nextel 610 fibres. Nextel 650 single filaments retain 70% of their room temperature strength at 1200°C, 200°C higher than Nextel 610 fibres [65]. The improvement in high temperature properties is attributed to a reduction in grain boundary diffusivity by the Y_2O_3 dopant. The single filament strength of Nextel 650 fibres is 2.5 - 2.7 GPa, 20% less than Nextel 610 fibres. Thermal aging at 1200°C for 100 hours indicates good microstructural stability and strength retention, however the maximum use temperature is limited to 1080°C due to the onset of creep and loss of strength. The best creep performance of any commercially available polycrystalline oxide fibre is still Nextel 720 fibre. However further reductions in creep of oxide fibres are possible, for instance yttrium aluminum garnet (YAG) fibres are the focus of a current developmental program at 3M [2].

YAG is the most creep resistant polycrystalline oxide and also has very slow grain growth kinetics at high temperature, suggesting that YAG fibres would be an ideal fibre for high temperature composites [66]. Fibres have been produced in the 3M laboratories with 0.7 GPa strength. Bend stress relaxation measurements indicate that these fibres would have a use temperature 50°C higher than Nextel 720 fibre [67]. YAG fibre heat treated to 1200°C has a fine grain size of 0.1 μm although the fibre contains a substantial amount of porosity. Elimination of this porosity would be expected to reduce creep rates further.

1.6. References

1. T. F. Cooke, "Inorganic Fibers – A literature Review", J. Am. Ceram. Soc; 1991 **74** (12) pg 2959 – 78.

2. C. Freeman, I. Alexander Final Report, Brite Euram Framework 4 project BE-1598 "Ultra High Temperature Ceramic Matrix Composites" June 1999 (UHT CMC).

3. F. Wawner, "Ceramic Fibres" In: "Fibre Reinforcements for Composite" AR Bunsell, ed, Elsevier, Amsterdam, 1988, pg 371.

4. A. Bunsell, "Development of Fine Ceramic Fibres for High Temperature Composites", Materials Forum, 1988, **12**, pg 1178 – 84.

5. F. Ko, "Preform Fiber Architecture for CMC's", J. Am. Ceram. Soc. 1989, **68** (2) pg 401 – 414.

6. S. Yajima, J. Hayashi, M. Omori, and K. Okamura, "Development of a SiC Fibre with High Tensile Strength," Nature, 1976, **261**, pg 683 - 85.

7. G. Simon, "Creep behaviour and structural characterization at high temperatures of Nicalon SiC fibres" J. Mat. Sci. 1984, **9**, pg 3658.

8. G. Simon,"Mechanical and structural characterization of the Nicalon silicon carbide fibre" " J. Mat. Sci. 1984, **19**, pg 3649 - 57.

9. T. Yarnamura, "Development of new continuous Si-TiC-O fibre using an organometallic polymer precursor" J. Mat. Sci. 1988, **23**, pg 2589.

10. T. Shimoo, H. Chen, and K. Okamura, "Mechanism of Oxidation of Si–C–O Fibers," J. Ceram. Soc. Jpn., 1992, **100** (7) pg 929 - 35.

11. A. Gihoudo, "The Ceramic Engineering Hand Book" Ceramic Society of Japan, Tokyo, Japan, 1989, pg 822.

12. A. Gihoudo, "The Ceramic Engineering Hand Book" Ceramic Society of Japan, Tokyo, Japan, 1997, pg 184.

13. K. Okamura, M. Sato, T. Seguchi, and S. Kawanishi, "High-Temperature Strength Improvement of Si–C–O Fiber by the Reduction of Oxygen Content," Proc. 1st Jpn.Int. SAMPE Symp, 1989, **1**, pg 929–34.

14. T. Seguchi, "High Temperature Ceramic Matrix Composites. Cambridge, UK: Woodhead" Ceram. Eng. Sci Proc. 1993, **14**, pg 51 – 57.

15. M. Takeda, Y. Imai, H. Ichikawa, T. Ishikawa, N. Kasai, T. Seguchi, and K.Okamura, "Thermomechanical Analysis of the Low Oxygen Silicon Carbide Fibers Derived from Polycarbosilane," Ceram. Eng. Sci. Proc. 1993,**14** (9-10) pg 540-47.

16. M. Takeda, J. Sakamoto, Y. Imai, H. Ichikawa, and T. Ishikawa, "Properties of Stoichiometric Silicon Carbide Fiber Derived from Polycarbosilane," Ceram. Eng.Sci. Proc. 1994 **15** (4) pg 133-41.

17. N. Hochet et al, "High temperature mechanical properties of LOX-E and M fibres" Microscopy, 1997, **185**, pg 243.

18. M. Takeda, "High performance silicon carbide fiber Hi-Nicalon for ceramic matrix composites" Ceram. Eng. Sci Proc. 1995, **16**, (5), pg 37-44.

19. M. Berger, "Microstructure and high temperature mechanical behaviour of new polymer derived SiC based fibers" Ceram. Eng. Sci Proc. 1998, **19**, (3-4), pg 39 – 46.

20. T. Ishikawa, "New type of SiC sintered fiber and its composite material" Ceram. Eng. Sci Proc. 1998, **19**, (3-4), pg 283-90.

21. J. Lipowitz "Structure and properties of polymer derived stoichiometric SiC fiber" Ceram. Eng. Sci Proc. 1995, **16**, pg 55-62.

22. M. Takeda "Microstructure and Oxidation Behaviour of Silicon Carbide Fibers Derived from Polycarbosilane" J. Am. Ceram. Soc. 2000, **83** [5] pg 1171–76.

23. J. Lipowitz "Composition and structure of ceramic fibers prepared from polymer precursors" Advanced Ceramic Materials, 1987, **2**, (2), pg 121 – 128.

24. H. Sowman, D. Johnson "Oxide Fibres From Chemical Ceramic Processes" Ceram. Eng. Sci. Proc. 1985, **6**, pg 1221 – 1230.

25. H. LaBelle, Jr., A.I. Mlavasky, "The Growth of Sapphire Filaments from the Melt", Nature, 1967, **216**, pg 574-575.

26. J. Pollock "Filamentary Sapphire – Growth and microstructural characterisation" Material Science, 1972, **7**, pg 631-48.

27. H Sayir "Temperature dependent brittle fracture of undoped and impurity doped sapphire fibers" Ceram. Eng. Sci Proc. 1993, **14**, (8), pg 581.

28. J. Sheehan et al "Mechanical properties of $MgAl_2O_4$ single crystal fibers" Ceram. Eng. Sci Proc. 1993, **14**, pg 660-70.

29. E. Courtright "Controlling microstructures in Al_2O_3- $Y_3Al_5O_{12}$ (YAG) eutectic fibers" Ceram. Eng. Sci Proc. 1993, **14**, pg 671-81.

30. S. Farmer "Microstructural stability and strength retention in directionally solidified Al_2O_3-YAG eutectic fibers" Ceram. Eng. Sci Proc. 1995, **1**, (5), pg 969-76.

31. G. Morscher "Bend stress relaxation of Al_2O_3-YAG eutectic fibers" Ceram. Eng. Sci Proc. 1995, **16**, (5), pg 959-68.

32. H. LaBelle, Jr, "EFG, The Invention and Application to Sapphire Growth", J. Crystal Growth 1980, **50**, pg 8-17.

33. H. LaBelle, Jr., "Growth of Inorganic Filaments" 1969, U. S. Patent No.3471266.

34. H. LaBelle, Jr., "Method of Growing Crystalline Materials" 1971, U. S. Patent No. 3591348.

35. H. LaBelle, Jr. & A.I. Mlavasky, "Method and Apparatus for Growing Inorganic Filaments, Ribbon from the Melt" 1972, US Patent No. 3650703.

36. H. LaBelle, Jr. & W.T. Little, "Crystal Growing Apparatus" 1972, U.S. Patent No. 3701636.

37. H. LaBelle Jr, A. Mlavasky, C. Cronan, "Production of Crystalline Bodies of Complex Geometries", 1974, U.S. Patent No. 3846082.

38. J. Haggerty, W. Menashi, J. Wenkus, "Method of Forming Refractory Fibers by Laser Energy", 1976, U. S. Patent No. 3944640.

39. C. Burrus, J. Stone, "Single-Crystal Fiber Optical Devices: A Nd:YAG Fiber Laser", Applied Physics Letters. 1975, **26**, (6), pg 318-320.

40. S. Aramaki, R. Roy "Phase Diagrams for Ceramasists", Am. Ceram. Soc. Pub, New York, 1964, #314, **1**, pg 203.

41. M. Stacey "Developments in Continuous Alumina Based Fibres", Br. Ceram. Trans. Journal. 1988, **87**, pg 168 – 172.

42. I. Harter, C. Norton Jr, L. Christie (The Babcock and Wilcox Co.), 1949, U.S. Patent No 2467889.

43. J. Birchall "Oxide Inorganic Fibres", "Concise Encyclopaedia of Composite Materials", Pergamon Press, London, 1989, pg 283.

44. J. Milewski "Whiskers", "Concise Encyclopaedia of Composite Materials", Pergamon Press, London, 1989, pg 1177.

45. W. Miller "Encyclopaedia of Textile Fibres and Non-Woven Fabrics", Wiley, New York, 1982, pg 438 – 50.

46. A. K. Dhingra "Advances in Inorganic Fibre Developments", in "Contemporary Topics in Polymer Science" AR Bunsell, ed, Plenum Press, 1982, pg 227 – 60.

47. L. Christie, Babcock and Wilcox Company, 1968, Br Patent Specification 1098595.

48. M. Morton, J. Birchall, J. Cassidy. 1974, U.K. Patent Specification 1360197.

49. T. Furuya, Y. Uchiyama, A. Kouda (Denki Kagaku Kogyo Kabushiki Kaisha), 1980, U.K. Patent Application GB 2028788A.

50. Toyota Motor Co. Ltd. Isolite Babcock Refractories Co. Ltd Japan Kokai Tokyo Koho "Filament Reinforced Aluminium Alloy" 1984, J.P.59 113139 (84,113,139), 29.

51. D. Johnson "Properties and Applications for 3M's Nextel 440 Ceramic Fiber" J. Materials and Processes.1987, **5**, pg 443 – 453.

52. A. Bunsell "Fiber Reinforcements for Composite Materials" J. Composite Materials. 1988, **2**, pg 73 – 148.

53. J. Romine "Microstructure of Dupont PRD 166 fibre" Ceram. Eng. Sci. Proc. 1987, **8** (8), pg 755.

54. V. Lavaste, "Comparative Properties of Dupont Fibre FP and PRD 166" J. Mat. Sci. 1995, **30**, pg 4215.

55. D. Gopal "Thermal Stability of Single Crystal and Polycrystalline Alumina Fibers and 85% Alumina 15% Silica Fibers", Ceram. Eng. Sci. Proc. 1995, **16**, pg 977-87.

56. A. Bunsell "Property, Structure and Characterisation of A Continuous Fine Alumina– Silica Fibre", Composite Science and Technology, 1990, **37**, pg 63 – 78.

57. H. Umezaki, O. Yasuyuki, K. Shimada, "Method for producing silica-alumina fiber", Sumitomo (Altex), 1994, US Patent 5,575,964.

58. K. Jakus et al "Mechanical Behaviour of Sumitomo Altex Fiber at Room and High Temperature", Ceram. Eng. Sci. Proc. 1989, **9-10**, pg 1338 – 49.

59. Sumitomo US Patent 4,961,889, 1990.

60. D. Johnson "Properties and Applications for 3M's Nextel 440 Ceramic Fiber and Comparison to Nextel 312" J. Materials and Processes, 1987, **1** pg 453 – 457.

61. M. Schmucker et al "High Temperature Behaviour of Polycrystalline Aluminosilicate Fibers With Mullite Bulk Composition – Microstructure and Properties", J. Eur. Ceram. Soc. 1996, **16**, pg 281 – 285.

62. D. Johnson "Nextel 480 Reinforcement Fiber" Ceram. Eng. Sci. Proc. 1987. **8**. (7-8), pg 74-6.

63. D. Wilson "High Temperature properties of Nextel 610 Alumina Based Nanocomposite Fibers", Ceram. Eng. Proc. 1993, **14**, pg 609 – 621.

64. D. Wilson "Microstructure and High Temperature Properties of Nextel 720 Fibers", 3M website, 1997.

65. D. M. Wilson and L. R. Visser, 3M Specialty Fibers and Composites. Ceramic Eng. Sci. Proc. 24th Annual Conference on Engineering Ceramics and Structures, January 2000, Cocoa Beach.

66. J. French, M. Harmer, H. Chan & G. Miller "Creep of duplex microstructures" J. Am. Ceram. Soc. 1994, **77**, pg 2857-65.

67. High Temperature Ceramic Matrix Composites, 4th Int. Conf. on High Temperature Ceramic Matrix Composites, ed. W. Krenkel., Wiley-VCH, 2001.

CHAPTER 2 SELECTION OF PRECURSORS FOR PREPARATION OF NON-OXIDE AND OXIDE FIBRES

2.1. Historical Review of Silane and Carbosilane Polymers in SiC Fibres

Textile fibres of silicon carbide were first successfully developed Japan and are now marketed under the trade name "Nicalon" by Nippon Carbon and Dow Corning. These fibres are based on the conversion of organosilicon polymers to an inorganic. The precursor organic material dimethyledichlorosilane is converted to polycarbosilane. This compound is heated at 280°C to adjust the molecular weight for spinability, by cross-linking the molecules. The "raw" spun fibres are cured by oxidation at 200°C to form the "green" fibres. The curing process produces cross-linking with oxygen. The green fibres are then heat treated at 1500°C to release hydrogen, methane and carbon monoxide leaving mostly silicon carbide with some residual oxygen.

The first recorded synthesis of a silane polymer was a perphenylpolysilane carried out by [1]. A similar later synthesis using dichlorodimethylsilane and sodium metal by Burkhard [2] was the first to be characterised. Permethylpolysilane is a highly crystalline polymer that is insoluble in common organic solvents (benzene or tetrahydrofuran) [3]. The polymer is also infusible, decomposing before reaching its melting point and owing to these properties it has been seen as an unpromising and uninteresting material for fibre formation [4]. The first work on carbosilane polymers was carried out by Fritz [5,6], using the thermal condensation polymerisation of tetramethylsilane and trimethylchlorosilane precursors. The tetramethylsilane was heated in a furnace at 700°C, with the unreacted silane repeatedly circulated through the furnace resulting in a polycarbosilane which had a molecular weight of ~800g mol^{-1}.

Ideally for the production of fibres a linear polymer chain is desirable with a molecular weight ranging from several tens of thousands to hundreds of thousands. The linear carbosilane polymer polysilmethylene was obtained by the ring opening polymerisation of 1, 3-disilacyclobutane by Nametkin [7] which had an exceptionally high molecular weight of up to ~3,000,000 g mol^{-1}. But despite the high molecular weight of this material, it was found to be unsuitable for spinning into fibres because of its gum like state [8-10]. The potential of ceramic materials derived from such polymer precursors was realised by Popper during his work at the British Ceramic Research Association (BCRA). He and his co-workers examined a large number of differing types of polymers and their conversion to ceramic material [11, 12]. It was not documented that any attempt had been made to produce ceramic fibres, but monolithic non-oxide ceramics made by this route included boron nitride, aluminium nitride, silicon nitride and silicon carbide. Some years later Yajima started resurgence in this field of silane polymers using the dechlorination of dichlorodimethylsilane (DCDMS) using lithium wire in THF to yield dodecamethylcyclohexasilane (DDMCHS) [13]. This could be further processed to yield a carbosilane polymer that was an effective precursor for the production of silicon carbide fibres. A resurgence soon followed by other groups, including those of [14], [3,15-19].

2.2. Development of Spinnable Carbosilane Polymers

Yajima was to pioneer the development of silicon carbide fibres using a variety of carbosilane precursors. As his understanding of the mechanisms involved in their conversion to the ceramic form grew, a series of improvements came about from his Mark 1-3 fibres. These were the first core-less non-oxide fibres, which did not rely on chemical vapour deposition (CVD) of material on to a core substrate. The bulk of the fibre is of the same composition and material.

2.2.1. Mark 1 Fibre

Yajima worked on the "Mark 1" fibre with the intention of producing a polymer with a sufficient molecular weight to allow melt spinning instead of dry spinning from a hydrocarbon or chlorinated hydrocarbon polymer solution. He first produced a polycarbosilane by the cleavage of the DDMCHS ring in an autoclave for 48hrs at 400°C in an argon atmosphere [13]. The product was fractionated to yield the "high" molecular weight fraction of approximately 1500 g mol^{-1}. This fraction was dissolved in benzene and from this solution it was possible to dry spin crude, very brittle 10 - 20μm diameter fibres using a glass rod dipped in the solution. When heat-treated to 1000°C/2hrs at reduced pressure (10^{-3} mm Hg), a 40% weight loss resulted. This demonstrated that a significant amount of volatile material remained. The infrared spectrum of the precursor polymer showed the presence of Si-R and Si-H bonds from the band at 2100 cm^{-1}.

Progressive heat treatments from 300 – 1000°C showed the disappearance of Si-H above 400°C which coincided with the polymer becoming fully cross linked and infusible in common organic solvents such as benzene, THF and chloroform. It was concluded that polymer cross-linking took place through the Si-H linkage. At more elevated temperatures the disappearance of further organic groups was detected until, at temperatures above 750°C, only Si-C and Si-O bands were present. X-ray diffraction (XRD) and scanning electron microscopy (SEM) techniques were used to characterize the heat treated fibre [20, 21] and found that at <800°C the fibres were composed of amorphous silicon carbide. At > 800°C a gradual increase in the extent of crystallinity of the silicon carbide was observed, still very small (calculated from measurements of the half-peak width of the XRD trace) at 3-7nm at 1500°C, confirmed by transition electron microscopy (TEM).

Later Yajima [22] demonstrated the relationship between the molecular weight of the polycarbosilane and the spinnability of the fibre. In order to produce continuous fibres, it is necessary to have the correct molecular weight distribution in the precursor polymer. Usually for production of synthetic fibres, high molecular weight linear polymers are thought to be desirable, but in the case of the carbosilane polymers, Yajima found that polymers having higher molecular weights did not spin as well as those containing only lower molecular weight molecules. The preparation of polycarbosilane from DDMCHS was considered to be difficult, expensive and time consuming.

An alternative simpler synthesis was devised by Yajima [23], in which DCDMS was reacted with molten sodium in xylene. After extraction, the product was heated in an electric furnace at 320°C/5hrs and volatiles were removed. The molecular weight was determined by vapour phase osmometry (VPO) with a lower average molecular weight of approximately 948 g mol^{-1}. Yajima used gel permeation chromatography (GPC) and revealed that the average molecular weight of the autoclaved polycarbosilanes increased as the polymerisation temperature increased [24]. At the same time the molecular weight distribution shifted to higher molecular weights. This was largely due to a dehydrogenation condensation reaction mechanism. Fibres produced by this method could be melt spun instead of dry spun and Yajima concluded that this method was very simple and economical. These fibres were known as "Mark 1" and the spinning characteristics of this fibre were such that the precursor fibre proved difficult to handle. It was brittle and only had sufficient strength to be handled when spun in relatively large diameters, and was therefore said to have poor spinnability.

2.2.2. Mark 2 & 3 Fibre

In an attempt to improve the spinnability of the polycarbosilane fibre Yajima added between 1% and 4% of dichlorodiphenylsilane [25, 26]. It was believed that the introduction of phenyl groups, which were more stable to temperature than the methyl groups, would result in the partial suppression of the dehydrogenation condensation reaction. It was anticipated that the molecular structure would be more linear, which was correct and resulted in a 30% improvement in the Yajima worked on the "Mark 1" fibre with the intention of producing a polymer with fibre (a 30% reduction in the green fibre diameter for the same given strength). The mechanical properties of the final silicon carbide "Mark 2" fibre were reported as superior to that of the Mark 1 fibre.

As part of an investigation into the process of thermal decomposition of organometallic polymers [27] also synthesized polyborodiphenylsiloxane (known as Python). Python was easily produced by dissolving boric acid and DCDMS in anhydrous N-butyl ether and refluxed in a nitrogen gas atmosphere for 18hrs, then heated at 300°C/1hr at reduced pressure. This gave polyborodiphenylsiloxane in a 92% yield. The spinnability of this Mark 3 polymer was greatly improved compared with that of Mark 1, so much so that when cured it could be handled and subjected to tensile testing. The tensile strength of the cured "Mark 3" fibre was in the range of 20-59 MPa. The work carried out on these polycarbosilane systems successfully led to the development of the first silicon carbide based ceramic fibre known commercially as Nicalon.

2.3. Precursors used in Oxide Ceramic Fibres

2.3.1. Historical Review of Sol-Gel

A process that has gained much notoriety in the glass and ceramic fields is the sol-gel reaction. This chemistry produces a variety of inorganic networks from silicon or metal alkoxide monomer precursors. Although first discovered in the late 1800's and extensively studied since the early 1930's, a renewed interest surfaced in the early 1970's when monolithic inorganic gels were formed at low temperatures and converted to glasses without a high temperature melting process [28-30]. Through this process, homogeneous inorganic oxide materials with desirable properties of hardness, optical transparency, chemical durability, tailored porosity, and thermal resistance, can be produced at room temperatures, as opposed to the much higher melting temperatures required in the production of conventional inorganic glasses [30-32]. The specific uses of these sol-gel produced glasses and ceramics are derived from the various material shapes generated in the gel state, i.e., monoliths, films, fibres, and monosized powders. Many specific applications include optics, protective and porous films, optical coatings, window insulators, dielectric and electronic coatings, high temperature superconductors, reinforcement fibres, fillers, and catalysts.

The sol-gel process involves the evolution of inorganic networks through the formation of a colloidal suspension (sol) and gelation of the sol to form a network in a continuous liquid phase (gel) [29]. The precursors for synthesizing these colloids consist of a metal or metalloid element surrounded by various reactive ligands. Metal alkoxides are most popular because they react readily with water. The most widely used metal alkoxides are the alkoxysilanes, such as tetramethoxysilane (TMOS) and tetraethoxysilane (TEOS).

However, other alkoxides such as aluminates, titanates, and borates are also commonly used in the sol-gel process, often mixed with TEOS. The first metal alkoxide was prepared from $SiCl_4$ and alcohol by Ebelmen [33] who found that the compound gelled on exposure to the atmosphere. However these materials remained of interest only to chemists and not materials scientists [34] for almost a century. It was finally recognised by Geffcken [35] in the 1930's that alkoxides could be used in the preparation of oxide films. This process was developed by the Schott glass company in Germany and was quite well understood [36]. Inorganic gels from aqueous salts have been studied for a long time [37] Graham showed that the water in silica gel could be exchanged for organic solvents, which argued in favour of the theory that the gel consisted of a solid network with continuous porosity. Competing theories of gel structure regarded the gel as a coagulated sol with each of the particles surrounded by a layer of bound water, or as an emulsion. The network structure of silica gels was widely accepted in the 1930's, largely through the work of Hurd [38], who showed that they must consist of a polymeric skeleton of silicic acid enclosing a continuous liquid phase.

The process of supercritical drying to produce aerogels was invented by Kistler [39], who was interested in demonstrating the existence of the solid skeleton of the gel, and in studying its structure. Around the same time, mineralogists became interested in the use of sols and gels for the preparation of homogeneous powders for use in studies of phase equilibria [40-41]. This method was later popularised in the ceramics community by Roy [42, 43] for the preparation of homogeneous powders. That work was not directed toward an understanding of the mechanisms of reaction or gelation, nor the preparation of monolithic shapes.

Much more sophisticated work, both scientifically and technologically, was going on in the nuclear fuel industry, but it was not published until later [44-45]. The goal of this work was to prepare small spheres (tens of μm's in diameter) of radioactive oxides that would be packed into fuel cells for nuclear reactors. The advantage of sol-gel processing was that it avoided generation of dangerous dust, as would be produced in conventional ceramics processing, and facilitated the formation of spheres. The latter was accomplished by dispersing the aqueous sol in a hydrophobic organic liquid, so that the sol would form into small droplets, each of which would subsequently gel.

The ceramics industry began to show interest in gels in the late 1960's and early 1970's. Controlled hydrolysis and condensation of alkoxides used for preparation of multicomponent glasses, was independently developed by Levene [46] and Dislich [47]. Ceramic fibres were made from organometallic precursors on a commercial basis by several companies [48-50]. However, the explosion of activity that continues today can be dated from the demonstration by Yoldas [51, 52] and Yamane [53] that monoliths could be produced by careful drying of gels. Technology preceded the science of sol-gel processing, but great strides have been made in the past few years in understanding the fundamental aspects of preparing homogeneous multicomponent ceramics (crystalline and amorphous) from alkoxide derived gels.

2.4. THE SOL-GEL PROCESS

In terms of chemical mechanisms, sol-gel processing can be divided into two distinct areas, namely the alkoxide route and the aqueous route. The former generally requires the use of an organic solvent, normally an alcohol, in order to act as mutual solvent for the organometallic precursor and the water for hydrolysis.

The latter route employs the principles of colloid chemistry to generate colloid sized particles from ionic species in an aqueous medium. The alkoxide route has attracted great attention in recent years however the aqueous systems are more economic (excluding expensive alcoholic solvents and precursors) and do have some interesting applications making them worthy of consideration. Therefore the sol-gel is an all-embracing term applied to any process whereby a high- temperature ceramic is made by the heat treatment of low-temperature precursors, in which the constituents are dispersed on a colloidal or molecular scale. Compared to traditional ceramics, where the initial particle size is typically> 1μm, the colloidal scale homogeneity allows the product to be sintered at higher rates and lower temperatures, giving a consequent reduction in flaw sizes in a bulk ceramic.

Proposed advantages and disadvantages to sol-gel processing are:

Advantages

1. Better homogeneity.

2. Better purity.

3. Low temperature preparation:

Savings in energy/Minimize evaporation losses.

Minimize air pollution/No reaction with container.

Bypass phase separation.

4. New noncrystalline solids outside the range of normal glass formation.

5. New crystalline phases from new noncrystalline solids.

6. Better glass products from the special properties of gels.

7. Special products, i.e., films and fibres.

Disadvantages

1. High cost of raw materials.
2. Large shrinkage during processing.
3. Residual microporosity.
4. Residual hydroxyl.
5. Residual carbon.
6. Health hazards of organic solvents.
7. Long processing times.
8. Difficulty in producing large pieces.

For the preparation of amorphous materials from alkoxides the sol-gel process can be broken down into the following stages.

1. Precursors, dissolution and mixing.
2. Sol to gel transition.
3. Forming (i.e., casting, fibre drawing and film formation)
4. Drying.
5. Gel to glass transition.

The materials can be subsequently fired to form crystalline phases.

2.5. The Alkoxide Route

The most commonly employed starting materials are metal alkoxides, which are available for a large range of elements and with various alkoxy groupings [54]. The solubility and reactivity of metal alkoxides varies widely, and some experimentation is frequently necessary to obtain the required solutions.

On occasions it may be unavoidable to compromise on the purity advantages given by alkoxide starting materials requiring the use of a metal salt, i.e. a nitrate, chloride or acetate, in order to get the metal precursor into solution. In order to achieve the advantages of improved homogeneity, the reacting species must be dispersed uniformly into a single-phase solution. Since most alkoxides are sensitive to hydrolysis by water a non-aqueous solvent is generally required, but in order to convert the organometallic compounds into species that would readily enter into condensation reactions, controlled hydrolysis must be achieved. This may necessitate a mutual solvent for the alkoxide, the polar water and any catalyst. The most widely used solvents are alcohols - typically methanol, ethanol and propanol.

It is important to realize that the choice of starting materials can have a marked effect on the resulting gel and ultimately on the glass. To achieve and maintain good homogeneity in multicomponent systems care must be taken to minimize self-condensation. This may be controlled by the processing conditions, i.e., the order of mixing, temperature and solvent type, as well as the choice of reactants; i.e., by using alkoxides of a similar reactivity [55]. Under order of mixing could be included attempts at controlled pre-hydrolysis of the least reactive alkoxides prior to the addition of more reactive components. Mixed alkoxides are also available for many systems, and they provide a further addition to accessible starting materials. In many cases, the solubility of the double alkoxide is higher than that of either single alkoxide. For example, the ethoxides of Al and Mg are only slightly soluble in cool ethanol, whereas the double alkoxide Mg $\{Al\ (OEt)_4\}_2$ is highly soluble [56]. This probably reflects the fact that double alkoxides are generally less associated in alcohols or other organic solvents than are the constituent alkoxides.

The following equations describe the fundamental reactions, which allow the conversion of monomeric organometallic precursors into gels and ultimately glasses or ceramics.

1) Hydrolysis with H^+/OH^- catalyst:

$$M(OR)_x + H_2O \leftrightarrow M(OR)_{x-1}OH + ROH$$

$$M(OR)_{x-1}OH + H_2O \leftrightarrow M(OR)_{x-2}(OH)_2 + ROH$$

Equation 2.1: Hydrolysis Reactions of Metal Alkoxides

2) Condensation

$$\equiv M\text{-}OH + HO\text{-}M\equiv \leftrightarrow \equiv M\text{-}O\text{-}M\equiv + H_2O$$

$$\equiv M\text{-}OH + RO\text{-}M\equiv \leftrightarrow \equiv M\text{-}O\text{-}M\equiv + ROH$$

$$\equiv M\text{-}OR + RO\text{-}M\equiv \leftrightarrow \equiv M\text{-}O\text{-}M\equiv + R\text{-}O\text{-}R$$

Equation 2.2: Condensation Reactions of Metal Alkoxides

M is a metal chosen from Al, In, Si, Ti, Zr, Sn, Pb, Ta, Cr, Fe, Ni, Co and several others. R represents an alkyl group. The condensation reactions also facilitate the reaction of compounds of different elements leading to the synthesis of multicomponent gel systems [57]. All the reactions can be regarded as equilibria with the extent of the reaction being determined by the species involved and the conditions under which the reactions take place. Another factor, which becomes important in the production of multicomponent gels is the relative rates of reaction of the alkoxides of different metals. Yoldas [58] has stated that the order of addition of the alkoxide components was important in producing a homogeneous gel, and the first component to be hydrolysed should be the most slowly reacting one - this generally being the silicon alkoxide. When this has been rendered an active polymerizing species, other alkoxides can be added which are then more likely to react with the already hydrolysed compounds rather than with themselves.

2.6. The Aqueous Route

It is also possible to produce amorphous pre-ceramic materials using colloidal systems in an aqueous medium. These techniques rely on generating a stable dispersion of colloidal sized particles in a solvent (in this case water) and destabilizing this sol in a controlled manner to give a solid gel from which the solvent can be removed, and then sintering to give a dense amorphous mass, which is subsequently crystallized after further heat treatment.

Sodium silicate solution "Na_2SiO_3"

↓ **Ion Exchange Resin**

Silicic acid $Si(OH)_4$ + NaO–resin

↓ **Condensation**

$(OH)_3$-Si-O-Si-$(OH)_3$ + H_2O

↓ **Cyclization and Growth**

Dense silica particle with hydroxylated surface

↓ **Further Condensation and Agglomeration**

Silica Gel

↓ Sintering and Crystalization

Polycrystalline Silica

Figure 2.1: Schematic of Aqueous Route to Polycrystalline Silica

The system that has probably received the most attention is silica, and many workers have described methods of producing dense silica glass from silica sols [59-60].

2.7. Specific Precursor Selection For Commercial and Experimental Polycrystalline Sol-Gel Derived Fibres

2.7.1. Alumina Precursor Materials

Among oxide ceramics, alumina (Al_2O_3) is generally considered the most desirable structural material. Alumina has excellent fracture toughness, high elastic modulus, a melting point in excess of 2000°C and very good thermochemical stability.

Aluminium Chlorhydrates

The property of transforming from a basic solution to a glassy gel is observed in basic salt solutions of group III and IV metals. Typically the viscosity of aqueous aluminium chlorhydrate solutions (Al/Cl = 2) is 100 Pa/s in the dry spinning range to 10^{12} Pa/s in the gel [61]. This behaviour may be contrasted with that of aluminium chloride solution, which shows a lower viscosity increase and crystallizes (at 11.8% Al_2O_3 equivalent) at ambient temperatures. Chlorhydrate solutions can be spun into glassy fibres, whereas any attempt to spin the salt is disrupted by the precipitation of crystals. Commercial aluminium chlorhydrate or ACH (typically $Al(OH)_5Cl$) is used to prepare some fibres.

ACH is made by dissolving aluminium metal in either aluminium chloride solution near 100°C, a limited amount of aqueous HCl, or aluminium oxychloride itself made around 150°C from aluminium hydroxide and aqueous HCl. Gel permeation chromatography (GPC) data show a typical chlorhydrate to comprise a range of species with a coarse fraction up to around 100 nm [62].

The polymeric species $Al_{13}(OH)_{24}(H_2O)^{7+}$ [63] is reported to be predominant in many sources of solution, although it has been suggested that further association in to around 40 Al units is more likely [61]. The viscosity of commercial ~24% alumina solutions may vary over the range 10 - 60 mPa. The lower figure is near that expected for the solutions of equiaxed polyions, limited agglomeration and open structuring of the coarser fractions would cause the highest figure. Gel fibres can be made from all commercial chlorhydrates, which solidify to glassy gels even when very slowly concentrated. In mixtures of spherical colloidal particles a polydispersity of only 6% [64] is needed to prevent crystallisation of a separate colloid phase, and it is speculated that polydispersity in the main species and the principle of maximum confusion [65] is sufficient to cause the formation of glassy gels. It was suggested by Assih [66] that the polyions absorb on to the coarser colloidal particles in chlorhydrate and prevent flocculation by setting up hydration barriers. Much of the chloride in solution appears to be complexed with the polyions and this further reduces the tendency of any positively charged coarse particles to flocculate.

Aluminium Carboxylates

Commercial or development alumina based fibres are also made from aqueous solutions of basic aluminium acetate borate ($Al(OH)_2(OOCH_3)^1/_3H_3BO_3$), aluminium formacetate ($AlOH(OOCH)(OOCCH_3)$) and aluminium nitroacetate solutions [11,12]. Aluminium oxynitrate solutions have also been used in noncommercial fibres. The solutions possess the gelling property of the chlorhydrates. Indeed, in mixed anion solutions the principle of maximum confusion should be enhanced by the presence of different anions, which reinforces the effect of cation polydispersity. Basic aluminium acetate ($AlOH(CH_3CO_2)_2$) is insoluble in water and its solubilisation by borate could be considered as an effect of randomisation of the solution structure.

Indeed dimethyl formamide (DMF) is also used by 3M to promote only the monoacetate aluminium compound [67-68] which also retained water solubility, when reacting aluminium powder with acetic acid. Aluminium formacetate is most favoured in a number of patents, mixed with a small amount of lactic acid (aluminium: lactate ratio 7:1). Lactic acid may be added to counteract gelation due to aluminium hydroxide formation, since the acetate and formate gel rapidly if heated above 85°C [69]. It is also likely that the bifunctional nature of lactic acid contributes to the solution spinnability by linking adjacent alumina species through the carboxylate and alcohol groups. Both chlorhydrate and the carboxylate solutions can be mixed with negatively charged commercial silica sols to make formulations of mullite composition. The sol mixing conditions can be critical as slow addition of silica sol to chlorhydrate causes flocculation, and intensive mixing is specified when chlorhydrate solution and sol are combined in the manufacture of alumina coated sols [70].

A further patent from Toray [71] compares the spinnability of aluminium chlorhydrate solutions with solutions in which chlorhydrate has been heated with lactic acid and organic acids with $pK_a < 3$. It was claimed that spinnability was enhanced when pK_a was < 3. Lactic acid did show an improvement on both chlorhydrate and chlorhydrate treated with acetic or formic acids, and it is speculated that the bifunctional nature of the additives may introduce a linear component to the underlying solution structure and improve spinnability.

Organometalic Precursors

Sumitomo [72] patented the preparation of fibres from polyaluminoxane precursors, which have been developed with the objective of maximizing the concentration of oxide species in the spun material.

The polymers are prepared by the partial hydrolysis of aluminium trialkyl or trialkoxy compounds with water. In earlier patents the molar ratio of water to aluminium organic compound, i.e., aluminium isopropoxide $Al(OC_3H_7)_3$ was 1, but more recently the ratio has dropped to 0.6. A degree of polymerisation is more suitable and it is likely that they are able to form linear structures by this method. A further refinement in their work is the reaction of preferably 10% of the attached organic groups with palmitic or stearic acid (14 – 16 methylene groups) in the earlier work or hydroxyethyl benzoate in a later example [73]. The result is to give a mixed polymer of structure O-Al-O with some isopropoxy (OC_3H_7) groups replaced at random by a palmitoyloxy, stearoyloxy, or derived hydroxybenzoate group. A copolymer is more soluble in a particular solvent than a homopolymer. This would give better spinnability according to Brinker's criterion, but in a linear system would also improve spinnability by improving the mobility of the polymer strands. Throughout the developments silica has been added as a polysilicate ethyl ester. In their earliest patents, Sumitomo created a dry spun precursor containing about 60% of polymer or 42% refractory. More recently, their formulations have approached melt spinning with a precursor, which is solid at room temperature and contains 95% polymer with residual isopropanol solvent.

High Temperature Heat Treatment and Crystallisation

Following heat treatment of an alumina precursor, α-alumina is thermodynamically the most stable form at all temperatures above ~250°C. α-alumina has been deposited directly from organic solution at 300°C [74] but is reluctant to form from hydrous oxide systems at low temperature. This feature has led to many practical difficulties and invention.

Decomposition and crystallinity data on alumina and its hydroxides are summarised in **Figure 2.2** [75], which includes more effects of seeding alumina precursors. Gibbsite [$Al(OH)_3$] is commercially the most important hydroxide and is precipitated from sodium aluminate solutions in the Bayer process and occurs naturally as a minor component in bauxites. Bayerite ($Al(OH)_3$) is typically precipitated from aluminium salt solutions. Both trihydroxides are built up of double layers of hydroxide in approximately hexagonal close packing with aluminium occupying $^2/_3$ of the interstices. In gibbsite the hydroxides are directly opposite those in the adjacent layer, whereas in Bayerite they match the opposing hollows [76]. The trihydroxides transform to boehmite when heated hydrothermally above 150°C, the structure [AlO(OH)] also has a layer structure with double layers of O^{2-}, but loss of water leads to rearrangement into in nearly cubic close packing [77]. Hydroxyl ions of one double layer are located over the depressions between hydroxyls in the adjacent layer so that the layers are linked by hydrogen bonds between their hydroxyls.

Gelatinous aluminium hydroxides or pseudoboehmite formed by precipitation between pH 4 and 9 can retain a high level of water even after drying to 100-110°C and tend to crystallise to boehmite on dehydration. The gelatinous materials follow less well-defined decomposition paths than the crystalline aluminium hydroxides, and the fibre precursors are of this general nature.

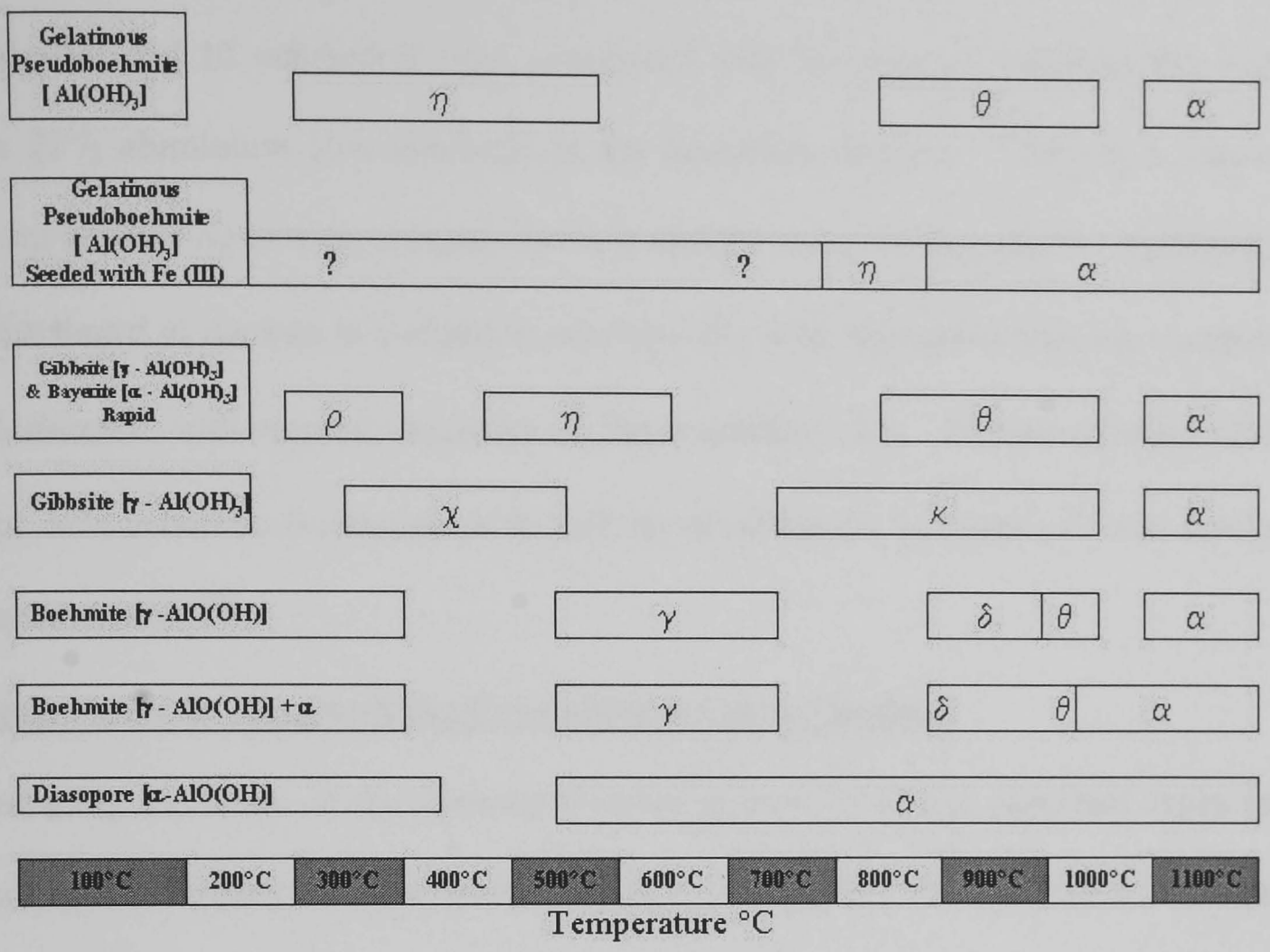

Figure 2.2: α-Alumina Formation From Hydrated Alumina's and Associated Intermediate Oxides

Diaspore [AlO(OH)], the remaining hydrous alumina, occurs naturally in some bauxites but can only be prepared with out prior nucleation [74] by hydrothermal processing above 300°C. The oxygens are again in layers but now with a hexagonal close packed arrangement that matches approximately the oxygen separations in the hexagonal close packed structure of α-alumina (0.44 versus 0.476 nm) [78]. Because of this structural match, diaspore transforms easily to α-alumina at low temperature. Crystalline boehmite dehydrates on heating to γ-alumina via its approximate cubic oxygen template to form a cubic close packed defect spinel structure. The trihydroxides that would crystallize to boehmite on careful dehydration, together with gelatinous alumina and the spinning precursors described above, all follow a transitional sequence on heat treatment.

The defect spinel arises because the unit cell in a spinel contains 24 metal ions in 8 tetrahedral and 16 octahedral sites, associated with 32 oxygens, whereas there are only $21^1/_3$ aluminium ions available in the transition alumina. There is increased structural ordering as temperatures increase and the transition proceeds. Aluminium is distributed at random in γ-alumina, whereas all of the tetragonal sites are occupied in δ-alumina, with ordered vacancies on the octahedral sites. Further ordering takes place in monoclinic θ-alumina with half the aluminiums in tetragonal and half in octahedral sites [79].

Strategies for Dealing with the Crystallization of α-Alumina

Continuing the focus on the hydrous alumina system, all of the precursor types are decomposed initially to amorphous alumina on heating beyond 400°C. Strong cohesive fibres may be made from the transitional aluminas, where the pore and defect size are reasonably contained and stratagies have been adopted to deal with the potentially damaging transformation to α-alumina.

High Alumina

A second strategy, used in the manufacture of Saffil or Safimax, is to add up to 5% silica to the alumina precursor, which has the effect of delaying the α-alumina transformation to >1300°C. This enables a number of transition aluminas to be sintered and controlled transformation to α-alumina. Intermediate products from a predominantely δ-alumina reinforcing fibre to a high α-alumina/mullite refractory form can be made. The crystallisation of α-alumina is not so destructive in this approach although product data shows that the strain to break of 0.7% in the largely δ-alumina "RF" grade could be reduced to as low as 0.35% in the high wear "RG" product where α-alumina may predominate [80].

Mullite and α-alumina are formed at the end of the sequence γ, δ, θ, α if the fibre temperature is raised from 1000°C to >1300°C. Initially γ alumina is precipitated with an average crystallite size of 5 nm, there is some crystal growth during the transition to θ, but α crystals when finally formed can grow to cross a fibre several micrometers in diameter. Birchall [81] has indicated that the strength of Saffil fibres falls sharply as the diameter is raised above that of the staple 3 – 5 μm product and this approach has not yet been used to make the coarser continuous fibres. Silica migrates in the fibres during sintering to give a surface of mullite composition.

Alpha Alumina Seeds

Du Pont introduced α-alumina milled to below 0.5 μm in the preparation of Fibre FP and recommended that at least 40% of the precursor be derived from the milled powder, thereby following standard bulk refractory practice. The introduction of milled ceramic reduces the volume change and associated shrinkage cracking on firing. The milled alumina will also seed the formation of α-alumina and remove the problems associated with delayed nucleation. The Du Pont procedure introduced an undesirable coarse component into the precursor formulation, which would both make spinning more difficult and limit the minimum fibre diameter. Kumagai and Messing [82] investigated the seeding of α-alumina from boehmite gels in more detail with nominally 0.1 and 0.4 μm seeds. They found an optimum level of 5×10^{13} of seeds per cm^3 of boehmite gel, which could be reached with a loading of 1.5% of the finer seeds of alumina, at which stage the ceramic was >98% sintered after 5 minutes at 1150°C. Levels of $10^{12}/cm^3$ seeds were ineffective, whereas too high a loading caused agglomeration.

The seeding and its effect on nucleation and subsequent sintering are effective at much lower levels (10% or less) than those used for Fibre FP. The relics of alumina

seeds have been observed in Almax continuous alumina fibres [83]. The refined introduction of α-alumina seeds at a low level seems to be a feature of technology generated in the mid 1980's. McCardle and Messing [84] demonstrated that the addition of γ-alumina seeds to boehmite reduces the boehmite dehydration temperature by about 20°C from 425°C but improves the grain structure of the ultimate high temperature α-alumina, to the extent that the ceramic reaches a limiting 2% porosity at 1200°C, while even at 1600°C untreated material is not sintered to this degree. This is still however a researched area of ceramics, where the reduction in temperature for the conversion of alumina precursors to α-alumina has been reported to be as low as 950°C [85]. Many other additives can be used to control the phase transformation temperature and grain growth of α-alumina, such as SiO_2, Cr_2O_3, MgO, Li_2O, B_2O_3 and ZrO_2 that are reviewed for use in polycrystalline alumina fibres [86-87]. In the transition from γ, δ, θ, α -alumina seeds affected only the temperature of the θ to α transformation.

The Use of Silica to Avoid Formation of Alpha Alumina

The selection of mullite ($3Al_2O_3.2SiO_2$) in bi-phasic fibre phase would be based on the intrinsically lower diffusivity in complex oxides compared to simple oxides, such as Al_2O_3, and hence reduced diffusional creep rates for a specific grain size [88-90]. Mullite is also highly resistant to shear-plasticity at high temperatures [91], presumably because of the large dislocation Burgers vectors and complex core structures. The absence of a large Al_2O_3 content also reduces the susceptibility of this phase to reduced fracture stress at intermediate temperatures. The simplest course is to avoid α-alumina completely and add enough silica to make a mullite fibre, which is a good refractory material in its own right.

Commercial fibres derived from formethanoate [92] or chlorhydrate/silica sol combinations [93] form γ-alumina and amorphous silica by 1000°C, and mullite is nucleated at about 1200°C [94]. The γ-alumina crystallite size is reported to be <60 nm when first formed with mullite, >50 nm in the final product. It is likely that the initial γ-alumina crystallite size is nearer the 5 nm reported for Saffil alumina [95] Mullite fibres have been made at 920°C in a laboratory study that used a more finely divided source of alumina [96] but the fibre was weak, possibly because free silica is not available to assist fibre sintering. Precursors of mullite composition sinter at a lower temperature than pure alumina and retain some porosity at 1000°C with an accessible surface area of 20 m^2/g, which is lost at 1200°C [67]. Mullite materials are fully sintered at 1000°C when a small amount of a glass former boria is added as a sintering aid. Sowman [97] showed that boria improves the strength of alumina silica fibres and its use in this role seems to be a feature of the earlier members of the Nextel series (Nextel 312, 440 and 480). Boria is, however, lost by vaporisation at high temperature and subtracts from the ultimate refractory performance of the fibres [98].

2.7.2. Silica Precursor Materials

Commercial silica sols are used in the manufacture of mullite fibres although the source and grade are often not declared in the patent literature. The simplest sols are negatively charged with pH near 10, and mole ratio SiO_2/Na_2O 60:130 [99] according to the sol surface area, the finest of these sols at 500 m^2/g having the highest sodium content. These materials would yield a mullite containing 0.2 - 0.5% Na_2O, which is unsatisfactory. The sodium may be removed by ion exchange or dialysis to form low sodium sols. The target SiO_2/Na_2O mole ratio is 130:500 and 3M embody Ludox LS (Du Pont), in their mullite related patent.

Derived sodium levels would be 0.05 - 0.2% in the product. Commercial sols are available with surface areas of up to 750 m^2/g. These are of lower silica concentration (10 – 15%) and are made by hydrolysis of tetraethylorthosilicate or silicon tetrachloride. 3M exemplifies a low concentration sol (Nalco 2326) in later patents as well as sols themselves made from tetraethylorthosilicate, and it seems that sodium is eliminated in the search for better refractory properties. ICI exemplifies silicone ethoxylate co-polymer surfactants (siloxane surfactants) as water miscible sources of silica. The silicone backbone is the hydrophobic component that is solubilised by pendant hydrophilic polyethylene oxide side chains, a typical compound DC-193 containing 13 silicone units with three allyl linked chains of 10 ethylene oxides. Miscibility with water is controlled by capping the side chains with propylene oxide units [100] or an acetoxy group. Being surfactants the siloxanes are aggregated into micelles on a molecular scale and in common with other ethoxylate surfactants are precipitated on a macroscopic scale when a solution is warmed to the cloud point temperature.

2.7.3. Zirconia Precursor Materials

Zirconia has a melting point of ~2670°C and therefore is an attractive material for use as a high temperature refractory fibre. Water soluble zirconium acetate [101] nitrate [102] chloride [103] and oxychloride [104] salts are widely used precursors for making continuous fibres by either dry spinning or commercially using the relic process (Zircar Fibres) [101]. They are also used with additional chelating ligands such as acetyl acetone [103] especially the alkoxides such as zirconium butoxide [105] or propoxide [106]. Colloidal precursors are also available in a number of particle sizes ranging from 5 – 200nm [107].

Stabilising additives are often used to promote formation of the stable high temperature cubic form (Y_2O_3, MgO and CaO) [108], although lanthanide elements can also be used [109-110], as tetragonal to monoclinic inversion occurs around 1170°C with an associated large volume change which would normally make a ceramic shatter. Typically a heat treatment to 1550°C is sufficient for conversion.

2.7.4. YAG Precursor Materials

Although laser optics have exploited the desirable properties of yttrium aluminium Garnet (YAG), which have been known for some time, its high melting point (1970°C), chemical inertness and excellent creep properties [111] have only been more recently the focus for ceramic fibre and bulk ceramics. A similar approach to aluminium precursors has been adopted for yttrium precursors, which can be blended with the aluminium precursor in the $Y_3Al_5O_{12}$ stochiometry or with an alumina rich eutectic composition. Analagous yttrium polymers can be made to those of the Sumitomo produced aluminoxane polymers for preparation of their commercial fibres. Chelating ligands can be used to stabilise the water-soluble acetate and carboxylate salts, to produce liquid precursors with the consistency of honey [112]. Both yttrium isopropoxide and butoxide have been used [113] in the same way as aluminium and a yttrium analogue of the chlorhydrate can be produced ($Y_2(OH)Cl_5.nH_2O$) [114].

A new concept emerged to improve the ceramic yield (oxide content when pyrolised) with yttrium compounds, by removing ligands and water of hydration by subjecting the water-soluble salt to a heat treatment just above its melting point [115]. YAG powder is used to produce a coarse grained fibre by combustion of Y and Al nitrates with glycine as fuel at 1000°C/1 hr to form $Y_3Al_5O_{12}$ powder and extruded with an acrylate plasticizer to form >100μm diameter fibres [116].

In a similar way colloidal yttria and alumina (boehmite) has been used with organic fiberising aids [117], but phase pure material is not achieved until much higher heat treatment temperatures (1650°C) as the precursors are not atomically intimate.

2.7.5. Spinel and Other Aluminate Precursor Materials

As with mullite and YAG, spinel ($MgAl_2O_4$) is an attractive material for use as a high temperature refractory fibre (MP 2100°C) and also has a high level of alumina in the structure. Numerous alumina precursors are available and the additional magnesia can be introduced as soluble salts, fine dispersed oxide powder [118], separate alkoxides [119] or double alkoxides [120]. To aid phase formation in the fired sol-gel, seed material of the $MgAl_2O_4$ spinel form can be produced by co-precipitated calcined hydroxides [121]. Less common aluminate sol-gels have also been prepared for fibre formation [122] to produce barium hexaluminate ($BaO.6Al_2O_3$).

2.7.6. Mullite Precursor Materials

Mullite has long been used as a high temperature refractory material in industry, but is not widely abundant as a natural mineral, the exception being on the Isle of Mull in Scotland. Mullite exhibits a high melting point (1920°C), good modulus, thermochemical stability and superior creep strength retention at high temperatures. There are wide ranges of economic, common alumina and silica precursors, which have been cited for use in the fabrication of mullite and other alumina based fibre systems that are summarised in **Table 2.1**. The combination of precursor economics and availability, high melting point, modulus, thermochemical stability and creep strength retention at high temperatures advocates the use of phase pure mullite as a high temperature candidate for use in sol-gel derived polycrystalline oxide ceramic fibres.

Without doubt the microstructure of the final product will be determined by the quality of raw materials used (purity, uniformity, molecular weight or size distribution and so on) as well as by process conditions. A key quality characteristic of continuous fibres is that they should be consistently strong over long lengths (many metres).

Al_2O_3 Precursor	**% Al_2O_3 Yield**	**SiO_2 Precursor**	**% SiO_2 Yield**
Pyrogenic Fumed Al_2O_3 (Powder)	~99	Pyrogenic Fumed Silica	~99
Fine α- Al_2O_3 (Powder)	>99	Fine Amorphous SiO_2	>99
Spray Dried Boehmite (Powder)	~70	Colloidal Silica	~50
Aluminium Chlorhydrate (Powder)	~48	Tetramethylorthosilicate (TMOS)	~40
Aluminium Formoacetate (Powder)	~37.5	Tetraethylorthosilicate (TEOS)	~40
Basic Aluminium Acetate (Borate Stabilised - Powder)	~32.8	Siloxanes	~30
Fumed Al_2O_3 Colloidal Sol	~30		
Aluminium Chlorohydrate Soln	~23		
Aluminium Isopropoxide (Powder)	~25		
Aluminium Chloride ($6H_2O$) (Powder)	~21.1		
Aluminium Sec-Butoxide (liquid)	~20.7		
Boehmite Colloidal Sol	~20		
Aluminium Di-Isopropoxide aceto acetic ester chelate (Liquid)	<20		
Aluminium Nitrate ($9H_2O$ - (Powder)	~13.6		

Table 2.1: Examples of Some Alumina/Silica Precursors Used For Fibre Production

Translated into mechanical properties this means a narrow spread of strengths and in turn this means avoiding contamination by small quantities of ambient dust, (Du Pont's PRD-166 fibre is less good in this respect than their FP).

Because of the unpredictable effects of most additives in such fibres on their high temperature properties, it is reasonable to expect that further improvements through reformulation will be discovered. In principle any of the aqueous sol-gel processes is capable of easy incorporation of alternative soluble or dispersible additives.

2.7.7. Summary

Silicon carbide fibres whilst having excellent room temperature mechanical properties are subject to degradation at high temperatures due to oxidation to silica and subsequent glass phase formation. Oxide fibres do not suffer from oxidation and are more resistant to high temperature aggressive environments. High alumina fibres are the most common due to the excellent mechanical properties and chemical inertness, but many phase transitions can occur (**Figure 2.2**) during processing to the final stable α form. Pure alumina fibres suffer from grain growth and severe loss of strength as the grain size increases with temperature, so tactics have been developed which inhibit this by controlled seeding of crystals or to form stable intermediate phases using larger quantities of secondary additives such as yttria or magnesia to form aluminates with high temperature creep resistant structures. A draw back to this is the lack of choice and high cost of the precursor materials used. Larger additions of silica are therefore more attaractive because it is economical and there are a number of precursors available, which could potentially create the correct sol system for extrusion. Such products in the past have been either a combination of silica and boric oxide to improve sintering or silca on its own, but none have been produced as a stoichiometric single-phase pure polycrystalline mullite fibre.

2.7.8. Aims

The main aims of this project will be to produce a stable, single-phase, fine-grained polycrystalline ceramic fibre via extrusion of sol-gel precursors. The spinning dope or sol should have a good shelf life enabling extrusion over several days, without the use of organic fugitive fiberising aids which contribute to the volatile components that reduce the final ceramic yield and economics of the material. Tensile strength after heat treatment >1200°C with improved creep properties at temperature, are the intended resulting mechanical properties. The approach will be based on manufacturing small batches of stoichiometric single phase pure mullite fibres using high purity precursors excluding persistent anions such as chloride or sulphate due to their adverse effects on residual porosity, sintering and defect formation.

2.8. References

1. F. Kipping, "Organic derivatives of silicon" J Chem Soc, 1924, **125,** pg 2291.

2. C. Burkhard, "Polydimethylsilanes" J Am Chem Soc, 1949, **71**, pg 963.

3. J. Wesson, T Williams, "Organosilane Polymers - Polydimethylsilylene", J Polym. Sci. Polym. Chem, 1979, **17**, pg 2833.

4. R. West, "Glasses and Composites" In, "Ultrastructure Processing of Ceramics" Chapter 19, L. Hench, D. Ulrich, eds. John Wiley and Sons, New York, 1984.

5. G. Fritz "Formation and properties of carbosilanes" Agnew. Chem Int. 1967, **5**, pg 677.

6. G. Fritz, J Grosse, D. Kummer. "Carbosilanes", Adv Inorg Chem Radiochem 1963, **7**, pg 349.

7. N. Nametkin, V. Wovin, Z. Wyalov. "Use of catalysts with carbosilanes" Izv. Akad Nauk. SSR Serkhim. 1964, **51** pg 203.

8. W. Kriner. J Polym Sci "Catalytic Polymerisation of 1,3-Disilacyclobutane Derivatives" 1966 (**A1**), **4**, pg 444.

9. D. Weynberg, L. Nelson "Platinum catalysed reactions of Silacyclobutanes and 1,3-Disilacyclobutanes" J Org Chem, 1965, **30**, pg 2618.

10. W. Bamford "Preparation and properties of polymethylenes: Use of Various Compounds of Group VII Metals as Catalysts" J Chem Soc, 1966, (**C1**) pg 137.

11. P. Chantrell, P Popper, "Inorganic polymers in ceramics" in chapter 7 "Special Ceramics", P Popper, ed, Academic Press, New York, 1965, pg 87.

12. P. Popper, "New electrical ceramics and inorganic polymers", Br. Ceram. Res. Assoc. Special Publication, 1967, **57**, pg 119.

13. S. Yajima "Continuous silicon carbide fiber of high tensile strength" Chem Lett, 1975, **9**, pg 931-934.

14. R. West, L. David "Polysilastyrene: Phenylmethylsilane-dimethylsilane copolymers as precursors to silicon carbide" Am. Ceram. Soc. Bull. 1983, 62, No 8. pg 899.

15. J. Wesson, T. Williams "Organosilane polymers" J Polym Sci Chem, 1980, **18**, pg 959.

16. J. Wesson, T. Williams "Organosilane polymers – Block copolymers" J Polym Sci Chem, 1981, **19**, pg 65.

17. C. Schilling, J. Wesson "Polycarbosilane precursors for silicon carbide" Am Ceram Soc. Bull 1983, **62**, pg 912.

18. R. Baney, J. Gaul, T. Hilty "Methylchloropolysilanes and derivatives prepared from the redistribution of methlchlorodisilanes" Organometallics, 1983, **2**, pg 859.

19. R. Baney, "Some organometalic routes to ceramics" in "Ultrastructure Processing of Ceramics, Glasses and Composites" John Wiley and Sons, New York, 1984.

20. S. Yajima, K. Okamura, J Hayashi "Structural analysis in continuous silicon carbide fiber of high tensile strength" Chem Lett, 1975, **9**, pg 1209.

21. S. Yajima, K. Okamura, J Hayashi, M Omori "Synthesis of the continuous SiC fiber with high tensile strength" J Am Chem Soc 1976, **59**, pg 324.

22. S. Yajima, C. Liaw, M. Omori, J. Hayashi "Molecular weight distribution of polycarbosilane as a starting material of the silicon carbide fiber with high tensile strength" Chem. Lett, 1976, 9, pg 435.

23. S. Yajima, M. Omori, J. Hayashi, K. Okamura, T. Matsuzama, C. Liaw "Simple synthesis of the continuous SiC fiber with high tensile strength" Chem. Lett, 1976, **9**, pg 551.

24. S. Yajima, Y. Hasegawa, J. Hayashi, M. limura "Synthesis of continuous silicon carbide fibre with high tensile strength and high Young's modulus" J Mat Sci., 1978, **13**, pg 2569-2576.

25. S. Yajima. "Development of high tensile strength silicon carbide fibre using an organosilicon polymer precursor" In: W Watt, BV Perov, eds. Handbook of Composites. Vol. 1. Amsterdam: North-Holland, 1980.

26. S. Yajima "Development of ceramics, especially silicon carbide fibres, from organosilicon polymers by heat treatment" Phil. Trans. R. Soc. London. 1980, Series **A 294**, pg 419-26.

27. S .Yajima, J. Hayashi, K. Okamura "Development of high tensile strength silicon carbide fibre using an organosilicon polymer precursor" Nature, 1978, **273**, pg 525.

28. L. Hench, "Use of inorganic gels for low temperature preparation of glasses" Chem. Rev. 1990, **90**, pg 35-40.

29. O. Lev, "Homogeneous inorganic glass from metal oxide precursors" Analytical Chemistry, 1995, **67**, (1), pg 22A-30A.

30. C. Brinker and G.W. Scherer, Sol-Gel Science: "The Physics and Chemistry of Sol-Gel Processing" Academic Press, Inc.: New York, 1990, pg 261.

31. C. Brinker; G. Scherer, "Sol-gel glass: Gelation and structure" J. Non-Crystalline Solids, 1985, **70**, pg 301-322.

32. K. Keefer, "Silicon Based Polymer Science", Advances in Chemistry1990, **224**, pg. 227-240.

33. J. Ebelmen, "Silicon alkoxide preparation by reaction of $SiCl_4$ with an alcoholic reagent", Ann. Rev. Phys. Chem, 1846, **57**, pg 331.

34. R. Mehrotra, "Metal Alkoxides", Academic Press, New York, 1978.

35. W. Geffcken and E. Berger, "Oxide film preparation" German Patent 736 411. 1939.

36. H. Schroeder, "Preparation of oxide films from alkoxides" Phys. Thin Films, 1969, **5**, pg 87-141.

37. T. Graham, "Use of organic solvents in silica gels" J. Chem. Soc., 1864, **17**, pg 318-327.

38. C. Hurd, "Polymeric structure of silicic acid derived from alkoxide precursors" Chem. Rev, 1938, **22**, pg 403-422.

39. S. Kistler, "Preparation of silica aerogel using the supercritical drying process" J. Phys. Chem., 1932, **36**, pg 52-64.

40. R. Ewell and H. Insley, "Precursor powder preparation from chemical intermediates" J. Res. NBS, 1935, **15**, pg 173-186.

41. R. Barrer and L. Hinds, "Phase equilibria studies of pure binary oxides using chemical starting materials" Nature, 1950, **166**, pg 562.

42. R. Roy, "Phase equilibria in the system $BaTiO_3$ – $CaTiO_3$" J. Am. Ceram. Soc, 1956, **39**, 4, pg 145-146.

43. R. Roy, "Gel route to homogeneous glass preparation" J. Am. Ceram. Soc, 1969, **52**, 6, pg 344.

44. R. Dell, "Reactivity of Solids", (Chapman and Hall, N.Y), pg. 553 - 566, 1972.

45. J. Woodhead, Silicates Ind, 1972, **37**, pg 191-194.

46. L. Levene and I. Thomas, "Process of converting metalorganic compounds and high purity products obtained there from" U.S. Patent 3,640,093, 1972.

47. H. Dislich, "Preparation of multicomponent glasses" Angewandt Chemie, 1971, **10**, 6, pg 363-370.

48. E. Wainer, German Patent 1,249,832, 1968.

49. H. Sowman, "Aluminium borate and aluminium borosilicate articles" U.S. Patent 3,795,524, 1974.

50. S. Horikuri, K. Tsuji, Y. Abe, A. Fukui, and E. lchiki, Japanese Patent 49-108325, 1974.

51. B. Yoldas, "Alumina gels that form porous transparent Al_2O_3" J. Mater. Sci., 1975, **10**, pg 1856-1860.

52. B. Yoldas, "Controlled drying of an alumina hydrate monolith " J. Mater. Sci., 1977, **12**, pg 1203-1208.

53. M. Yamane, A. Shinji, and T. Sakaino, "Sol-gel preparation of a silica monolith" J. Mater. Sci., 1978, **13**, pg 865-870.

54. D. Gaur, "Metal Alkoxides", Academic Press, New York, 1978, pg 225.

55. M. Yamane, S. Inoue and K. Nakazawa, "Controlled hydrolysis of alkoxide precursors" J. Non-Cryst. Solids, 1982, **48**, pg 153-9.

56. S. Govil and R. C. Mehrotta, "Increased solubility of double ethoxides of Al and Mg in organic solvents", J. Org. Chem., 1975, **5**, pg 267.

57. H. Dislich, "Preparation of TiO_2-SiO_2 multicomponent glasses" Angewandt. Chem, 1972, **11**, pg 133-7.

58. B. Yoldas, "Monolithic glass formation by chemical polymerization" J. Mat. Sci., 1979, **14**, pg 1843-9.

59. R. Keller, "The Chemistry of Silica", J. Wiley, New York, 1979.

60. E. Rabinovich, J. Mac Chesney, D. Johnson Jnr, J. Simpson, B. Meager, F. DiMarcello, D. Wood and E. Sigety, J. Non-Cryst. Solids. 1984, **63**, pg 155-61.

61. M. Taylor "Fine Ceramic Fibers", Dekker, Amsterdam, pg 72, 1999.

62. K. Goslins (Unilever Ltd), Eur. Patent Application 79301204.8, 1980.

63. D. Teagarden, "Aluminium chlorohydrate: Physiochemical properties" J Pharm Sci 1989, **70**, (7), pg 762.

64. P. Pusey. "Some Effects of Polydispersity on the Scattering of Radiation by Colloids". Symposium on the Polydispersity Problem in Colloid Science, University of Nottingham, 15-16th September 1987.

65. C. Brinker, G.W. Scherer. "Sol-Gel Science" Academic Press, San Diego, 1990, pg 261.

66. T. Assih, A. Ayral "Raman study of alumina gels" J Mat Sci 1988, **23**, pg 3326.

67. K.A. Karst, H.G. Sowman (Minnesota Mining and Manufacturing Co.), U.S. Patent 4047963, 13 September 1977.

68. T. Wood, D.M. Wilson, H.G. Sowman (Minnesota Mining and Manufacturing Co.), Eur. Patent Application 0294208, 1988.

69. H. Sowman, Aluminium Borate and Aluminium Borosilicate Articles, U.S. Patent 3,795,524, 1985

70. G. Alexander, GH Bolt. U.S. Patent 3,007,878, 1961.

71. H. Uemura, S Ouchi, K Fuada (Toray Industries), Jap. Patent 59211623, 1984.

72. Sumitomo Chemical Co. Ltd. U.K. Patent 1457801, 1976.

73. Y. Kimura Kokai Tokyo Koho, Japanese patent 8288218, 1987.

74. S. Cho, S. Venigalla, J. Adair "Morphological forms of alpha alumina particles synthesized in 1,4-butanediol solution", J. Amer. Ceram Soc 1996, **79** pg 88-96.

75. W. Gitzen, "Decomposition and crystalisation data of intermediate aluminas and hydroxides" J Amer Ceram Soc, 1970, **53**, pg 125.

76. A. Wells. "Structural Inorganic Chemistry", 5th ed. New York: Oxford University Press, 1984, pg 635.

77. H. Sowman "Oxide Ceramic Fibres", Ceram. Eng. Sci. Proc. 1987, **10**, pg 1127 – 1136.

78. D. Lide, "Handbook of Chemistry and Physics", 76th ed. Boca Raton: CRC Press, London, 1995, pg 144.

79. J. Birchall. In: A Kelly, Yu N Rabotnov, eds. "Handbook of Composites. Vol. 1. Strong Fibres", Dekker Amsterdam, 1985, pg131.

80. ICI Chemicals and Polymers Ltd. Saffil Alumina Fibre literature: "Cost Effective Reinforcement for Metal Matrix Composites", 1990.

81. J. Birchall "Oxide Inorganic Fibres", "Concise Encyclopaedia of Composite Materials", Pergamon Press, London, 1989.

82. M. Kumagai, "Controlled transformation and sintering of a boehmite sol-gel by alpha alumina seeding" J Am Ceram Soc 1985, **68** (9) pg 500-505.

83. V. Lavaste, M. Berger, A Bunsell "Microstructure and mechanical characterisation of alpha-alumina based fibres" J Mat Sci 1995, **30**, pg 4215-4225.

84. J. McCardle, "Seeding with gamma alumina for transformation and microstructure control in boehmite-derived alpha alumina" J. Am Ceram Soc 1986, **69** (5):C98-C101.

85. N. Bahlawane, "New sol-gel route for preparation of pure alpha alumina at 950°C" J. Am. Ceram. Soc, 2000, **83**, 9, pg 2324-6.

86. A. Garvish "Influence of additives on the phase inversions in alumina fibres", Ogneupory, 1988, **10**, pg 15-20.

87. K. Lysak "Obtaining polycrystalline alumina fibres", Ogneupory, 1983, **8**, pg 6-9.

88. P. Lessing "Creep of polycrystalline mullite" J. Am. Ceram. Soc. 1975, **68**, pg 149.

89. R. Nixon, "Mullite" Am. Ceram. Soc, 1990, **73**, pg 579.

90. W. Clegg, "The Science of Engineering Ceramics II", Trans. Tech.Publ, New York, 1998, pg 315.

91. C. Dokko "High temperature mechanical properties of mullite under compression" J. Am. Ceram. Soc. 1977, **60**, pg 150.

92. H. Sowmann, US Patent No 4,047,965 "Non Frangible Alumina-Silica Fibers", 1977.

93. J. Simmons, "Preparation of Mullite Based Fibers via Sol-Gel Processing", Ceram. Eng. Sci. Proc., 1990, **11**, 9-10, pg 1512-25.

94. 3M Nextel™ Ceramic Textiles Technical Notebook, Nextel 550 2002, pg 6.

95. M. Stacey "Developments in Continuous Alumina-Based Fibres", Br. Ceram. Trans.J. 1988, **87**, pg 168-172.

96. A. Bhattacharya, A. Hartridge, K. Mallick, "A novel aqueous route for the synthesis of mullite fibre" J Mat Sci Lett, 1996, **15**, pg 1654-1656.

97. H. Sowman, "Sol-Gel Technology", Noyes Publications, New York, 1988, pg 162.

98. 3M Nextel™ Ceramic Textiles Technical Notebook, Nextel 312, 2002, pg 13.

99. J. Rule (DuPont and Co.), U.K. Patent 699557, 1953.

100. Tegopren Silicone Surfactants, Th. Goldschmidt AG. Chemische Fabriken Goldmidtstrasse 100 D4300 Essen 1, Germany, 1990.

101. A. Naumann, Union Carbide Corp. German Patent. 2007209, 1990.

102. A. Hartridge "Synthesis and characterization of partially and fully stabilized zirconia fibres made from an inorganic precursor", J. Mats. Res. 2001, **16**, 8, pg 122.

103. Y. Abe, "Preparation of polycrystalline zirconia fibres using zirconyl chloride sols" J. Mats. Sci. 1998, **33**, pg 1867.

104. P. Chakrabarty "Zirconia fibre mats prepared by a sol-gel spinning technique", J. Eur. Ceram. Soc. 2001, **21**, pg 355 – 361.

105. T. Yogo "Preparation of polycrystalline zirconia fibres from a zirconium butoxide derived precursor" J. Mats. Sci. 1990, **25**, pg 2394.

106. G. Chatterjee, "Zirconium oxide fibers" J. Mats. Sci. Lett. 1990, **9**, pg 845.

107. E. Funkenbusch, (Minnesota Mining and Manufacturing Co.) U.S. Patent 4,937,212, 1994.

108. D. Marshall, "High strength zirconia fibers", J. Am. Ceram. Soc. 1987, **70** (9) pg 187 –88.

109. G. Emig, "Sol-gel process for spinning continuous (Zr,Ce)O_2 fibers" Materials Science and Engineering, 1994, **189**, pg 311 – 17.

110. M. Naskar "Rare earth doped zirconia fibres by sol-gel processing" J. Mats. Sci 1996, **31**, pg 6263 – 7.

111. G. Corman "High temperature creep of some single crystal oxides" Ceram. Eng. Sci. Proc. 1991, **12**, 9-10, pg 1745-1767.

112. A. Apblett, "Polymeric precursors for Yttria" J. Mats. Sci 1996, **31**, pg 6123 – 5.

113. A. Towata,"Preparation of polycrystalline YAG/alumina composite fibers and YAG fiber by sol-gel method" J. Composites, 2001, **32**, pg 1127-31.

114. A. Ikesue "Fabrication of polycrystalline, transparent YAG ceramics by a solid state reaction method", J. Am. Ceram. Soc. 1995, **78**, 1, pg 225-8.

115. S. Sung "Method for making ceramic fibers from a water soluble pre-ceramic polymer solution" (The Babcock & Wilcox Co) U.S. Patent 561,226, 1995.

116. D. Popovich "Fabrication and mechanical properties of polymer melt spun yttrium aluminium garnet (YAG) fiber", J. Adv. Ceram. Res, 1997, 12, pg 322-5.

117. B. King "Polycrystalline yttrium aluminium garnet fibers from colloidal sols" J. Am. Ceram. Soc. 1995, **78**, 8, pg 2141-8.

118. D. Sporn "Ceramic fibres from sol-gel precursors", J.Ceram. Proc. Sci, 1997, **25**, pg 22-4.

119. J. Pasquier, "Synthesis of $MgAl_2O_4$ spinel: seeding effects on formation temperature", J. Mats. Sci. 1991, **26**, pg 3797-3802.

120. K. Jones, "Spinel formation from magnesium aluminium double alkoxides" Mat. Res, 1986, **73**, pg 228-33.

121. R. Bratton "Translucent sintered $MgAl_2O_4$", J. Am. Ceram. Soc, 1974, **57**, 7, pg 283-5.

122. T. Davies, "Preparation of barium hexa-aluminate ceramic fibres and refractories", Brit. Cerams. Trans. 2000, **99**, 2 pg 85-7.

CHAPTER 3 METHODS OF ANALYSIS

INTRODUCTION

Various analytical tools were used to characterise the sol-gel fibres and precursors throughout this study, namely Controlled-Stress Rheometry, Thermal Analysis, Fourier Transform Infrared Spectroscopy (FT-IR), Inductively Coupled Plasma Emission Spectroscopy (ICP), X-ray Fluorescence (XRF), X-ray Diffraction (XRD), Nuclear Magnetic Resonance Spectroscopy (NMR), Scanning and Transmission Electron Microscopy (SEM/TEM).

3.1. Controlled-Stress Rheometry (Cone and Plate)

The equipment used was a Carrimed CSL 500 controlled-stress rheometer (**Figure 3.1**). This is a cone and plate or parallel-plate design in which the material of interest is sheared between a rotating geometry and a stationary base plate. A Peltier heating element is used to control temperature very accurately to 25°C.

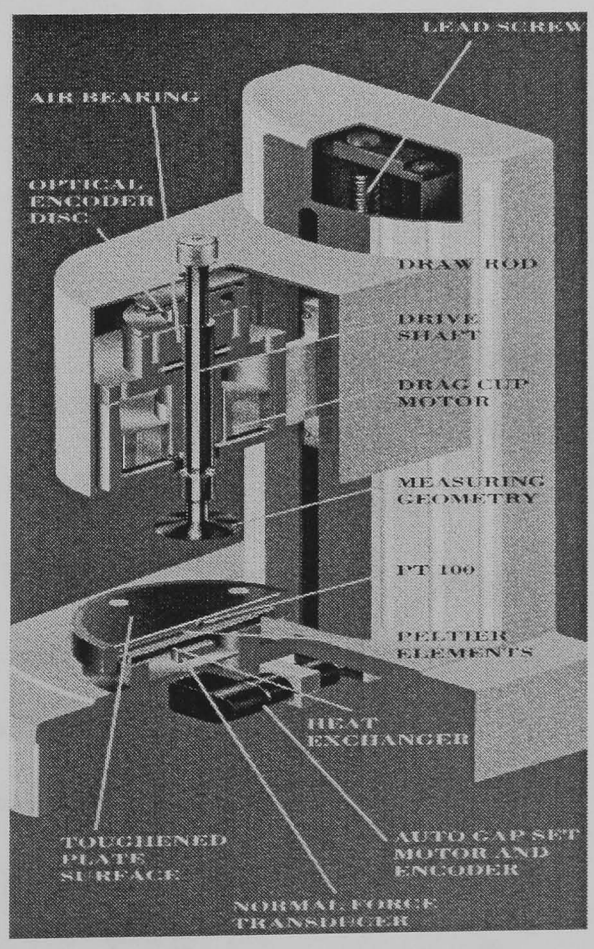

Figure 3.1: Controlled Stress Rheometer Equipment Schematic

The sample is mechanically oscillated at a strain that does not exceed the linear viscoelastic region (LVR) of the material [1]. Both shear stress or rate and viscosity of a sol-gel can be measured using this technique, which gives an indication of how the material will deform during the high shear forces exerted during extrusion through a spinnerette. A capillary rheometer would be better suited for this purpose, as it simulates extrusion, but the standard die holes are in the mm not μm dimensions.

3.2. Thermal Analysis (TGA, DTGA, DSC)

Thermal analysis was carried out on fibre samples in air using a TA Instruments TGA (Thermo Gravimetric Analysis) equipment model STA 1400H (**Figure 3.2**). This allows physical and chemical properties of a substance to be determined as a function of temperature and/or time, while the sample is subjected to a controlled temperature program. In this case both weight loss and the rate (DTGA) at which it occurs with temperature were recorded whilst the sample was heated from room temperature up to 1400°C. In the DSC (Differential Scanning Calorimetry) mode a difference in heat flow to or from a sample and to or from a reference is monitored as a function of temperature [2].

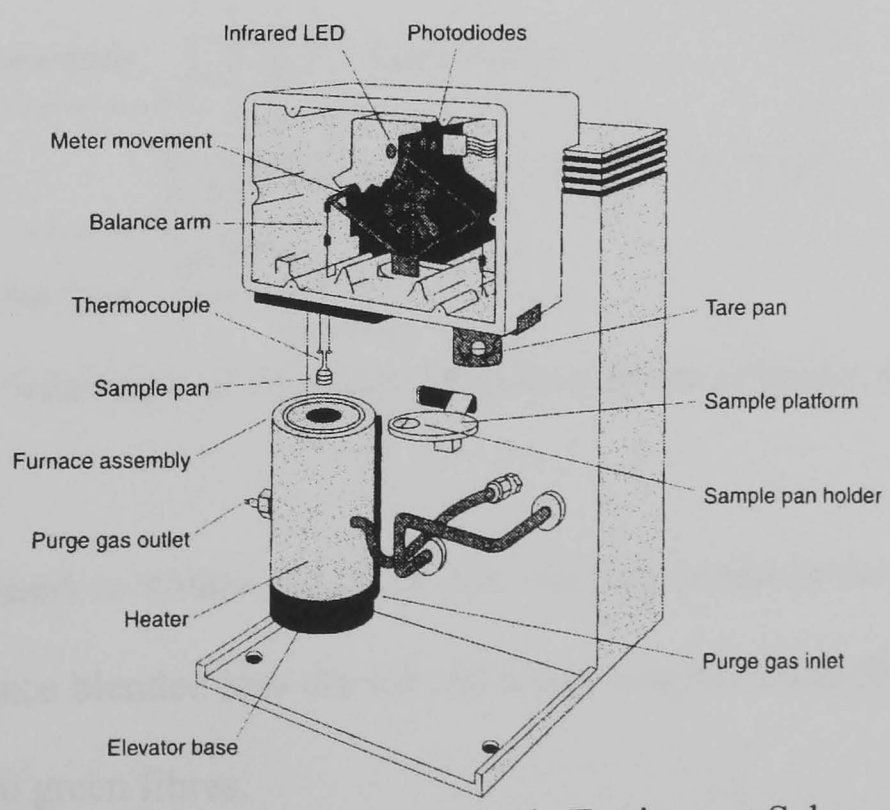

Figure 3.2: Thermo Gravimetric Analysis Equipment Schematic

Negative heat flow (endothermic reactions) in these materials are indicative of evaporation of solvent or other evolved volatiles, whilst a positive heat flow (exothermic reaction) is indicative of pyrolysis of components or heat evolution due to the phase transformation of material from the amorphous to crystalline state.

3.3. Fourier Transform Infrared Spectroscopy (FT-IR)

The equipment used was a Bio Rad FTS-40. An FT-IR Spectrometer is an instrument which acquires broadband Near Infra Red (NIR) to Far Infra Red (FIR) spectra (**Figure 3.3**). Unlike a dispersive instrument, i.e. grating monochromator or spectrograph, an FT-IR Spectrometer (Fourier Transform Infra Red) collects all wavelengths simultaneously (Multiplex or Felgett Advantage). FT-IR is a method of obtaining infrared spectra by first collecting an interferogram of a sample signal (using an interferometer), then performing a Fourier Transform (FT) on the interferogram to obtain the spectrum [3].

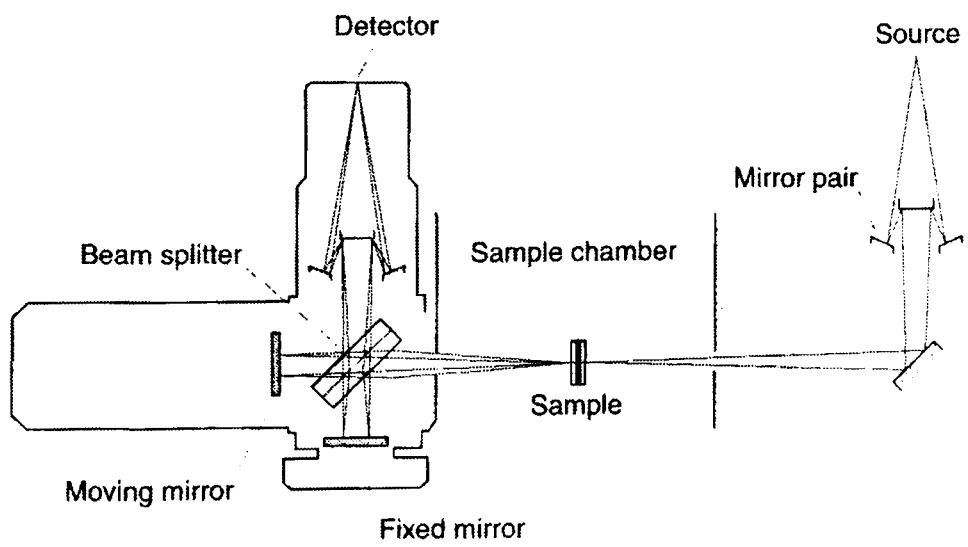

Figure 3.3: Schematic of a Fourier Transform Infrared Spectroscopy

The technique was used to obtain details of the reaction products formed from the precursor systems, once blended into the sol and rotary evaporated to form the sol-gel prior to extrusion into green fibres.

3.4. Inductively Coupled Plasma Emission Spectroscopy (ICP)

The equipment used was a SPECTRO ICP. The analytical principle used in the ICP system is optical emission spectroscopy. A liquid is nebulized and then vaporised with in the Argon plasma and the atoms and ions contained in the plasma vapour are excited into a state of radiated light (photon) emission (**Figure 3.4**). The radiation emitted can be passed to the spectrometer optic, where it is dispersed into its spectral components and from the specific wavelengths emitted by each element, the most suitable line for the application is measured by means of a CCD (Charge Coupled Device) [4]. The radiation intensity, which is proportional to the concentration of the element in the sample, is recalculated internally from a stored set of calibration curves and can be shown directly as percent or measured concentration.

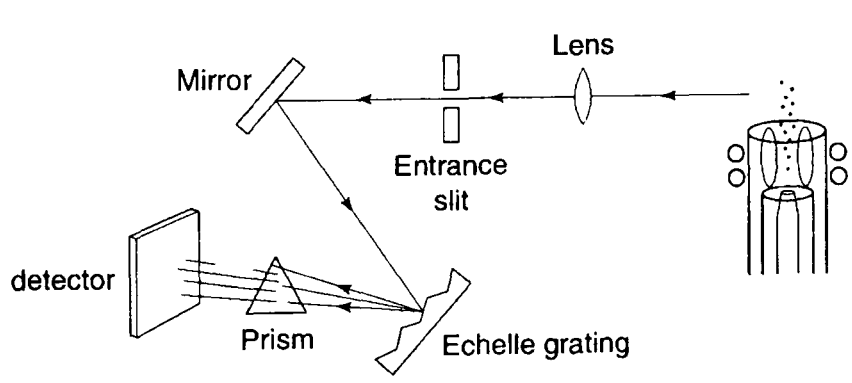

Figure 3.4: Simultaneous ICP Apparatus

The main purpose of using the technique was to determine trace element impurities in the precursor materials being used to produce sol-gels.

3.5. X-ray Fluorescence (XRF)

The equipment used was a Philips PW1480 Wavelength Dispersive XRF, with a Rhodium tube. X-ray spectrometry methods are founded on Moseley's relationship, showing that the reciprocal of the wavelength of characteristic radiation for any given spectral line of a series (i.e. K, L, M etc.) is directly related to the square of the atomic number.

An electron can be ejected from its atomic orbital by the absorption of a light wave (photon) of sufficient energy [5]. The energy of the photon (hν) must be greater than the energy with which the electron is bound to the nucleus of the atom. When an inner orbital electron is ejected from an atom, an electron from a higher energy level orbital will transfer into the vacant lower energy orbital. During this transition a photon may be emitted from the atom and this fluorescent light is called the characteristic X-ray of the element. The energy of the emitted photon will be equal to the difference in energies between the two orbitals occupied by the electron making the transition. Due to the fact that the energy difference between two specific orbital shells, in a given element, is always the same (i.e., characteristic of a particular element), the photon emitted when an electron moves between these two levels will always have the same energy. Therefore, by determining the energy (wavelength) of the X-ray light (photons) emitted by a particular element, it is possible to determine the identity of that element.

For a particular energy (wavelength) of fluorescent light emitted by an element, the number of photons per unit time (generally referred to as peak intensity or count rate) is related to the amount of that analyte in the sample. The counting rates for all detectable elements within a sample are usually calculated by counting, for a set time, the number of photons that are detected for the various analytes "characteristic" X-ray energy lines. Therefore, by determining the energy of the X-ray peaks in a sample's spectrum, and by calculating the count rate of the various elemental peaks, it is possible to qualitatively establish the elemental composition of the sample and to quantitatively measure the concentration of these elements.

In WDXRF spectrometry, the polychromatic beam emerging from a sample surface is dispersed into its monochromatic constituents by the use of an analysing crystal according to Bragg's law. The wavelength for any measured line is computed from knowledge of the crystal parameters and diffraction angles. A selection of crystals is necessary in order to cover the wavelength range of interest. In a sequential WDXRF spectrometer the crystal is turned and the spectrum is measured sequentially scanning the wavelengths by changing the 2θ angle. In both cases the elements and their concentration are identified by the spectral intensities. A lithium tetraborate ($Li_2B_4O_7$) fusion technique was employed to prepare the samples for testing, instead of a pressed pellet technique allowing better homogeneity and a flat, smooth surface morphology. Typically a 1g sample of Tema milled fired fibre would be fused in 10g of flux and a standard oxides program ran to determine the components in the final fired fibres.

3.6. X-ray Diffraction (XRD)

The equipment used was a Philips 1830 X-ray Diffractometer with a twin goniometer and settings were 40mA and 40kV, in the range of 5-70° 2θ. The radiation source was Cu $K\alpha_1$, λ=1.54056. Crystalline structures are described as a periodic array of atoms aligned along a three dimensional lattice, the periodic nature of these structures generates a series of atomic planes oriented in several directions throughout the crystalline lattice. Each atomic plane is repeated periodically and therefore generates a family of plane separated by a specific distance "d" called the d-spacing. Each family of planes is then characterised by its specific d-spacing and by its orientation along the unit cell as defined by the Miller indices (hkl). It can be shown that every crystalline structure generates a unique set of atomic planes and therefore a unique set of d-spacing.

No two crystals can have the same set of d-spacing, hence specifying a set of d-spacing is therefore sufficient to define a structure entirely and it can be shown that the d-spacing's are geometrically related to the unit cell parameters of a crystal. This is the practical basis to determine experimentally crystal structures using X-ray diffraction. In an X-ray diffraction experiment, a beam of X-rays is reflected off subsequent layers of atomic planes at the surface of the crystal. X-rays reflected off the inner atomic layers have to travel an extra path length, which depend on the d spacing "d" and the reflection angle "θ". If this extra path length is equal to an integral number of wavelengths "λ" of the X-ray light, then all the X-rays reflected off subsequent layers are in phase and interfere constructively to produce an intense reflected beam. If not, X-rays reflected off subsequent layers interfere destructively and no reflection can be detected. The geometrical condition for reflection/diffraction is expressed in the Bragg equation $\lambda=2d\cdot\sin\theta$. Hence, by scanning "θ" over a powdered sample of crystal where all possible planar orientation are probable, a beam of X-ray can be detected for each specific value of d spacing. This generates an X-ray pattern exhibiting X-ray peaks at each value of "θ" for which the Bragg equation is satisfied.

The phases formed within the fired polycrystalline fibres are of particular relevance to the expected thermal and mechanical properties and stability. The technique can establish the degree of reaction between the precursors and guide the use of firing schedules for satisfactory conversion to the correct ceramic phases. Low angle work can be used to determine the size of porosity in fibres, with relation to temperature and densification. Crystallite size has also been determined using the peak height method, by comparison with a standard reference material (100% crystalline) for progressively fired fibre samples.

Low Angle XRD Measurements

Low angle XRD analysis has been proven to be useful in determining the size of the voids in synthetic zeolite structures. Hence the technique can also be used to determine the internal porosity due to phase formation and sintering of ceramics as traditional methods such as Specific Surface Area and Helium Picnometry rely on an open pore structure, relying on the intrusion of gas molecules into the pore structure. which is either very fine or enclosed in the fibre core. This non-intrusive technique can therefor detect nano-sized porosity as demonstrated for synthetic zeolite mesoporous structures.

In order to exploit the technique the Bragg Equation must be transposed from;

$$n\lambda=2d \sin\theta$$

Equation 3.1: The Bragg Equation

To;

$$d=\lambda/2\sin\theta \text{ (in angstroms (Å))}$$

Equation 3.2: Transposed Bragg Equation

In order to relate the °2θ values from the xrd scan to the size of the pore in Angstroms and then multipling by 10 converts to nm.

The wavelength of the $K\alpha_1$ Copper X-ray source is:

$$\lambda \text{ Cu}= 1.54056$$

- The pore size in nm is:

$$1.54056/(\sin(°2\theta \times \pi/180)*20)$$

Equation 3.3: Pore Size Calculation in nm

3.7. Nuclear Magnetic Resonance Spectroscopy (NMR)

The spectrometer used for solid state NMR was a Varian UNITY 300MHz Inova with a 7.05 T Oxford Instruments magnet. The resonance frequency for ^{29}Si and ^{27}Al are 60 and 70MHz respectively. Liquid helium (-269°C) is used to cool the innermost part of the superconducting coil, which creates the magnetic field, and liquid nitrogen (-195°C) surrounds it to keep the helium from evaporating too fast. The sample is placed in the top of the spectrometer, where an air jet spins the sample tube to give a more uniform sample to scan. When a sample is made for solution NMR spectroscopy, the solvent or part of the solvent used should be deuterated to replace of the ^{1}H of the solvent molecule. Hydrogen has one proton as its nucleus while deuterium has a proton and a neutron in its nucleus. This is necessary to "lock" the NMR on a specific frequency so the spectrum will not drift around during acquisition. Once the magnetic field is applied and the sample is locked and spinning, a spectrum is acquired. An RF (radio frequency) generator "pulses" the sample with a short burst of radio waves. These waves are absorbed and transmitted through the sample to the receiver, which detects the signal from the sample. This information is then transmitted to the computer where it is translated and analysed.

Nuclear Magnetic Resonance spectroscopy involves the nuclei of atoms, not the electrons and the chemical environment of specific nuclei is deduced from information obtained about the nuclei [6]. Because different nuclei resonate at different frequencies a different frequency radio wave must be used. This also means that similar atoms in different environments, such as hydrogen attached to oxygen and hydrogen attached to a carbon, flip at different frequencies.

By determining at which frequencies these different nuclei flip, it is possible to determine the structure of a molecule. As there are a number of precursors blended together in the sol, it is uncertain how the competing reactions may proceed towards the formation of the final polycrystalline ceramic fibre. The environment of the predominant Si and Al nuclei, which form the mullite crystalline phase can be monitored as they change and related to the XRD data. This helps to determine the expected intermediate path taken during sintering and densification. Both green sol-gels and fibres were fired to progressively higher temperatures and evaluated by this technique.

3.8. Scanning Electron Microscopy (SEM)

The equipment used was a Topcon ABT-60 Scanning Electron Microscope (SEM), using an acceleration voltage typically of 15Kv. SEM is a rapid and non-destructive technique used to investigate the microstructure, morphology and elemental composition of a wide range of materials. The combination of the electron imaging system with the ability to perform elemental analysis (EDX) of very localised or larger areas of the sample makes it a very useful technique for materials investigations and characterisation. In light microscopy, a specimen is viewed through a series of lenses that magnify the visible light image. However SEM does not actually view a true image of the specimen, but rather produces an electronic map of the specimen that is displayed on a cathode ray tube (CRT), (**Figure 3.5)** [7]. Electrons from a filament in an electron gun are beamed at the specimen in a vacuum chamber and the beam forms a line that continuously sweeps across the specimen at high speed which irradiates the specimen and in turn produces a signal in the form of either x-ray fluorescence, secondary or backscattered electrons. The signal produced by the secondary electrons is detected and sent to a CRT image.

The scan rate for the electron beam can be increased so that a virtual 3-D image of the specimen can be viewed. By changing the width (w) of the electron beam, the magnification (M) can be changed where:

$$M=W/w$$

Equation3.4: Relationship Between Magnification and Electron Beam Width

and W is the width of the CRT. Since W is constant, the magnification can be increased by decreasing the width of the electron beam (w).

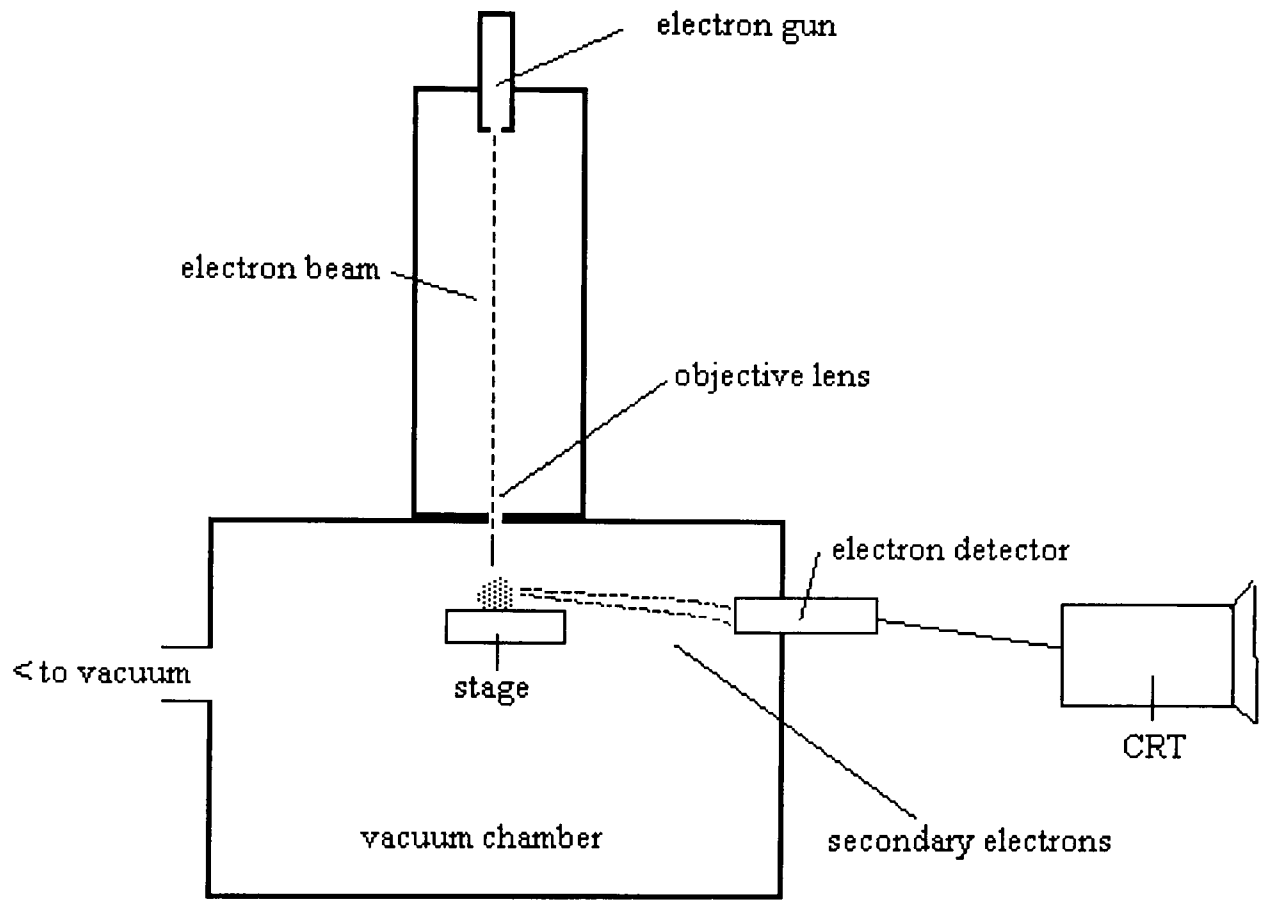

Figure 3.5: Schematic of a Typical Scanning Electron Microscope

Secondary electrons (SE) are formed by the ejection of electrons from the near sample surface as a result of inelastic collisions with the incident electron beam. SE's are low energy electrons (<50eV) and are controlled by the topographical properties of the sample surface.

The advantages of SE imaging over conventional optical microscopy include the much higher resolution and the larger depth of field. SE images show a 3-D perspective of the sample surface. Specimens for SE imaging are normally coated with a conductive layer of gold to prevent the build up of negative charge, which applies to polycrystalline ceramic fibres. Backscattered electrons (BSE) are incident beam electrons emitted as a result of elastic collisions with specimen electrons. BSE's have much higher energies compared to SE's (energies approaching that of the incident beam). The BSE signal intensity from a flat sample is purely a function of atomic number such that heavier elements in the sample will appear brighter in the image than lighter elements. The greater the difference in atomic number the greater the contrast will be. Specimens for BSE imaging should always be flat because sample topography also controls BSE emission, so samples are normally polished to a high standard and coated with a conductive layer of carbon. Qualitative EDX analysis of most elements (including C, N, O, F) is possible [8]. Elemental analysis is achieved by collecting the X-rays generated when the incident electron beam interacts with the atoms of the sample. Each element in the sample produces X-rays with characteristic energies whose peak intensities are related to the amount of the elements present. The energies of these X-rays are converted into electrical signals in a Si (Li) detector and are processed to produce an intensity spectrum in counts per second.

The EDX analyser is also used to display the compositional information in the form of X-ray distribution images or maps. X-ray maps are visually and informative because they show the spatial distribution and relative concentrations of different elements within a sample or a small area of the sample. They are particularly useful at showing up concentration gradients and determining inter-element associations.

General imaging of fired fibres was conducted in the secondary electron mode, to determine the change in surface morphology as crystal phases formed or grain growth occurred. EDX elemental mapping was also used to determine the distribution of elements such as Sulphur during the firing of impure precursor fibres.

3.9. Transmission Electron Microscopy (TEM)

The transmission electron microscope (TEM) has become the premier tool for the microstructural characterisation of materials. In practice, the diffraction patterns measured by X-ray methods are more quantitative than electron diffraction patterns, but electrons have an important advantage over X-rays – electrons can be focused easily [9]. The optics of electron microscopes can be used to make images of the electron intensity emerging from the sample. For example, variations in the intensity of electron diffraction across a thin specimen, called "diffraction contrast," is useful for making images of defects such as dislocations, interfaces, and second phase particles. Beyond diffraction contrast microscopy, which measures the intensity of diffracted waves, in "high-resolution" transmission electron microscopy (HRTEM or HREM) the phase of the diffracted electron wave is preserved and interferes constructively or destructively with the phase of the transmitted wave. This technique of "phase-contrast imaging" is used to form images of columns of atoms. TEM is such a powerful tool for the characterisation of materials that some microstructural features are defined largely in terms of their TEM images.

Besides diffraction and spatial imaging, the high-energy electrons in TEM cause electronic excitations of the atoms in the specimen. Two important spectroscopic techniques make use of these excitations: In energy-dispersive X-ray spectrometry (EDS), an X-ray spectrum is acquired from small regions of the specimen illuminated with a focused electron beam, usually using a solid-state detector.

Characteristic X-rays from each element are used to determine the concentrations of the different elements in the specimen. A schematic diagram of a TEM is shown in **Figure 3.6**. A modern TEM may have the capability of imaging the variations in diffraction across the specimen (diffraction contrast imaging), imaging the phase contrast of the specimen (high-resolution imaging), obtaining diffraction patterns from selected areas of the specimen, and performing EDS spectroscopy measurements with a small, focused electron beam.

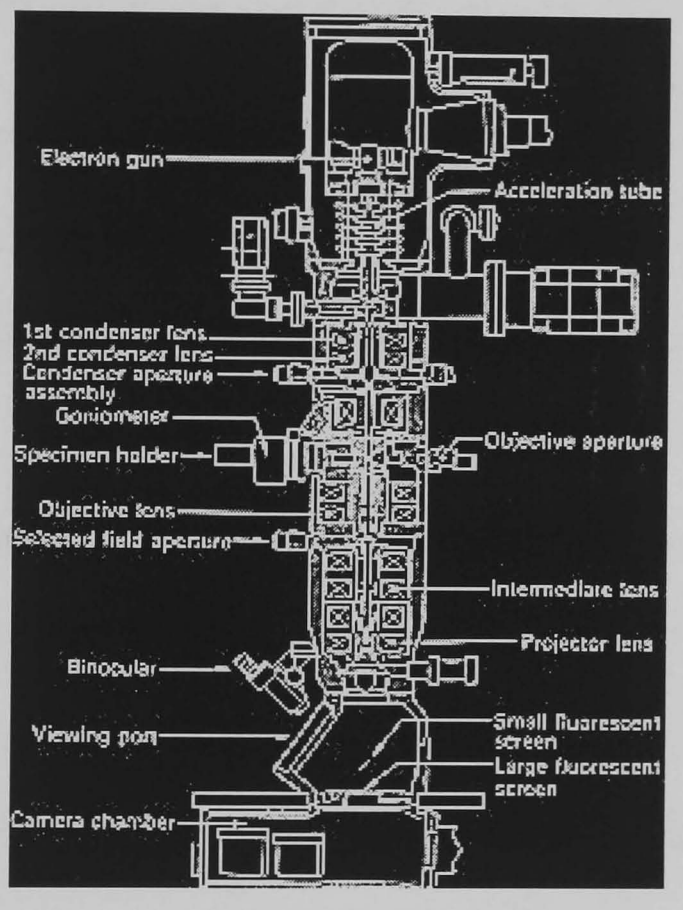

Figure 3.6: Schematic of a Transmission Electron Microscope (TEM)

Thin sections of fibres were prepared by Ion beam milling and analysed on a Jeol 2000 Transmission Electron Microscope, to determine the very fine features of the microstructure (nm), which cannot be seen using SEM. This was particularly useful for observing fine porosity, defects, grain size, residual grain boundary phases and distribution of minor phase additives such as zirconia. Both SEM and TEM are used extensively as characterisation tools in the development of polycrystalline non-oxide and oxide fibres.

3.10 Room Temperature Mechanical Tensile Tests

Room temperature single fibre tensile tests were carried out on a Discaptelec purpose built fibre tensile testing machine. Fibre gauge lengths were typically 25mm, card mounted as illustrated in **Figure 34** using a cross head speed = 3.0mm/min.

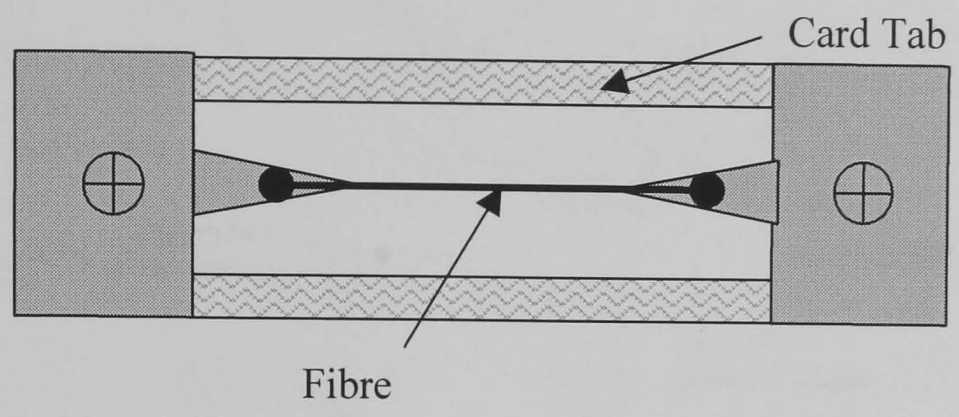

Figure 3.7: Card Fibre Testing Template (For 25mm Gauge Length)

Average fibre diameter was determined using an optical microscope (+/-3μm), described as follows along the length of the fibre.

Diameter measurements

The Watson Image Shearing Eyepiece (WISE) is an optical measurement method, which was used to measure fibre diameters (**Figure 3.8**). A dichromic beam splitter is used to produce red and green images of the object under study (fibre), which are manipulated by mirrors. The eyepiece is calibrated by examining an array of lines, equally spaced at a known spacing. The initial reading on the dial for mirror angle adjustment in the non-shear position is noted and the difference from final reading when full shearing has superimposed a red image from one line on a green image from the next is used with the known spacing of the lines to produce a calibration factor. The difference in readings for zero (position A) and full shear (position C) of the fibre image is then multiplied by the scaling factor to give diameter.

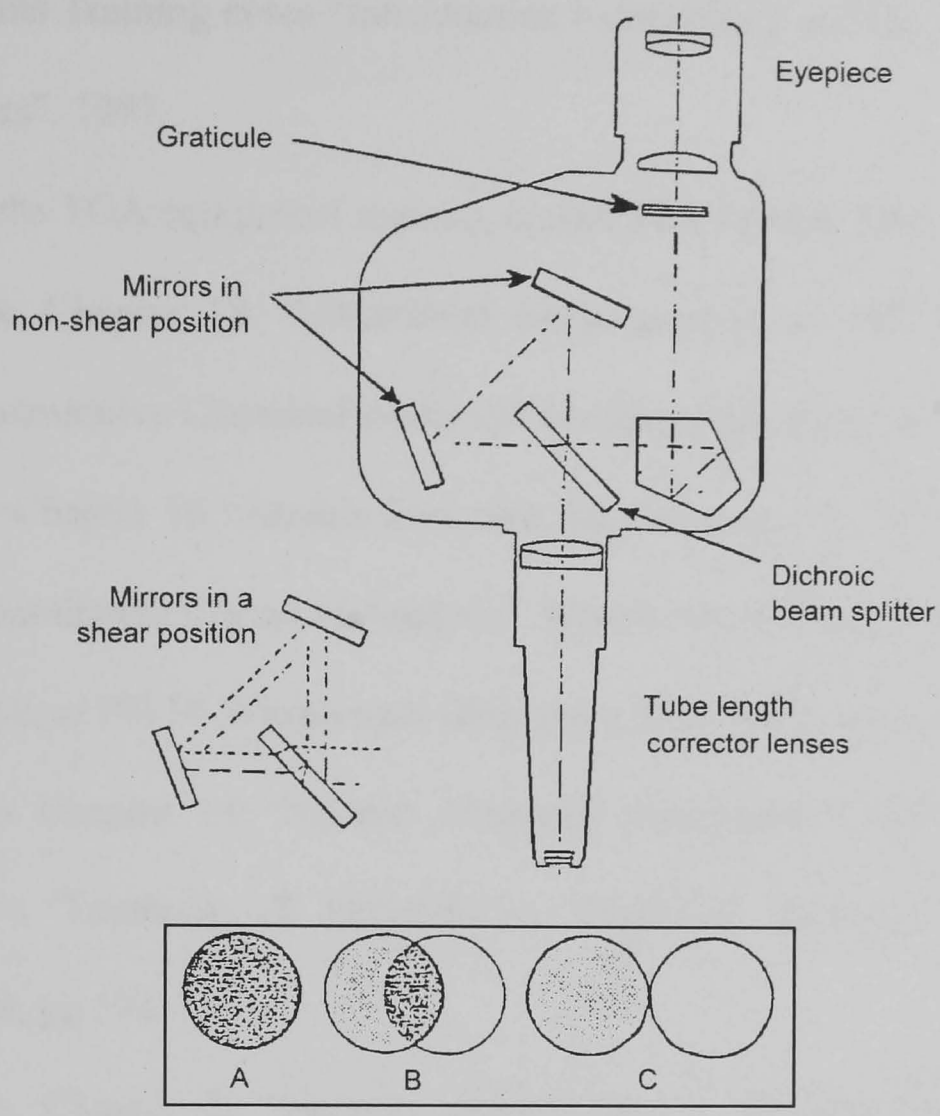

The principal of image shearing from zero shear (A) through half shear (B) to full shear (C)

Figure 3.8: Watson Image Shearing Eyepiece (WISE) Used to Measure Fibre Diameters

Tensile strength is then calculated by:

$$\text{Tensile Strength} = (4 \times \text{Load} \times 10^3)/(\pi * \text{Diameter}^2)$$

Equation 3.5: Calculation of Tensile Strength of a Single Fibre

(Load in N, Diameter in m, Tensile Strength in GPa)

3.11. References

1. TA Instruments Training notes "Introduction to Rheology and the use of controlled stress rheometers", 1997.

2. TA Instruments TGA equipment manual, model STA 1400H, 1992.

3. J. Mendham Chapter 18 "Vibrational Spectroscopy" in "6th Edition Vogel's Textbook of Quantitative Chemical Analysis" Prentice Hall, Singapore, 2000, pg 698.

4. J. Mendham Chapter 16 "Atomic Emission Spectroscopy" in "6th Edition Vogel's Textbook of Quantitative Chemical Analysis" Prentice Hall, Singapore, 2000, pg 624.

5. Philips Analytical PW14 Wavelength Dispersive XRF instrument manual, 1990.

6. J. Mendham Chapter 14 "Nuclear Magnetic Resonance Spectroscopy" in "6th Edition Vogel's Textbook of Quantitative Chemical Analysis" Prentice Hall, Singapore, 2000, pg 571.

7. J. Goldstein, Chapter 2, "Electron Optics" in "2nd Edition Scanning Electron Microscopy and X-ray Microanalysis", Plenum Press, pg 21, 1992.

8. J. Goldstein Chapter 6, "Qualitative X-ray Analysis" in "Scanning Electron Microscopy and X-ray Microanalysis", 2nd Edition, Plenum Press, New York, 1992, pg 348.

9. J. Goldstein Chapter 1, "Introduction" in "Scanning Electron Microscopy and X-ray Microanalysis", 2nd Edition, Plenum Press, New York, 1992, pg 5.

CHAPTER 4 FORMATION OF FIBRES AND FIRING

(PRELIMINARY WORK)

4. FABRICATION AND FIRING OF CONTINUOUS POLYCRYSTALLINE OXIDE FIBRES FROM SOL-GEL PRECURSORS

4.1. General Processing Considerations

A gel is prepared by solidification of a liquid sol, which in the ideal concept is a classical sol of stabilised monodispersed colloidal particles, such as silica sol. Following initial work by Yoldas [1] in the 1970's, a large literature base is now built up on the use of metal alkoxides as sol-gel precursors. The alumina based fibres that are now commercially available and those under development [2] are all made using the sol-gel process. From a simple geometric consideration, the fibre diameters are much smaller than the dimensions of bulk ceramics and the fine scale homogeneity is needed to keep features such as surface texture within viable limits. The principal commonality among all of these is that the fibres are first formed, and then fired under controlled conditions to a ceramic. Processes used for oxide fibres are somewhat similar to those used for some carbon or other non-oxide fibres, essential differences being in the precursors used and the conditions for pyrolysis and sintering. The resulting oxide fibres may comprise amorphous or polycrystalline phases or a mixture of the two. Fugitive organic components may be added to the precursors for their effects on stability of the fiberisable composition or on the rheological properties required for the fibreising process. Preferably, such properties would permit continuous formation of filaments at speeds sufficient for commercial feasibility.

From a technological viewpoint, it would be convenient to divide the sol-gel fibre-making process into a sequence of logical stages as follows:

1. Selection of raw materials
2. Preparation of a spinning solution or dope
3. Spinning of the dope to make a gel fibre
4. Drying and decomposition of the gel to make a porous fibre
5. Sintering and crystallization of the decomposed gel to make a stable, strong ceramic product

It is possible to separate stages 1-3 and drying in stage 4. Decomposition, sintering, and crystallization are not so easily separated and are best considered against the framework of aluminium hydrous oxide and oxide chemistries.

4.2. Wet and Dry Fibre Spinning

The majority of the alumina based fibres are made by dry spinning, in processes whereby the gel is formed by evaporation of solvent. Aluminosilicates are technically made by melt spinning (solidification of a melt). Wet spinning, in which the spinning dope is coagulated in a liquid medium, is not used to prepare alumina fibres. The term dry spinning covers a range of different processes and devices. The continuous alumina fibres in are all extruded as a jet of sol from spinning holes and mechanically drawn onto a rotating drum. The fibres may be drawn initially in air at near ambient temperatures as described by 3M. This avoids over rapid drying of the sol, which causes premature "skinning" of the sol surface before the fibre is fully drawn.

The spinning liquid “sol” must be capable of forming stable jets that can be drawn to fine diameters and then [3], transform smoothly to a solid (in this case gel) fibre, at a rate that is harmonised to allow draw but to suppress the growth of surface ripples in the jetting/draw operation.

The transformation from liquid to solid should be continuous, with the liquid viscosity increasing until a glassy gel is formed without phase change. Researchers have investigated fundamental spinning behaviour in silicate sols made by alkoxide hydrolysis [4]. They concluded that the continuous transformation is a prerequisite that is met in weakly branched structures, enabling high levels of concentration without gelation. The incentive to produce inorganic fibres higher in alumina content than can conveniently be manufactured by melt spinning is twofold. The success of melt spun fibres in thermal insulation at temperatures up to 1400°C led to a demand for fibres capable of use at higher temperatures and the potential high stiffness of alumina rich fibres was attractive for composite manufacture. The high modulus of alumina (α-alumina, 530 GPa), its relatively low density (α- alumina, 4.0 kg/m^3) and its inert nature make it an attractive candidate for metal reinforcement [5]. The low viscosity of molten alumina and its high melting point (2070°C) preclude melt spinning, so that processes had to be developed to avoid the melting step.

4.2.1. The Slurry Process

The process consists essentially of three stages, slurry preparation, yarn spinning and firing. An aqueous suspension of particulate alumina is prepared, the aqueous phase of which may contain dissolved organic polymers to increase viscosity and to stabilise the suspension, together with additives to control grain size at the sintering stage. The aqueous phase may also contain a dissolved alumina precursor (i.e., an aluminum salt) to aid densification at the sintering stage. The slurry is then extruded into air, collected, dried and fired in two steps, an initial firing at low temperature to control shrinkage, and a final flame firing to complete conversion to the high temperature stable form (α-alumina) and to eliminate porosity.

The fired fibre may be coated with a thin layer of silica to increase fibre strength by about 50% as a result of the heating of surface flaws. The major fibres made by this process were Fibre FP [6] and Almax [7] and the diameter of individual filaments was about 20 and 10μm respectively. The grain size of the α-alumina in these fibres is about 0.5μm. The properties of FP fibres have been improved by modifying the composition with 20wt% of tetragonal zirconia. The fibre (PRD 166) showed a 50% improvement in strength over the α-Al_2O_3 FP fibre but otherwise the morphology was the same [8].

4.2.2. Solution or Sol-Gel Spinning

An alternative process to slurry spinning is the spinning of viscous, concentrated solutions (aqueous or alcoholic/hydrocarbon) of aluminum compounds that are precursors to the oxide, followed by the drying and heat treatment of the green gel fibres [9]. A commercial example of a non-aqueous alumina precursor is Sumitomo's patented polyaluminoxane polymer derived from partial hydrolysis of triethylaluminium dissolved in benzene [10]. Basic aluminium salts are popular since they are water soluble (essentially cationic aluminium sols), for example 3M use basic aluminium formate. The hexahydrated aluminium cation, $[Al(H_2O)_6]^{3+}$, is stable only in highly acidic solution and as the solution becomes more basic, hydrolysis of the ion occurs and polymeric species are formed in which aluminum atoms are linked by oxygen bridges. Eventually, complex polynuclear species such as $[AlO_4Al_{12}(OH)_{24}(H_2O)_{12}]^{7+}$ are formed [11]. The viscosity of solutions containing such species rises rapidly with the equivalent Al_2O_3 content and, at an equivalent Al_2O_3 concentration of about 45 wt%, a gel or glass like solid is produced.

In the preparation of alumina fibres, a syrupy solution of a basic aluminum salt (i.e. aluminium chlorhydrate) is prepared, to which may be added soluble organic polymers to control rheology (spinning aids), and sources of oxides such as SiO_2, MgO, B_2O_3 may be added as grain-growth inhibitors. The viscosity of the solution used for spinning will depend on the type of spinning process to be used and the type of fibre it is desired to produce staple fibre or continuous filament. For continuous filament, a solution having a viscosity between 10 and 100 Pas is desirable. This is extruded through spinnerette holes between 100 and 200 μm diameter into dry air (<65% RH) and the fibre drawn down in diameter during collection. When discontinuous fibre is to be produced, centrifugal spinning may be used, in which droplets of solution are projected into dry air from a rapidly rotating disk; or gas-attenuation spinning may be employed, in which fibres are produced by drag in a stream of gas. For this type of spinning, solutions having a viscosity between 0.5 and 2.0 Pas will be used, in which the equivalent $A1_2O_3$ concentration is 25-30 wt%.

Drying of the fibres in flight produces solid-gel fibres containing the equivalent of 45 wt% $A1_2O_3$. Other methods investigated include soaking an organic textile fibre (usually cellulose) in an inorganic salt solution, heating to burn out the organic material, and then firing to sinter and densify the oxide relic [12]. The relic process has been successfully adapted to making ZrO_2 fibres [13] and is used by Zircar USA in the manufacture of these and other less common oxide fibres, such as lanthanide and actinide oxides.

4.2.3. Filtration

Control of particulate is a problem when sols are spun through holes; the critical particle sizes are much smaller than the hole diameter.

Both 3M and ICI patents mention filtration down to the 1μm level, with the finer holes (50μm) being particularly sensitive to blockage. Rates per spinning site are higher in centrifugal spinners, where holes are not essential and spinning can be done from cup or vain atomizers, inertial forces predominate in the discharge of fibres from the spinning atomizer, and speeds of more than 10,000 rpm may be used on a 10cm wheel. These spinners will operate without protective filtration, but the disturbances caused by particulate are ejected from the spinning area and appear as shot, which is intimately blended with the fibre.

4.2.4. Rheology For Spinning

Spinning Aids and Spinning

Researchers such as Brinker have shown that linear species in solution are not essential for spinnability [4], however the process is greatly improved if the sol does contains such polymers or additives. Alumina fibres either contain linear long chain polymers (polyethylene oxide – "Polyox™") or a linear structure can be created in the precursor sol. The length of the stable Newtonian jet or ability to form a continuous length of unbroken sol when extruded through a spinnerette hole is given by the equation derived by [14]:

$$L=12d_0(We^{0.5}+3We/Re)$$

Equation 4.1: Stable Newtonian Jet Length of a Sol During Extrusion

where We is the Weber number = $U_0^2 d_0 p/\sigma$ for flow from the hole and Re is the Reynolds number = $U_0^2 d_0 p/\eta$, p = solution density, σ = surface tension, η = viscosity

The viscosity, hole diameter and solution velocity in the hole are characteristics of most variation. Whilst a fibre is being drawn it reaches its final diameter quickly, so that in an ideal Newtonian case the approximate time of flight in the stable region would be given by:

$$t_{approx} = \text{stable jet length/windup rate}$$

Equation 4.2: Period of Stable Newtonian Jet Length of a Sol During Extrusion

The idealised (Newtonian) drying times are too short in the staple centrifugal spinning processes and a linear polymer spinning aid is needed to increase the stable jet length to give the fibre time to dry and avoid atomisation. Bayer showed that linear polymers in solution could cause huge increases in stable jet lengths in low viscosity systems. As the sol concentration and viscosity is normally higher for extruded continuous fibres, it would be expected that stable jet length should increase. It has been demonstrated that this is not the case in real systems [15], where the continuous transition from liquid to solid implies a viscoelastic region. Ziabicki suggested that jet integrity is derived from the cohesive energy density of the material, and in practice the stable jet length starts to decrease at high measured viscosities. The cohesive energy density changes with the material, and an approximate ranking of systems, and the ease of spinning, is given by the spin/draw ratio(s) achievable in a real process:

$$\upsilon = U_L/U_0$$

Equation 4.3: Cohesive Energy Density Change with Spin/Draw Ratio

where U_L is the fibre windup velocity and U_0 the velocity in the spinning holes.

Spin draw ratios can be increased by the addition of a small percentage (<1%) of linear chain polymers, increasing the liquid throughput in the spinning holes improving the economy of the spinning process. A larger hole size can increase liquid throughput, are easier to clean and facilitate the introduction of particulates into the sol.

At a fixed liquid rate, shear rate in the holes given by:

$$\gamma = (32 \times \pi) \times Q/\pi r^2$$

(Q = liquid rate and πr^2 = area of spinneret hole)

Equation 4.4: Shear Rate of a Sol During Extrusion

The rate of shear is reduced and deposition of particulates on the hole wall [16]. Preferred spinning aids are polyethylene oxide (PEO) of intermediate molecular weight (~ 2000-10000) or polyvinyl alcohol (PVA) of ~2000.

4.2.5. Drying.

Once the still plastic gel filament is formed from the sol, it is vulnerable to internally generated vapour [17] and decomposition products. An aqueous aluminium chlorhydrate gel filament when dried contains more than 40% alumina along with 10 - 25% free water, which must be carefully removed in the first stage of heat treatment. Rapid heating causes boiling of the solvent and results in blistering and macroporosity in the fibre. Mild drying conditions are required for the first 300°C or so and control of humidity may be required, as the vapour pressure for water is high, the drying rate slows above this. All of these points are important considerations that are required when formulating a system for the manufacture of a continuous fibre with good mechanical properties, once converted to the polycrystalline ceramic oxide form.

4.3. Mullite As A Material For Use in Polycrystalline Continuous Fibres

In terms of physical properties, mullite ($3Al_2O_3.2SiO_2$) is a refractory ceramic oxide, combining a high melting point (1920°C), low thermal expansion, intrinsically low creep rate (for a specific grain size), good mechanical strength and inertness at high temperatures in oxidising atmospheres [18]. A major factor in selection of mullite as a complex oxide was the low cost and large number of readily available precursors for sol spinning. Although there are a large number of aluminium and silicon precursors, which have been used for mullite synthesis, there are specific requirements for fibre spinning concerning the development of an air stable sol with appropriate rheology, whilst achieving complete densification after pyrolysis. The absence of excess alumina should give an improvement in microstructural stability, above ~1200°C, (unlike the Nextel 720 alumina -mullite fibre) which suffers from the intervention of metastable pseudo tetragonal phases (2:1 mullite) coupled with the exsolution of residual alumina phase, with associated loss of strength [19]. The preferred stable phase is orthorhombic (3:2) mullite as identified by the resolved doublet peaks at 26° 2θ corresponding to the {120} and {210} planes seen using XRD.

4.3.1. Precursor Selection For Sol-Gel Fibre Production

The precursor choice may be a combination of alkoxides or colloidal dispersions (or mixtures of these types) and may also include the addition of an inorganic salt. The different mixtures produce different levels of molecular homogeneity, alkoxides developing Al-O-Si bonds in the pre-mullite gel whilst colloidal dispersions remain chemically distinct until the reaction sintering stage. A variety of silicon and aluminium precursors are available, some displaying problems at either the spinning or the fibre pyrolysis stage.

For example, aluminium chlorhydrate (ACH) is particularly desirable as an alumina precursor as it is extremely water soluble, forms extrudable gels and yields 45-48% Al_2O_3 after thermal decomposition. However this always results in porous fibres [20] presumably due to Cl^- (17% in ACH) loss during the pyrolysis/sintering steps, illustrated in **Figure 4.1**:

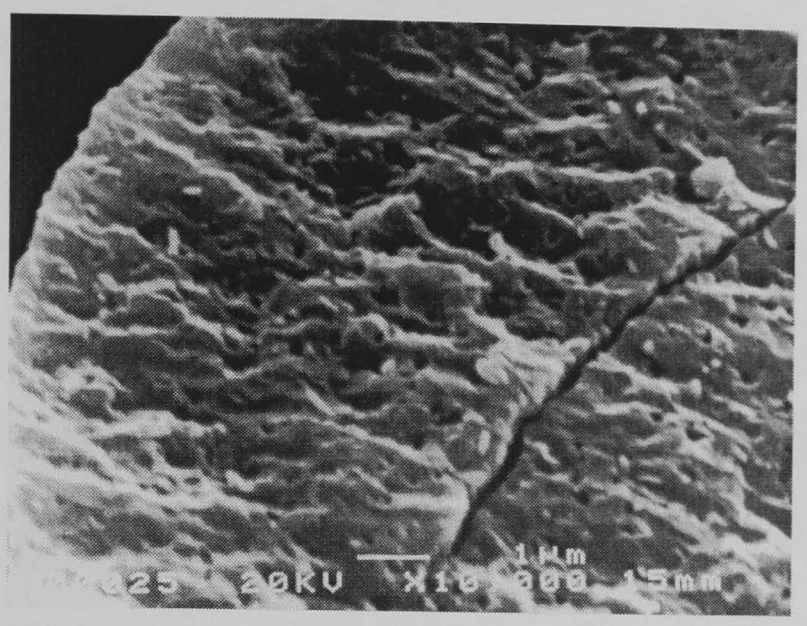

Figure 4.1: SEM Micrograph of an ACH/SiO_2 fibre fracture surface fired at 180°C/hr to 1400°C/4 hrs.

Work by [21] also reported high levels of porosity and bloating on the fibre surface when using ACH as a precursor. He attributed this to the high decomposition temperature of the Cl^- ions, and came to the conclusion that "ACH was an inadequate starting material for the preparation of dense mullite fibres". 3M have stated that chloride causes weak fibres and recommends ~ 1% of chloride based on the refractory oxide content of the precursor solution, or less than 0.2% chloride in the final ceramic [22]. Compared to alkoxides chloride precursors are known to give a more bottlenecked pore structure, and generally a coarser structure in catalysts [23]. It is speculated that residual chloride moves to the surface of the pores and coarsens the structure by increasing grain boundary mobility. Fibres of reasonable quality can, however, are made from chlorhydrates when additional precautions are taken.

The ICI Saffil and Safimax spinning solutions contain a surfactant and by control of spinning conditions are drawn at about 10°C below the surfactant precipitation temperature or cloud point [24]. At this condition the surfactant micelles have grown large enough to be aligned axially by the spinner draw but not so large that they form oversized macropores on decomposition. The ceramic product is 40% porous with an accessible area near 150 m^2/g. The average pore diameter is 5 nm, and 80% of the pores are axially aligned. The fibres demonstrated good tensile strength and stiffness in the porous condition, and were more likely to sinter to a dense product. Du Pont advised that strong fibres could not be made from a spinning solution where all the ceramic is derived from aluminium chlorhydrate. Following bulk ceramic practice they recommended that at least 40% of the fibre is derived from a dispersion of α-alumina in chlorhydrate.

The addition of fine alumina, as well as seeding the gel, will reduce the shrinkage forces in what is quite a large diameter fibre and prevent cavities forming during the earliest stages of decomposition. Therefore from these observations and results the use of alternative alumina precursors, free from Cl^- ions was considered to be the right way to proceed. In order to proceed with the selection of appropriate precursors for the fabrication of stochiometric mullite polycrystalline fibres, the following considerations must be applied:

- Chloride free (or equally a persistent anion free i.e. SO_4^{2-}) system
- High purity
- Relatively inexpensive
- Water soluble (inexpensive solvent)
- Stable in air (no expensive process conditions)

- Easy to handle by-products from synthesis
- Gel formation tendency, rather than crystallisation due to saturation
- Naturally viscoelastic sol
- Stable rheology with time
- Newtonian shear behaviour
- Controllable drying characteristics
- High ceramic yield
- Dense, strong, thermally stable fired ceramic microstructure

Newtonian shear behaviour is a very important characteristic for extrusion of continuous fibres and is often not considered by the researcher in the literature. Initial experiments can rely on pulling fibres by hand, using an attenuation device such as a glass rod for individual fibres or a hairbrush for multiple fibres. This technique allows acquisition of fibres of the diameter of interest, to study the most of the points above, but will not ultimately determine if the material can be easily processed by extrusion through a spinnerette into a continuous fibre.

Considering the attributes required, a review of the mullite precursor systems in the literature and commercial fibre production indicates that the alumina precursor is key to obtaining the desired properties. Alumina is the highest weight percentage proportion and will influence the properties of the sol considerable. Generally the alumina precursor forms the gel network, due to its extensive aqueous chemistry, which will dictate the rheology, formability and drying characteristics of the sol during its processing into green precursor fibres. Looking to the most common potential precursor systems identified before in **Table 4.1** there are limited options for precursors with similar alumina yield to aluminium chlorhydrate (ACH).

Al_2O_3 Precursor	% Al_2O_3 Yield
Pyrogenic Fumed Al_2O_3 (Powder) - δ - Al_2O_3	~99
Fine α- Al_2O_3 (Powder)	>99
Spray Dried Boehmite (Powder) - AlOOH	~70
Aluminium Chlorhydrate (Powder) - $Al(OH)_5Cl$	~48
Basic Aluminium Formoacetate (Powder) - $AlOHOOCHOOCH_3$	~37.5
Basic Aluminium Acetate (Borate Stabilised - Powder) - $(Al(OH)_2(OOCH_3).^1/_3H_3BO_3)$	~32.8
Fumed Al_2O_3 Colloidal Sol - δ - $Al_2O_{3\,(aq)}$	~30
Aluminium Chlorohydrate Soln - $Al(OH)_5Cl_{\,(aq)}$	~23
Aluminium Isopropoxide (Powder) - $Al(OC_3H_7)_3$	~25
Aluminium Chloride ($6H_2O$ - Powder) – $AlCl_3$	~21.1
Aluminium Sec-Butoxide (Liquid) - $Al(OC_4H_9)_3$	~20.7
Boehmite Colloidal Sol – $AlOOH_{\,(aq)}$	~20
Aluminium Di-Isopropoxide aceto acetic ester chelate (Liquid)	<20
Aluminium Nitrate ($9H_2O$) (Powder) - $Al(NO_3)_3.9H_2O$	~13.6

Table 4.1: Potential Alumina Precursor Materials for Sol-Gel Fibre Preparation

Aluminium chloride, whilst being highly soluble, contains chloride ions, does not form a gel easily and is prone to crystallisation when saturated. This can be overcome by dissolution of further aluminium metal, again forming an ACH precursor. Precursors such as boehmite, pyrogenic or alpha alumina powder have very high yields of alumina and have no organic content. Limited aqueous solubility will not provide a viscoelastic sol/suspension, thus requiring additional organic fiberisation aids for filament formation. Aluminium formoacetate and basic aluminium acetate (BAA) are normally very insoluble without the addition of a stabilising anion. A modified BAA is used by 3M in the manufacture of Nextel 312, 440 and 480 (boron modified mullite) using borate as a stabilising anion. A significant proportion of unwanted boric oxide results, as $^1/_3$ of a mole is required to stabilise each mole of BAA. This can greatly reduce the refractoriness (compared to stochiometric mullite - $3Al_2O_3.2SiO_2$) as the melting point is suppressed and boron will volatilise as $Al_2O_3.^1/_2$ B_2O_3 above 1035°C [25], according to the phase diagram data in **Figure 4.2**:

Al_2O_3–B_2O_3–SiO_2

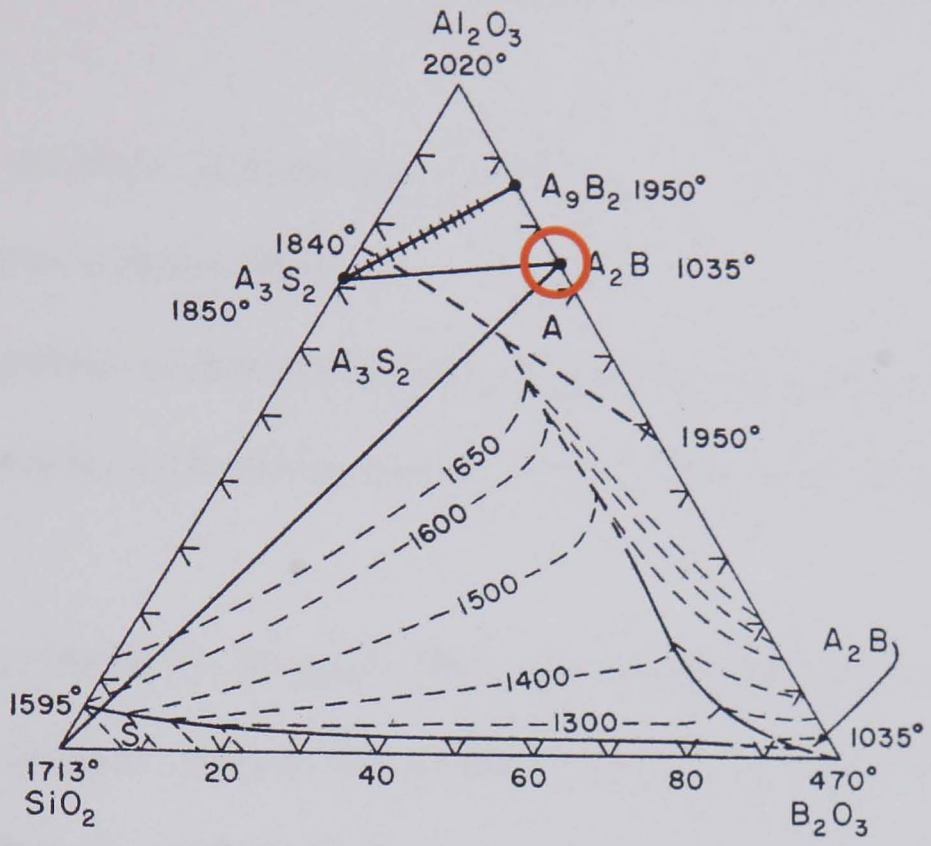

Figure 4.2: Al_2O_3 - SiO_2 - B_2O_3 Ternary Phase Diagram

Considering these facts, it seemed likely that potential precursors should be limited to hydrolysable aluminium alkoxides and a water soluble aluminium salt absent of persistent anions, such as a carboxylate. Two systems were selected for preparation of high alumina mullite sol-gels for the purpose of making hand drawn then extruded fibres.

4.4. References

1. B. Yoldas "Alumina gels that form porous transparent Al_2O_3" J. Mat. Sci, 1975, **10**, pg 1856-1860.

2. D. Wilson "New High Temperature Oxide Fibres", 3M Co., St. Paul, MN, Research Literature on web site, 2004.

3. O. Faust, "Practicalities of spinning technology" Kolloid. Zeits. 1932, **61**, pg 257.

4. C. Brinker, R. Assink "Spinnability of silica sols" J. Non-Cryst Solids 1989, **111**, pg 48-54.

5. A. Dhingra "Advances in Inorganic Fibre Developments", in "Contemporary Topics in Polymer Science", Plenum Press, New York, 1982, pg 227 – 60.

6. Du Pont, USA Patent 3, 808,015, 1972.

7. Mitsui Minning Co Ltd, European patent 260868-A, March 1988.

8. A. Bunsell "Microstructure and Mechanical Characteristics of α-Alumina Based Fibres", J. Mats. Sci, 1995, **30**, pg 4215 – 4225.

9. P. Brache "Inorganic Composites Materials – A Survey of Recent Developments", Pergamon Press, London, 1994.

10. Y. Abel, ICCM – IV, "Progress in Science and Engineering Composites", Ceram. Eng. Sci. Proc, 1982, **5**, pg 1427 – 1434.

11. H. Sowman "Oxide Ceramic Fibres", Ceram. Eng. Sci. Proc, 1987, **10**, pg 1127 – 1136.

12. J. Birchall "Alumina Fibres: Preparation, Properties and Applications", Ceram. Eng. Sci. Proc, 1985, **8**, pg 115 – 53.

13. B. Hamling, US Patent 3, 860,529 Union Carbide, Jan 1975.

14. C. Weber "Stable Newtonian jet length during extrusion" Math. Mech. **11**, Pg 136, 1931.

15.A. Ziabicki "Fundamentals of Fiber Formation", J. Non-Cryst Solids 1987, **109**. pg 48-54.

16. M. Von Smoluchowski "Mathmatical theory of the coagulation of colloidal particles" Z. Phys. Chem. 1917, **92**, pg 129.

17. R. Dwivedi, "Drying behaviour of alumina gels" J Mat Sci Lett 1986, **5**, pg 373-376, 1986.

18. A. Alper "High Temperature Oxides" Part IV, Academic Press, New York, 1971, Pg 37-76.

19. F. Deleglise "High temperature behaviours of two nanocomposite oxide fibres", Key. Eng. Mat. 1999, **164**, pg 265.

20. S. Andrew, "Theory and practice of the formulation of heterogeneous catalysts" Chem. Eng. Sci, 1981, **36**, 9, pg 1431-1435.

21. K. Okada "Mullite Long Fibres Prepared By Sol - Gel Method Using Water Solvent System", Key Engineering Materials Vols. 1997, **132**, pg 1946-1949.

22. K. Karst, Minnesota Mining and Manufacturing Co, U.S. Patent 4047963, 13 September 1977.

23. S. Andrew, "Theory and practice of the formulation of homogeneous catalysts" Chem. Eng. Sci 1981, **36**, 9, pg 1483-1492.

24. M. Stacey, Imperial Chemical Industries PLC UK GB, Eur. Patent Application 881117, p13. Patent 318203, 1987.

25. P. Gielisse, System Al_2O_3-B_2O_3-SiO_2, Quart.Prog. Rept., 931-8, The Ohio State Univ. Res. Foundation pg 6, 1961 in "The American ceramic society "Phase Diagrams for Ceramasists", 1964 and 1969 volumes: Al_2O_3 - SiO_2 - B_2O_3 (Fig 763), 1964.

CHAPTER 5 EXPERIMENTAL POLYCRYSTALLINE FIBRE PRODUCTION USING CHLORIDE FREE MULLITE SOL-GELS

5.1. Alkoxide Mullite Sol

The first sol is based on an alkoxide/inorganic salt system that does not contain any chloride ions and has been demonstrated to form fibres by hand drawing, but not extrusion. Okada [1] studied this aqueous non volatile system using water as the solvent with aluminium nitrate (AN - ~14% Al_2O_3), aluminium isopropoxide (AIP – 25% Al_2O_3), and tetraethylorthosilicate (TEOS), at various AIP:AN ratio's in that order of addition. The AN imparts an acidic environment to assist in the hydrolysis of AIP and TEOS to give a stable clear sol according to the following simplified reaction scheme:

(AN) (AIP) (TEOS) (Aluminosiloxane)

$$Al(NO_3)_3 + 2Al(^{Ipr}C_3H_7O)_3 + Si(C_2H_5O)_4 + [H_3O]^+ \Rightarrow -[Al\text{-}O\text{-}Si]\text{-}_n + 6C_3H_7OH + 4C_2H_5OH$$

Equation 5.1: Hydrolysis of Mullite Alkoxide Sol Precursors

A large organic content is then removed as alcohol during the rotary evaporation, sol concentration stage. Okada reported that an AIP/AN Ratio <0.5 results in thixotropic flow (shear thickening) and no fibre formation. A ratio of >0.5 results in pseudoplastic (shear thinning) flow and a poorly spinnable solution whilst Newtonian flow and fibre formation results from a ratio of 1:1 or more preferable 2:1. The additional AIP was reported to suppress the three dimensional polymerisation of TEOS to colloidal silica sol [2]. Fibres could be drawn by hand to 100 cm, with a homogeneous - Al - O - Si - intermediate gel backbone, with a ceramic yield of ~50% and crystallised to dense, pore and crack free polycrystalline mullite when fired to 1000°C.

In order to evaluate the claims a sol was made using the preferred AIP/AN Ratio of 2:1, according to Okada, as follows:

1. Distilled Water – 2988g

2. Aluminium nitrate nonahydrate 98% – 900g (Aldrich, 23,797-3)

3. Aluminium isopropoxide 98% – 979.2g (Aldrich, 22,041-8)

4. Tetraethylorthosilicate (TEOS) 98% – 457.6g (Aldrich, 190-3)

5.1.2. Mixing Procedure

Okada's paper did note advise on the order of addition of precursors, it was necessary through experimentation to change the above sequence to produce a clear colourless sol. Aluminium nitrate (AN) was added to the distilled water and mixed using a Silverson high shear mixer until completely dissolved. The aluminium isopropoxide (AIP) powder was added slowly to the mixture and the temperature was not allowed to rise above 30°C (hydrolysis of AIP was found to be exothermic) as a white hydrated aluminium hydroxide precipitate would form. The use of a water bath with the addition of ice or ammonium chloride was used to cool the sol during mixing.

Hydrolysis of aluminium isopropoxide evolves isopropyl alcohol, which improves dispersion of tetraethylorthosilicate (TEOS) within the aqueous solvent. TEOS is added slowly over a period of around 20 min. The sol, when completely mixed, is then filtered using a Whatmann No 1 filter paper assisted be a vacuum pump to remove any particulate contamination. Once the sol had been made it required rotary evaporation at reduced pressure in order to reduce the volume of solvent and increase the sol viscosity.

5.1.3. Rotary Evaporation

After initial blending and hydrolysis of the precursors, the resultant intermediate sol was processed further, via rotary evaporation, to remove excess solvent and some reaction products (i.e. organic acids, alcohols, esters) with the aim of forming a viscous Newtonian liquid, having low shear characteristics under shear stress (during extrusion). The batch of sol was rotary evaporated using a 10 litre Buchi R152 Rotavapor (**Figure 5.1**).

The process exploits the reduction in boiling point of a liquid (or mixture of liquids) under reduced pressure to allow distillation of solvents and reaction products at near ambient temperature. The air tight system was evacuated by means of a controlled vacuum pump and the sol was rotated in the evaporation flask, whilst partially submerged in a heated bath of water. Evaporation of the most volatile component(s) proceeds first i.e. alcohols and organic acids, followed by water. The vapour condensed in the water-cooled column and the condensate was collected in the flask. To avoid vapour condensation inside the vacuum pump chamber and spoiling the innards, a cold finger trap was constructed in line between the apparatus and the pump. This involved connecting a quickfit glass "finger trap" in line, which was submerged in a dewer of liquid nitrogen. The vapour that passes through the finger is dried by virtue of vapours present condensing and freezing out at sub –190°C temperatures.

Typical conditions used are as follows:

Water Bath	40°C
Flask Revolution	45rpm
Flask Volume	3 litre for 3 kg, 10 litre for 6 kg batch
Vacuum Pump	70Mb +/-3 (Initial Setting)
Vacuum Pump	20Mb +/-3* (Final Setting)
Liquid Nitrogen	Approx every 30 mins (Dewer Refill)

*It is important to note that the pressure was gradually decreased in increments of 10Mb from 70 to 20Mb, between which, the sol was allowed to settle and the time recorded for future reference. The yield of extrudable sol depended on the system used and its viscosity, which in turn dictated the evaporation duration. The sol was processed until the viscosity was such that fibres could be drawn by hand using a glass rod, in ambient air.

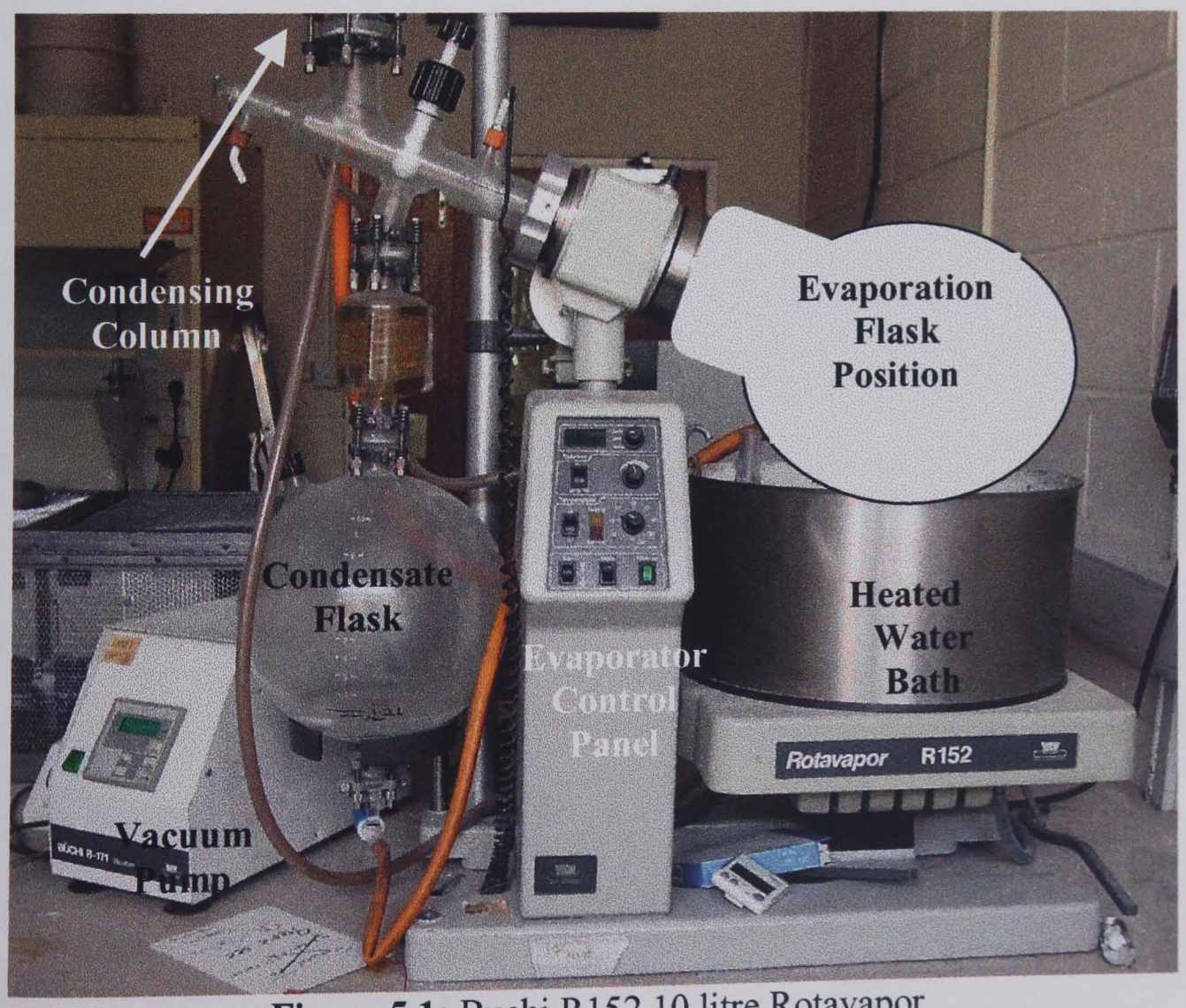

Figure 5.1: Buchi R152 10 litre Rotavapor

5.1.4. Fibre Formation, Stability and Rheology

The sol was hand drawn into short fibres (up to 5cm) using a glass rod and exhibited elasticity and hygroscopic characteristics when left exposed to the air. A gravimetric experiment was conducted exposing the sol to the atmosphere for 24hrs on a watch glass at 25°C. A weight gain of ~5% was recorded, confirming absorption of moisture from vapour, which may have been due to the aluminium nitrate which normally exists as the nonahydrate ($Al(NO_3)_3.9H_2O$). Addition of 0.1% of fiberising aid "Polyox™" (polyethylene oxide $-[CH_2\text{-}O\text{-}CH_2)]_{-n}$ MW 600,00) reduced the elasticity and fibre dimensions remain stable once produced, with no improvement in hygroscopic nature. Over a 48 hr period it became obvious that the shelf life of the sol would be short, as the sol began to increase in viscosity during storage, eventually going solid after 7 days. This would not be a desirable attribute if the sol were processed over an extended period of time. Another fresh batch of sol (without Polyox) was prepared at a slightly higher initial viscosity (removal of more liquid) for extrusion using a delivery pump/spinnerette system, as a higher shear rate was expected.

5.1.5. Sol Extrusion to Produce Green Fibres

The sol was transferred from the evaporation flask to the reservoir of the extrusion equipment shown in **Figure 5.2**. It was then extruded under a positive nitrogen gas pressure (5 - 20bar) into a delivery pump and through a porous sintered metal filter. The sol experienced considerable shear prior to delivery at the spinnerette, which reduced viscosity. This was further affected by the shear created as the sol passed through the spinnerette holes (dependant on size and depth).

The spinnerettes used were made by laser drilling of commercial stainless steel blanks, with hole sizes in the range of 80 - 100μm (**Figure 5.3**).

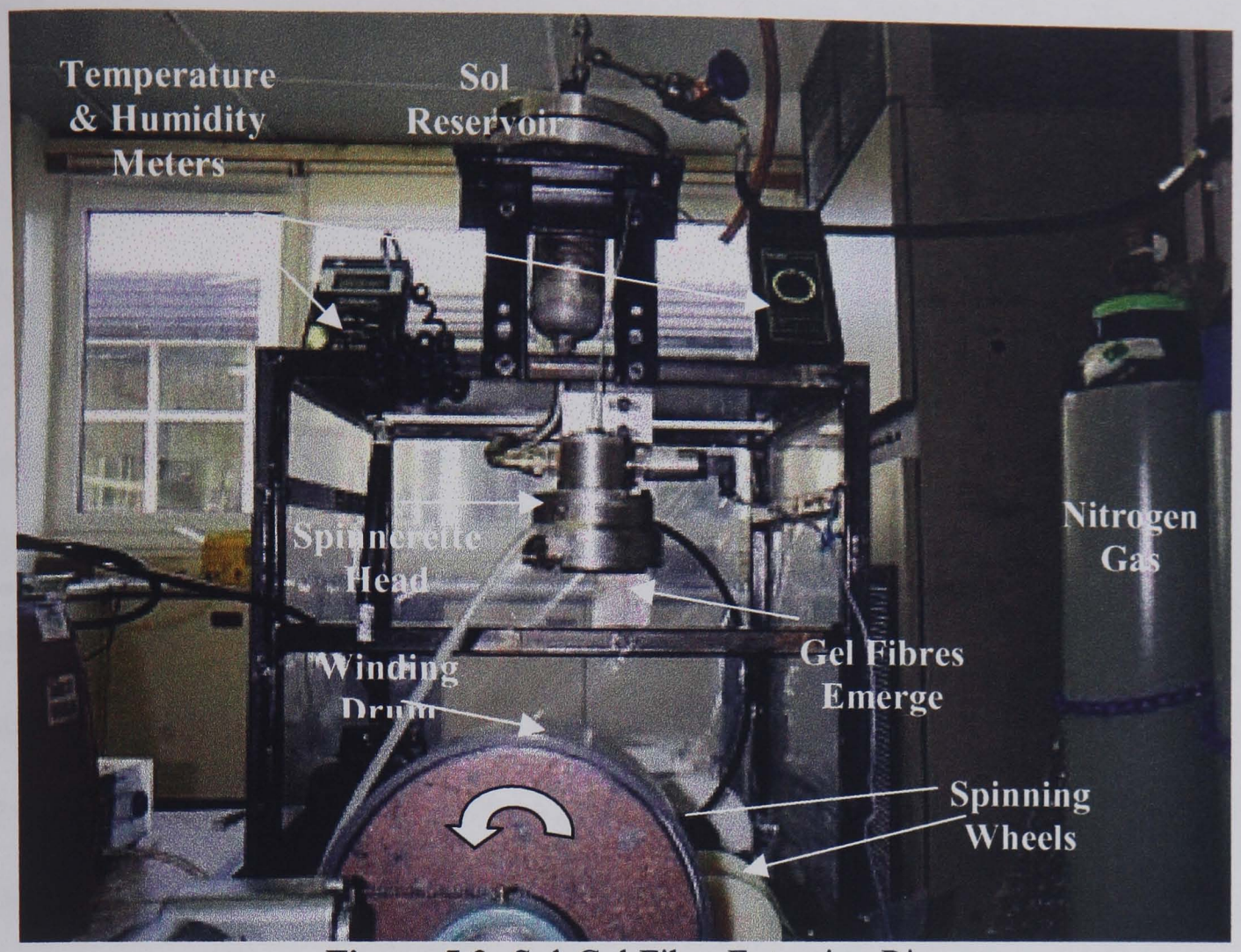

Figure 5.2: Sol-Gel Fibre Extrusion Rig

Figure 5.3: Spinnerette used for fibre extrusion - 100μm

The emerging green filaments (jets) flowed under the influence of gravity and started to dry and form a gel fibre, influenced by the increase in surface area and the volatility of the solvent system used. The partially dry gel fibres were wound onto a winding drum (or spinning wheels), at controlled speed, drawing the filament diameter down (typically from 100 to 30μm). The temperature and relative humidity of the surrounding atmosphere was also monitored, typically 25°C and 65% respectively.

The green fibres made from the alkoxide were then removed from the drum and lined up on a refractory alumina plate for firing in order to convert them to the polycrystalline oxide.

5.1.6. Thermal Analysis

Thermal analysis was carried out on a fibre sample in air which allowed both weight loss and the rate (dt/TGA) at which it occured to be monitored with temperature, whilst the sample was heated from room temperature to 1400°C @ 180°C/hr. From the dt/TGA profile (**Figure 5.4**) the weight loss (68%) was completed by ~380°C. In the DSC mode (Differential Scanning Calorimetry) exothermic peaks in the range of room temperature to ~350°C were seen relating to combustion of carbonaceous and nitrate derived functionalities, with a further exothermic peak at 978°C indicative of mullite crystallisation.

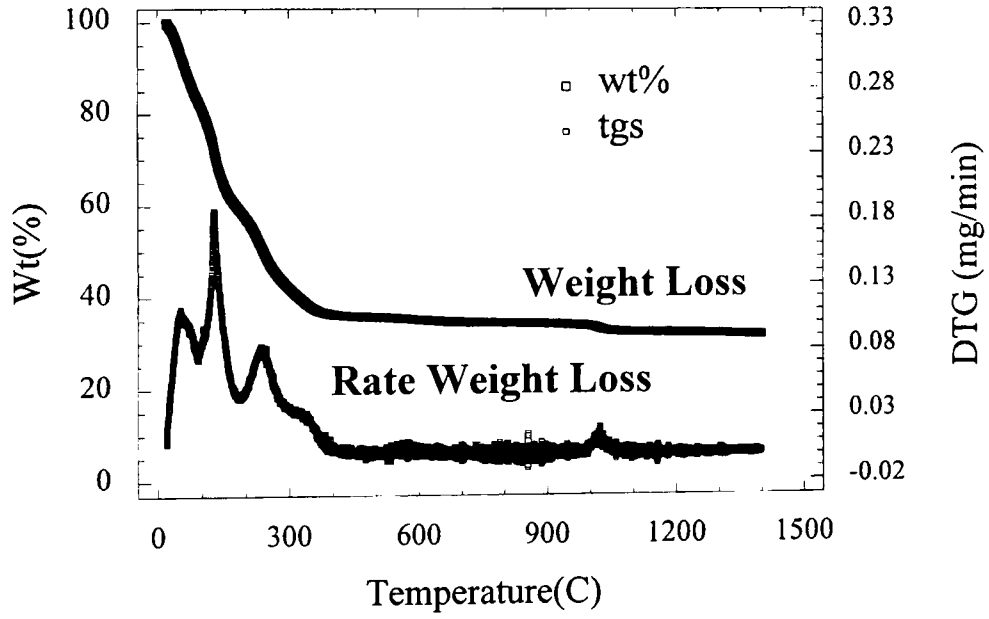

Figure 5.4: dt/TGA Trace For a 2AIP:1AN/TEOS Mullite Fibre at 180°C/hr to 1400°C

5.1.7. XRD (X-Ray Diffraction) Analysis

XRD analysis showed evidence of initial mullite formation at 1000°C, in the form of the 2:1 phase (supported by DSC data) seen by the single XRD peak at 26.1° 2θ.

All amorphous phases were absent at 1100°C and 3:2 mullite formed exclusively at 1200°C. This system appears reactive in terms of phase evolution, as would be expected from an alkoxide system.

5.1.8. SEM Analysis

Some interesting features are apparent after heat treatment up to 1400°C, i.e., a very fine-grained microstructure (~100nm) compared to the commercially produced fibres. Irregular, non-circular cross-sections as previously observed with other commercial mullite fibres such as Nextel 312, 440 and 480. The amount and size of the intergranular pores was reduced compared to an ACH based mullite fibre, which resulted in a noticeable increase in strength and flexibility. **Figure 5.5** shows the improved microstructure due to the selection of a non ACH sol-gel system.

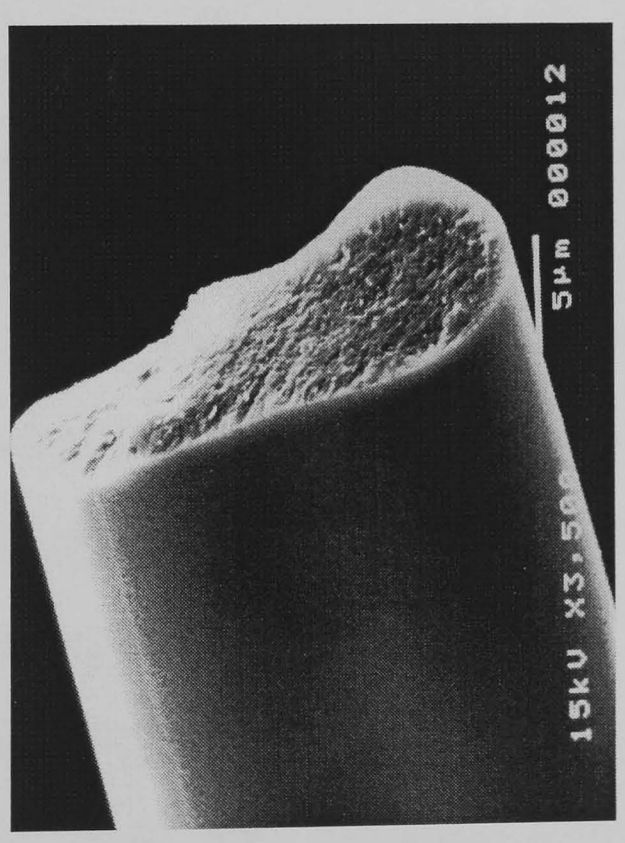

Figure 5.5: SEM micrograph of 2:1 AIP:AN/TEOS fired at 180°C/hr to 1400°C/4hrs

Although this system produced a much-improved microstructure, it still posed difficulties in producing a stable green fibre primarily because of its high affinity for water.

Due to this characteristic, a second alternative chloride free system was formulated and evaluated, which used an aluminium carboxylate precursor and colloidal silica.

5.2. Inorganic Salt/Colloidal Sol - AAT Mullite Sol System

5.2.1. Properties of Aluminium Carboxylates

There are good reasons for using aluminium carboxylate solutions for sol-gel fibre production as they possess the gelling properties of the chlorhydrates and the tendency to precipitate insoluble hydrous aluminium hydroxides was reduced by the principle of maximum confusion. The presence of different anions reinforces the effect of cation polydispersity. Basic aluminium acetate is normally insoluble in water and 3M enhanced solubilisation, by the addition of borate (H_3BO_3 – Boric acid), which was considered as an effect of randomisation of the solution structure. Boric oxide plays a role as a glass former in refractory materials, which improves the flexibility and textile quality of a fibre [3] but high temperature performance was reduced. If the borate were substituted for an alternative ion such as the tartrate (as tartaric acid) this would not result in glass formation in the same way as borate and the refractoriness of the fibres would not be impaired.

5.2.3. Commercial Grade Aluminium Acetotartrate (AAT)

A commercially available aluminium carboxylate AAT (Reheis, Chemicals Eire - used as an astringent) was identified as a potential candidate for fibre production. The material properties include chloride free, high water solublility and high alumina yield (~24%, half that of ACH) similar to stabilised aluminium acetate adducts used commercially for the production of continuous alumina fibres. The material is reported to have a formula weight of 216g/mol^{-1}:

$$\mathbf{Al(OH)_{0.61}\ (CH_3COO)_{1.65}\ (OOC(CHOH)_2COO)_{0.37}\ H_2O_{1.47}}$$

Concentration of such salt solutions via heating and evaporation at reduced pressure should give rise to an increase in viscosity and form linear co-ordination between molecules. This would be energetically likely as the bi-dentate tartrate ($^{-}OOC(CHOH)_2COO^{-}$) structure would be less stericly hindered in the linear form resulting in viscoelastic properties, which would lead to good fibre drawing., an advantage for fibre formation. The fibre forming characteristics of AAT were confirmed by blending with distilled water and then concentrating up by rotary evaporation. The material became viscoelastic and could be drawn by hand into fibre using a glass rod. The material was also extruded through a spinnerette using the sol-gel fibre extrusion rig, again forming fibres successfully. In order to aquire a mullite composition a suitable silica source was required.

5.2.4. Commercial AAT/Ludox AM-30 Mullite Sol

In order to produce a mullite sol for fibre preparation, several silica precursors were evaluated for compatibility in aqueous solution with AAT:

- TEOS - A white gelatinous precipitate formed due to rapid hydrolysis in the presence of the acetic acid liberated by AAT.
- Aerosil® 200 Pyrogenic fumed silica (Degussa-Huls) – This dispersed easily with a noticeable increase in viscosity probably due to hydrogen bonding between water and the hydrophilic surface silanol (Si-OH) groups. The sol-gelled slightly when concentrated and exhibited shear thinning flow behaviour when extruded.
- Dow Corning D193 Siloxane Surfactant – The material dispersed well, but gelled severely to a wax consistency when concentrated, not allowing transfer to the extrusion equipment. ICI [4] used this successfully with ACH, which is less acidic.

- Commercial grade colloidal silica (Dupont, Ludox®) – The AM-30 grade was selected because of its reported acid stability [5]. The silica sol dispersed well and fibres were easily pulled by hand and extruded. Green filaments were strong and could be handled easily. The sol-gel exhibited little thickening over a few days.

It was concluded that the most compatible, economic and stable sol system was that based on colloidal silica. Also the green fibres were stable in air and had reasonable strength, allowing them to be handled.

A larger batch of mullite sol was made up containing the Ludox AM-30 was made with:

Distilled Water – 3006g

Aluminium Acetotartrate - 1543.2g (Reheis, Chemicals Eire)

A Silverson mixer was used to blend 1473.25g of the AAT solution and 75g of Ludox AM-30 to obtain mullite stoichiometry. The final step is to filter the resultant solution using a vacuum pump and a No 1 Whatmann filter paper. The sol was rotary evaporated as before until it was suitable for forming fibres. Green fibres could be drawn down to diameters in the region of 10 - 20μm at best, which were very stable and strong at room temperature, displaying no hygroscopic character. This grade of silica was selected due to its stability in acidic media, via the partial replacement of some surface silicon atoms, which would normally form neutral silanol groups (see **Figure 5.6**).

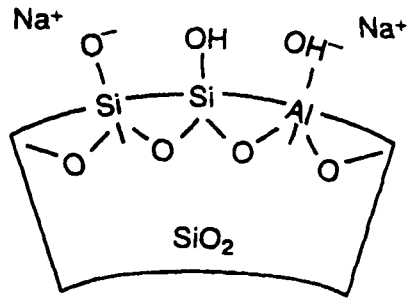

Figure 5.6: Simplified Surface Substitution by Al^{3+} of Ludox AM-30 Colloidal Silica

As aluminium is trivalent compared to silicon being tetravalent a single fixed negative charge is created, independent of pH, which allows stability up to neutral pH.

5.2.5. Thermal Analysis

A fibre sample was analysed by TGA/DSC in air, heated from room temperature up to 1400°C @ 180°C/hr. From the dt/TGA profile (**Figure 5.7**) weight loss was complete (79%) at ~450°C. This was confirmed by the DSC trace, with an associated large exothermic peak at 376°C which would be coincidental with the oxidation of the carboxylate groups, followed by a smaller exotherm at 900°C which would support the formation of γ-alumina seen from XRD data. There was no mullite crystallisation peak observed at ~980°C as before using alkoxide precursors.

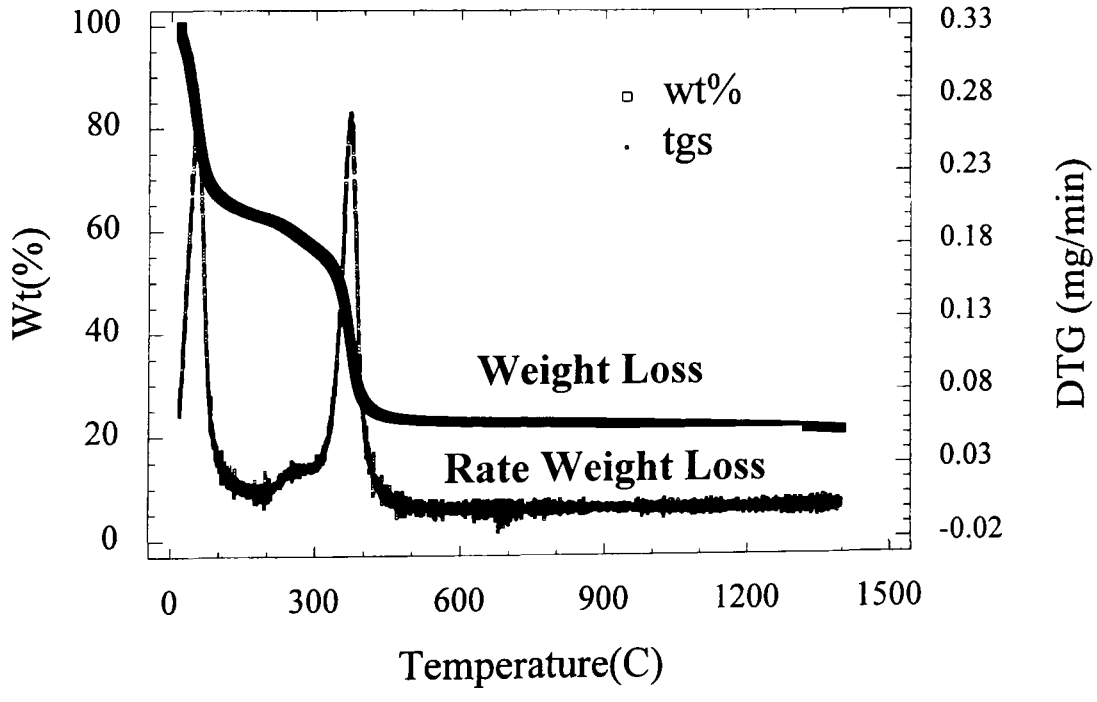

Figure 5.7: dt/TGA Trace For a Commercial AAT/Ludox AM-30 Mullite Precursor sol at 180°C/hr to 1400°C

5.2.6. XRD (X-Ray Diffraction) Analysis

XRD revealed the formation of intermediate γ-alumina between 900°C with a minor amorphous phase evolving at 1200°C, with exclusive 3:2 mullite conversion at 1300°C (as indicated by the orthorhombic mullite doublet peak residing between at 25.9 and 26.4° 2θ). The initial formation of alumina intermediates suggests that the silica in the colloidal form (12nm) is less reactive than that of the alkoxide system, therefore leading to mullite formation at a higher temperature without transition through the metastable 2:1 phase (as seen in Nextel 720 fibre heat treated to 1200°C or above).

5.2.7. SEM Analysis

SEM revealed fibre diameters (10-100μm) with most fibres having irregular shaped cross-sections. Fibres less than 20μm in diameter were crack-free, whilst larger fibres contained drying cracks (**Figure 5.8**), with the level of cracking increasing with diameter.

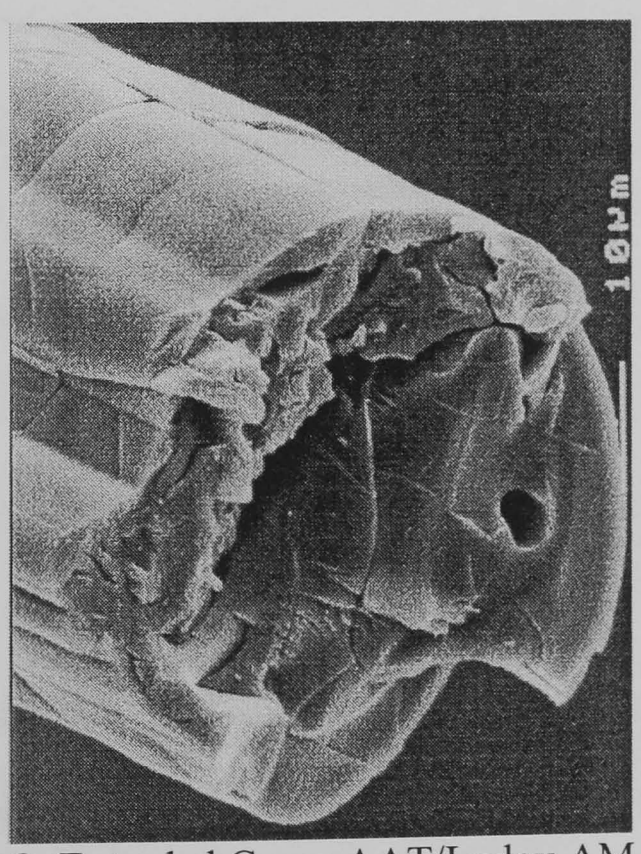

Figure 5.8: Extruded Green AAT/Ludox AM-30 Fibre

Higher magnification (**Figure 5.9**) of fired fibres revealed a very uniform grain structure throughout the fibres, but the grain size was relatively large (up to ~1μm) with a high level of intergranular porosity. In mullite containing materials, the presence of elongated grains (non equiaxed) can be attributed to the presence of a siliceous glass phase [6], which is consistent with XRD observations.

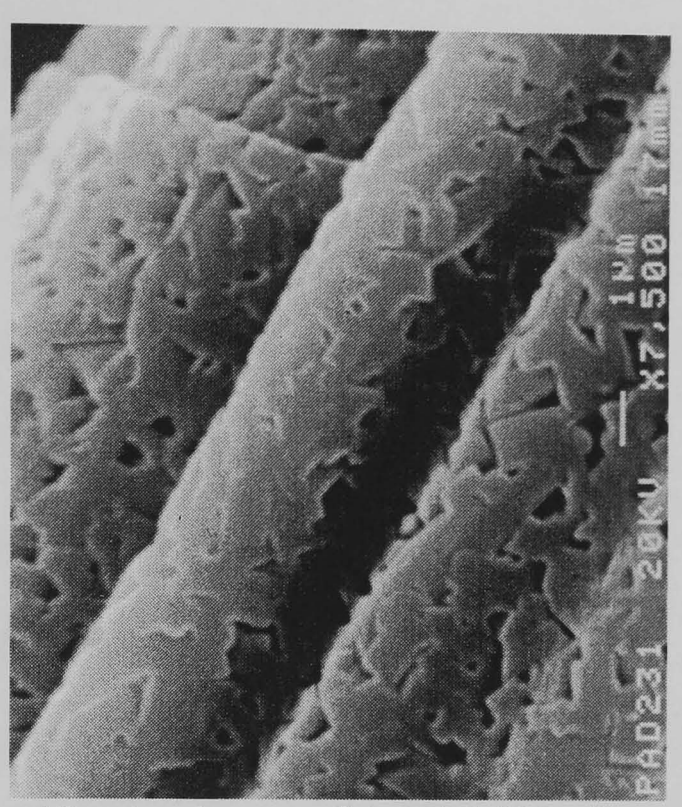

Figure 5.9: High magnification image of AAT/C.SiO_2 fibre showing grain growth and porosity after 1400°C heat treatment

5.3. Summary of Chloride Free Mullite Sols

Both precursors systems have their advantages and disadvantages with regards fibre formation. Those produced from the AIP/AN:TEOS system have a very fine grained microstructure with no intergranular porosity when fired to 1400°C, aided by the broad temperature range over which the pyrolysis occurs. This system requires a fugitive fiberising aid to assist the viscoelastic nature needed to form small diameter filaments. Also this system demonstrated its instability in ambient conditions through its high affinity for water shown by its hygroscopic nature, which makes post extrusion handling difficult.

The AAT:Ludox AM-30 colloidal silica system however exhibited excellent fibre forming features, green fibres are stable in air and are easily handled, some larger fibres suffer from severe drying defects. Unfortunately there was considerable grain growth with a high level of intergranular porosity when heat-treated to 1400°C. There are two obvious mechanisms by which this could occur:

1. Narrow temperature range over which the pyrolysis occurs.
2. Rapid densification and crystallisation of the amorphous phase.

Between the two mullite sol systems, there are desirable attributes which would enable fibre formation by extrusion, stable green fibres and a fine grained mullite microstructure at an economic cost. The advantages and disadvantages of both systems are summarised in **Table 5.1 and 5.2:**

Alkoxide Mullite Sol: 2:1 AIP:AN/TEOS

ADVANTAGES	DISADVANTAGES
Chloride Free	Sol is Unstable & Green Fibres are Hygroscopic.
Crack Free When Diameter is Reduced	Sol is very Elastic Even With Fiberising Aids.
Forms Mullite Phase at Low Temperatures (<1000°C) & Fine Microstructure from Homogeneous Mixing	Care During Heat Treatment is Required.
Porosity is Reduced Compared to ACH Fibres	

Table 5.1: Advantages and Disadvantages of the Alkoxide Mullite Sol

Inorganic Salt/Colloidal Sol: AAT/Ludox AM-30 Silica

ADVANTAGES	DISADVANTAGES
Stable Sol Viscosity	Fired Fibres Show Porosity and Cracking
Chloride Free	Forms a Coarse Microstructure
Requires No Fiberising Aid	
Green Fibres Are Strong and can be Handled	
Forms Mullite Phase at >1200°C Due to Inhomogeneous Mixing	

Table 5.2: Advantages and Disadvantages of the Inorganic Salt/Colloidal Sol

The general trend was that the alkoxide system was problematic in the sol form, but the microstructural characteristics were favourable and vice versa for the inorganic salt/colloidal sol system. It was therefore hypothesised that it would not be unreasonable to produce a stable, extrudable sol that yielded strong stable green fibres that on firing would yield a fine grained homogeneous mullite microstructure. The next chapter deals with the approach of blending the two precursor systems to create such an effect.

5.4. References

1. K. Okada "Mullite Long Fibres Prepared By Sol - Gel Method Using Water Solvent System", Key Engineering Materials, 1997, **132-136**, pg 1946-1949.

2. T. Nishio, "Preparation of mullite fiber by sol-gel method", J. Ceram. Soc. Jpn, 1991, **99**, pg 654-59.

3. K. Karst, Minnesota Mining and Manufacturing Co, 1977, U.S. Patent 4047963, 13.

4. Tegopren Silicone Surfactants, Th. Goldschmidt AG. 1990, Chemische Fabriken Goldmidtstrasse 100 D4300 Essen 1, Germany.

5. Dupont Product data Bulletin "Ludox Colloidal Silica Sols", 1993.

6. M. Sacks "A review of powder preparation methods and densification procedures for fabricating high density mullite", J. Am. Ceramic Soc. 1990, **6**, pg 167-208.

CHAPTER 6 OPTIMISATION AND CHARACTERISATION OF FIRED FIBRES

6.1. Commercial AAT Mixed Mullite (50:50) Fibres

During the preliminary experimental work as detailed in chapter 5, the characteristics of the two chloride free sol systems were determined. The concept of a blended or mixed sol was introduced which would exploit the benefits of the two systems. This was initially pursued by thoroughly mixing a 50:50 weight ratio of the aluminium acetotartrate/colloidal silica and the alkoxide [1] mullite sols in their dilute form, prior to rotary evaporation. The resulting material was a highly viscous, straw-coloured sol exhibiting viscoelastic tendency. Stable green fibres were subsequently hand drawn with a glass rod to demonstrate the fibre forming ability of the sol and the resulting fibres examined.

6.1.1. Thermal Analysis

Green fibres were analysed by TGA/DTG at a ramp rate of 20°C/min in air, in order to establish the pyrolysis pattern and weight loss of the precursor fibres during conversion to the oxide form (**Figure 6.1**).

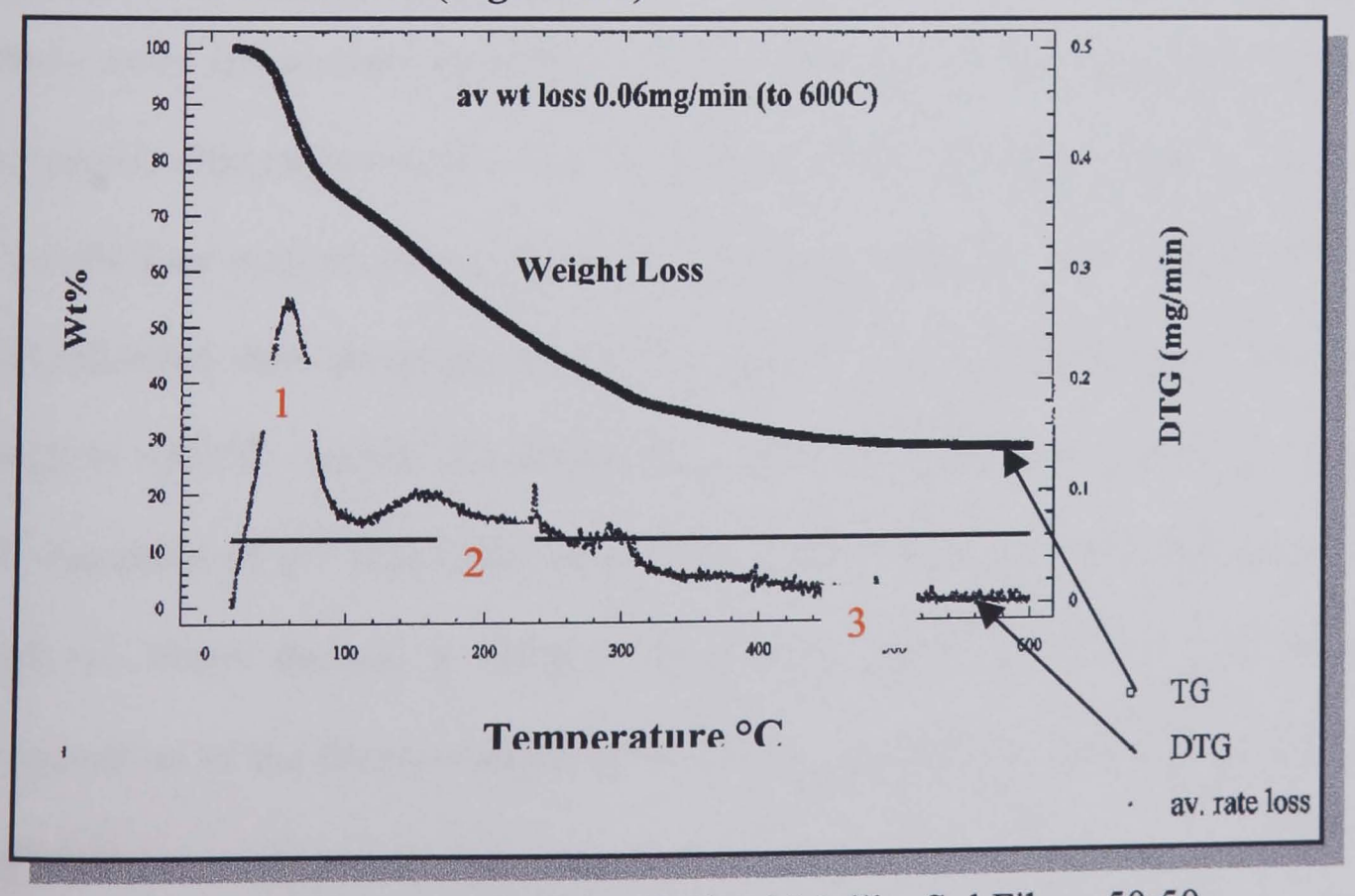

Figure 6.1: Pyrolysis Profile of Mixed Mullite Sol Fibres 50:50

The rapid loss of residual water and volatile alcohol residues occurs from the onset of firing (1). The next region (2) was carboxylic acid and nitrate group removal. The final region (3) before conversion to an amorphous oxide fibre, is largely due to oxidation of carbon, which originated from incomplete oxidation of organic precursors during region 2. This was due to the slightly reducing atmosphere in an electric furnace. This was consistent with a visual inspection of the fibres when the firing was interrupted at that stage. Fibres had a black appearance, unlike the white appearance associated with fully oxidised fibres. Comparison of the mixed system with the two mullite sols, (Chapter 5 Fig 5.4 (Alkoxide) and Chapter 5 Fig 5.7 (AAT/Colloidal silica)) showed that the pyrolysis profile is much more uniform.

The alkoxide system had a total weight loss of 75% of the initial material (25% ceramic yield), 65% of which was lost between room temperature and 300°C, due to 3 broad events as denoted by the 3 peaks. The rate of weight loss for the peaks ranged from 0.08, 0.1 and 0.18mg/min. The AAT/Colloidal silica profile showed a total weight loss of 80% of the initial material (20% ceramic yield), 75% of which was lost between room temperature and 400°C, due to 2 distinct events as denoted by the 2 sharp peaks. The rate of weight loss for both peaks is very high at 0.25mg/min. As the weight loss occured over a narrow temperature range and some precursors (i.e. AAT) exhibited short abrupt decomposition regions, care was taken during this stage through to ~500°C. Ideally the weight loss should be more even across this range. With exception of the first large weight loss region (1) due to residual water, the mixed sol fibres showed a broader temperature range over which the steady decomposition of the fibres occured up to 300°C, completing 60% of the total 70% weight loss.

In principal this should limit the possibility of uncontrolled exothermic reaction from oxidative decomposition, reduce entrapment of decomposition vapours during the fibre's plastic period and inhibit pore formation. Therefore the firing of such fibres should be less complex and more forgiving of the firing rate. For manufacture of commercial alumina based fibres retention of strength requires careful firing to control evolution of volatiles, when converting the plastic gel fibre into the amorphous oxide. Rapid heating will cause boiling of the solvent and results in blistering and macroporosity in the fibre. Mild drying conditions are used for the first 300°C or so and control of humidity may be required, as the vapour pressure for water is high, the drying rate slows above this.

During decomposition the gel is converted from a soft plastic to a brittle porous ceramic, and there is again a risk of generating coarse porosity especially when the fibre is still in the plastic state. There is very little direct information on the precursors used to make alumina based fibres, although manufacturers patents give an indication of the conditions needed to avoid the generation of critical macropores during fibre decomposition. All of the precursor types are decomposed initially to amorphous alumina on heating beyond 400°C. Extremes of temperature during decomposition are generally avoided, particularly exotherms. 3M pay particular attention to slow rates of temperature rise between 200°C and 500°C to avoid ignition of organics when decomposing their carboxylate precursors, in an oxidising atmosphere. The adiabatic exotherms are very high for Aluminium formoacetate or Diacetate is –2095 to –2326 kJ/mole of alumina, steam hydrolysis to convert the organic to hydroxides is nearly thermally neutral (67 kJ /mole of alumina).

This is practised by 3M and Sumitomo, an alternative could be to decompose the fibre in a nitrogen atmosphere during this temperature range, although volatilisation of the decomposition vapours may become an issue. ICI used a similar technique after drying their Saffil fibres between 200°C and 500°C [2], the steam also assists in removal of chloride ions as HCl vapour and the overall decomposition of chlorhydrate to alumina is strongly endothermic. Once it had been established that the sol was suitable for drawing fibres, it was evaluated for extrusion. Generally many sol systems can be formed into fibres using drawing techniques, which do not exert large shear forces, but when extruded through small, constrained holes this can have a significant impact on the sol flow characteristics. If shear thinning of the sol occurs, the integrity of the filament transitioning from sol to gel as it dries can become weak and continuous filament drawing difficult. This was not the case.

The sol was extruded through a 100 x 100μm hole "top hat" spinnerette and the resulting green fibres (**Figure 6.2**) wound onto a rotating collection drum. Apart from the inherent flow characteristics of the sol, the major factors that affected the transition of the sol to the green fibres was sol temperature, air temperature and relative humidity. The preferred ranges for these parameters were established as:

1. Room Temperature 20 - 30°C
2. Relative Humidity 55 - 65%
3. Sol Temperature 20 - 25°C

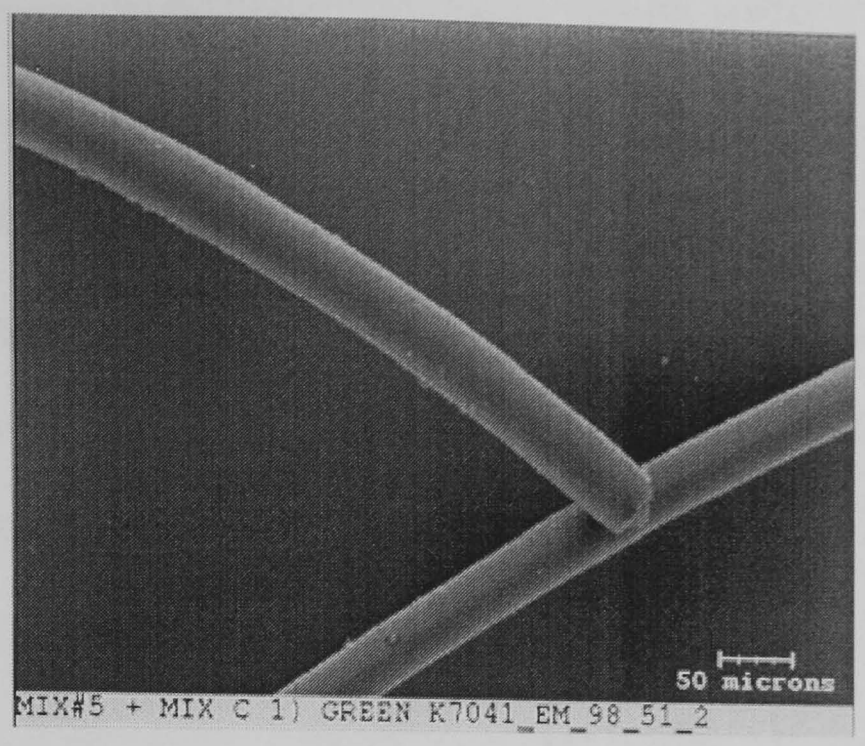

Figure 6.2: SEM Micrograph of Mixed Mullite 50:50 Green Extruded Fibres

Green fibres were then fired at a ramp rate of 180°C/hr to temperatures between 1200°C and 1600°C/4hrs for SEM evaluation.

6.1.2. SEM Analysis of Fired Fibre

Scanning Electron Microscopy (SEM) demonstrates the smooth fine-grained microstructure obtained from this mixed sol system (**Figure 6.3**) unlike the severe drying defects observed with the AAT colloidal silica system previously.

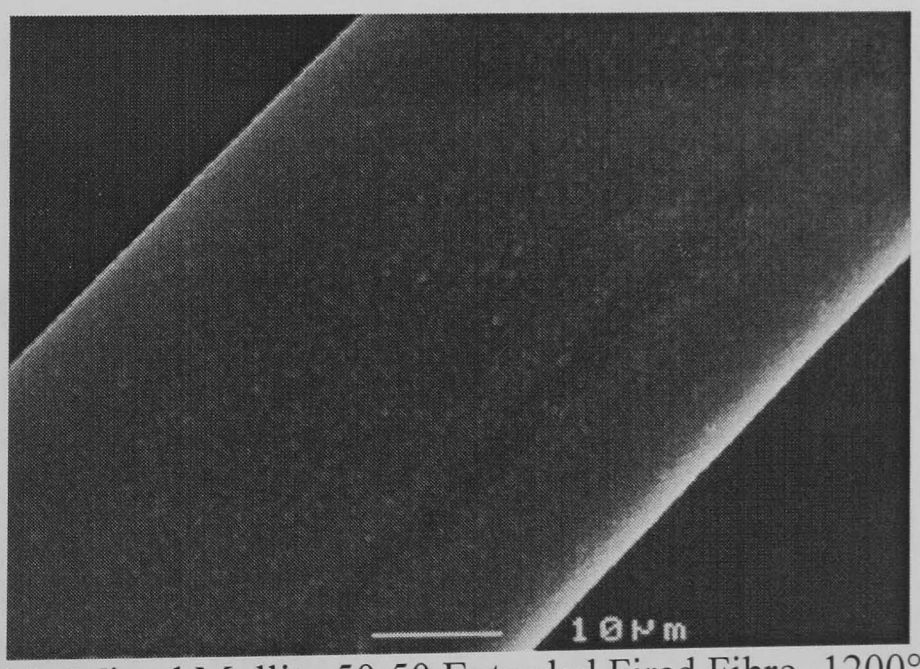

Figure 6.3: Mixed Mullite 50:50 Extruded Fired Fibre -1200°C/24hrs

SEM analysis showed that fracture surfaces were similar in appearance to Nextel 720 and showed a fine and uniform grain structure, which was free from obvious porosity when fired up to 1300°C.

As the temperature was increased there was a gradual increase in grain size and the level of porosity, but the pore size remained fine at ~100nm right up to 1500°C from rough visual evaluation of images. At temperatures in excess of this both grain and pore size became much larger. Defects in the form of large holes were found in some fibres - these are likely to be due to the presence of fine bubbles in the sol. Radial drying cracks were found in some of the larger diameter fibres, all fibres with diameters less than 25μm were crack free. The sol exhibited a good shelf life (without any obvious thickening or ageing with time) over a period of a few weeks, easily fibersised, no fiberisation additives required, handleable green fibres, no drying problems and dense fired microstructure with noticeable strength.

6.1.3. SEM – Elemental Mapping

In order to determine if the precursors had remained homogeneous through the firing process in the polycrystalline fibres, EDS elemental mapping analysis was carried out on fibres fired to 1200°C/4hrs. **Figure 6.4** shows maps for Si and Al distribution over a fibre cross-section. The yellow/orange areas indicate a high concentration of the element being determined, which are evenly distributed across each map confirming the retention of precursor homogeneity during the sintering and densification stage.

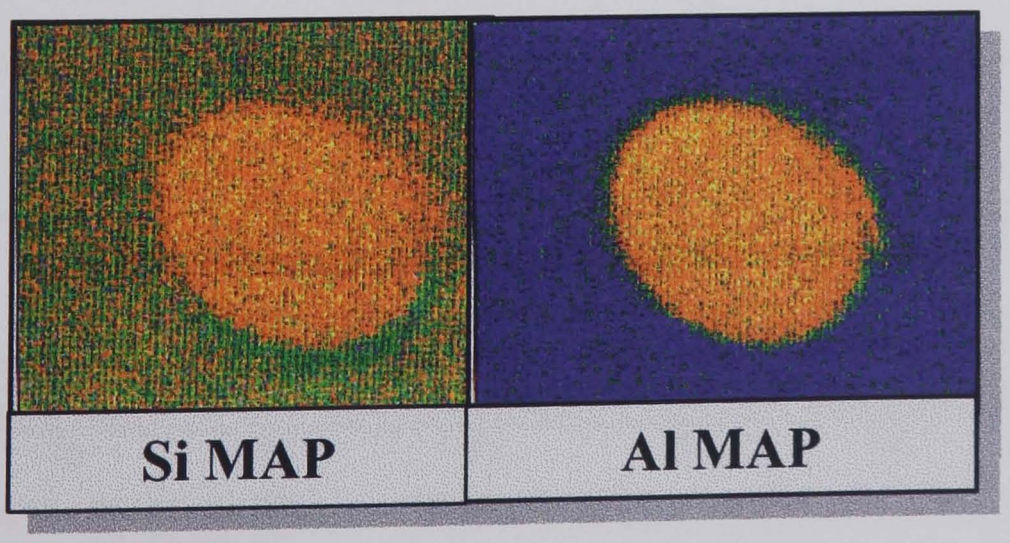

Figure 6.4: EDS Elemental Mapping of a Fibre Cross Section

6.1.4. XRD Analysis

Samples of fibre were fired in the temperature range 1000 – 1600°C/4hrs at a ramp rate of 180°C, crushed and X-ray diffraction analysis was carried out on them. Up to 1100°C there was very little evidence to suggest any major crystallisation of the fibres, especially at 26 °2θ, which is a peak specific to mullite ($Al_6Si_2O_{13}$). Above this temperature mullite forms exclusively, as the stable stoichiometric 3:2 orthorhombic phase, pronounced by the resolved doublet at 26 °2θ. Mullite continued to form as the temperature increased, with an increase in peak intensity, to the exclusion of any other crystalline phases (**Figure 6.5**). Mullite formation in the mixed sol system was different to that of the two individual sols. This formed only mullite at 1200°C and above, without the formation of any significant intermediate alumina or silica phases.

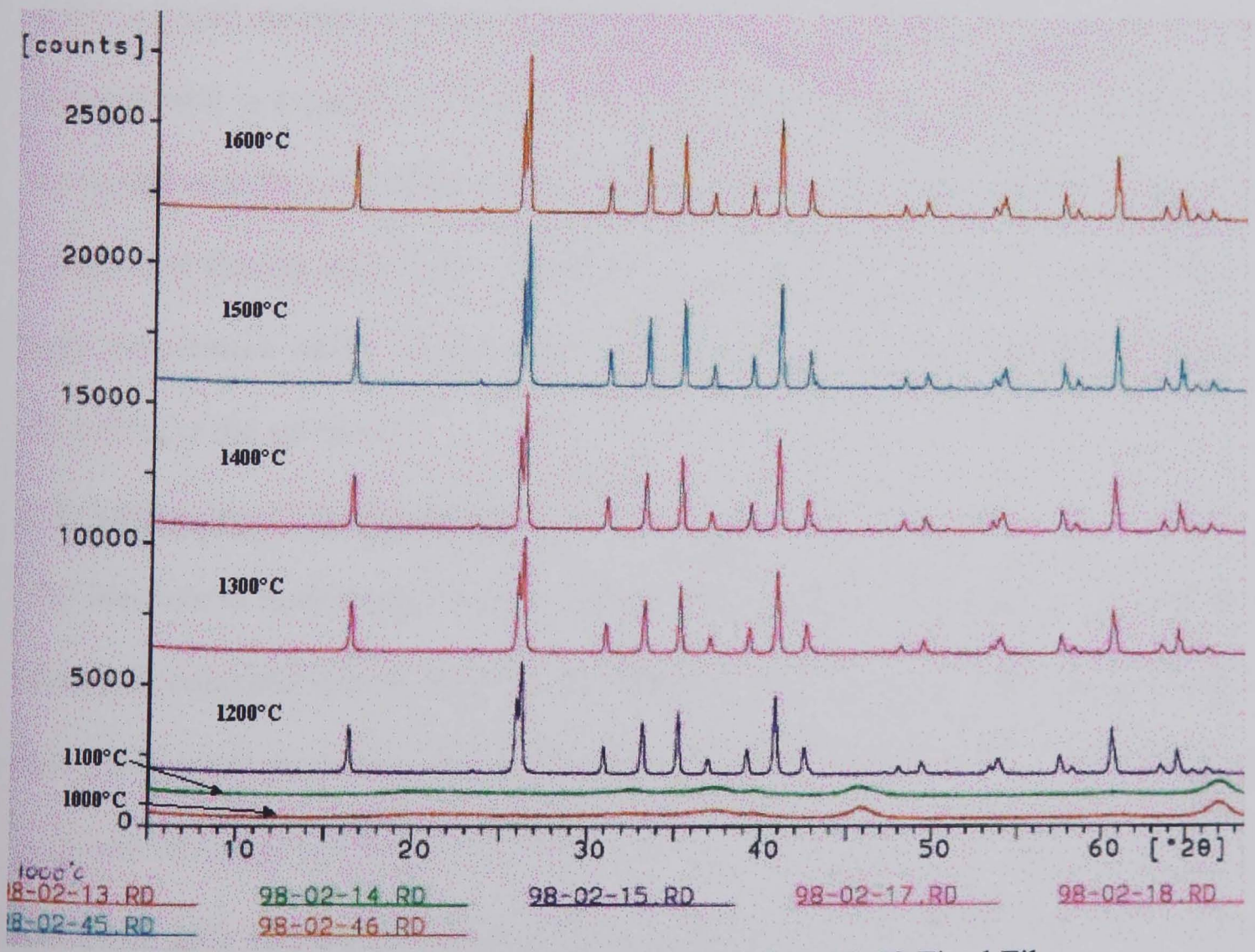

Figure 6.5: XRD Patterns for Mixed Mullite 50:50 Fired Fibres

The alkoxide system started to form mullite initially at 600°C and was almost fully crystallised as orthorhombic mullite by 1000°C, with little change in peak intensity above this. This confirmed the high degree of homogeneity between the component precursors. The AAT/colloidal silica system showed a much later formation of mullite, completely amorphous at 800°C, via γ-alumina intermediate (900-1100°C) forming mullite exclusively at 1200°C, implying a poorer homogeneity between precursors. It seemed that the introduction of AAT and AM-30 colloidal silica disrupted the homogeneity of the alkoxide system and impeded the onset of mullite formation. As the colloidal silica was probably the least reactive component of the sol, being colloidal (12nm) this would control the degree of mullite formation. Also because the system was so complex and contains many different constituents, the principle of "maximum confusion" [3] may apply, which suggested "it is easier to vitrify a liquid containing many elements, because it is difficult for the constituents to organise into a crystal". As room temperature strength of ceramics is generally associated with fine crystalline microstructures (especially important for fine diameter fibres), and fluxing impurities i.e. alkalies and produce glass phases which deform at high temperature under load, another fine and pure colloidal silica would be more desirable for the sol system.

6.2. Alternative Colloidal Silica

The aim was to investigate the effect of the reduced soda, de-ionised and ammonium stabilised colloidal silicas on the fibre spinning process and mullite crystallite size. Sols were made as before, with direct substitution of the AM-30 with the candidate colloidal silica, accounting for the difference in silica content. Alternative colloidal silica sols with varying colloid size (7nm to 30nm) were evaluated to replace Ludox AM-30 (acid stable sol), used for mixed mullite fibre production.

Sols were generally translucent in appearance, except that containing Degussa K328. which is opaque/off white in appearance due to its large particle size of 30nm. The sols were extruded through a 100 x 100μm hole spinnerette and wound onto a rotating collection drum. Fibres were produced from all sols and fired to 1200, 1250 and 1300°C/24hrs and XRD used to. Microstructural development was characterised by XRD, in order to estimate mullite crystallite size. High angle diffraction patterns (20 > 40° 2θ) were used for lattice parameter measurements for mullite found at 26° 2θ. The half-peak width of the XRD peak was used to estimate the crystallite using the Debye-Scherrer equation;

$$D=K\lambda/\beta \cos\theta$$

Equation 6.1: Dedbye-Sherrer Equation for Mullite Crystallite Size Estimation

where K is a constant (K = 0.91), D is the mean crystallite dimension normal to the diffracting planes, λ is the X-ray wavelength (λ = 0.15406 nm for Cu target), β is the peak width (in rad) at half maximum peak height and θ is the Bragg angle. Results of these individual tests are listed in **Table 6.1**:

	1200°C	**1250°C**	**1300°C**
Degussa K328 - 28% SiO_2, 30nm/80m^2/g	**(α-Al_2O_3)**	217	349
Ludox TMA - 34% SiO_2, 22nm/140m^2/g (DI)	138	201	229
Ludox LS-30 - 30% SiO_2, 12nm/215m^2/g (0.1% Na_2O)	191	251	251
Ludox SM-AS 25% SiO_2, 7nm/360m^2/g (0.05 - 0.08 % Na_2O Occluded within particles)	53	83	217
Ludox AM-30 30% SiO_2, 12nm/220m^2/g (0.24% Na_2O)	175	300	321

Table 6.1: XRD Mullite Crystallite Size Data (nm) For Alternative Silica Sols

Poor handleability resulted from all of the new sols except Ludox SM AS (7nm colloid size, soda free). All except Degussa K328 form mullite at 1200°C, the large colloid size results in a higher sintering temperature between the precursors. Ludox SM-AS had the smallest crystallite size (7nm) and contained little Na_2O as it is ammonium stabilised. Comparing fired fibres made from this to Nextel 720 (Mullite/α-Al_2O_3) commercial fibre the microstructure was similar in dimensions (**Figure 6.6**).

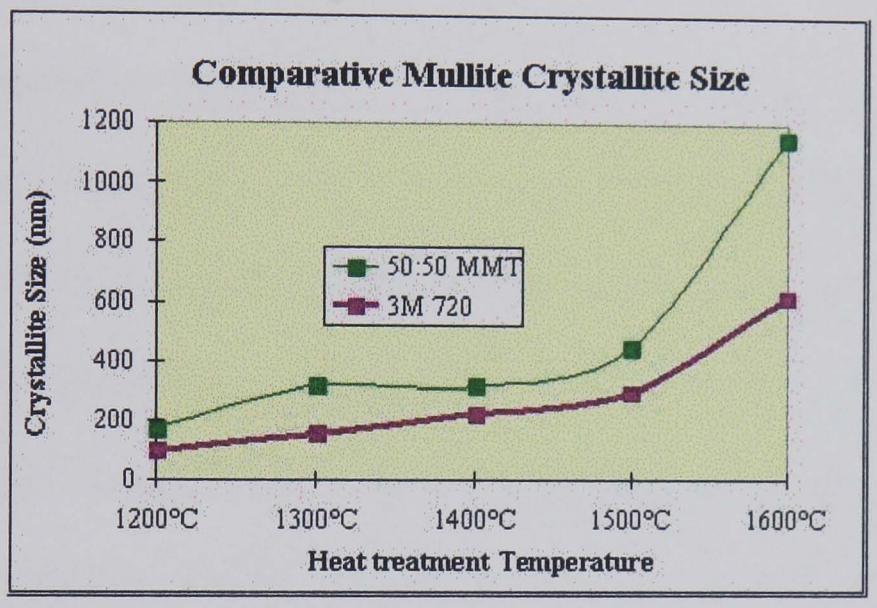

Figure 6.6: Mullite Crystallite size of Experimental and Commercial Fibres

The low soda content, in addition to a very small colloid size and high surface area of Ludox SM-AS, resulted in a mixed mullite precursor, which was less viscous and therefore aided upto a point the fibre spinning process. SEM analysis of heat-treated fibres revealed two further advantages of using this silica source. Firstly the reduction in viscosity of the precursor sol resulted in a reduction in the diameter of fibres from ~50µm to less than 20µm with many as small as 10µm in size. This had the effect of eliminating the radial drying cracks observed in the larger diameter fibres. The second important microstructural improvement was that the presence of large (few µm size) voids observed in many of the earlier fibres had also been significantly reduced.

This was also as a result of the reduction in viscosity of the precursor sol - air bubbles within the sol now had a tendency to rise to the surface of the sol prior to extrusion. The size of any bubbles trapped within the fibre were now less than ~1μm. As fired fibres made from Ludox SM-AS showed reasonable strength, further development continued with the substitution of Ludox AM-30 as a low soda containing small colloid sol appears advantageous.

6.3. Precursor Ratio Optimisation of Commercial AAT Mixed Mullite Fibres

Further optimisation of the mixed system using Ludox SM-AS, was further investigated to determine the effect of varying the ratio of the two sol systems. A series of sols were produced (on a weight ratio basis) of the Alkoxide and AAT individual sols to form a range of "mixed mullite sols" and fibres were extruded from each of the blends produced, to determine if this was the optimum ratio fibres. Details of the sols characteristics were recorded in order to produce an arbitrary ranking (0= poor and 3= good) to assist in the selection of the most appropriate composition for further scrutiny. The criteria used was based on extrudability, winding, elimination of drying cracks and fired strength in addition to SEM observations of the microstructure. This is summarised in **Table 6.2**:

Mix	% Alkoxide	% AAT/ SM-AS	Extrudability	Winding	SEM Apperance 1200/1400°C/4hrs
1	90	10	Poor	Poor	Dense, fine grains, cracked
2	80	20	Poor	Poor	Dense, fine grains, crack Free,
3	70	30	Moderate	OK, slow	Fibres very hygroscopic, none fired
4	60	40	Moderate	OK, breaks	30 um, Dense Crack Free, Some Bubbles.
5	50	50	Good, continuous	OK, slow but continuous	30 um, Dense Crack Free, Some Bubbles.
6	40	60	Good, continuous	OK, slow but continuous	Clean Surface, Some Cracks, Irregullar Shape ,Weaker
7	30	70	Moderate	Difficult, fibres stick together	Severe Cracking
8	20	80	Moderate	OK, fibres stick together	Severe Cracking
9	10	90	Holes blocked	None wound	N/A

Table 6.2: Sol Ratio Optimisation Results After Extrusion

6.3.1. SEM Analysis of Fired Fibres

Fibres were fired to 1200 and 1400°C/4hrs for SEM analysis. The results of the 1400°C/4hrs firing are summarised below. The 'best' mixed mullite extruded fired fibres were those with the ratio of 50:50 (**Figure 6.7**) and 60:40 (**Figure 6.8**). Both of these fibres exhibit a smooth surface with fine grains and minor porosity.

Fibres rich in AAT, i.e., 30:70 (**Figure 6.9**) and 20:80 (**Figure 6.10**) suffered progressively worse grain coarsening and porosity with a change in the crystal morphology, particularly seen in **Figure 6.10**.

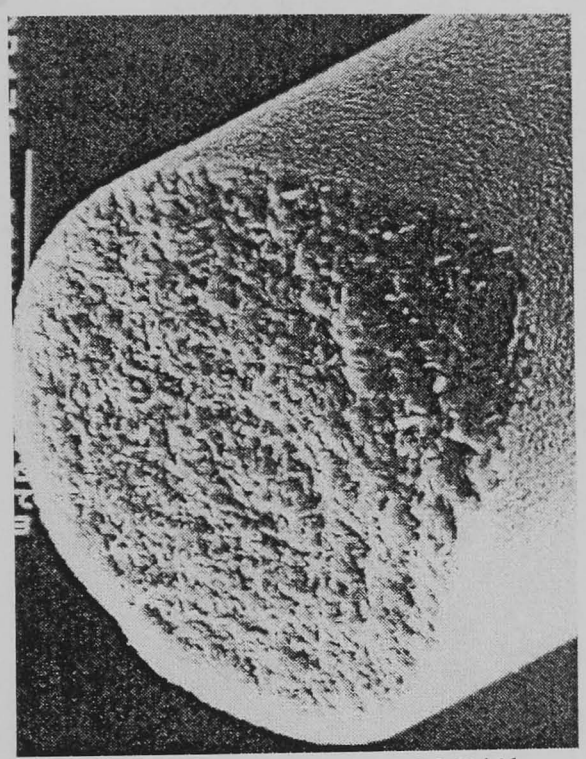

Figure 6.7: 50:50 1400°C/4hrs

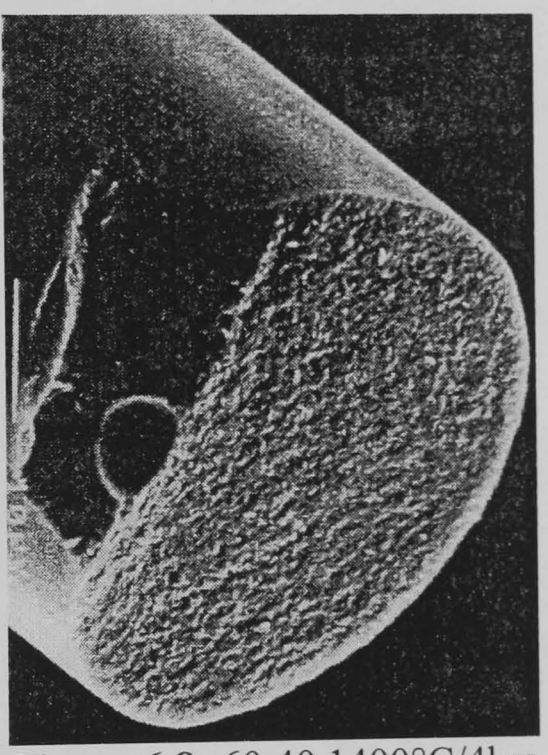

Figure 6.8: 60:40 1400°C/4hrs

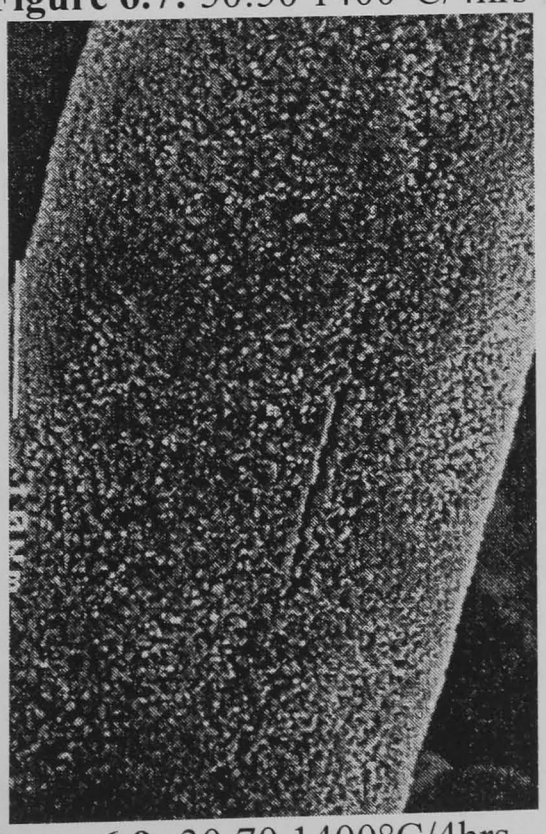

Figure 6.9: 30:70 1400°C/4hrs

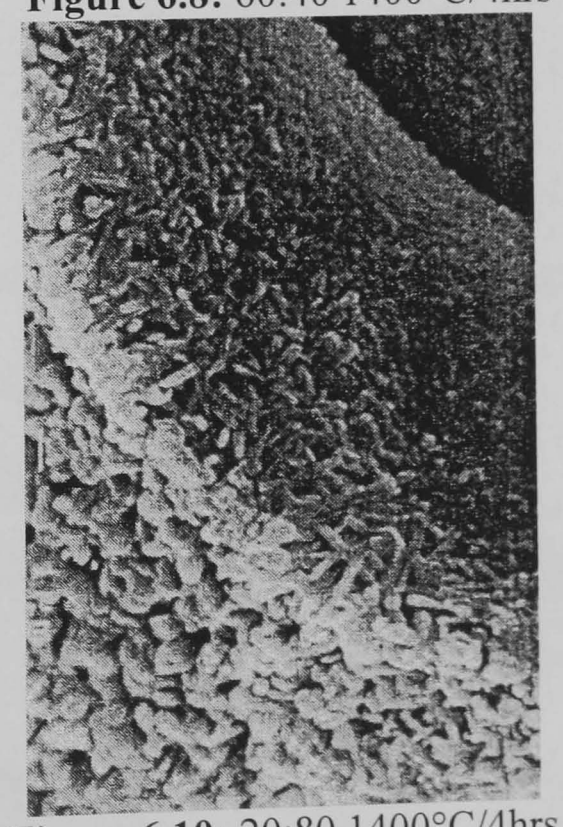

Figure 6.10: 20:80 1400°C/4hrs

6.3.2. Commercial AAT 55:45 Mixed Mullite Fibres

A further batch of sol was prepared with 55wt% of the Alkoxide precursor and 45wt% of the AAT:Colloidal silica sol. Fibres were extruded from the sol for heat treatments and subsequent SEM analysis. It was confirmed that the best fiberising and microstructural properties were produced from a 55:45 blend of the alkoxide/inorganic salt:colloidal silica, a typical SEM micrograph illustrates the advantages of the mixed sol (**Figure 6.11**):

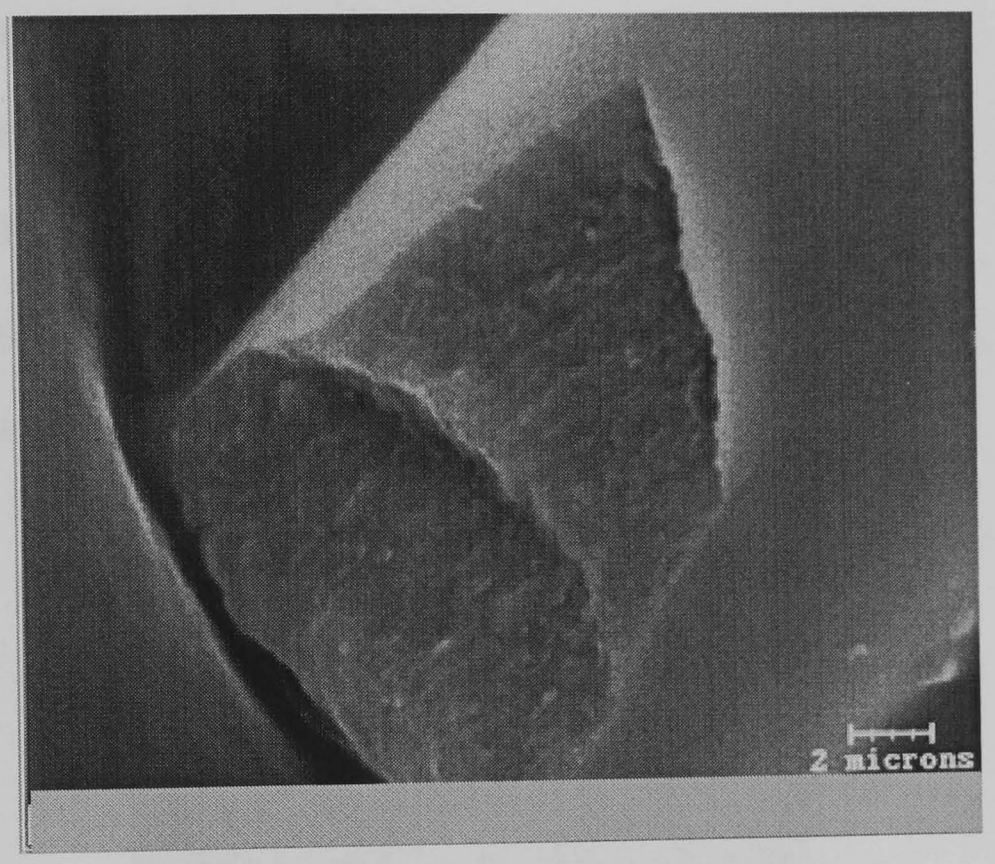

Figure 6.11: 55:45 Mixed Mullite Fibre Heat Treated 180°C/hr to 1400°C/4 hours

It can be seen that the fibre has undergone consolidation from its green precursor into a fine grained oxide fibre, during firing. TGA/DSC and XRD analysis show almost the same characteristics as for the 50:50 material.

6.4. Commercial AAT (55:45) Zirconia Additions

In order to maintain a fine microstructure during sintering and use at temperatures up to 1400°C an additive was required to aid sintering, and avoiding residual intragranular microporosity and inhibiting grain growth.

Zirconia is a well known sintering aid and grain growth inhibitor, two different commercial sources of colloidal sol were identified which were compatible with the sol chemistry. Nyacol colloidal zirconia sol (10nm zirconium acetate based - 20.2% ZrO_2) and MEL zirconium hydroxynitrate based sol (29.5% ZrO_2). The author has experience of using an optimum 5wt% addition of zirconia as an effective grain growth inhibitor, in melt produced CaO-MgO-SiO_2 fibres. The fibres were extruded as before and heat treated from 1200°C to 1600°C for SEM analysis. Addition of the MEL zirconia sol resulted in very fine (~10μm) green fibres with an "hour glass" effect along the fibre length (**Figure 6.12**) due to the extreme shear thinning characteristics of the sol which gave rise to die swell (expansion and relaxation) of the material once emerged from the hole. The fibres were therefore difficult to make with a consistent fibre diameter variation in the longitudinal direction.

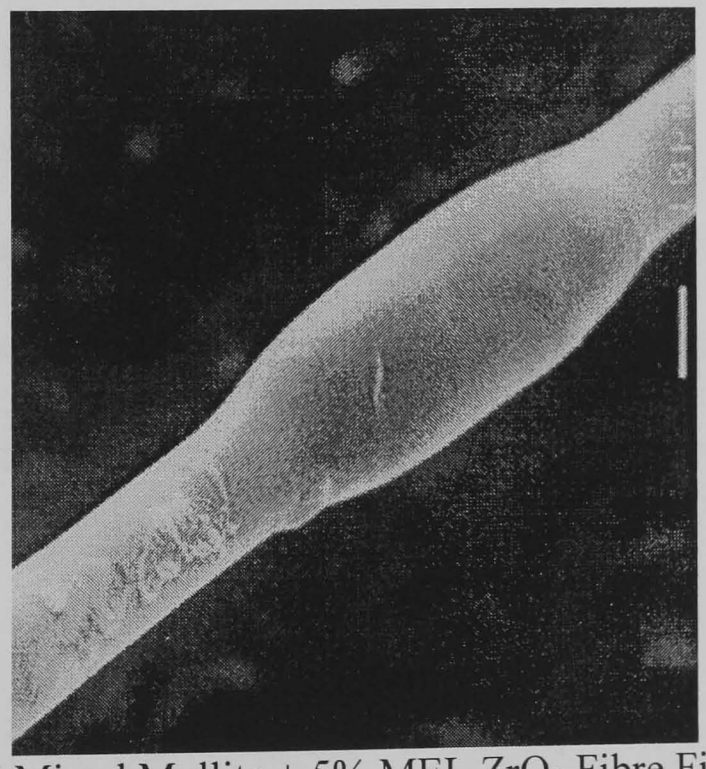

Figure 6.12: 55:45 Mixed Mullite + 5% MEL ZrO_2 Fibre Fired to 1400°C/4hrs

The increase in viscoelasticity may be attributed to the structure of zirconium hydroxynitrate [4], in solution, as it exists as a cationic linear polymer (**Figure 6.13**) with extensive hydroxy bridging.

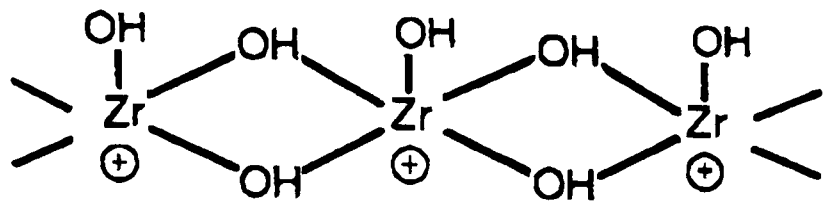

Figure 6.13: MEL Sol - Zirconium Hydroxynitrate Linear Polymeric Species

6.4.1. SEM of Zirconia Doped Fired Fibres

The results suggested that adding zirconia reduced the grain size and level of porosity on exposure to 1400°C/hrs, however at 1500°C (1600°C in the case of MEL doped material) there is a significant increase in the grain size and pore size compared to fibres without the zirconia additions. The Nyacol material was preferred and used for further doping. At this point, a stable stoichiometric mullite system had been developed with a good microstructure, having few defects, aided by using zirconia as a sintering aid. However the commercial AAT precursor was to become obsolete and unwanted impurities (forming calcium aluminate - hibonite $CaO.6Al_2O_3$), had been discovered by XRF analysis (**Table 6.3**) and confirmed by XRD. Potentially the CaO contamination could affect the microstructure and high temperature creep properties of a fibre, due to β-Alumina formation. β-Alumina is a term used to describe the combination of sodium (usually) or various alkali and alkali earth metal oxides with alumina, in the idealised composition $Na_2O.11Al_2O_3$ [5].

Oxide	% Impurity
CaO	0.43
ZrO_2	0.17
Na_2O	0.18
SO_4^{2-}	0.06

Table 6.3: Oxide Impurities In Commercial AAT Determined By XRF Analysis

The distinctive needle like crystal morphology of β-alumina is apparent in **Figure 6.10** and was probably responsible in part for the architecture seen in the morphology of the simple AAT/Colloidal silica system (Chapter 5, Figure 9).

A similar morphology of non-equiaxed grains is also a feature of mullite formed in the presence of a siliceous glass phase. Potentially reactions at high temperature can form vitreous CaO-Al_2O_3-SiO_2 phases such as anorthite ($CaO.Al_2O_3.4SiO_2$), which would soften and allow creep to occur due to viscous flow of the glass. With this problem in mind attention was focused on obtaining an alternative or producing an AAT precursor in the lab without CaO contamination.

6.5. Alternative Lab AAT With Low Impurity Levels

Failing to find an alternative commercial supply of AAT led to several lab methods being explored for the small-scale preparation of Lab AAT or another suitable carboxylate. These can be produced in several ways, but ultimately are composed of aluminium acetate (basic) and a carboxylic acid. The acid used is governed by the degree of dissociation of that acid, dependant also on its sequestering nature of the aluminium ion (mono or polydentate). Typically polydentates are tartaric, citric, maleic, itaconic and adipic acids. Three aluminium salts were chosen, based on the alumina yield and water solubility for reaction with the appropriate carboxylic acid(s) in aqueous solution to produce a higher purity precursor:

(i) Aluminium Sulphate/Acetic/Tartaric Acid/Barium Carbonate

Removal of sulphate ions using $BaCO_3$ yields a less soluble sulphate than calcium, therefore almost eliminating the Ba^{2+}contamination, however FT-IR reveals little and incomplete reaction to form AAT.

(ii) Aluminium Isopropoxide/Acetic/Tartaric Acid

AIP was hydrolysed in the presence of the acids in a ratio of **acetic : tartaric acid** of **1:1** and **3:1** respectively, with the latter being unstable and precipitating while the former produced a clear viscous fibre forming sol with an more significant FT-IR spectra closer to commercial aluminium acetotartrate.

However, the intensity of the peak due to salt formation at ~1584cm^{-1} is low and contains large peaks between 1475 - 1584cm^{-1} as a result of the reaction of free acids with isopropyl alcohol, forming esters during the hydrolysis of aluminium isopropoxide.

(iii) Basic Aluminium Acetate/Tartaric Acid

Basic aluminium acetate (BAA) is normally a water insoluble material, commercially available with a $^1/_3$ molar addition of boric acid to stabilise and promote solubility in water. Tartaric acid was successfully used in a similar manner to boric acid, with careful dissolution at boiling point on a hot plate and stirrer to produce a clear straw coloured viscous fibre forming sol, having the following stoichiometry:

$$\mathbf{(Al(OH)_{0.61}\ (CH_3COO)_{1.39}\ (OOC(CHOH)_2COO)_{0.37})}$$

FT-IR spectra and DSC/TGA traces showed almost identical features compared with commercially available AAT, but with lower levels of impurities as analysed by XRF <0.03% CaO, 99.8% Al_2O_3, with ~0.2% SiO_2. The maximum equivalent oxide yield of alumina was ~7% w/w in solution due to problems with considerable practrical increase in reaction time (days compared to hours) of the tartaric acid and BAA above this concentration.

6.6. Lab AAT (55:45) 5% Zirconia Addition

The new precursor was introduced into the standard composition containing Nyacol colloidal zirconia (10nm), as detailed below.

Procedure for Mixing Precursors

Lab AAT

Distilled Water – 3006g

L-Tartaric Acid 99%– 555g (Aldrich T, 10-9)

Basic Aluminium Acetate (BAA) – 988.2g (Fluka 06157)

Mixing Procedure

The BAA is added slowly to the already dissolved tartaric acid/water mixture whilst stirring with a high shear mixer in a 5 litre beaker. When each of the components have been thoroughly mixed transfer the contents of the 5l beaker to two smaller 2l Pyrex thick walled glass beakers. Make a mark on the side of the beakers showing the fill line. A magnetic stirrer should then be added to each of beakers. After doing this a sheet of cling film should be stretched over the top of each of the beakers and fastened down with tape. Each of the beakers should then be placed on a hotplate in order to evaporate the mixtures down. To enable vapour to escape the cling film can be punctured a few times with a needle. Usually around about 400 ml of solution is evaporated off from each of the beakers. Once this has been achieved the beakers should be removed from the hotplates and refilled to the fill line previously marked using distilled water. The resultant solutions are then filtered using a vacuum pump and a No 1 Whatmann filter paper.

Alkoxide Sol

Water – 2988g

Aluminium Nitrate Nonahydrate 98% – 900g (Aldrich 23,797-3)

Aluminium Isopropoxide 98% – 979.2g (Aldrich 22,041-8)

Tetraethylorthosilicate (TEOS) 98% – 457.6g (Aldrich , 190-3)

Mixing Procedure

Once again mixing should be carried out using a high shear mixer and also in the order of addition shown above. Once the aluminium precursors have benn dissolved the TEOS is added slowly over a period of around 20 min, as this hydrolyses at a slower rate.

Mixed Mullite Sol

A blend of Lab AAT, alkoxide sol and colloidal silica and zirconia res is made in the following way:

Lab AAT – 1473.25g + 150g SMAS = Mix C

1500g of Mix C + 1500g of Mul 5 + 66.28g ZrO_2

A further hotplate evaporation is made to remove a total volume of 800ml prior to rotary evaporation detailed previously. The sol was extruded and heat treated in the same way as before. The fibre surface was very smooth, (**Figure 6.14**) the fracture surface free from cracks and porosity. Granulation and porosity only appears between 1500 – 1600°C.

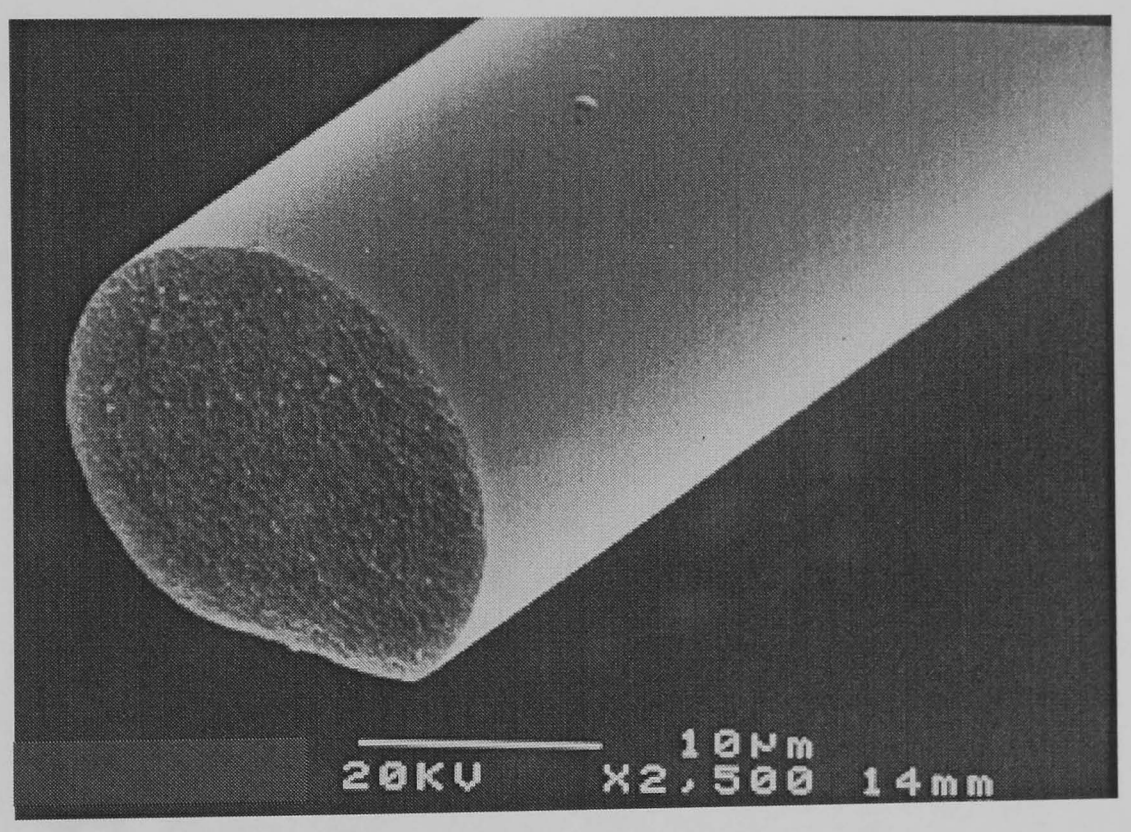

Figure 6.14: Lab AAT Mixed Mullite Fibre Fired to 1400°C/4 hours (55:45 + 5 wt% Nyacol ZrO_2).

6.6.1. Thermal Analysis

Weight loss was complete (75%) at ~450°C a large exothermic peak was observed at 376° (oxidation of the carboxylate groups), followed by a smaller exotherm as 964°C formation of γ-alumina seen by XRD.

6.6.2. XRD Analysis

Features of the individual sols blended to form this system are apparent in **Figure 6.15** as broad peaks at ~45° and 21.5° which may be a disordered or nanocrystalline form of γ-Al_2O_3 (JCPDS 15-776 cubic spinel) and nanocrystalline ZrO_2 (JCPDS 17-923 tetragonal), respectively, as seen in the AAT/Colloidal silica sol. Mullite crystallises at 1200°C. The in situ precipitation of zirconia is mainly observed above 1200°C when the broad peak at ~30° appears, corresponding to tetragonal ZrO_2.

This phase is not normally stable without the addition of a stabilising ion such as Y^{3+} [6]. However this may be explained by the extremely even distribution of the initial fine (10nm) colloidal material used which can be seen as fine black regions in the TEM **Figure 6.17**, compared to TEM **Figure 6.16** without zirconia. Peak broadening due to <100nm initial mullite crystal size does not clearly distinguish between tetragonal (2:1) and orthorhombic (3:2) (JCPDS 10-425) forms below 1200°C, but at 1300°C the ~26° double peak is a resolved corresponding to the [120]-[210] orthorhombic planes [7].

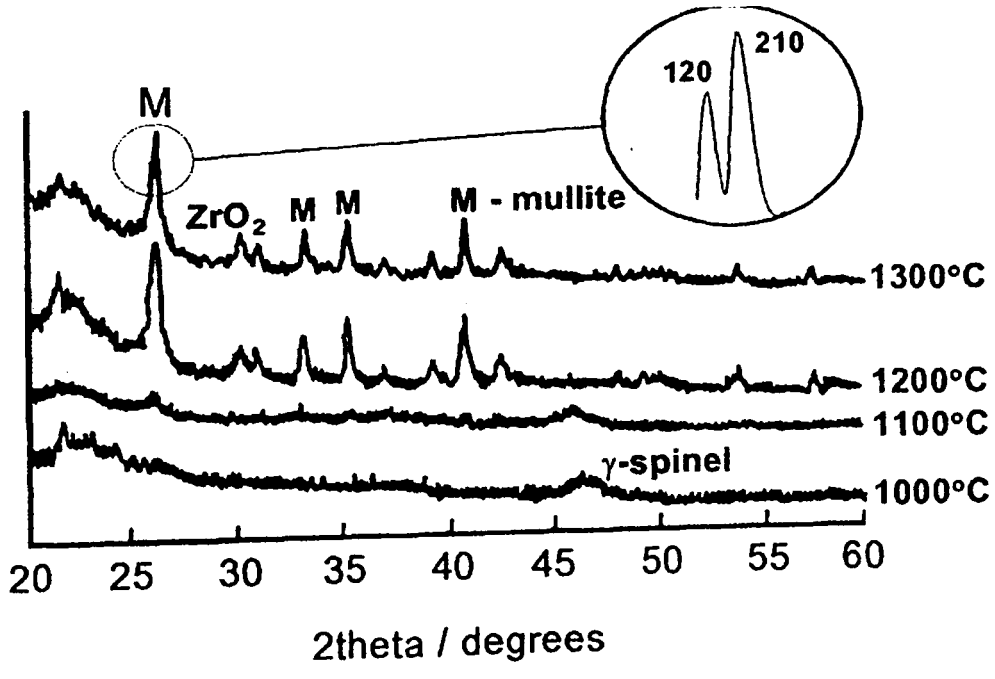

Figure 6.15: XRD Trace with Varying Pyrolysis Temperatures

6.6.3. TEM Analysis

Analysis of fibres fired at 1400°C/4 hrs was conducted using Transmission Electron Microscopy (TEM).

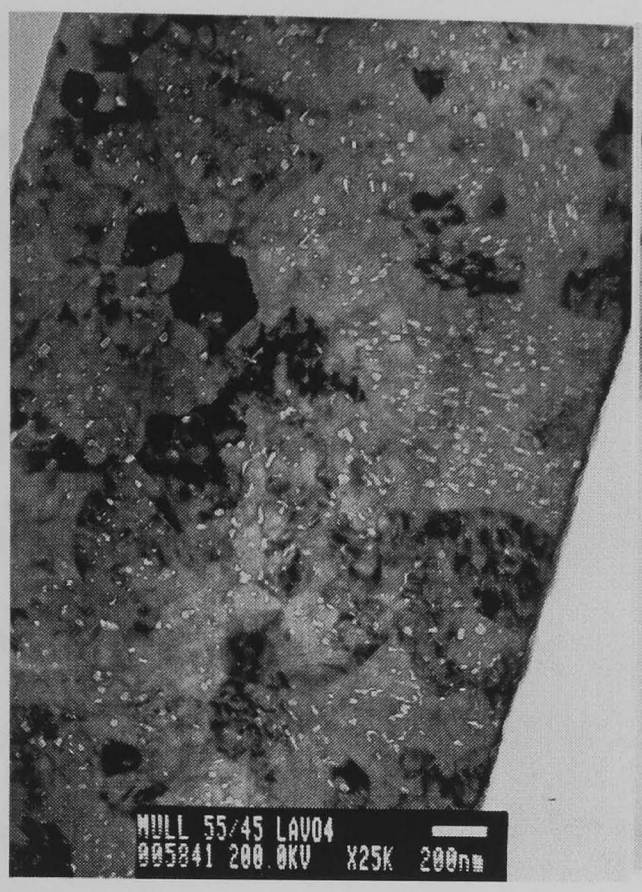

Figure 6.16: Mixed Mullite (55:45)

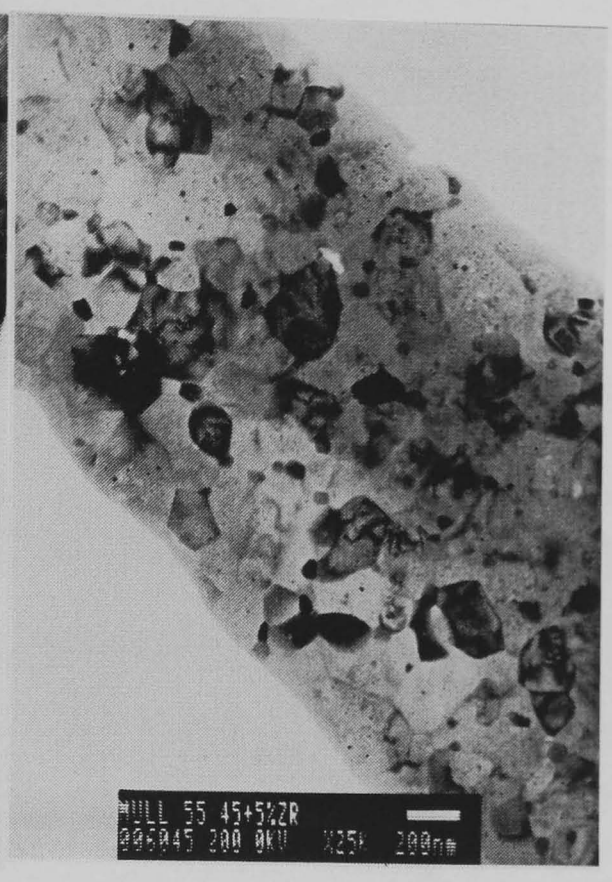

Figure 6.17: Mixed Mullite Fibre + 5% ZrO_2

The images shown in **Figures 6.16 and 6.17** demonstrated the marked change in nano-scale, mainly intragranular, porosity; this is reduced in the presence of the precipitated nanosized ZrO_2, which is visible at grain boundaries and within mullite crystals. The small grain size of the zirconia means that it is therefore thermodynamically stable in the tetragonal form below ~50nm, without the normal inversion to monoclinic (baddeleyite). The inhibition of grain growth, following mullite crystallisation, has enhanced the efficiency of sintering via grain-boundary transport to residual pores to yield dense fibres. An important element of this mechanism is the uniform distribution of nanoscale additive particles, which is only obtainable via dissolution in the initial sol and re-precipitation during conversion of gel to the crystalline state.

In order to define more accurately the optimum addition of zirconia for sintering and grain refinement, a series of zirconia additions in the range 0 to 5% were made and fibres evaluated further.

6.7. Lab AAT (55:45) With Incremental Zirconia Additions

Further batches of fibre were produced with 1% incremental additions of Nyacol AC colloidal zirconia (0 – 5%) in order to establish how the zirconia affects the microstructure of the fibre.

6.7.1. XRF Analysis

XRF analysis shows that impurities such as CaO, K_2O and Na_2O, which are the major contaminants responsible for producing glassy phases are relatively low, at least in terms of the detection limits (~<0.05%) of the equipment. The experimental fibres are listed in **Table 6.4** with commercial Nextel 720 fibre for comparison.

Sample	*0% ZrO_2*	*1% ZrO_2*	*2% ZrO_2*	*3% ZrO_2*	*4% ZrO_2*	*5% ZrO_2*	*Nextel 720*
Na_2O	<0.05	<0.05	<0.05	<0.05	<0.05	0.07	<0.05
MgO	<0.05	<0.05	<0.05	<0.05	<0.05	<0.05	<0.05
Al_2O_3	**72.0**	**73.1**	**72.6**	**72.6**	**72.1**	**72.3**	**85.5**
SiO_2	**28.7**	**27.4**	**26.9**	**25.5**	**25.6**	**23.9**	**14.3**
Fe_2O_3	0.05	0.08	<0.05	<0.05	0.06	<0.05	**0.5**
Y_2O_3	<0.05	<0.05	<0.05	<0.05	<0.05	<0.05	<0.05
ZrO_2	**<0.05**	**0.92**	**1.90**	**2.67**	**3.61**	**4.39**	<0.05
HfO_2	<0.05	<0.05	<0.05	0.06	0.08	0.09	<0.05
LOI @ 1025°C	<0.01	0.01	<0.01	0.01	<0.01	<0.01	N/A
Total	***100.7***	***101.5***	***101.5***	***100.8***	***101.5***	***100.7***	***100.3***

Table 6.4: XRF Analysis of Fired Fibres

Worthy of note is the high Fe_2O_3 level in Nextel 720, which has been found in some 3M patents for preparing bi-component continuous fibres. 3M use this as a 30% colloidal ferric oxide (OMG Americas "Cem-All"™) to promote isomorphic seeding of α-alumina, in this alumina rich-mullite fibre.

Such compounds as haematite (α-Fe_2O_3), goethite (α-FeO(OH)), and lepidocrocite (γ-FeOOH) have the same structure as corundum (α-Al_2O_3), diaspore, and boehmite, respectively [8].

6.7.2. TEM Analysis

It was evident that there was a gradual reduction in intergranular porosity (**Figures 6.18 - 21**) with increasing addition of zirconia up to a threshold of 3-5% were there was little difference in the overall microstructure. The optimum addition for elimination of nanoporosity appeared to be at ~5% w/w, this composition was therefore preferred over the pure mullite fibre.

Figure 6.18: 1% ZrO_2 1400°C/4hrs

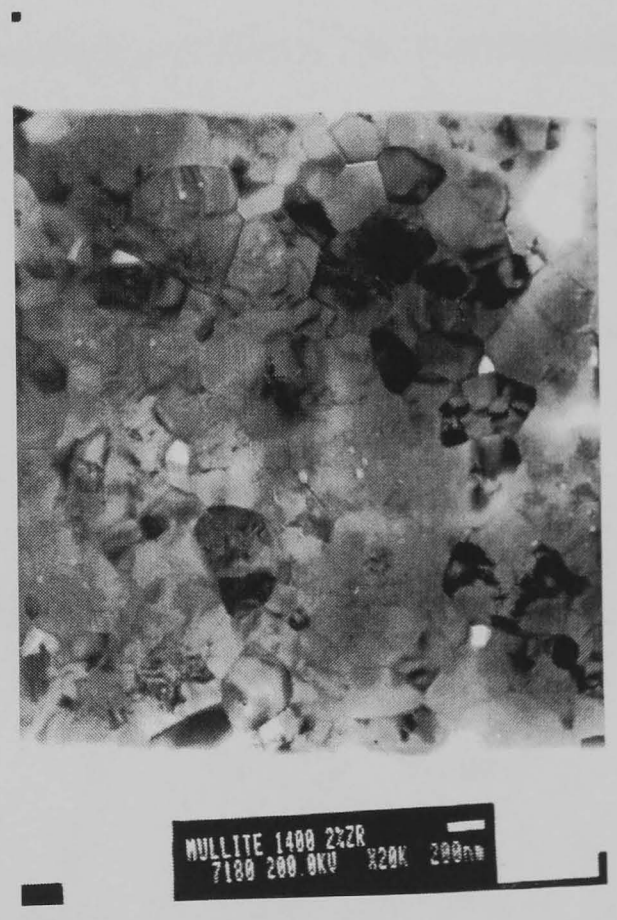

Figure 6.19: 2% ZrO_2 1400°C/4hrs

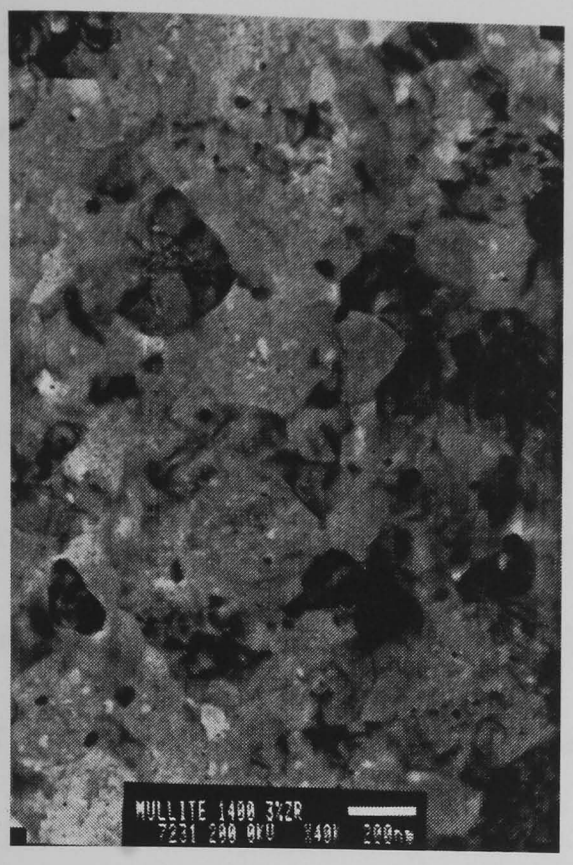

Figure 6.20: 3% ZrO_2 1400°C/4hrs

Figure 6.21: 4% ZrO_2 1400°C/4hrs

6.7.3. XRD Analysis

One sample of each fibre containing 0%, ~5% zirconia and Nextel 720 were evaluated for mullite crystallite size after heat treatments from 1200 – 1600°C/24hrs. This showed that zirconia does indeed inhibit grain growth with increased temperature. The preferred ~5% zirconia – mullite fibre is very similar to the commercial Nextel 3M mullite – alumina fibre.

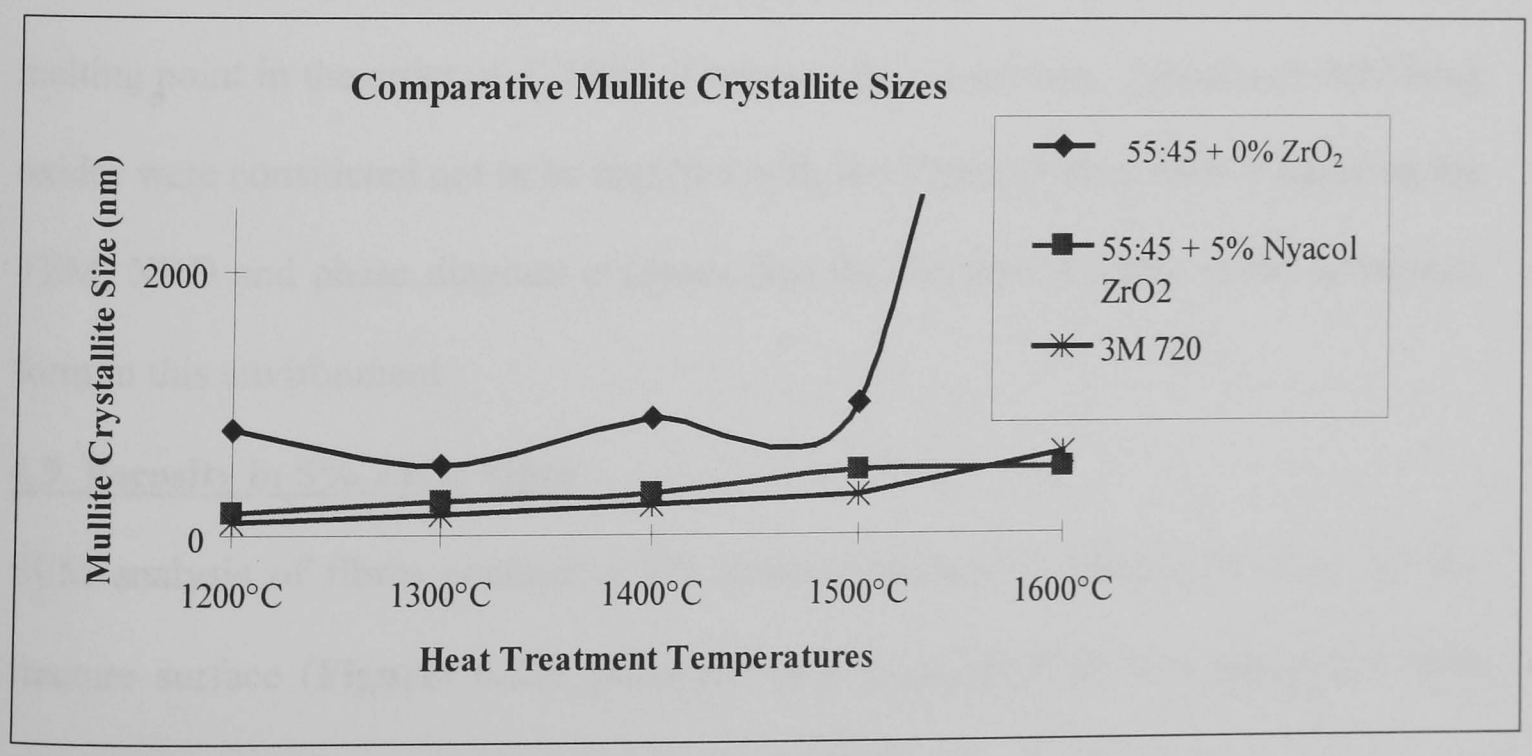

Figure 6.22: Mullite Crystallite Size Comparison of Doped and Non Doped Fibres

6.8. Stabilising Additives for Zirconia

Zirconia appeared to assist the sintering and stabilisation of grain growth up to 1400°C and improved the overall stability of the fibre at high temperatures. Normally stabilisation of the zirconia has to be considered, as the tetragonal phase will transfer to the monoclinic or cubic phase, if diffusion occurs at high temperatures and the improvement in toughness is lost in mullite monolithic ceramics. Fibres made using a larger colloidal zirconia source (~100nm) had been shown to transform to monoclinic zirconia above 1200°C, this would be expected as these colloids are initially large and are less thermodynamically stable. This incurs a volume expansion of 3 - 5% resulting in crack propagation, producing small defects. Partial stabilisation of zirconia in the tetragonal phase requires typically a 3 - 5 mole % addition of stabilising additives; examples of such additives for zirconia are yttria, ceria, magnesia and calcia. The ternary Al_2O_3 - SiO_2 – ZrO_2 [9] phase diagram in the American ceramic society "Phase Diagrams for Ceramasists", 1964 and 1969 volumes was consulted to determine the stability of zirconia with the stoichiometric 3:2 mullite system. Zirconia is insoluble in the mullite phase and therefore is thermodynamically compatible, only forming the zircon ($ZrSiO_4$) phase, which has a melting point in the order of 1775°C, if excess silica is present. Additional stabilising oxides were considered not to be required with the 10nm zirconia colloid based on the TEM, XRD and phase diagram evidence that the zirconia is stable in the tetragonal form in this environment.

6.9. Porosity in 5% ZrO_2 Fibre

SEM analysis of fibres containing 5% zirconia showed a dense outer crust on the fracture surface (**Figures 6.23**), polished samples highlighted core separation after 1500°C/4 hours (**Figure 6.24**) and not up to 1300°C.

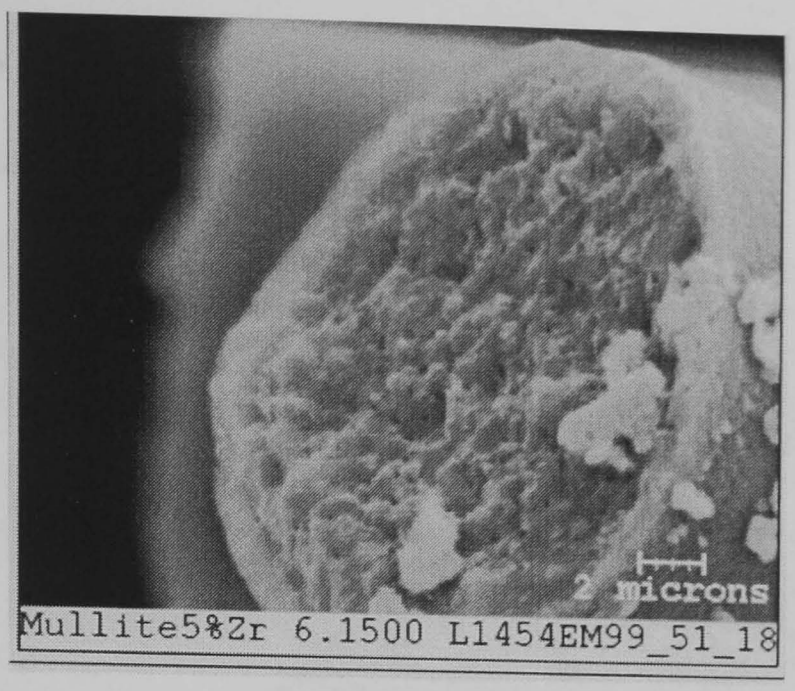

Figure 6.23: SEM 1500°C/4hrs

Fibres with a larger cross sectional diameter appeared to exemplify this feature the most.

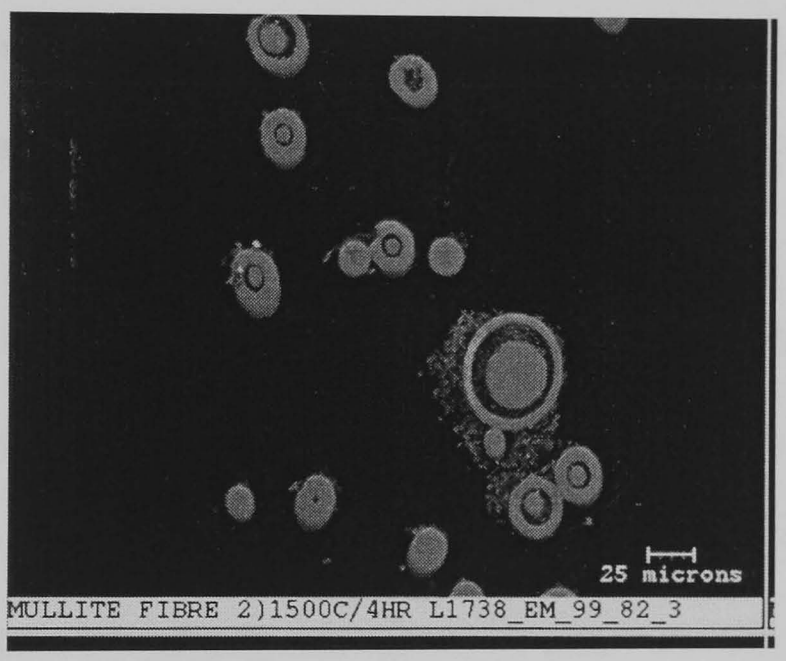

Figure 6.24: SEM 1500°C/4 hours (Polished)

Further analysis on polished samples using quantitative EDS revealed that the inner and outer core areas do not differ significantly from the expected stoichiometric 3:2 mullite + zirconia composition, even with temperature (1100°C, 1300°C and 1500°C). SEM also revealed that even fibres fired to 1100°C (still amorphous) and polished show this separation effect. EDS analysis on further samples was used to map for non metallic elements and it was found that sulphur was detected as a significant element

in the inner core only (dense red area), as seen in **Figures 6.25 (SEM) & (EDS)**. This phenomenon was found to affect fibres of all diameters.

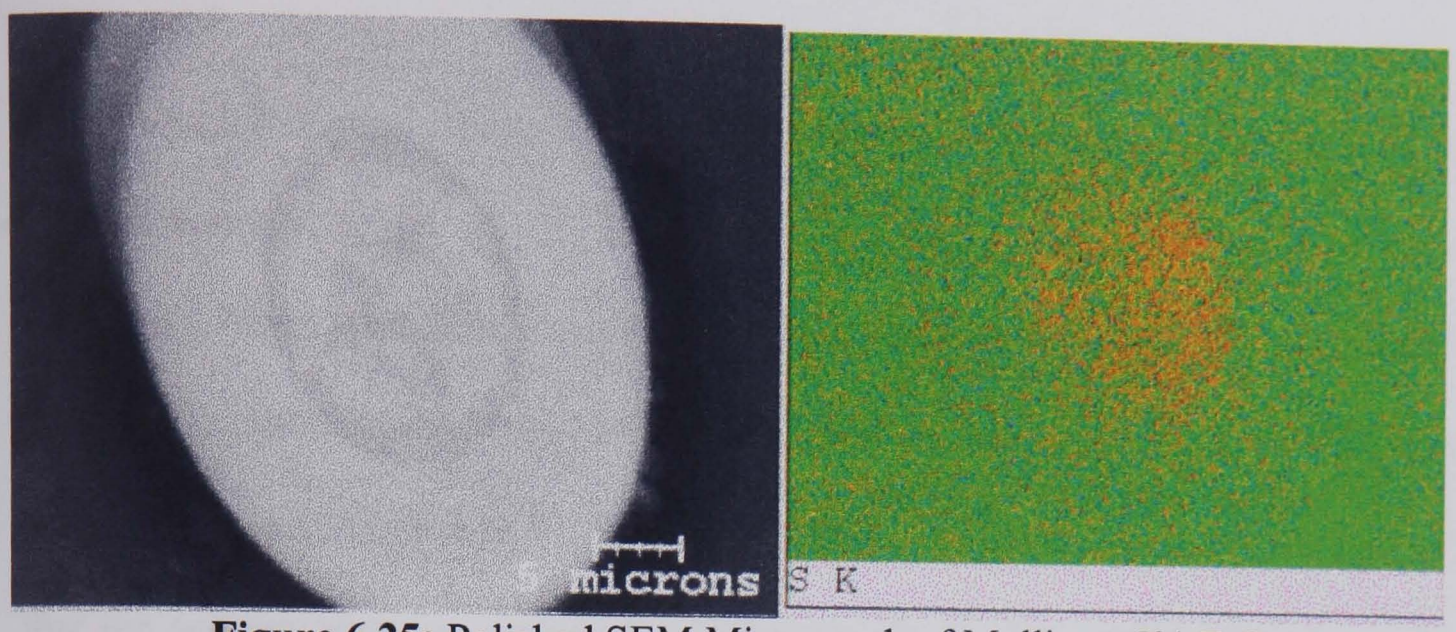

Figure 6.25: Polished SEM Micrograph of Mullite + 5% ZrO_2 Fibre Heat Treated to 1300°C/4 hours and EDS Map

As XRF did not show a high value for sulphur (0.06% SO_4^{2-}- **Table 6.3**) ICP analysis of the individual sols was carried out. The alkoxide containing <10ppm and the lab AAT was found to contain 460ppm Sulphur, which was derived from the BAA component. Similar EDS mapping was carried out on unfired fibres and did not show sulphur preferentially abundant in the inner area, therefore it was more likely that this occured by diffusion during firing. Careful pyrolysis of the sulphate ions minimised the porosity of the final sintered polycrystalline fibre, due to small voids being created which allowed full densification at high temperatures.

6.10. Sulphur Free Lab AAT

It was clear that the major source of sulphur was from the insoluble BAA, the options to eliminate sulphur completely from BAA, resulting in sulphur free mullite sols were as follows:

1. Alternative higher purity commercial grade – **not available.**
2. Specific ion exchange for sulphate, replaced with an innocuous anion i.e. OH^- or CH_3COO^- – **not easily available.**

3. Precipitation of SO_4^{2-} using a soluble Barium salt i.e. nitrate, acetate – even if stoichiometric quantities of Barium were used only ~80% of soluble S was removed.
4. Thorough oxidative calcination to remove sulphur as a volatile component i.e. SO_X – **evaluated.**

Additional fibres were fired in smaller tows and analysed. This time no cores were seen, further batches of fibres were also evaluated examining specific fibre diameters. from the smallest eg 5μm to the largest ~30μm producing the same result suggesting that the sulphur was not completely eliminated in the first batch due to such large quantities being fired at one time. This shows that if fibres are batched fired, sufficient oxygen, ventilation and removal of combustion gases is important.

6.11. Sol Rheology

In order to assess the affects of ageing of the mixed mullite + 5% ZrO_2 sol a series of three sols were made at different concentrations, by controlling the volume of condensate removed during rotary evaporation. A standard 3kg batch was made in each case and the following volume of condensate removed:

Low Solids = $1000cm^3$

Medium Solids = $1100cm^3$

High Solids = $1200cm^3$ (Typical sol)

The importance of being able to extrude a sol through a spinnerette at high shear rates, over a period of time with continuity is important for the manufacture of continuous polycrystalline oxide fibres. If the sol becomes too viscous, it may be difficult to overcome the yield stress required to move it through the hole. Equally if it is not viscous enough, it will shear easily and will not have sufficient strength to remain as a strong green filament [10].

This results in poor Newtonian drying times (as with lower viscosity. less concentrated sols used for staple fibres), which impedes draw down to its final fine diameter. Newtonian flow behaviour is important, as the viscosity will change in a linear manner with the shear applied, without sudden and dramatic change.

Typical shear rates for hole diameters used in continuous fibre production can be derived, at a fixed liquid rate, shear rate (γ) in the holes is given by:

$$\gamma = (32 \times \pi) \times Q/\pi r^2$$

Q = flow rate (cm^3/s^{-1})

πr^2 = area of spinneret hole

Equation 6.2: Shear Rate of a Sol During Extrusion

It can be seen that the larger hole size and the greater the number of holes in a spinnerette of fixed area also reduces the shear rate considerable (**Table 5**).

Spinneret	Shear Rate s^{-1}
100μm - 100 holes	162
80μm - 100 holes	253
80μm - 20 holes	1267
70μm - 20 holes	1655
70μm - 20 holes	1655
60μm - 20 holes	2253
50μm - 20 holes	3244

Table 6.5: Shear Rates for Standard Spinnerette and Hole Geometries

As the sol concentration and viscosity is normally higher for extruded continuous fibres, it would be expected that stable jet length should increase. It has been demonstrated previously [11], that jet integrity is derived from the cohesive energy density of the material, and in practice the stable jet length starts to decrease at high measured viscosities. As this material sheared to a slightly lower viscosity it makes it easier to draw into continuous filaments.

Viscosities were measured on each sol over a period of five weeks using a Carrimed CSL (500) cone and plate rheometer using the following settings:

Platform to spindle clearing	43μm
Cone	2 cm 1 59 degrees (43μm Truncation)*
Air Pressure	30 psi
Platform Temperature	20°C
Equilibration Time	10 sec
Run Time	2 min
Shear Stress	(0-10,000)Pa ~Linear Increase

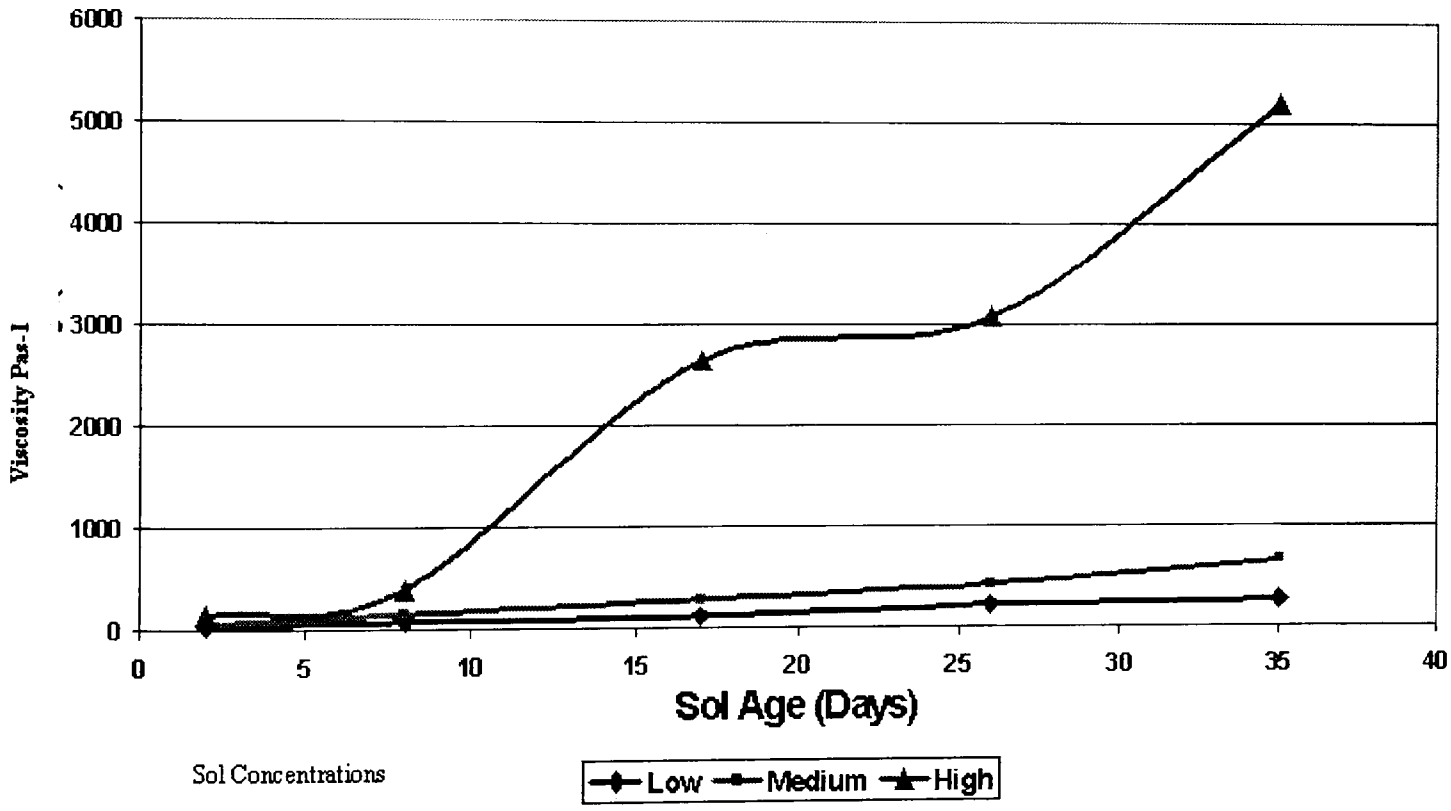

Figure 6.26: Viscosity Vs Time at a Shear Rate of 1 s^{-1}

At a constant low shear rate the sols containing more liquid show very consistent ageing over time, as viscosity has changed only ten fold over five weeks, unlike the high solids sol which has changed nearer thirty five fold (**Figure 6.26**). After 7 – 8 days it shows a dramatic increase in viscosity.

If the sol is shear thinning then the higher the initial viscosity, the more tolerant it will be and more versatile for extrusion through different spinnerette holes and multiplicities. Typically the shear rate would be a few hundred for the spinnerettes used during these experiments (80 - 100µm - 100 holes). Looking at the affect of shear rate Vs viscosity (Faint grey line) of the low solids sol (**Figure 6.27**) it shear thins down from a viscosity of ~100Pas^{-1} to 70Pa^{s-1} with a maximum shear rate of 40 s^{-1}. This is implies that the material is prone to shear thinning, but retains Newtonian flow behaviour as the shear stress Vs shear rate is linear.

Figure 6.27: Low Solids Sol Shear Stress and Viscosity Vs Shear Rate

The high solids sol also demonstrates a shear thinning behaviour and Newtonian flow, but is less easily sheared according to the maximum shear rate of ~2.5 s^{-1} achieved (**Figure 6.28**). This means that the viscosity should remain higher during extrusion and the ability of the fibre to be drawn (if viscoelastic) should be higher.

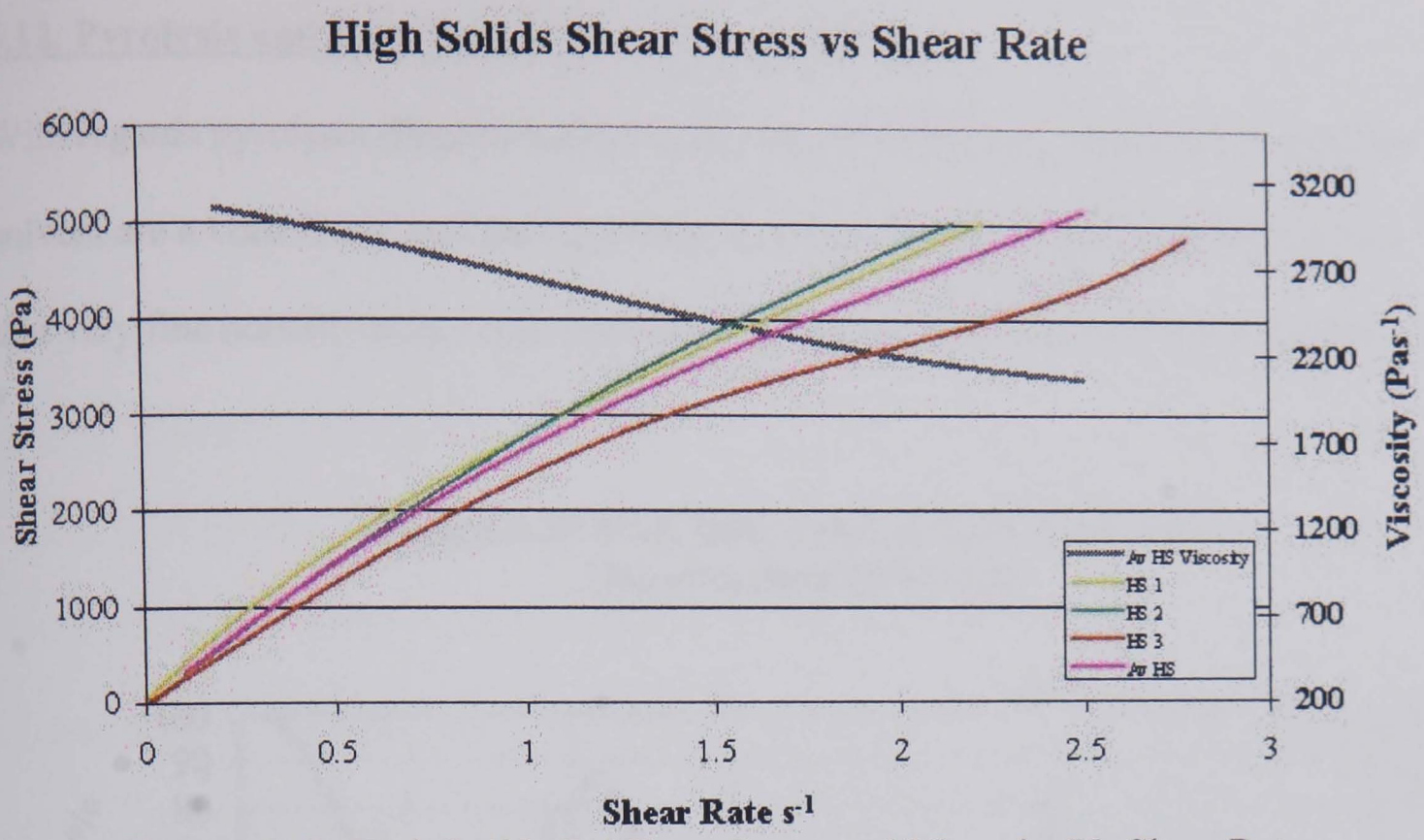

Figure 6.28: High Solids Sol Shear Stress and Viscosity Vs Shear Rate

All of the sols were extruded on the day a viscosity measurement was taken using the 100µm - 100 hole spinnerette and fibre collected. The low solids sol was difficult to collect and draw as the viscosity was very low as it emerged from the holes and remained very sticky collecting on the winding drum and sticking together.

The medium solids sol was slightly better and improved slightly with time, but still problematic to dry and wind. The high solids sol was much better, easily wound during the first week for more than 10 minutes at a time without breakage.

A gradual increase in gas pressure and pump speed was required over the remaining period to maintain the same extrusion conditions. Seven days was considered optimum, after this, green fibre quality was not as good. The cohesive energy density therefore appears to be better for a higher viscosity in this system, which is contrary to the literature [12], although the addition of a linear chained organic polymer is said to increase cohesive energy density of most systems. As the Aluminium Acetotartrate appears to be extremely viscoelastic on its own, it is fair to say that this acts as an inorganic spinning aid allowing high viscosity, more shear resistant sols to be dry spun and drawn down into strong green fibres.

6.12. Pyrolysis and Low Temperature Phase Formation

With regards pyrolysis (**Figure 6.29**) a large volume (>70%) of fugitive organics and solvent are a volatilised and ignited during the initial firing process it is also possible that very fine porosity may occur when leaving the pre-consolidated fibre structure.

Figure 6.29 TGA/DSC Trace of Extruded Fibres (Heating Rate 20°C/min)

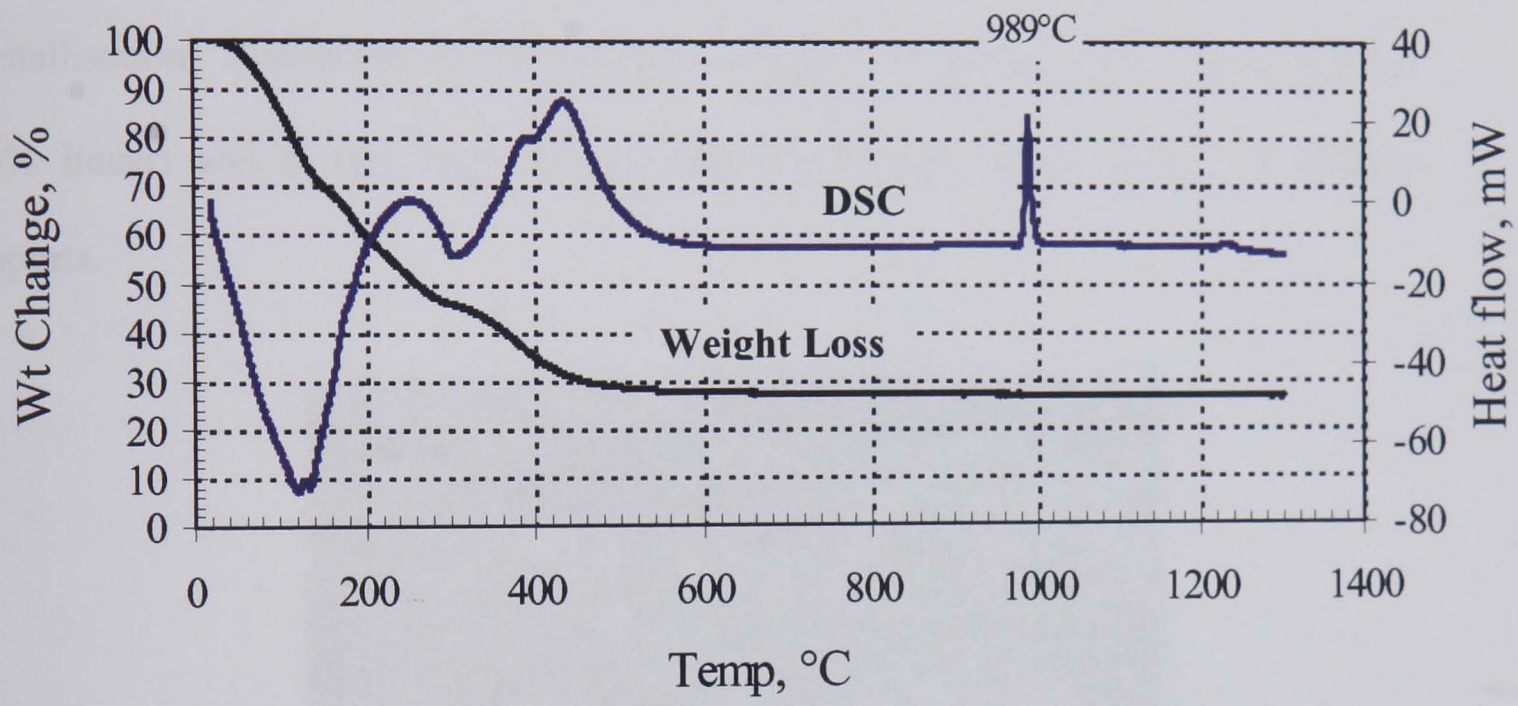

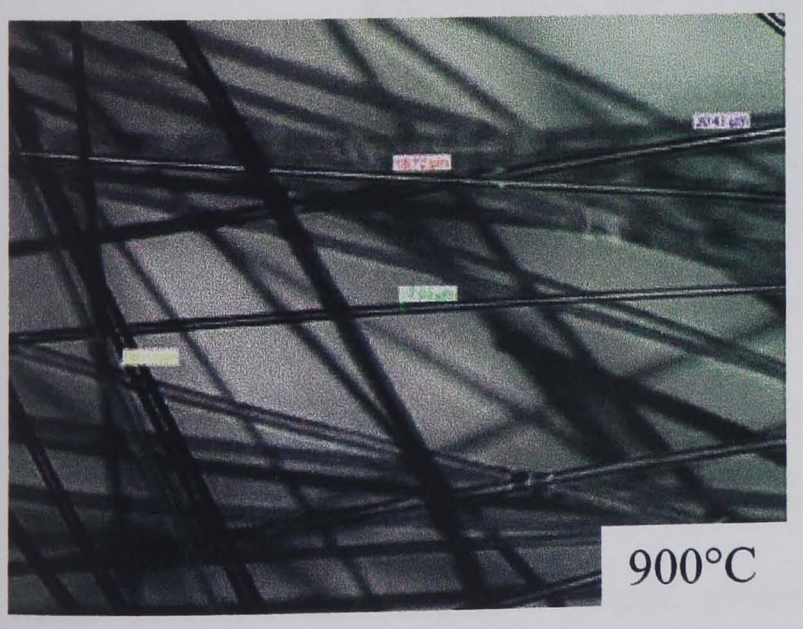

Figure 6.30: Fired to 900°C/24hrs

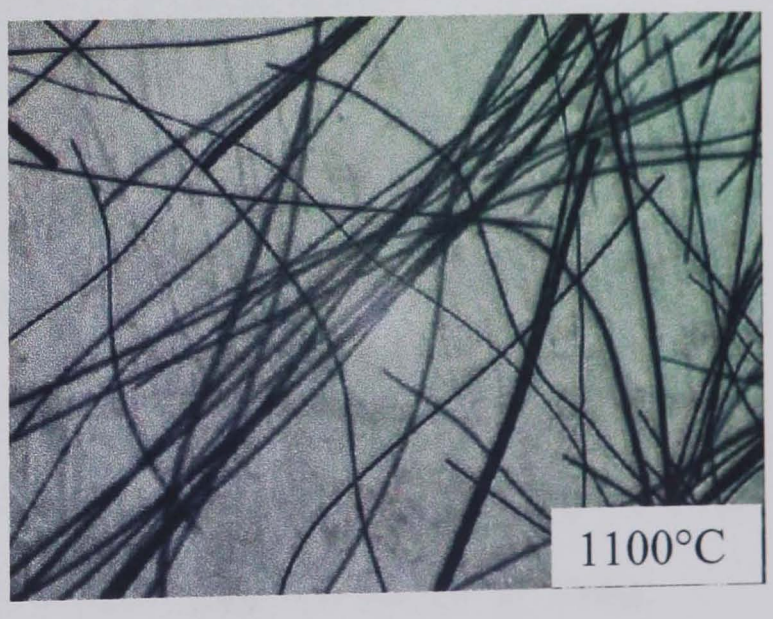

Figure 6.31: Fired to 1100°C/24hrs

From the TGA/DSC trace of the fibres it appeared that the initial crystallisation reactions occured at ~990°C which could be the formation of γ-alumina or initiation of mullite crystallisation which then proceeds to form mullite exclusively above 1200°C, once all of the amorphous silica phase has been consumed. Many fibres appear "kinked", the optical images of mullite + 5% ZrO_2 fibres shown in **Figures 6.30 – 32** showed that kinks were more predominant after heat treatments of >900°C, which coincides with intermediate γ-alumina phase formation and subsequent mullite crystallisation. Formation of the γ-alumina phase is associated with large shrinkage (26% linear) and a very high surface area <1000m^2/g, hence its use in catalyst supports.

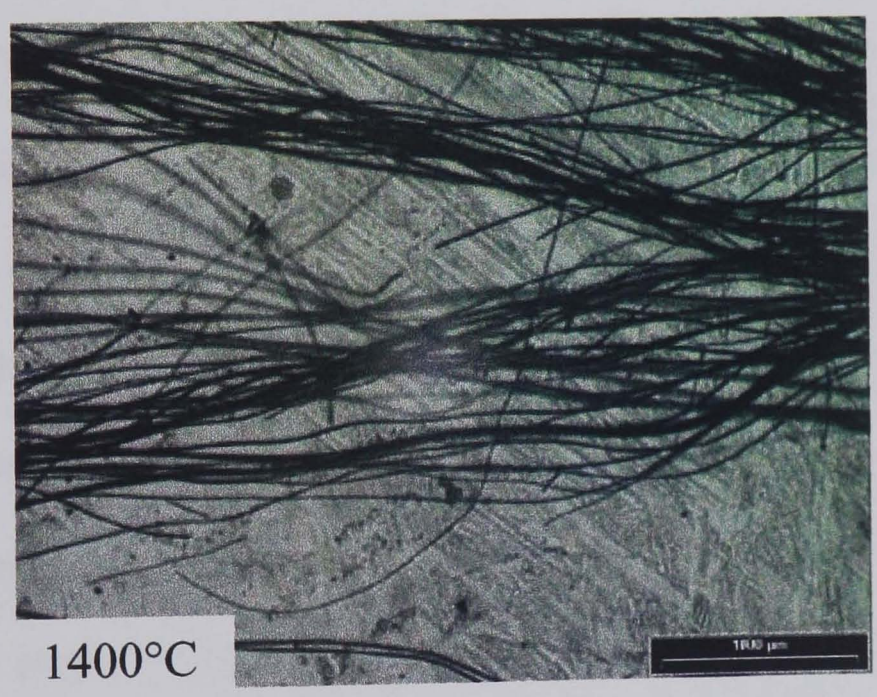

Figure 6.32: Mullite + 5% ZrO_2 1400°C/24hrs

Fibres were visibly more kinked once fired to >900°C, which produced a stress point that introduced a strength determining defect in the fibre. As the defect appeared when devitrification occured it was probably related more to factors affecting crystallisation and crystal size as opposed to the loss of volatile components in the precursor fibre.

6.13. Porosity

Porosity is generated when aluminium hydroxides are dehydrated. Porous aluminas are important commercial adsorbents and catalyst supports, and there is a large volume of literature on their preparation from aluminium hydroxides. Details of porosity development such as size, size distribution, shape, and overall pore volume are sensitive to process conditions and impurities in the hydroxides. The stoichiometric amount of alumina in the hydrous aluminas ranges down from 83.5% in boehmite to 50% in a gelatinous alumina, and this alone gives a large scope for variation. Since the work of Yoldas, there have been extensive studies on aluminium alkoxide, especially sec-butoxide, decomposition. The range of surface areas after decomposition, 1-800 m^2/g, is a measure of the breadth of precursor and process variation [13]. Wilson and Stacey [14] investigated the decomposition of a well crystallised boehmite initially to γ, then at higher temperatures through δ to θ, then α-alumina. They showed that the oxygen layers remained intact during the decomposition, which consumed the sheets of hydroxyl between them, leaving lamellar micropores 0.8 nm across on a repeat 3.5- 4 nm spacing. The decomposition and transition is topotactic, with the shape of the original boehmite crystal maintained in the transformed product. The theoretical surface area of these micropores is 180 m^2/g, and a maximum of 107 m^2/g was measured by nitrogen adsorption possibly because the pores were too fine to allow proper penetration of the nitrogen molecules. As the transition proceeded there was some sintering, cross linking, and merging of pores, which were faceted and 6 nm across in δ rising to 9 nm in θ, with a final rounded 25-70 nm in α-alumina.

Wilson and Stacey's data on accessible surface area, mean pore size, and total pore volume are effectively those for single boehmite crystals, they show that even in this simple system, working from a dense hydrous alumina, there is an accelerated growth in pore size as α-alumina is formed. Polycrystalline transition aluminas are not sintered when α-alumina nucleates above 1100°C. After nucleation α-alumina, crystals grow rapidly to a large size and entrap the remaining porosity. The reduced volume of α-alumina (density 3.99 kg/m^3) compared to the transition aluminas (density 3.65 kg/m^3) will facilitate this behaviour. The rapidly advancing α-crystal front could sweep out small pores in the transitional alumina [15]. It is also observed that some pores are occluded inside whole α-alumina crystals and this is consistent with Wilson's speculation that the larger pores had coalesced inside the original boehmite relic. It has been shown that nucleation in bulk transitional aluminas gives a weak product with a high level of residual porosity [16], not sintered at 1200°C and uncontrolled rapid growth of α-alumina effectively destroys a pure alumina fibre. Also the formation of α-alumina has a damaging effect on alumina-boria-silica [17] and mullite containing fibres [18].

6.14. Low Angle XRD Non Intrusive Porosity Measurements

Low angle XRD analysis has been proven to be useful in determining the size of the voids in synthetic zeolite structures. Hence the technique was used to determine the internal porosity due to phase formation and sintering as traditional methods such as Specific Surface Area and Helium Picnometry did not work. These methods rely on the intrusion of gas molecules into the pore structure, which is either very fine or enclosed in the fibre core. This non-intrusive technique was used in order to detect nanometer sized porosity as demonstrated for synthetic zeolite mesoporous structures.

Fibres were heat treated at 180°C/hr to 400, 600, 900, 990, 1100. 1200 and 1400°C/4hrs as well as unfired (green) has been carried out using a low angle scan (2 – 10 °2θ). Results of the analysis are given in **Figure 6.33** showing the size of "features" in nm for each given heat treatment.

$$n\lambda=2d \sin \theta$$

Equation 6.3: The Bragg Equation

To;

$$d=\lambda/2\sin\theta \text{ (in angstroms (Å))}$$

Equation 6.4: Transposed Bragg Equation

In order to relate the °2θ values from the xrd scan to the size of the pore in Angstroms and then multipling by 10 converts to nm.

The wavelength of the $K\alpha_1$ Copper X-ray source is:

λ Cu= 1.54056

□ The pore size in nm is:

$$1.54056/(\sin(°2\theta \times \pi/180)*20)$$

Equation 6.5: Pore Size Calculation in nm

There appears to be small dimensional "features" in all fibres to greater or lesser extent regardless of heat treatment, however distinct trends can be seen between the green (unfired) material up to ~900°C. A 400°C heat treatment results in a broad size range of porosity, due to removal of free and bound water plus combustible organics and does not alter significantly through to 600°C. This appears to coarsen and become larger in number (counts) as the firing temperature increases, which is coincidental with the formation of porous intermediates such as γ-alumina.

Above 900°C the levels recede with increasing temperature, which would correspond with sintering and densification to ultimately form dense stoichiometric mullite.

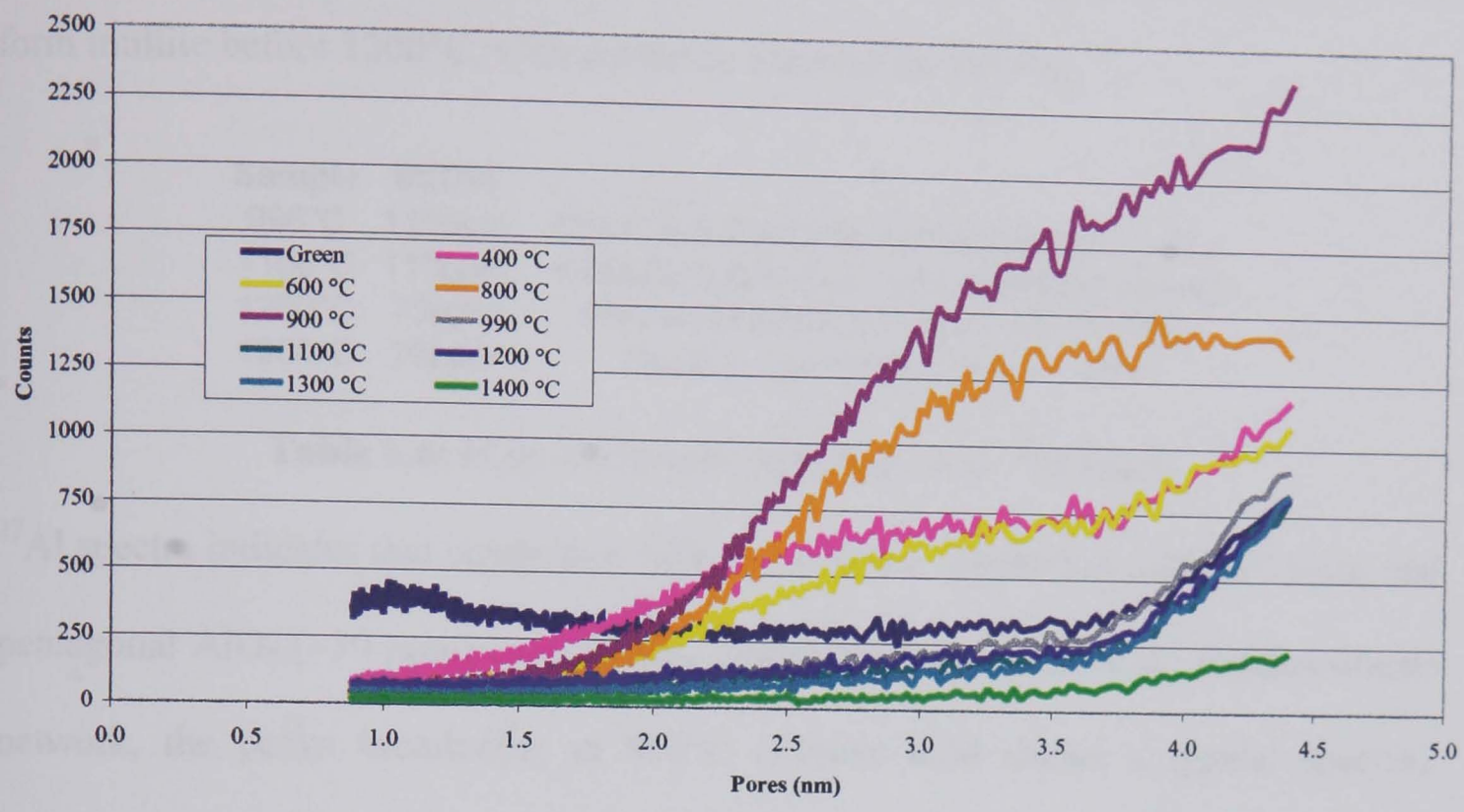

Figure 6.33: Low Angle XRD of Fast Fired (180°C/hr) Mullite + 5% ZrO_2 fibres

As the TGA was carried out at a relatively fast ramp rate of 20°C/min (1200°C/hr) it is possible that the DSC crystalisation temperature observed for γ-alumina at 989°C is higher than the actual temperature at which it occurs. This would explain why a subsequent further increase in porosity is seen at 900°C and then densification at 990°C and above.

6.15. Fibre Characterisation Using Solid State NMR

^{29}Si NMR spectra and ^{27}Al spectra were acquired on a Varian UNITY 300MHz Inova spectrometer with a 7.05 T Oxford Instruments magnet. The resonance frequency for ^{29}Si and ^{27}Al are 60 and 70MHz respectively. Chemical shifts were referenced to tetramethylsilane (TMS) for Si and aluminium chloride for Al. The samples were the same as used for low angle XRD, but milled in a tungsten carbide "Tema Mill".

The 110 ppm Si peak at 990°C and 1100°C corresponds to tetrahedral SiO_2 rich domains from the heterogeneous gel (derived from colloidal SiO_2). With increasing temperature the free SiO_2 is reacted with the aluminosilicate-surrounding network to form mullite before 1200°C, with complete reaction by 1300°C.

Sample	Si(O)4	
990°C	110ppm	Silica Rich Domains, heterogeneous mixing
1100°C	110ppm	Silica Rich Domains, heterogeneous mixing
1200°C	75ppm	Free silica starts to react to form mullite
1300°C	75ppm	Reaction complete to form mullite

Table 6.6: Main Chemical Shift Peaks For ^{29}Si Nuclei

^{27}Al spectra indicates that octahedral AlO_6 (~3.5 ppm), tetrahedral AlO_4 (57 ppm) and pentagonal AlO_5 (~30 ppm) co-ordinated aluminium is present in the aluminosilicate network, the peaks broadening at 950°C (**Figure 6.34** shows a typical spectra). Above 950°C the broad peak containing the three components resolves into AlO_6 and AlO_4 with a corresponding shift to ~6 ppm and 60 ppm, respectively at 980°C. At 990°C the appearance of a new, more intense AlO_4 peak at 46 ppm is typical of orthorhombic mullite. The 46 ppm AlO_4 peak has been ascribed to a T* site in which three (triclustered) $A1O_4$ tetrahedra are linked to a common oxygen atom [19]. With increasing temperature both peaks become more resolved with the tetrahedral peak becoming less broad due to continuing structural refinement of stoichiometric mullite at 1300°C. These observations are consistent with the phase identification determined using X-ray diffraction analysis.

Sample	Al(O)4	Al(O)5	Al(O)6	
Green			0.22ppm	
400°C	-	-	-	
600°C	57ppm	28ppm	0.85ppm	
800°C	57ppm	30ppm	3.35ppm	4&5 inc rel to 6, Peaks shifting to higher frquency
900°C	50ppm	29.3ppm	3.6ppm	
950°C		30.9ppm		Broad peak, little structure, contains all 3 forms
980°C	60.5ppm		6.1ppm	Resolved, tet & Oct
990°C	45.9ppm		-1ppm	6 retained, 4 now more substantial
1100°C	45.9ppm		-2.9ppm	Resolved, tet & Oct
1200°C	45.3ppm		-2.9ppm	Resolved, tet & Oct
1300°C	43.4ppm		-3.5ppm	Resolved, tet most structure (less broad)
1400°C	42ppm		-3.5ppm	

Table 6.7: Main Chemical Shift Peaks For ^{27}Al Nuclei

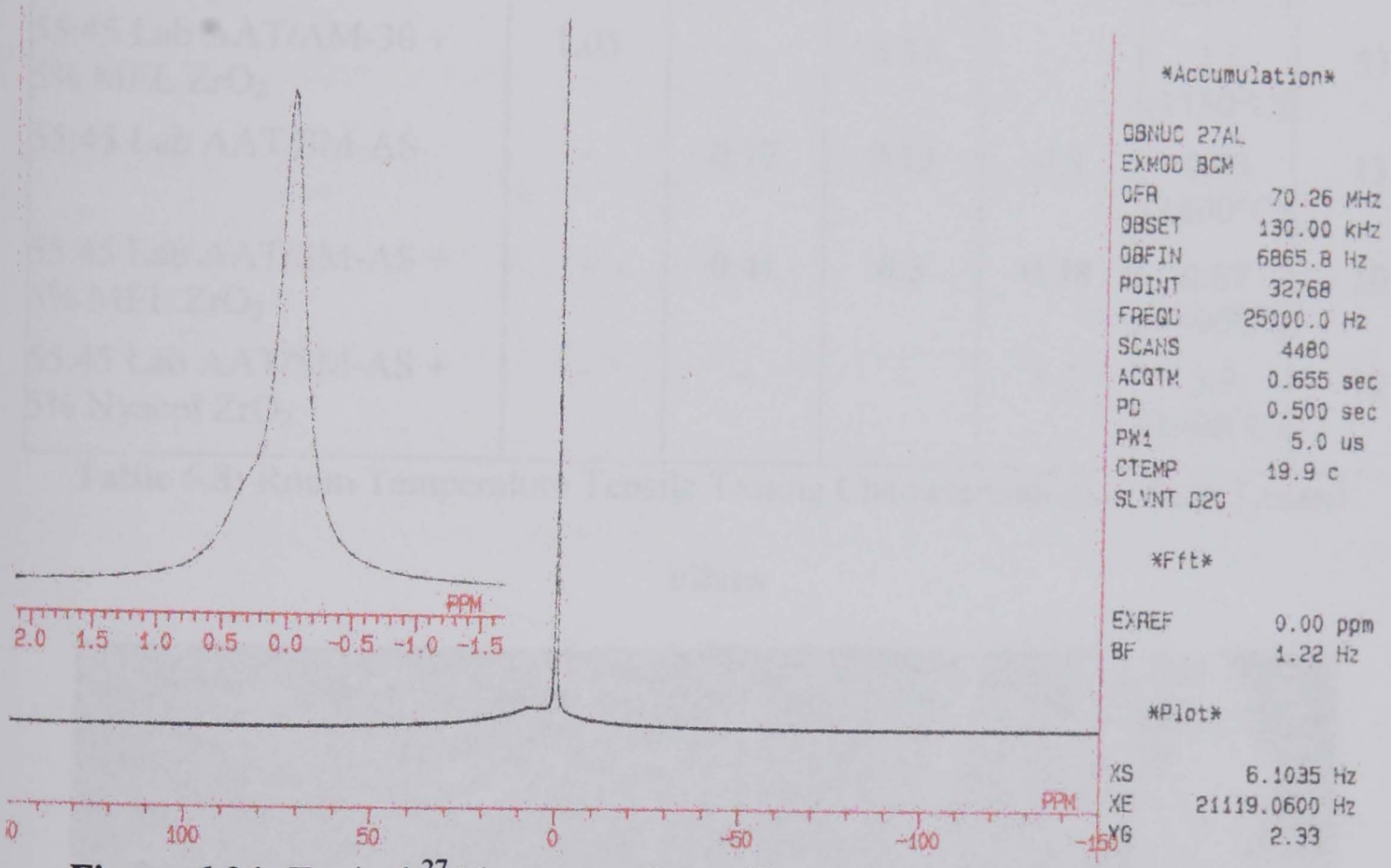

Figure 6.34: Typical ^{27}Al spectra of a mullite and 5% zirconia sol-gel prior to extrusion

6.16. Preliminary Room Temperature Mechanical Tensile Tests

A selection of fibres made during the development work were evaluated after heat treatments of 4hrs in the temperature range 1150 – 1400°C, results are summarised in **Table 6.8**.

This revealed that, potentially, the mixed mullite compositions containing zirconia ~5% could produce very respectable mechanical strengths of 2.5 – 2.9GPa, after heat treatments at 1400°C for 4 hours, although the average values were lower than expected due to processing defects such as kinks, cracks and bubbles as seen in **Figure 6.35**.

	Average Tensile Strength (GPa)					
Composition	**1150°C 4hrs**	**1200°C 4hrs**	**1300°C 4hrs**	**1400°C 4hrs**	**Maximum Strength (GPa)**	**Ave. Diameter (μm)**
50:50 Com. AAT/ AM-30	-	0.04	0.09	0.05	0.17 (1200°C)	30
55:45 Lab AAT/AM-30 + 5% MEL ZrO_2	1.05	-	0.35	-	2.5 (1150°C)	33
55:45 Lab AAT/SM-AS	-	0.17	0.13	0.3	0.43 (1400°C)	13
55:45 Lab AAT/SM-AS + 5% MEL ZrO_2	-	0.41	0.3	0.38	0.67 (1400°C)	10
55:45 Lab AAT/SM-AS + 5% Nyacol ZrO_2	-	-	-	1.2	2.9 (1400°C)	10

Table 6.8: Room Temperature Tensile Testing Characterisation of Heat Treated Fibres

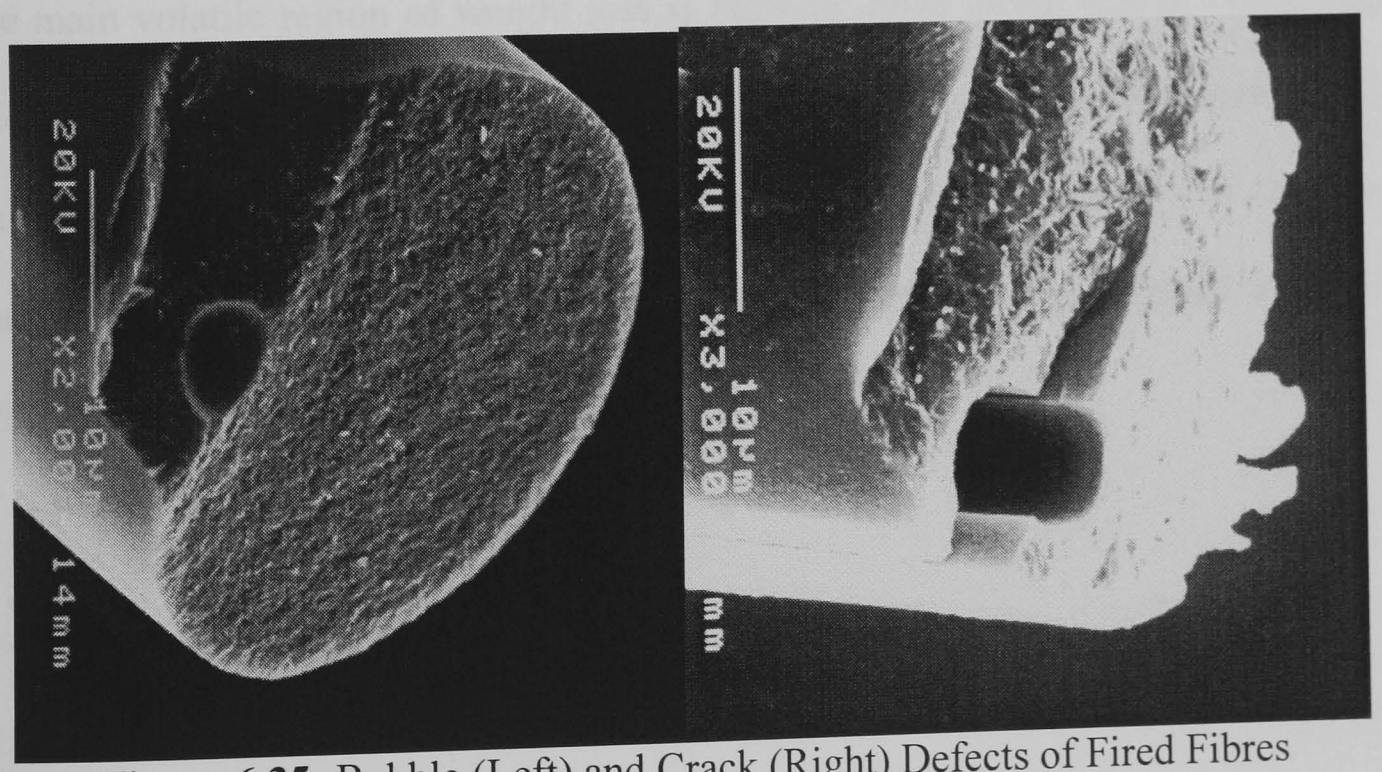

Figure 6.35: Bubble (Left) and Crack (Right) Defects of Fired Fibres

6.17. Effect of Firing Rate on the Microstructure

As porosity may be evolved either from loss of water or conversion of combustible components to carbon dioxide, nitrogen oxides or water, a heat treatment regime was determined from dta data, to pass through the regions of high rate of weight loss during pyrolysis (**Table 6.9**).

	Stage 1	Stage 2	Stage 3	Stage 4	Stage 5	Stage 6
Ramp Rate °C/hr	10	15	5	30	30	180
Target °C	60	120	310	510	600	1400
Duration hr	2	2	2	2	30	4

Table 6.9: Multi Step Slow Firing

The idea is to reduce the rate at which fugitive precursor components are converted to gases or vapours of larger volume, reducing the size of the voids created when leaving the still plastic precursor fibre during pyrolysis. A long dwell at 600°C is required as the slow firing produces a more reducing atmosphere in the kiln which forms a visible black carbon deposit on the surface of the fibres. The effect of reducing the firing rate is clear from the comparison of 180°C/hr (**Figure 6.36**) and 18°C/hr (**Figure 6.37**). The main volatile region of weight loss is reduced down to the loss of water, acetic acid and remaining residual propanol from the offset. The combustion/carbonisation mainly of the organics is controlled such that the removal is gradual and consistent. The effect of moist air and nitrogen atmospheres were also investigated as to their effects, but without any merit.

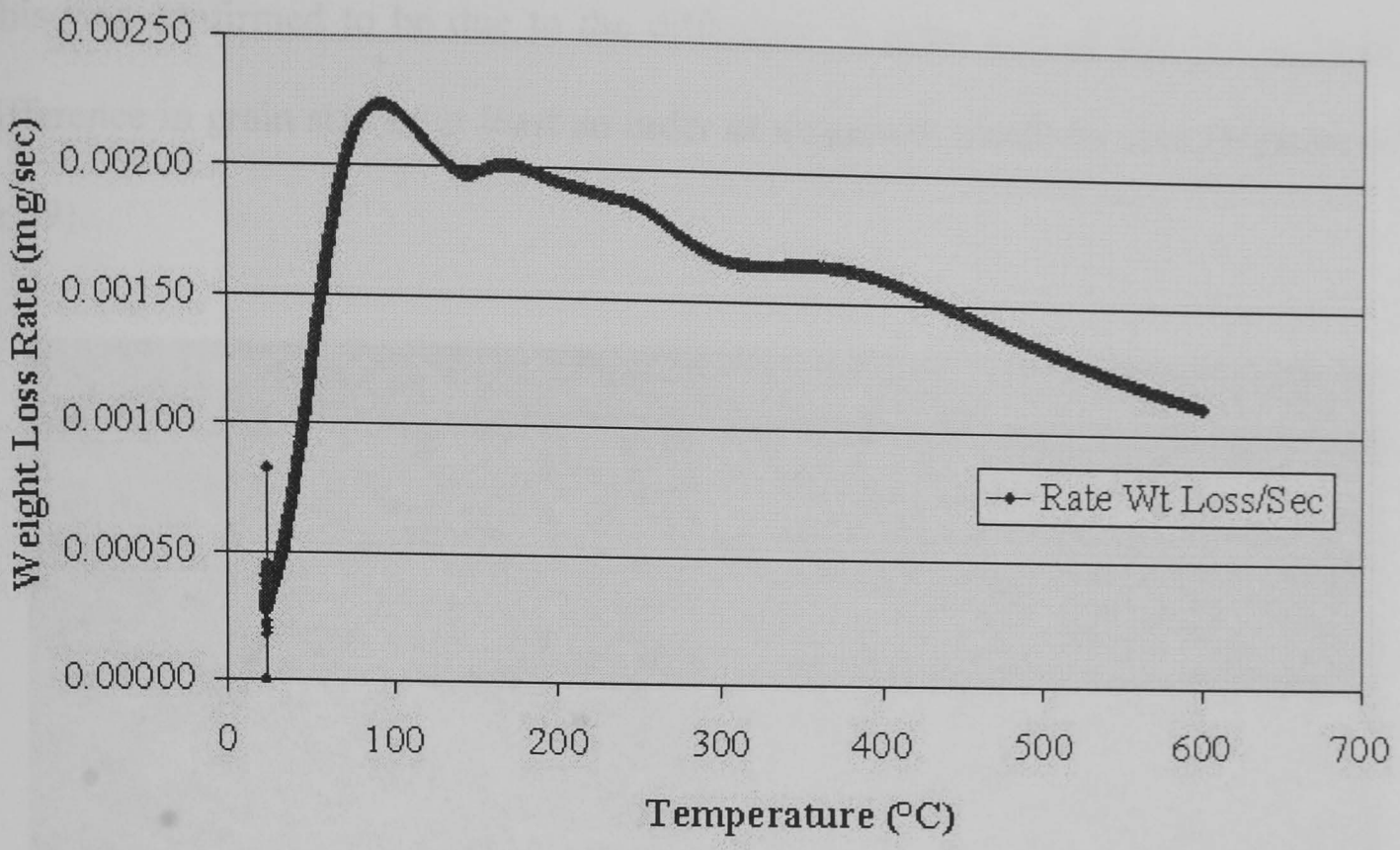

Figure 6.36: Rate of Weight Loss/second @ 180°C/hr

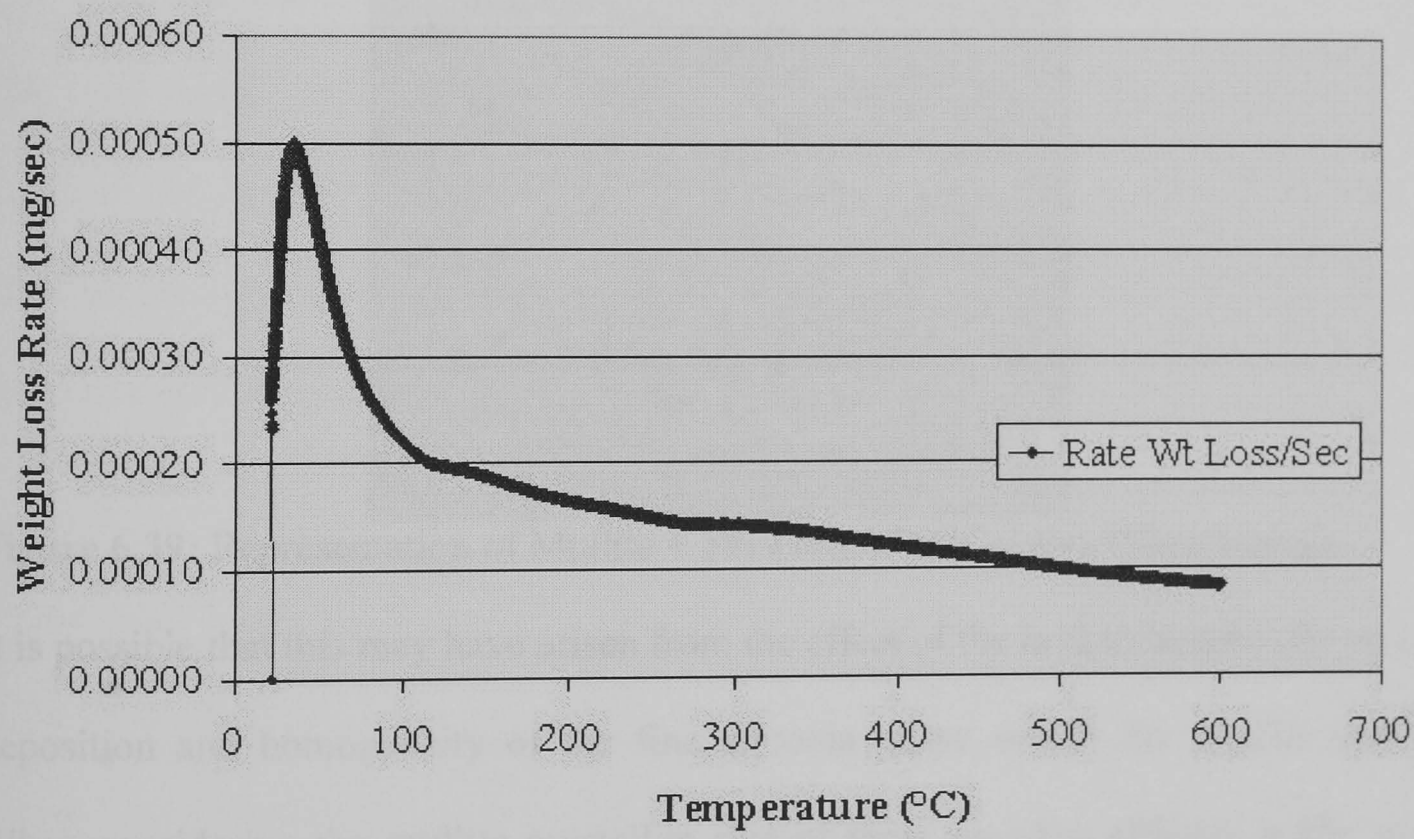

Figure 6.37: Rate of Weight Loss/second @ 18°C/hr

Samples of fast fired (180°C/hr) and slow fired fibres fired to 1400°C were analysed by SEM in order to determine the effects of grain size in relation to firing conditions. It was visible that the slow fired fibres were much more translucent than those fired more rapidly, implying less light scatter due to fine grain size.

This was confirmed to be due to the difference in grain size of the two samples, a difference in grain size of at least an order of magnitude could be seen (**Figures 6.38 & 39**).

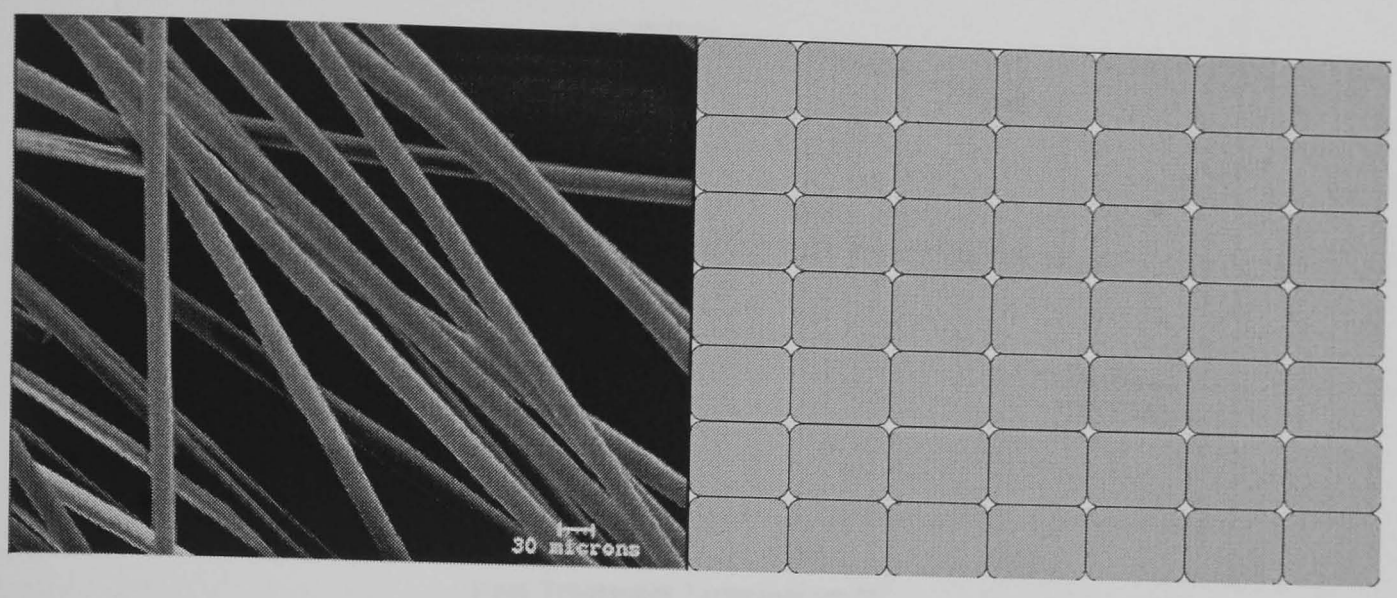

Figure 6.38: Representation of Mullite + 5% ZrO_2 1400°C/24hrs (180°C/hr)

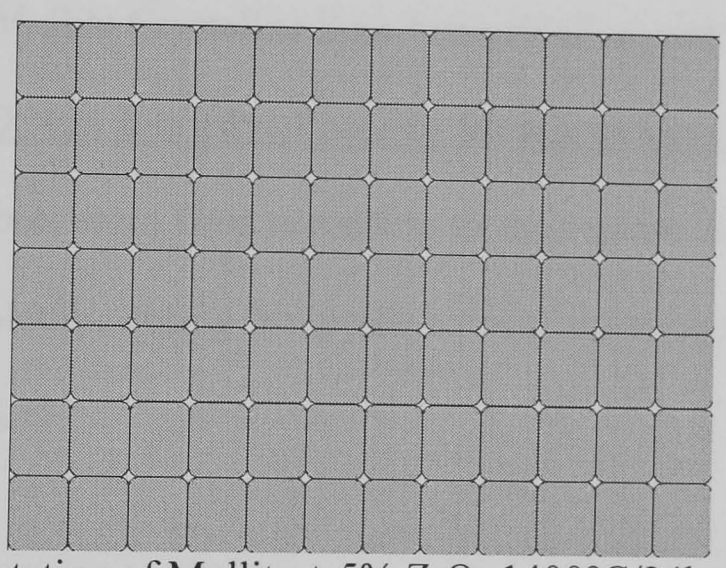

Figure 6.39: Representation of Mullite + 5% ZrO_2 1400°C/24hrs (Slow Firing)

It is possible that this may have arisen from the effect of the heat treatment rate on the deposition and homogeneity of the fine zirconia phase within the mullite matrix. When considering the mullite crystallite size of these powders **(Figure 6.40)**, with respect to temperature it can be seen that the firing rate has a marked effect.

Both powder samples when fired slow have a smaller and uniform crystallite size than those fired fast, as seen from SEM images. As diffusion is not inhibited in this system the firing rate may determine the precipitation or deposition of the zirconia grains, influencing their ability to control grain growth.

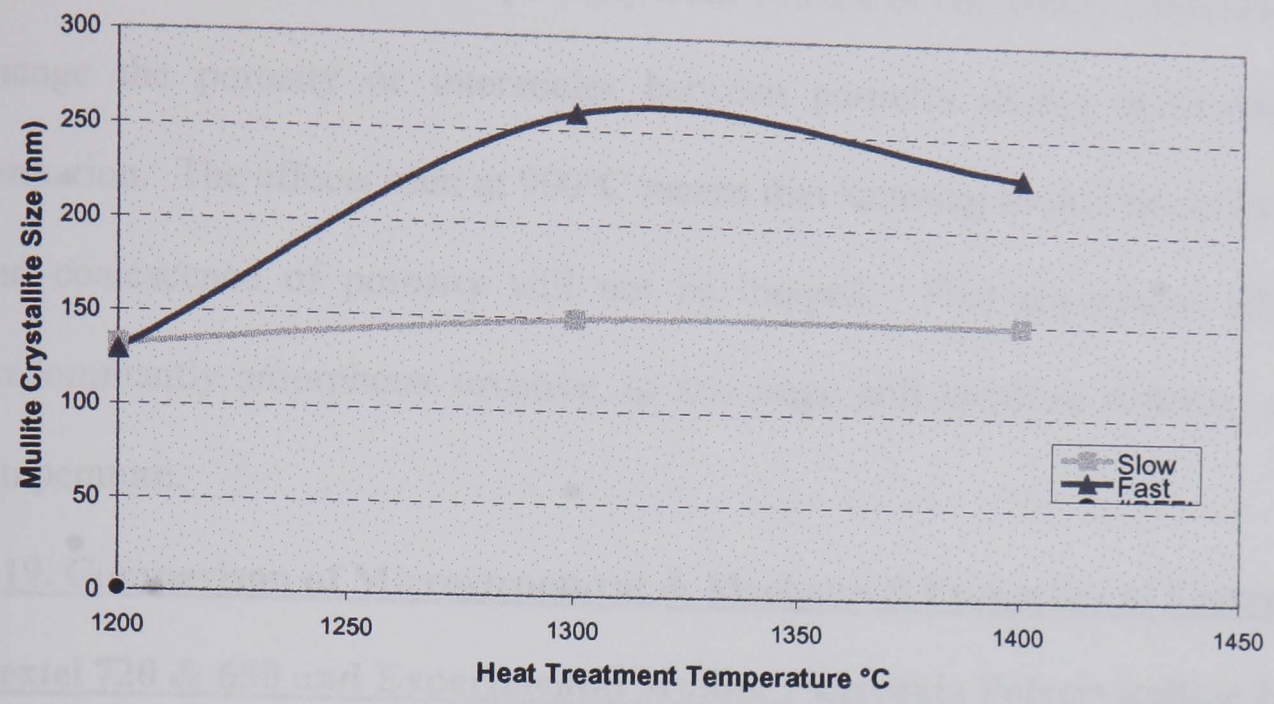

Figure 6.40: Mullite Crystallite Size Analysis (Fast and Slow Firings)

6.18. Low Angle XRD Non Intrusive Porosity Measurements Slow Fire

Mullite + 5% ZrO_2 fibres were fired according to the regime in **Table 6.5** to see the effect on porosity evolution during the pyrolysis and sintering process. The results are plotted in **Figure 6.41**.

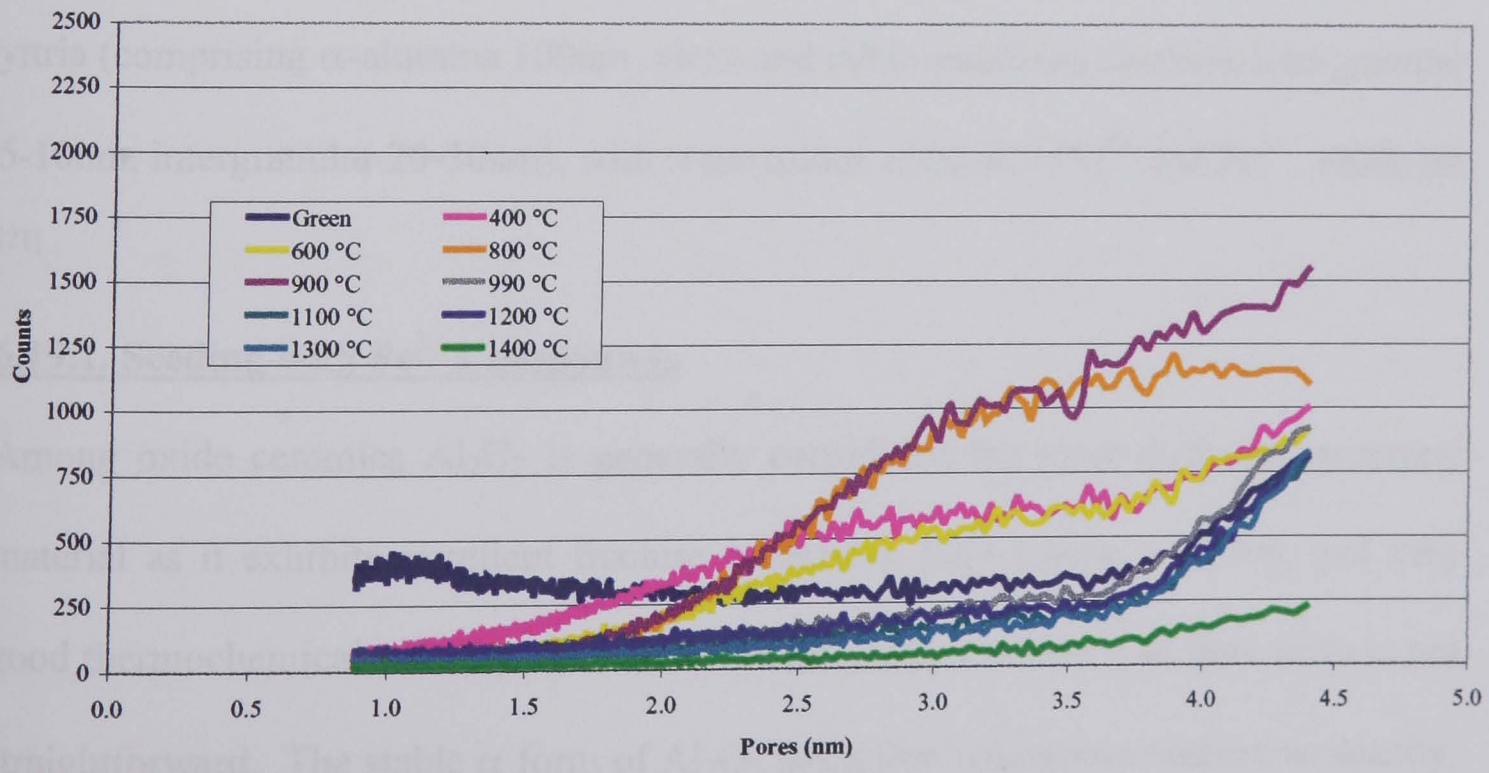

Figure 6.41: Low Angle XRD of Slow Fired Mullite + 5% ZrO_2 fibres

The main observable change is the reduction in the number of counts for 800°C and especially 900°C. This implies that the slower firing rate does not make any real difference on the evolution of porosity from volatile or combustion products, but does change the porosity or intersticies between particles during intermediate phase formation. The effects seen at 900°C means that sintering should be easier to initiate and coalescence of porosity will not be trapped. Free amorphous silica in the predominantly amorphous structure, at this stage will facilitate sintering above this temperature.

6.19. Comparison of Microstructural & Mechanical Properties of Commercial Nextel 720 & 650 and Experimental Mullite + Zirconia Polycrystalline Fibres.

Nextel 720 as received is a dense polycrystalline fibre with a circular 12μm diameter and a room temperature tensile strength of 2.1GPa [20]. Its chemical composition is 85% alumina, 15% silica (comprising α-alumina and mullite - <500nm) with some minor addition of Ferric Oxide (<0.5%). Nextel 650 as received is a dense polycrystalline fibre with a circular 11μm diameter and a room temperature tensile strength of 2.55GPa. Its chemical composition is 89% alumina, 10% zirconia, 1% yttria (comprising α-alumina 100nm, yttria and cubic stabilised zirconia, intragranular 5-10nm, intergranular 20-30nm), with some minor addition of Si^{4+} and Fe^{3+}, 1000ppm [21].

6.19.1. Seeding with Fe^{3+} Compounds

Among oxide ceramics Al_2O_3 is generally considered the most desirable structural material as it exhibits excellent fracture toughness, high elastic modulus, and very good thermochemical stability. However the fabrication of Al_2O_3 in fibre form is not straightforward. The stable α form of Al_2O_3 has a low volumetric nucleation density, which leads to large grain size.

In addition to large grains, crystallisation often leads to high levels of porosity. which inhibit sintering. Thus, control over the nucleation process during crystallisation is essential if the fine grain sizes required for high strength are to be achieved. This has been described in 3M's predominantly alumina based Nextel 610 fibre for this purpose at an addition of 0.65%. It was demonstrated that finely ground haematite would nucleate α-alumina at about 120°C below the temperature required for an unseeded boehmite [22]. On further heating the material proceeds to a fully sintered ceramic at 1300°C, whereas the unseeded alumina was still 20% porous. 3M [23] described the seeding of sols with ferric nitrate solution that has been treated with ammonium bicarbonate and excess nitrate and ammonium removed by dialysis. The precursor initially forms amorphous alumina, which transforms to either η or γ-alumina between 800°C and 900°C. Further transformation to α-alumina generally occurs between 900°C and 1025°C, and the structure can be fully sintered by heating at 1300°C for about 10 minutes. They also specify a ferric nitrate solution, hydrolysed by boiling, as a source of seeds.

This technique is a considerable advance on earlier practice, and the results imply a higher concentration of nuclei than that reported by [24]. The technique is used to make Nextel 610 (99% α-alumina) and appears to yield a stronger fibre product. Further refinement is described, i.e., holding the fibre between the seeding and sintering temperatures gives a novel porous α-alumina with spheroidal crystallites ~100 nm in diameter and an accessible surface area of 19 m^2/g. Adding silica delays the nucleation and gives a finer α-alumina crystal, and it is likely that seeding is used to make the Nextel 720 α-alumina /mullite composite fibre, due to the level of iron present.

6.19.2. Microstructural Stability of Nextel 720 and 650 With Temperature

Limited samples of Nextel 720 and 650 commercial fibres were obtained to determine their microstructural stability and mechanical strength, before and after high temperature heat treatments. Nextel 720 has been under development prior to the work in this thesis, the Nextel 650 product became available as an experimental fibre at the end of this research project. Both fibres are straight, shiny and almost translucent in the as received form, once heat treated at 1200 – 1400°C for 4 – 100 hour the appearance changes significantly. From the comments in **Table 6.10a and b** it can be seen that the Nextel 650 fibre is most effected by temperature and duration. After 1200°C/100 hrs the fibre becomes very brittle with some suggestion of grain growth due to the change in the appearance of the fibre. Severe kinking and grain growth occurs after heating to 1300°C, becoming more pronounced with increasing temperature and time. **Figures 6.42a and b** illustrate the difference in grain size between (**a**) 1300°C/4 hrs to (**b**) 1400°C/4 hrs.

N650	4 hrs	10 hrs	25 hrs	100 hrs
1200°C	straight, shiny	straight, shiny	straight, shiny	straight, white, brittle
1300°C	kinked, white, brittle	kinked, white, brittle	kinked, white, brittle	kinked, white, brittle
1400°C	v.kinked, white, v.brittle	v.kinked, white, v.brittle	v.kinked, white, v.brittle	v.kinked, white, v.brittle

Table 6.10a: Nextel 650 Heat Treatments vs Duration at Temperature

N720	4 hrs	10 hrs	25 hrs	100 hrs
1200°C	straight, shiny	straight, shiny	straight, shiny, opalescent	straight, shiny, opalescent
1300°C	straight, shiny	straight, shiny	straight, shiny, opalescent	straight, shiny, opalescent
1400°C	straight, shiny	straight, shiny	straight, opalescent, brittle	straight, shiny, white, brittle

Table 6.10b: Nextel 720 Heat Treatments vs Duration at Temperature

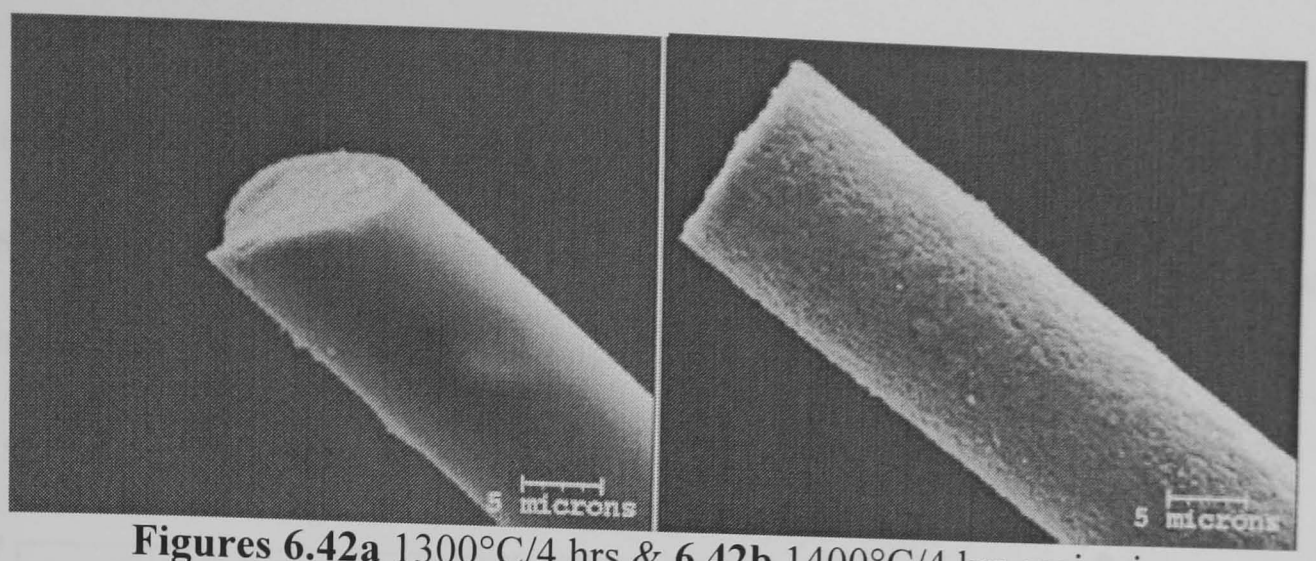

Figures 6.42a 1300°C/4 hrs & **6.42b** 1400°C/4 hrs grain size

The addition of zirconia is said to be instrumental in reducing the effect grain growth in this fibre system and rare earth oxides are reported to reduce creep by several orders of magnitude [25]. The fine distribution of zirconia can be seen in the TEM micrograph (**Figure 6.43)** as small black speckles, this has a similar resemblance to the microstructure of mullite + 5% ZrO_2 experimental fibres, fired to 1400°C/4hrs.

Figure 6.43: TEM Nextel 650 As Made Fibre

6.19.3. Tensile Test Evaluations

Mechanical tests were carried out (where possible) on 25mm gauge lengths of fibres listed in **Table 6.10a and b** using a tensile test machine, results are summarised in **Figure 6.44**. The results show that Nextel 720 fibre is less effected by temperature and time at temperature than the 650 fibre, as only 1200°C heat treated 650 fibres could be mounted for testing.

Both fibres, especially 720 (<1400°C) show an initial decline and then increase in tensile strength. This may be due to annealing of the fibres and reducing internal porosity, as the fibres are believed to be fired at the sintering temperature for only a few minutes.

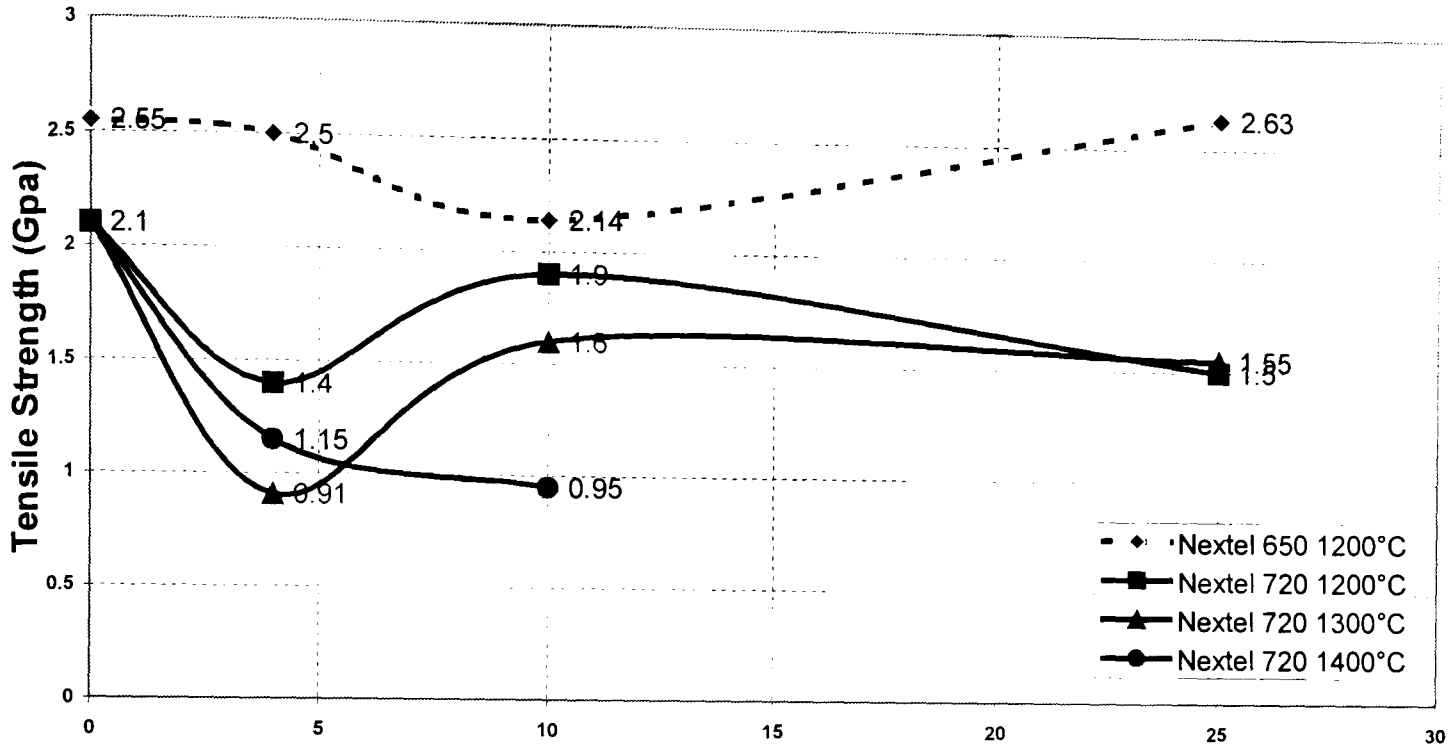

Figure 6.44: Tensile Strength of Nextel 720 and 650 vs Heat Treatment Temperature and Time

A comparison of the limited samples of commercial fibres and experimental fibres was made after heat treatment at 1250°C/4hrs as this is 50°C above the recommended use temperature of Nextel 720 which is the best commercial polycrystalline oxide fibre on the market at the time of publication. Heat treatments of experimental mullite + 5% zirconia fibres was carried under load, using cristobalite (SiO_2) microscope slides to pin the fibres down on an alumina firing plate to avoid kink formation due to high shrinkage. Tensile tests were carried out as described previously.

Fired fast to 1250°C/4hrs				Fired fast to 1250°C/4hrs			
Nextel 650	**Diameter μm**	**Load**	**GPa**	**Nextel 720**	**Diameter μm**	**Load**	**GPa**
1	11.3	0.21	2.05	1	11.6	0.21	1.95
2	11.5	0.21	2.06	2	11.4	0.23	2.26
3	12	0.25	2.17	3	11.4	0.20	2.32
4	11.6	0.26	2.41	4	10.6	0.22	2.30
5	10.8	0.23	2.52	5	11	0.22	2.20
6	11.1	0.24	2.44	6	11.2	0.20	1.89
7	10.9	0.22	2.38	7	11.6	0.18	2.15
8	11.1	0.25	2.55	8	10.4	0.16	1.81
9	11.3	0.26	2.56	9	10.5	0.18	1.84
10	10.9	0.24	2.52	10	11	0.16	1.65
Average	**11.25**	**Average**	**2.37**	**Average**	**11.07**	**Average**	**2.04**
	(11)		**(2.55)**		(12)		(2.1)
STD DEV	**0.37**	**STD DEV**	**0.20**	**STD DEV**	**0.45**	**STD DEV**	**0.24**

Table 6.11: Tensile Test Results of Best Commercial Fibres after 1250°C/4hrs Heat Treatment

The first observation is that the standard deviation of both fibre diameter and and tensile strength of the Nextel 720 and 650 is very low which is what would be expected from a well controlled commercial process. Fibre diameters differ considerably for the experimental fibres, especially those extruded 12 days after the original high solids sol had been rotary evaporated ready for extrusion. This is much more viscous than that of 7 days, which was considered optimum (**Figure 6.26**).

7 days, fired fast to 1250°C/4hrs			
Batch A	**Diameter μm**	**Load**	**GPa**
1	18.6	0.71	2.61
2	18.4	0.87	3.27
3	14.8	0.65	3.78
4	14.8	0.62	3.60
5	14	0.56	3.64
6	19.6	0.61	2.03
7	12.8	0.62	4.79
8	11.6	0.45	4.26
9	11.6	0.36	3.41
10	13.1	0.41	3.04
Average	**14.93**	**Average**	**3.44**
STD DEV	**2.95**	**STD DEV**	**0.79**

Table 6.12a : Tensile Test Results of Batch A Experimental Fibres after 1250°C/4hrs

7 days, fired slow to 1250°C/4hrs				12 days, fired fast to 1250°C/4hrs			
Batch B	**Diameter μm**	**Load**	**GPa**	**Batch C**	**Diameter μm**	**Load**	**GPa**
1	16.8	0.17	0.77	1	32.4	0.18	0.21
2	17.8	0.06	0.24	2	23.2	0.15	0.36
3	18.8	0.20	0.72	3	13.2	0.16	1.17
4	17.6	0.11	0.45	4	20.8	0.19	0.56
5	17.8	0.14	0.55	5	20.8	0.26	0.77
6	14	0.12	0.76	6	18.4	0.24	0.92
7	17.8	0.13	0.51	7	19.4	0.19	0.64
8	16	0.13	0.66	8	19.6	0.18	0.61
9	13.6	0.13	0.89	9	20	0.10	0.33
10	24	0.18	0.40	10	14.4	0.15	0.91
Average	**17.42**	**Average**	**0.59**	**Average**	**20.22**	**Average**	**0.65**
STD DEV	**2.87**	**STD DEV**	**0.20**	**STD DEV**	**5.22**	**STD DEV**	**0.30**

Table 6.12b: Tensile Test Results of Batch B and C Experimental Fibres after 1250°C/4hrs Heat Treatment

There was a large standard deviation of tensile strength for the experimental fibres compared to commercial fibres, although both firing rate and age of the sol seem to have a significant impact. Slow fired fibres have been shown to develop a finer microstructure than those fired under a faster regime, however they appear to be consistently weaker. This may be due to the subsequent handling of the amorphous fibres and the high temperature heat treatment step. In practice the slow firing technique would not be an economically viable option. When the gel is converted to a brittle ceramic, its strength depends critically on the size of defects in the fibre. For strengths similar to commercial alumina based fibres products flaws must be smaller than ~0.4 μm [26] for polycrystalline ceramic fibres. Flaws can be introduced at a number of stages in the process and individual manufacturers have developed their own means of making fibres of adequate mechanical properties. It is well known that single fibre strengths decrease as diameter increases [27]. Fast firing of 12 day aged sol prior to extrusion shows a much reduced tensile strength compared to the optimum 7 days. These fibres now show a more uniform consistency in mechanical strength and a realisation of the potential properties that were first seen for preliminary testing of mullite + 5% zirconia fibres (**Table 6.8**).

As crystal size is extremely fine and uniform in the experimental fibres, the grain boundarys will also be small and their contribution as flaws will be minimised.

6.19.4. High Temperature Creep Properties - Bending Stress Relaxation Creep Test

Grain size is also an important factor when considering the high temperature creep behaviour of polycrystalline fibres, if grains are larger ie. undergone grain growth then there are less grain boundaries available to facilitate creep. If sliding can occur between grain boundaries when the material is in tension, then the fibre length will change i.e. extend. This implies that the material is not fully stable under those conditions and movement of the material can occur, this is particularly undesirable if the material is part of a moving part in a high temperature environment. A simple ranking test can be used in order to investigate the effect of these zirconia additions on the creep properties of the fibres, bend stress relaxation (BSR) tests were conducted on fibres. Unlike the tensile tests, creep tests were performed on the fibres at temperature, after first being heat treated to that temperature in order to stabilise the material. Creep in polycrystalline fibres is normally attributed to grain boundary sliding, the primary controlling mechanisms are anelastic (delayed elasticity) and are broadly distributed in relaxation times [28]. In order to investigate the effect of the zirconia addition on the creep properties of the fibres, bend stress relaxation (BSR) tests were conducted on fibres previously heat treated at 1200°C and 1400°C. The tests were carried out in air and all fibres were of a similar diameter (10 - 15μm). Fibres were tied around alumina rods and measured as reported by [29]. Tests on Nextel 720 were carried out in parallel to provide a direct comparison. A schematic of the principal is outlined in **Figure 6.45**:

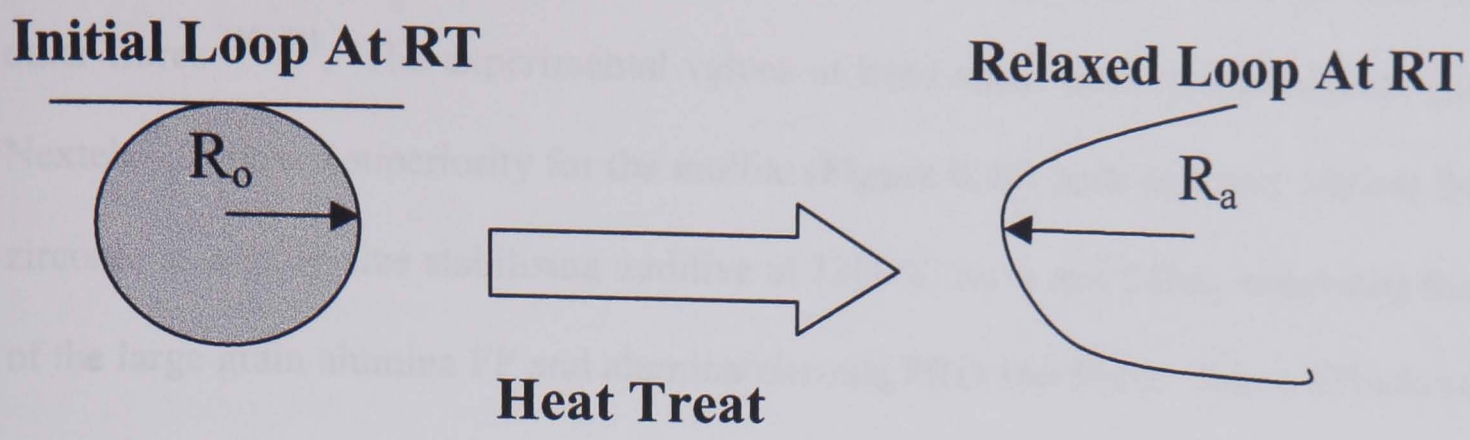

Figure 6.45: Dicarlo BSR Test Schematic

The index of performance (m) is the ratio of radius of bending before and after holding in a furnace at a specific temperature:

$$\varepsilon_0 = \frac{z}{R_o} \qquad \sigma_0 = \varepsilon_0 * E_{fibre} \qquad m = 1 - \frac{Ro}{R_a}$$

were E is the elastic modulus of the fibre ε_0 and σ_0 are the initial deformation and stress at the surface of the fibre, z is the radius of the tested fibre and R_o is the radius of the rod. Alumina rods were used with 1cm diameter. If stress relaxation occurs then $R_a < R_o$ and the material has undergone creep during the test and the m ratio is <1.

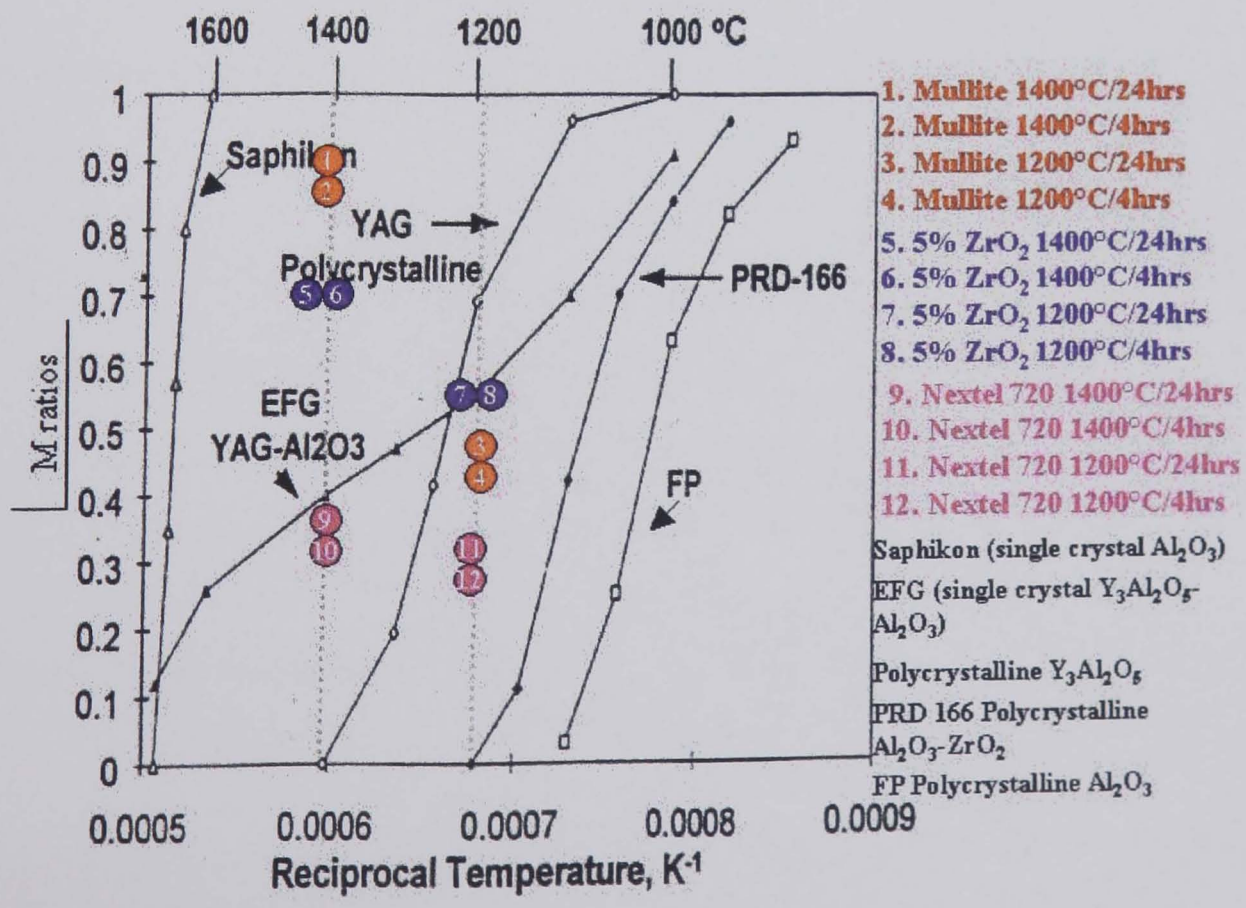

Figure 6.46: Dicarlo BSR M Ratio Values Vs Temperature

High temperature creep properties (BSR) were then compared to literature data for other fibres [30, 31]. The experimental values of bend stress ratio (m) for mullite and Nextel 720 show a superiority for the mullite (**Figure 6.46**) both with and without the zirconia as a grain size stabilising additive at 1200°C for 4 and 24hrs, exceeding that of the large grain alumina FP and alumina/zirconia PRD 166 fibres. Since diffusional creep is sensitive to grain size the comparison was also made for 1400°C heat treatments. Grain growth in the 1400°C heat treated mullite fibres, with and without zirconia, showed the expected further improvement in creep resistance that now exceeds that for polycrystalline YAG and EFG YAG-Al_2O_3.

6.20. References

1. K. Okada "Mullite Long Fibres Prepared By Sol - Gel Method Using Water Solvent System", Key Engineering Materials Vols. 1997, **132**, pg 1946-1949.

2. M. Stacey, Imperial Chemical Industries PLC UK GB, Eur. Patent Application 881117, Patent 318203, 1987.

3. P. Agrawal "The devitrification of amorphous oxides" J. Phys; 1979, **12**, pg 2073-85.

4. R. Stevens, An Introduction to Zirconia (written for MEL), "Zirconia and zirconia Ceramics", 1986, pg 14-16.

5. F. Cotton "Advanced Inorganic Chemistry, 6th Edition" Wiley-Interscience Pub. New York, 1999, pg 178.

6. D. Rawlings "Technical Ceramics" in "Materials Science", 4th Ed., Perganon Press, London, 1990, pg 318.

7. D. Jeng, "Sintering and crystallisation of mullite powder prepared by sol-gel processing" J.Mat.Sci. 1993, **28**, pg 4904.

8. U. Schwertman Iron Oxides in the Laboratory, Wiley-Interscience Pub, Weinheim 1991, pg 178.

9. P. Budnikov "The Al_2O_3 - SiO_2 – ZrO_2 system" Phase Diagrams for Ceramicist's, 1964 and 1969 volumes, American ceramic society Fig 772, 1964.

10. C. Weber "Stable Newtonian jet length during extrusion" Math. Mech. **11**, pg 136, 1931.

11. A. Ziabicki "Fundamentals of Fiber Formation", J. Non-Cryst Solids 1987, **109**, pg 48-54.

12. M. Von Smoluchowski "Mathmatical theory of the coagulation of colloidal particles" Z. Phys. Chem. 1917, **92**, pg 129.

13. M. Astier, "Porosity of alumina gels prepared by hydrolysis of aluminium s-butylate with limited amounts of water" J. Chem. Tech. Biotechnol 1980, **30**, pg 691-698.

14. S. Wilson, "Microstructural evolution of high temperature crystallised boehmite" J. Coll. Int. Sci. 1981, **82**, pg 507.

15. J. Birchall "Oxide Inorganic Fibres", "Concise Encyclopaedia of Composite Materials", Pergamon Press, London, 1989.

16. J. McArdle, "Transformation and microstructure control in boehmite-derived alumina by ferric oxide seeding" Adv. Ceram. Mat. 1988, **3** (4), pg 387-392.

17. H. Sowman, "Sol-Gel Technology", Noyes Publications, New York, 1988. pg 162.

18. K. Karst (3M), U.S. Patent 4047963, 13 September 1977.

19. M. Schmucker "Polycrystalline aluminosilicate fibres with bulk mullite composition", J. Non. Cryst. Solids, 1998, **226**, pg 99.

20. 3M Ceramic Textiles Technical Notebook, pg 15, 2002.

21. D. Wilson, L. Visser, "Nextel™ 650 Ceramic Oxide Fiber: New Alumina Based Fiber For High Temperature Composite Reinforcement", Ceram. Eng. Sci. Proc. 24th Annual Conference on Engineering Ceramics , Cocoa Beach, FL Jan 2000.

22. D. Wilson "Alumina Fiber Development at 3M", Proceeding of the 14th Intl. Conf. on Metal Matrix, Carbon and Ceramic Composites, Cocoa Beach, 1990, pg 105.

23. T. Wood (3M), European Patent Application 0294208, 1988.

24. M. Kumagai, "Controlled transformation and sintering of a boehmite sol-gel by α-alumina seeding" J Am Ceram Soc 1985, **68** (9) pg 500-505.

25. D. Wilson "High performance oxide fibres for metal and ceramic composites" Presented at the Processing of Fibers & Composites Conference, Barga, Italy. May 22, 2000.

26. L. Sawyer, R. Arons "Characterization of Nicalon: Strength, structure and fractography" J Am. Ceram Soc 1987, **70** (11), pg 798-810.

27. F. Anderegg "Single fibre strength as a function of diameter" Ind Eng Chem, 1939, **31** pg 290-298.

28. A. Norwick, "Anelastic Relaxation in Crystalline Solids", Academic Press, 1982.

29. J. Dicarlo, "Creep limitations of current polycrystalline ceramic fibers", Composites Science and Technology, Elsevier Science Ltd, 51, pg 213 – 222, 1994.

30. G. Morscher "Fiber creep evaluation by stress relaxation measurements", Ceram. Eng. Sci. Proc. 12, pg 1032, 1991.

31. G. Morscher "Bend stress relaxation of YAG-Alumina eutectic fibers" Ceram. Eng. Sci. Proc., 16, pg 532, 1995.

CHAPTER 7 CONCLUSIONS AND FURTHER WORK

7. CONCLUSIONS

7.1. Introduction

Polycrystalline ceramic fibres hold great potential as high temperature reinforcement materials as they are chemically inert and resistant to oxidation in air, at high temperatures. Silicon carbide and other non-oxide fibres possess excellent mechanical properties at room temperature, but suffer from oxidation during prolonged use at 1200°C. Fibres have been developed with low oxygen contents (<0.5%) resulting in better oxidation resistance, but still are limited. Current commercial continuous polycrystalline oxide ceramic fibres whilst being chemically inert and oxidation resistant suffer from loss of strength, grain growth and creep limiting them to a maximum use temperature of 1200°C. 3M (Minnesota Mining and Manufacturing) are the market leaders in the manufacture of polycrystalline oxide continuous fibres and initially developed aluminosilicate fibres with considerable levels (>10%) of boric oxide (i.e. 62% Al_2O_3, 24% SiO_2, 14% B_2O_3) [1]. This has been reduced over the years and the alumina-silica ratio adjusted nearer to stoichiometric $3Al_2O_3.2SiO_2$ mullite and more recently alumina rich mullite. All of these fibres have been processed without rendering the fibre thermally stable, resulting in either a mixture of intermediate alumina, alumino-silicate or amorphous phases.

The exception is the more recent Nextel 720 multiphasic α-alumina/2:1 mullite ($2Al_2O_3.SiO_2$) alumina rich fibre. The alumina rich 2:1 mullite phase becomes unstable and converts to stoichiometric ($3Al_2O_3.2SiO_2$) mullite at temperatures of 1200°C. Minor phase formation is also initiated by impurities, such as sodium leading to residual glass formation at grain boundaries [2].

More recently during the life of this project their focus has been on development of a non silicate system based on a fine α-alumina matrix with yttria stabilised nano dispersed zirconia. The fibres retain their tensile strength very well up to 1200°C, but become very brittle above this temperature due to crystallisation and grain growth. As such they are regarded as being inferior to the Nextel 720 fibre and the maximum use temperature is limited to 1080°C [3], whilst 720 is 1150°C.

The main aims of this project have been to address these points to produce a stable, single phase, fine grained polycrystalline ceramic fibre via extrusion of sol-gel precursors. The intended outcome was to produce a fibre resulting in improved mechanical properties, particularly retention of a high proportion of the initial tensile strength of the fibre after heat treatment to >1200°C and improved creep properties at temperature. The selection of stoichiometric mullite ($3Al_2O_3.2SiO_2$) as a fibre phase was based on the intrinsically lower diffusivity in complex oxides compared to simple oxides, such as Al_2O_3, and hence reduced diffusional creep rates [4-6], for a specific grain size. Mullite is also highly resistant to shear plasticity at high temperatures [7], presumably because of the large dislocation Burgers vectors and complex core structures. The absence of a large Al_2O_3 content also reduces the susceptibility of this phase to reduced fracture stress at intermediate temperatures. A specific target was an improvement in microstructural stability, above – 1200°C, over the 3M-720 (Al_2O_3-mullite) fibre which exhibits a change in mullite constitution and crystal symmetry coupled to exsolution of Al_2O_3, with associated strength loss [2].

An additional factor in selection of mullite as a complex oxide was the low cost and large number of readily available precursors for sol-gel production. The approach was based on manufacturing small batches of stoichiometric single phase pure mullite fibres using high purity precursors excluding persistent anions such as chloride or sulphate due to their adverse effects on residual porosity, sintering and defect formation. The spinning dope or sol should have a good shelf life enabling extrusion over several days, without the use of organic fugitive fiberising aids which contribute to the volatile components that reduce the final ceramic yield and economics of the material. Traditionally many alumina and mullite fibres have been based on the use of simple aqueous sol-gel systems which utilise aluminium chlorhydrate (typically $Al(OH)_5Cl$) as the main alumina precursor and colloidal silica. Both of these precursors are widely and economically available in a variety of grades.

3M prefer the use of aluminium carboxylates, which have similar gel and fiberisation properties to ACH, but do not contain persistent anions such as chloride, only organic groups which are easily converted to CO_2 and H_2O during pyrolysis. Other manufacturers [8] have favoured the use of alkoxides, which generally converted to inorganic polymers via hydrolysis in an alcoholic system, which is more expensive and difficult to handle.

Preliminary work focused on two systems derived from the literature, one an aqueous alkoxide system [9] and the other based on existing aluminium carboxylate manufacturing technology [1].

7.2. Simple Chloride Free Mullite Sols

The two chloride free systems were screened for suitability based on their Newtonian flow behaviour, sol stability and microstructural stability with temperature and apparent strength.

The alkoxide system was found to display the best Newtonian flow behaviour at an aluminium isopropoxide : aluminium nitrate ratio of 2:1 as reported by Okada, allowing easy extrusion through spinnerette holes. However the reported viscoelastic character was not apparent which allows the fibre diameter to be reduced via draw down after extrusion. TGA/DSC showed that the pyrolysis of green fibres occurred over broad temperature range, allowing solvent and combustible material to be removed in a more controlled manor with a ceramic oxide yield of 32%. SEM demonstrated a very fine grained, dense microstructure with no intergranular porosity when fired up to 1400°C. XRD analysis showed evidence of initial mullite formation at 1000°C, in the form of the 2:1 phase (supported by DSC data) seen by the single XRD peak at 26.1° 2θ. All amorphous phases being absent at 1100°C and 3:2 mullite formed exclusively at 1200°C. This system would require a fugitive fiberising aid to assist the viscoelastic nature needed to form small diameter filaments. Also instability at ambient conditions was observed, apparent from its hygroscopic nature, which makes post extrusion handling difficult.

The second system based on aluminium acetotartrate (AAT) and Ludox AM-30 colloidal silica exhibits Newtonian flow behaviour, sol stability and excellent fibre forming drawing features. Green fibres are stable in air and are easily handled. TGA/DSC showed that pyrolysis of this system occurs over a wider temperature range than the alkoxide, but also the weight loss events occur over narrow temperature ranges to yield 21% oxide ceramic. This is due to the loss of water, free acetic acid and carboxylate salt groups and carbon formed under slightly reducing firing conditions.

XRD revealed the formation of intermediate γ-alumina at 900°C with a minor amorphous phase evolving at 1200°C with exclusive 3:2 mullite conversion at 1300°C (as indicated by the orthorhombic mullite doublet peak residing between at 25.9 and 26.4° 2θ). The initial formation of alumina intermediates suggested that the silica in the colloidal form (12nm) is less reactive than that of the alkoxide system, therefore leading to mullite formation at a higher temperature without transition through the metastable 2:1 phase (as seen in Nextel 720 fibre heat treated to 1200°C or above). SEM showed that considerable grain growth occured with a high level of intergranular porosity when heat-treated up to 1400°C. Elongated non-equiaxed mullite grains were attributed to the presence of a siliceous glass phase [10] which is consistent with XRD observations. The results showed that the alkoxide system is problematic, but the microstructural characteristics are favourable and vice versa for the inorganic salt/colloidal sol system. It was therefore hypothesised that it would not be unreasonable to produce a stable, extrudable sol, which yielded strong stable green fibres, which on firing would yield a fine grained homogeneous mullite microstructure.

7.3. Blending Sols

The sols were arbitrarily blended at a weight % ratio of 50:50 in the dilute form and then rotary evaporated down to a viscosity suitable for extrusion through a spinnerette. Newtonian flow was maintained and fibres were extruded through 100μm holes, and drawn down to below 30μm. The preferred drying conditions were an air temperature of 20 - 30°C, relative humidity 55 - 65%, fibres dried in air easily and were stable and easy to handle. TGA/DSC showed that the pyrolysis profile was much more uniform than that of the individual sols, resulting in a 25% ceramic oxide yield with the rate of weight loss being lower.

SEM analysis showed that fracture surfaces were similar in appearance to Nextel 720 with a fine, uniform grain structure, which is free from obvious porosity when fired up to 1300°C. As the temperature was increased there was a gradual increase in grain size and the level of porosity, but the pore size remained fine at ~100nm right up to 1500°C, at temperatures in excess of this both grain and pore size became much larger. EDS elemental mapping of fibre cross-sections showed that the distribution of the Si and Al precursors was homogeneous.

XRD analysis revealed that phase evolution in the mixed sol system was different to that of the two individual sols. Stoichiometric 3:2 orthorhombic mullite formed only at 1200°C and above, without the formation of any significant intermediate alumina (a small peak due to cubic spinel - γ-alumina at 46 °2θ) or silica phases. From the individual sols the colloidal silica was the least reactive component and hence its introduction to the mixed sol coupled with the principle of "maximum confusion" [11] would explain the inhibited reaction and formation of mullite. The effect of silica colloid size and reactivity to form mullite in the mixed sol was evaluated using water dispersible grades with sizes ranging from 7 – 30nm. It was found that the largest colloid was least reactive and no mullite was observed by XRD until 1250°C, unlike all of the other sols. The smallest colloids resulted in the finest mullite crystals. As room temperature strength of ceramics is generally associated with fine crystalline microstructures (especially important for fine diameter fibres) and fluxing impurities i.e. alkalies and produce glass phases which deform at high temperature under load, another fine and pure colloidal silica would be more desirable for the sol system.

Ludox AM-30 (sodium aluminate stabilised) was therefore replaced with the ammonia stabilised Ludox SM-AS sol having a low soda content and small colloid size of 7nm.

Other advantages of using a finer silica sol was the reduction in sol viscosity, allowing easier draw down to smaller fibre diameters and reduced bubble entrapment in green fibres. The best-mixed sol ratio was established with a series of experiments conducted using 10% incremental changes and finally 5% at the preferred level. The sols were made as before and assessed based on sol ageing stability, extrudability, draw down rate, green fibre strength and stability in air. Materials were also fired in air to 1200°C and 1400°C/4hrs and assed for handleability and grain growth using SEM. Fibres with a 55:45 alkoxide:AAT/Colloidal silica ratio were proven best overall. Fibres rich in the AAT sol showed significant grain coarsening up to 1400°C with needle like crystals, which have been seen in Nextel 720 fibres after heat treatment [2]. Further examination with XRD found a calcium aluminate phase (Hibbonite - $CaO.6Al_2O_3$). ICP analysis of the precursors found that the commercial AAT from Reheis Chemicals Ltd contained calcium, sodium, zirconium and sulphur totalling ~1% as oxides, which are sometimes retained as intermittent impurities dependant on their process operations. As no guarantee of purity beyond these limits and a withdrawal of the product ensued a lab manufactured precursor was produced using Basic Aluminium Acetate, distilled water and tartaric acid.

7.4. Substitution of Commercial AAT Precursor With a Lab Produced Precursor

The resulting solution contained <0.03% CaO, 99.8% Al_2O_3, with ~0.2% SiO_2 in the ~7% w/w Al_2O_3 solution, attempts to increase the Al_2O_3 content resulted in prolonged digestion times and solid residue from incomplete reaction. The solution was substituted into the optimised mixed mullite sol system and fibres formed and fired as before. Strong dense mullite fibres resulted as with the impure commercial AAT.

Tensile tests at room temperature on heat treated fibres were conducted and the best average strength was 430Mpa (after 1400°C/4hrs) for the lab produced AAT compared to 170MPa for the 50:50 mixed commercial AAT fibre after only 1150°C/4hrs. These results were considerable lower than that expected for heat-treated Nextel 720 and 650 which is typically ~2GPa.

7.5. Microstructural Refinement Using Nano Dispersed Tetragonal Zirconia

In order to maintain a fine microstructure at temperatures up to and above 1400°C an additive was required to aid sintering avoiding residual intragranular microporosity and inhibiting grain growth [12] **Wilson (2000)**. Zirconia is a well-known sintering aid and grain growth inhibitor, two different commercial sources of colloidal sol were identified, which were compatible with the sol chemistry. Nyacol colloidal zirconia sol (10nm zirconium acetate based - 20.2% ZrO_2) and MEL zirconium hydroxynitrate based sol (29.5% ZrO_2). The former was preferred as the latter made sol viscosity much lower and too much shear was experienced even at the lowest extrusion rates, resulting in non-uniformity of fibre lengths. Addition levels were investigated from 0 – 5% by weight. Analysis of fired fibres (1400°C/4hrs) was conducted using Transmission Electron Microscopy (TEM) demonstrating the marked change in nano-scale, mainly intragranular, porosity in the presence of the precipitated nanosized zirconia. Very small grains of the zirconia (< ~50nm) were visible at grain boundaries and within mullite crystals and therefore thermodynamically stable in the tetragonal form without the normal inversion to monoclinic (baddeleyite).

SEM confirmed the inhibition of grain growth, following mullite crystallisation due to enhanced sintering efficiency via grain-boundary transport to residual pores to yield dense fibres.

An important element of this mechanism is the uniform distribution of nano-scale additive particles, which is only obtainable via dissolution in the initial sol and re-precipitation during conversion of gel to the crystalline state. The preferred addition level was ~5%, XRD confirmed that the mullite crystal size was less than with the addition and than without and almost identical to the commercial Nextel 720 fibre. Solid state NMR was conducted on fast fired fibres (green to 1400°C range) for ^{29}Si and ^{27}Al nuclei. It concurred with XRD results, concluding that silica rich tetrahedral evolved along with a mixture of tetrahedral and octahedral aluminium, resolving to form mullite at 1200°C to completion at 1300°C in the orthorhombic 3:2 stoichiometric mullite form.

7.6. Sol Rheology and Ageing With Time

Sol rheology was investigated with three different concentration sols to simulate different viscosities and propensity to ageing (viscosity increase) with time. At a constant low shear rate the less concentrated sols show very consistent ageing over time, as viscosity has changing only ten fold over five weeks, unlike the high solids sol, which changed nearer thirty five fold. After 7 – 8 days it showed a dramatic increase in viscosity, retaining Newtonian flow and the higher the initial viscosity, the more tolerant it will be and more versatile for extrusion. This meant that the viscosity remained higher during extrusion and the ability of the fibre to be drawn is higher. This was confirmed by experimental observations and seven days was considered optimum, after this green fibre quality was not as good.

7.7. Effects of Firing on Microstructure and Mechanical Properties

Firing of fibres was found to be important when carried out as a batch process. as sufficient exposure to both the heat source (Silicon Carbide radiative elements) and air permits removal of small quantities of SO_4^{2-} as SO_x from the core of the fibre at fast (180°C/hr) firing rates. Fibres are preferable constrained during firing in order to reduce the distortion or "kinks" from linear shrinkage (typically <30% at 1400°C) which corresponded to crystallisation during firing. The rate at which the fibre is fired also determines the resulting nano porosity and grain size of the amorphous precursor fibre through to the fully crystalline state.

Non-intrusive low angle XRD was used to detect nano sized pores in fibres fired from 400 – 1400°C/4hrs at slow and fast firing rate. Both showed a peak for porosity after 900°C, reducing at ~990°C due to formation of γ-alumina in this range, a weaker response incurred from the slow fired fibres. The slow firing at temperatures below this was controlled such that the removal of combustible material is gradual and consistent. As diffusion is not inhibited in this system the firing rate may determine the precipitation of the zirconia grains, influencing their ability to control grain growth, as seen by SEM. At high magnification (x 20,000) it confirmed an approximate factor of two increase in crystal size from slow to fast fired material, supported by the translucent to opaque visible appearance of fired fibres at 1400°C. XRD mullite crystallite sizes were seen not only to be smaller for slow fired material (~150nm vs ~250nm), but consistent without growth from 1200°C – 1400°C/4hrs.

7.8. Microstructural Comparison of Commercial and Experimental Fibres

Samples of Nextel 650 and 720 fibres were heat treated at 1200, 1300 and 1400°C for 4, 10, 25 and 100hrs. Visual inspection showed that the shiney lustre of the fine grained Nextel 650 fibre was lost when heat-treated at 1300°C for any period of time, becoming white, kinked and brittle to touch. SEM confirmed that grain growth was starting to become a dominant effect. Even after 100hrs at 1200°C this had occurred suggesting that the classification temperature of 1080°C is proscribed correctly due to fibre degradation. Nextel 720 fibre showed some opalescence after 25 – 100hrs at 1200°C due to some slight grain growth, which became more prominent at 1300°C and with increased duration. At 1400°C this still applied except the fibre became more brittle with time due to excessive, probably alumina grain growth. The experimental mullite + 5% ZrO_2 fibre did become more opalescent but grain size remained smaller than the Nextel fibres.

7.9. Mechanical Testing

Room temperature single fibre tensile tests were carried out on experimental and commercial Nextel 650 and 720 fibres after heat treatment to temperatures that the fibre would see in service. Initial tests confirmed that the experimental zirconia doped fibres showed the best retention of tensile strength after firing up to 1400°C/4hrs, as the mircrostructure remained fine. Further batches of optimised fibres proved that fibres extruded after 7 days, using a sol described to be as high solids (high ceramic yield) was preferred and demonstrated superior post heat treatment tensile strength compared to the commercial fibres. The zirconia addition to Nextel 650 is claimed to reduce grain growth in the fibre, clearly this is not sufficient to deter the continued grain growth of α-alumina crystals above 1300°C, unlike in the experimental fibres.

In order to investigate the effect of the zirconia addition on the creep properties of the fibres, bend stress relaxation (BSR) tests as described by Dicarlo [13] were conducted on fibres heat treated at 1200°C and 1400°C. The tests were carried out in air and all fibres were of a similar diameter (10 - 15μm). Tests on Nextel 720 were carried out in parallel to provide a direct comparison. Comparison of values for the experimental fibres was made with that found from the literature for commercial fibres [14, 15], both single crystal and polycrystalline. The bend stress ratio (m) for experimental single phase mullite fibres was seen to be superior to Nextel 720, both with and without the zirconia as a grain size stabilising additive at 1200°C for 4 and 24hrs, exceeding that of the large grain alumina FP and alumina/zirconia PRD 166 fibres. Since diffusional creep is sensitive to grain size the comparison was also made for 1400°C heat treatments. Grain growth in the 1400°C heat treated mullite fibres, with and without zirconia, showed the expected further improvement in creep resistance which now exceeds that for polycrystalline YAG and EFG YAG-Al_2O_3.

7.10. Further Work

It has been shown that a single phase mixed oxide polycrystalline ceramic fibre can be produced on a lab scale with improved microstructural characteristics by careful control of precursors and their purity. Also the addition of a small quantity of grain stabilising additives can further enhance the microstructure to retain high temperature stability to 1400°C. Currently the variation of fibre strength within a batch or between batches can be large (~1GPa) compared to that seen for commercial Nextel fibres (0.2GPa).

In order to exploit the promising characteristics of the zirconia doped mullite fibre, more emphasis is required on producing the material in larger batches or as a continuous production process with tighter tolerances. In line firing would be one such way in order to control defects from kinks due to excessive shrinkage during firing. QinetiQ (formally DERA), Farnborough are proposing to run a 3 year project within their ceramics group to develop the proven chemistry in to a commercially viable product. Their target is to produce a fibre that is aimed mainly at supplying the UK and European composites requirements for use up to 1400°C in sufficient quantity and to be commercially viable for potential use in gas turbines and aircraft engines.

An ideal optimised structure for high temperature filaments would preferable be a single crystal fibre with a complex oxide structure, limiting creep, and a high melting point. As seen in the literature they are difficult to prepare, expensive and are not suitable for weaving into cloth for use as reinforcement for ceramic matrix composites. Yttrium aluminium garnet ($Y_3Al_5O_{12}$ – YAG) is the most creep resistant polycrystalline oxide currently known and also has very slow grain growth kinetics at high temperature, suggesting that YAG fibres would be an ideal fibre for high temperature composites. Fibres have been produced in the 3M laboratories with a room temperature strength of 700 MPa. Bend stress relaxation measurements indicate that these fibres would have a use temperature 50°C higher than Nextel 720 fibre. YAG fibre heat treated to 1200°C has a fine grain size of 0.1 μm although the fibre contains a substantial amount of porosity. Elimination of this porosity would be expected to reduce creep rates further.

A similar approach to that used to fabricate the experimental mullite and mullite – zirconia fibres may well yield a further improvement in microstructural stability at high temperatures, although Yttrium precursors are considerable more expensive than those used for traditional alumina or mullite based fibres. Further improvements in resistance to oxidation at high temperatures may be possible for non-oxide fibres by using barriers coatings on them. Such a coating could be a high temperature stable oxide sol-gel, such as mullite. This would allow exploitation of their low density, typically <2.5kg/m^3 (most useful oxide typically 3 - 4kg/m^3) and high tensile strength.

7.11. References

1. K. Karst, H.G. Sowman (Minnesota Mining and Manufacturing Co.), U.S. Patent 4047963, 13 September 1977.

2. F. Deleglise "High temperature behaviours of two nanocomposite oxide fibres". Key. Eng. Mat. 1999, **164**, pg 265.

3. D. Wilson, L. Visser, "Nextel™ 650 Ceramic Oxide Fiber: New Alumina Based Fiber For High Temperature Composite Reinforcement", Ceram. Eng. Sci. Proc. 24th Annual Conference on Engineering Ceramics , Cocoa Beach, FL Jan 2000.

4. P. Lessing "Creep of polycrystalline mullite" J. Am. Ceram. Soc. 1975, **68**, pg 149.

5. R. Nixon "International use of Mullite", J. Am. Ceram. Soc, 1990, **73**, pg 579.

6. W. Clegg, "The Science of Engineering Ceramics II", Trans. Tech.Publ, New York, 1998, pg 315.

7. C. Dokko "High temperature mechanical properties of mullite under compression" J. Am. Ceram. Soc. 1977, **60**, pg 150.

8. Sumitomo Chemical Co. Ltd. U.K. Patent 1457801, 1976.

9. K. Okada "Mullite Long Fibres Prepared By Sol - Gel Method Using Water Solvent System", Key Engineering Materials Vols. 1997, **132**, pg 1946-1949.

10. M. Sacks "A review of powder preparation methods and densification procedures for fabricating high density mullite", American Ceramic Society Publication – Mullite and mullite matrix composite, ceramic transactions, 1990, **6**, pg 167-208.

11. P. Agrawal "The devitrification of amorphous oxides" J. Phys; 1979, **12**, pg 2073-85.

12. D. Wilson "High performance oxide fibres for metal and ceramic composites" Presented at the Processing of Fibers & Composites Conference, Barga, Italy, May 22, 2000.

13. J. Dicarlo, "Creep limitations of current polycrystalline ceramic fibers". J. Composite Science and Technology, 1994, **51**, pg 213 – 222.

14. G. Morscher "Fiber creep evaluation by stress relaxation measurements". Ceram. Eng. Sci. Proc. 1991, **12**, pg 1032.

15. G. Morscher "Bend stress relaxation of YAG-Alumina eutectic fibers" Ceram. Eng. Sci. Proc, 1995, **16**, pg 532.